THÈSE

En vue de l'obtention du
DOCTORAT DE L'UNIVERSITÉ DE TOULOUSE

Délivré par l'Université Toulouse 3 - Paul Sabatier

Présentée et soutenue par
HAIYANG GENG

Le 28 septembre 2022

Analyses moléculaires du traitement et de l'apprentissage visuels chez les abeilles mellifères

---

Ecole doctorale : **BSB - Biologie, Santé, Biotechnologies**

Spécialité : **NEUROSCIENCES**

Unité de recherche :
CRCA - Centre de Recherches sur la Cognition Animale

Thèse dirigée par
Martin GIURFA et Isabelle MASSOU

Jury
M. Claudio LAZZARI, Rapporteur
Mme Emmanuelle JACQUIN-JOLY, Rapporteure
M. Cédric ALAUX, Examinateur
M. Martin GIURFA, Co-directeur de thèse
Mme Isabelle MASSOU, Co-directrice de thèse

Contents

List of abbreviations:

AL: Antennal Lobe

AOTu: Anterior Optic Tubercle

APL: Anterior Paired Lateral

CB: Central Brain

CRISPR: Clustered Regularly Interspaced Short Palindromic Repeats

CS: Conditioned Stimulus

CX: Central Complex

DA: Dopamine

DRA: Dorsal Rim Area

DSB: Double-Strand Break

Egr1: Early Growth Response gene-1

FISH: Fluorescence In Situ Hybridization technology

GABA: Gamma-Aminobutyric Acid

GLMM: Generalized Linear Model

GPCR: G-protein-coupled receptors

Hr38: Hormone Receptor 38

IEG: Immediate Early Gene

ISH: In Situ Hybridization

L-: Long wavelength

LMC: Laminar Monopolar Cell

LMM: Linear Mixed Modal

LTD: Long-term Depression

LTM: Long Term Memory

LTP: Long-term Potentiation

M-: Medium wavelength

MB: Mushroom Body

NC: No Choice

OA: Octopamine

OL: Optic Lobe

PB: Protocerebral Bridge

PER: Proboscis Extension Response

RNAi: RNA Interference

RT-qPCR: Reverse Transcription Quantitative Polymerase Chain Reaction

S-: Short wavelength

sgRNA: Single-guide RNA

sKC: Small Kenyon Cell

TALENs: Transcription Activator-like Effector Nucleases

TH: Tyramine

US: Unconditioned Stimulus

VL: Vertical Lobe

VR: Virtual Reality

ZFNs: Zinc Finger Nucleases

5-HT: Serotonin

Acknowledgments

It was my first time studying abroad, and my heart was full of excitement, anticipation, pressure and some fear. However, as time went by, facing the language problems of studying abroad, cultural differences, technical problems in experiments and the COVID-19, I almost gave up my dream of science. Fortunately, frustration taught me to move forward and do better. I am thankful for these experiences, as they gave me the opportunity to learn and grow so much. There are too many people to thank: family, mentors, colleagues, friends... It is because of your help and support that I had the motivation to continue to work hard and follow my dreams.

First of all, I would like to thank my two co-supervisors, Professor Martin Giurfa and Mrs. Isabelle Massou.

I am thankful to Prof. Giurfa for giving me the opportunity to study in Toulouse. Completing a PhD project was one of the great adventures of my life, but looking back on my academic career over the past four years, I realized that recruiting a PhD like me, was an even bigger and riskier adventure for my supervisors. You are the world's top scientist, read a lot, and seem to have a library in your mind. Thank you for your understanding, support and trust! Once again, I would like to thank Professor Martin for providing me with such a valuable opportunity to learn and grow, the premise of my nearly four-year study abroad in France. Without this premise, the later stories would not exist. Thank you for everything. I could not ask for a better mentor.

I would also like to thank my co-supervisor, Isabelle Massou. Thank you for your help and for your advice. Thank you for patiently guiding me through all the experimental steps on the bench. Thank you for showing me how to address PhD questions in a proper and efficient manner. You are a most valuable contributor to our lab and team. So many of my experiments benefited from your technical advice and knowledge.

I thank the examiners of this thesis, Drs. Emmanuelle Jacquin-Joly, Cedric Alaux and Claudio Lazzari, for investing their time in reading and commenting on my work.

I thank the members of my PhD committee, Drs. Marie-Laure Parmentier and Steeve H. Thany, for encouragement, guidance and feedback throughout the years, it took me to complete this thesis.

I gratefully acknowledge the contribution of Drs. Gregory Lafon, Aurore Avarguès-Weber and Alexis Buatois to the behavioral experiments in Chapters 2 and 3. Without their important

Curriculum Vitae

• Personal Information •

Name：	Haiyang GENG	**Age：**	31 (07/05/1991)
Phone：	(+33) 0781966256	**E-mail：**	haiyang.fafu@gmail.com
Address：	12, ALL DES RAMIERS, 31520 RAMONVILLE ST AGNE, FRANCE		

• Education •

2018-2022	**PhD candidate**, Neurosciences, Biology-Health-Biotechnology School, University Paul Sabatier - Toulouse III, France
2015-2018	**Masters**, College of Bee Science, Fujian Agriculture and Forestry University, China
2011-2015	**Bachelors**, College of Bee Science, Fujian Agriculture and Forestry University, China

• Achievements in Scientific Research •

A）Publications

1   **Geng H(∗)**, Lafon G(∗), Avarguès-Weber A, Buatois A, Massou I, Giurfa M. (2022) Visual learning in a virtual reality environment upregulates immediate early gene expression in the mushroom bodies of honey bees. Commun Biol. 14;5(1):130. doi: 10.1038/s42003-022-03075-8.

2   Lafon G(∗), **Geng H(∗)**, Avarguès-Weber A, Buatois A, Massou I, Giurfa M. (2022) The neural signature of visual learning under restrictive virtual-reality conditions. Front Behav Neurosci. 16:846076. doi: 10.3389/fnbeh.2022.846076.

3   Marchal P, Villar ME, **Geng H**, Arrufat P, Combe M, Viola H, Massou I, Giurfa M. (2019) Inhibitory learning of phototaxis by honeybees in a passive-avoidance task. Learn Mem. 26(10):1-12. doi: 10.1101/lm.050120.119.

4   Wang, X., Lin, Y., Liang, L., **Geng, H**., Zhang, M., Nie, H., & Su, S. (2021). Transcriptional Profiles of Diploid Mutant Apis mellifera Embryos after Knockout of csd by CRISPR/Cas9. Insects, 12(8), 704. https://doi-org.insb.bib.cnrs.fr/10.3390/insects12080704

5   Nie, H(∗), **Geng H(∗)**, Lin Y, Xu S, Li Z, Zhao Y, Su S. (2018) Genome-wide identification and characterization of fox genes in the honeybee, Apis cerana and comparative analysis with other bee fox genes. International Journal of Genomics vol. 2018, Article ID 5702061, 12 pages, 2018. doi: 10.1155/2018/5702061.
     (∗) 1st authorship shared

6   Nie, H, Xu S, Xie C, **Geng H,** Zhao Y, Li J, Huang WF, Lin Y, Li Z, Su S. (2017) Comparative transcriptome analysis of Apis mellifera antennae of workers performing different tasks. Molecular Genetics & Genomics, 293(1):237-248. doi: 10.1007/s00438-017-1382-5.

7   Zhang, S, Shao Q, **Geng H**, Su S. (2017) The effect of royal jelly on the growth of breast cancer in mice. Oncology Letters, 14(6):7615-7621. doi: 10.3892/ol.2017.7078.

8   Li, Z, Huang S, Huang W, **Geng H**, Zhao Y, Li M, Chen Y, Su S. (2016) A scientific note on detection of honeybee viruses in the darkling beetle (Alphitobius diaperinus, Coleoptera: Tenebrionidae), a new pest in Apis cerana cerana colonies. Apidologie, 47: 759. https://doi.org/10.1007/s13592-016-0430-1.

9   Jin, L., Mehmood, S., Zhang, G.C., Song, Y., Su, S., Huang, S., Huang, H., Zhang, Y., **Geng, H**., & Huang, W. (2020). Visualizing Sacbrood Virus of Honey Bees via Transformation and Coupling with Enhanced Green Fluorescent Protein. Viruses, 12.

B）Posters

- **H. Geng**, H. Nie, M. Zhang, S. Mehmood, S. Su. Targeted nucleotide editing using CRISPR/Cas9 system in the honeybee, *Apis mellifera* L. **First International Workshop on Insect Genome Editing**. Shanghai, China. 28-31 October, 2017

- **H. Geng**, M. Paoli, G. Lafon, B. Paffhausen, I. Massou, M. Giurfa. CRISPR/Cas9-mediated knockout of *Amlop1* opsin reduces color learning efficiency of honeybees in a passive-avoidance task. **International Congress of Neuroethology**. Lisbon, Portugal, 24-29 July, 2022

C）Patent

- S. Su, **H. Geng**, etc. A method for removing honeycomb eggs for microinjection in *Apis mellifera*. Application number 201710703765.5 (in the patent office of FAFU)

・Skills・

Expert	CRISPR/Cas9 gene-editing system in the honeybee	Beekeeper
Proficient	RNAi system in the honeybee	qPCR
	Proboscis extension reflex (PER)	ICARUS
	In situ hybridization	Cloning
	Artificial insemination in honeybees	3D printing
Novice	Laser capture microdissection (LCM) technology	Arduino
	3D virtual reality (VR)	Calcium imaging

・Languages・

Chinese, mother language

English, B2

Abstract

English Abstract

Honey bees are endowed with the capacity of color vision as they possess three types of photoreceptors in their retina that are maximally sensitive in the ultraviolet, blue and green domains owing to the presence of corresponding opsin types. While the behavioral aspects of color vision have been intensively explored based on the easiness by which free-flying bee foragers are trained to color stimuli paired with sucrose solution, the molecular underpinnings of this capacity have been barely explored. Here, to fill this void, we developed studies that spanned the exploration of opsin properties and changes of gene expression in the bee brain during color learning and retention in controlled laboratory protocols.

We characterized opsin distribution in the honey bee visual system, focusing on the presence of two types of green opsins (*Amlop1* and *Amlop2*), one of which (*Amlop2*) was discovered upon sequencing of the bee genome. We confirmed that *Amlop1* is present in ommatidia of the compound eye but not in the ocelli, while *Amlop2* is confined to the ocelli. We developed a CRISPR/Cas9 approach to determine possible functional differences between these opsins. We successfully created *Amlop1* and *Amlop2* adult mutant bees by means of the CRISPR/Cas9 technology, and we also produced *white-gene* mutants as a control for the efficiency of our method. We tested our mutants using a conditioning protocol, in which bees learn to inhibit attraction to chromatic light based on electric-shock punishment (Icarus protocol). *White* and *Amlop2* mutants learned to inhibit spontaneous attraction to blue light, while *Amlop1* mutants failed to do so. These results indicate that responses to blue light, which is also partially sensed by green receptors, are mediated mainly by compound-eye photoreceptors containing *Amlop1*, but not by the ocellar system in which photoreceptors contain *Amlop2*. Accordingly, 24 hours later, *white* and *Amlop2* mutants exhibited an aversive memory for the punished color that was comparable to control bees, but *Amlop1* mutants exhibited no such memory. We discuss these findings based on controls with eyes or ocelli covered by black paint and interpret our results in the context of chromatic vs. achromatic vision via the compound eyes and the ocelli, respectively.

Finally, we analyzed immediate early gene (IEG) expression in specific areas of the bee brain,

following color vision learning in a virtual reality (VR) environment. We changed the degrees of freedom of this environment and subjected bees to a 2D VR, in which only lateral movements of the stimuli were possible, and to a 3D VR, which provided a more immersive sensation. We analyzed levels of relative expression of three IEGs (*kakusei*, *Hr38*, and *Egr1*) in the calyces of the mushroom bodies, the optic lobes and the rest of the brain, after color discrimination learning. In the 3D VR, successful learners exhibited *Egr1* upregulation only in the calyces of the mushroom bodies, thus uncovering a privileged involvement of these brain regions in associative color learning. Yet, in the 2D VR, *Egr1* was downregulated in the OLs, while *Hr38* and *kakusei* were coincidently downregulated in the calyces of the MBs in the learned group. Although both VR scenarios point towards specific activations of the calyces of the mushroom bodies (and of the visual circuits in the 2D VR), the difference in the type of expression detected suggests that the different constraints of the two VRs may lead to different kinds of neural phenomena. While 3D VR scenarios allowing for navigation and exploratory learning may lead to IEG upregulation, 2D VR scenarios in which movements are constrained may induce higher levels of inhibitory activity in the bee brain. Overall, we provide a series of new explorations of the visual system, including new functional analyses and the development of novel methods to study opsin function, which advances our understanding of honey bee vision and visual learning.

Keywords: Vision, Visual Learning, Honey Bee (*Apis mellifera*), Opsin Genes, Photoreceptors, CRISPR/Cas9, Inhibition of Color Attraction, Virtual Reality, Brain, IEG expression, Mushroom Bodies, Optic Lobes

Résumé Français

La capacité de vision en couleurs des abeilles mellifères repose sur l'existence de trois types de photorécepteurs dans leur rétine dont la sensibilité maximale dans les domaines de l'ultraviolet, bleu et vert est conférée par trois types d'opsines localisées dans ces photorécepteurs. Alors que les aspects comportementaux de la vision des couleurs des abeilles ont été explorés de manière intensive grâce à la facilité avec laquelle les butineuses en vol libre peuvent être entraînées à des stimuli visuels associés à une solution de saccharose, les fondements moléculaires de cette capacité ont été à peine explorés. Afin de combler ce vide, nous avons développé des études qui vont de l'exploration des propriétés des opsines aux analyses de changements de l'expression des gènes dans le cerveau de l'abeille pendant l'apprentissage et la rétention des couleurs dans des protocoles contrôlés en laboratoire.

Dans un premier temps, nous avons caractérisé la distribution des opsines dans le système visuel des abeilles mellifères, en nous concentrant sur deux types d'opsines sensibles maximalement au vert (*Amlop1* et *Amlop2*), dont l'une (*Amlop2*) a été découverte lors du séquençage du génome de l'abeille. Nous avons confirmé qu'*Amlop1* est présent dans les ommatidies de l'œil composé mais pas dans les ocelles, tandis qu'*Amlop2* est confiné aux ocelles. Nous avons développé une approche CRISPR/Cas9 pour déterminer les différences fonctionnelles entre ces deux opsines. Nous avons créé avec succès des abeilles mutantes adultes *Amlop1* et *Amlop2* au moyen de la technologie CRISPR/Cas9 et nous avons également développé des mutants pour le gène *white* afin de contrôler l'efficacité de notre méthode. Nous avons testé les mutants générés dans un protocole de conditionnement dans lequel les abeilles apprennent à inhiber leur attraction à une lumière chromatique par son association à une punition choc électrique (protocole Icarus). Les mutants *white* et *Amlop2* ont appris à inhiber l'attraction spontanée à la lumière bleue alors que les mutants *Amlop1* n'ont pas réussi à le faire. Ces résultats indiquent que les réponses à la lumière bleue, qui est également détectée partiellement par les récepteurs verts, sont médiées principalement par des photorécepteurs contenant *Amlop1*, mais pas par le système ocellaire contenant *Amlop2*. En conséquence, 24 heures plus tard, les mutants *white* et *Amlop2* ont montré une mémoire aversive pour la couleur punie qui était comparable à celle des abeilles témoins, mais les mutants *Amlop1* n'ont montré aucune mémoire. Nous discutons à partir des performances de contrôles avec les

yeux ou les ocelles recouverts par une peinture noire et interprétons nos résultats en fonction de l'utilisation de la vision chromatique ou achromatique via les yeux composés ou les ocelles, respectivement.

Finalement, nous avons analysé l'expression de gènes précoces (IEG) dans des zones spécifiques du cerveau de l'abeille suite à un apprentissage associatif de couleurs dans un environnement de réalité virtuelle (RV). Nous avons varié les degrés de liberté de cet environnement et soumis les abeilles à une RV 2D dans laquelle seuls les mouvements latéraux des stimuli étaient possibles et à une RV 3D qui procurait une sensation plus immersive. Nous avons analysé les niveaux d'expression relative de trois IEG (*kakusei*, *Hr38* et *Egr1*) dans les calices des corps pédonculés, les lobes optiques et du reste le cerveau suite à l'apprentissage discriminatif de deux couleurs. Dans la RV 3D, les abeilles apprenant la tâche ont montrant une régulation à la hausse d'*Egr1* uniquement dans les calices des corps pédonculés, montraint ainsi une implication privilégiée de ces régions du cerveau dans l'apprentissage associatif des couleurs. Pourtant, dans la RV 2D; *Egr1* a été régulé à la baisse dans les OL, tandis que *Hr38* et *kakusei* ont été aussi régulés à la baisse dans les calices des corps pédonculés des abeilles ayant appris la tâche de discrimination. Bien que les deux scénarios de RV pointent vers des activations spécifiques des calices des corps pédonculés (et des circuits visuels dans la RV 2D), la différence dans le type d'expression détecté suggère que les différentes contraintes des deux types de RV peuvent conduire à différents types de phénomènes neuronaux. Alors que les scénarios de RV 3D permettant la navigation et l'apprentissage exploratoire peuvent conduire à une régulation à la hausse des IEGs, les scénarios de RV 2D dans lesquels les mouvements sont limités induiraient des niveaux plus élevés d'activité inhibitrice dans le cerveau de l'abeille. Cette thèse propose ainsi une série de nouvelles explorations du système visuel, y compris de nouvelles analyses fonctionnelles et le développement de nouvelles méthodes pour étudier la fonction des opsines, qui font progresser notre compréhension de la vision des abeilles mellifères et de leur apprentissage visuel.

Mots-clés : Vision, Apprentissage visuel, Abeille mellifère (*Apis mellifera*), Opsines, Photorécepteurs, CRISPR/Cas9, Inhibition de l'Attraction Chromatique, Réalité Virtuelle, Cerveau, Expression de précoces (IEGs), Corps Pédonculés, Lobes Optiques

Introduction

1. Color vision

Visible light is electromagnetic radiation, which is absorbed by photopigments present in photoreceptors located in the retina, creating thereby visual sensations and experiences in the brain. Light exhibits both particle-like and wave-like properties. Both aspects are connected by the formula $E_\lambda = h\nu = hc/\lambda$, with E_λ being the energy of a single photon of wavelength λ and h being the Planck constant. The wavelength λ and the frequency ν of the electromagnetic wave are connected by $c = \lambda\nu$, with c being the velocity of light in vacuum (Fig. 1).

The visible spectrum is the portion of the electromagnetic spectrum that is visible and can be detected by the eye. The human eye can see light as colors within a range that goes from approximately 400 nm (human violet-blue) to approximately 700 nm (human red) (Fig. 1). Many other animals also see colors but differ from humans in the wavelength range they perceive. For instance, some species of both vertebrates and invertebrates are able to perceive ultraviolet (down to ~300 nm) and/or near infrared (up to ~800 nm) light, depending on the visual pigments expressed by their photoreceptors (Nathans, 1999).

1.1 Human Photoreceptor function and types

There are two types of photoreceptors (cone photoreceptors and rod photoreceptors; Fig. 2) sensing light, color or shape, among other visual cues, and delivering the message to the brain through the optic nerve in the case of the vertebrate visual system (Rodieck and Rodieck, 1998). Rods photoreceptors are sensitive to low-light levels and participate in nocturnal vision; they allow identifying black and white hues and are usually concentrated at the outer edges of the retina so that they are used in peripheral vision. Cones, in opposition, are specialized for detecting color at high bright light. Cone cells in the retina are classified according to their different spectral sensitive, as mentioned above. They provide the basis to decompose the spectral light through three different channels, each with a different spectral tuning (Chen et al., 2005).
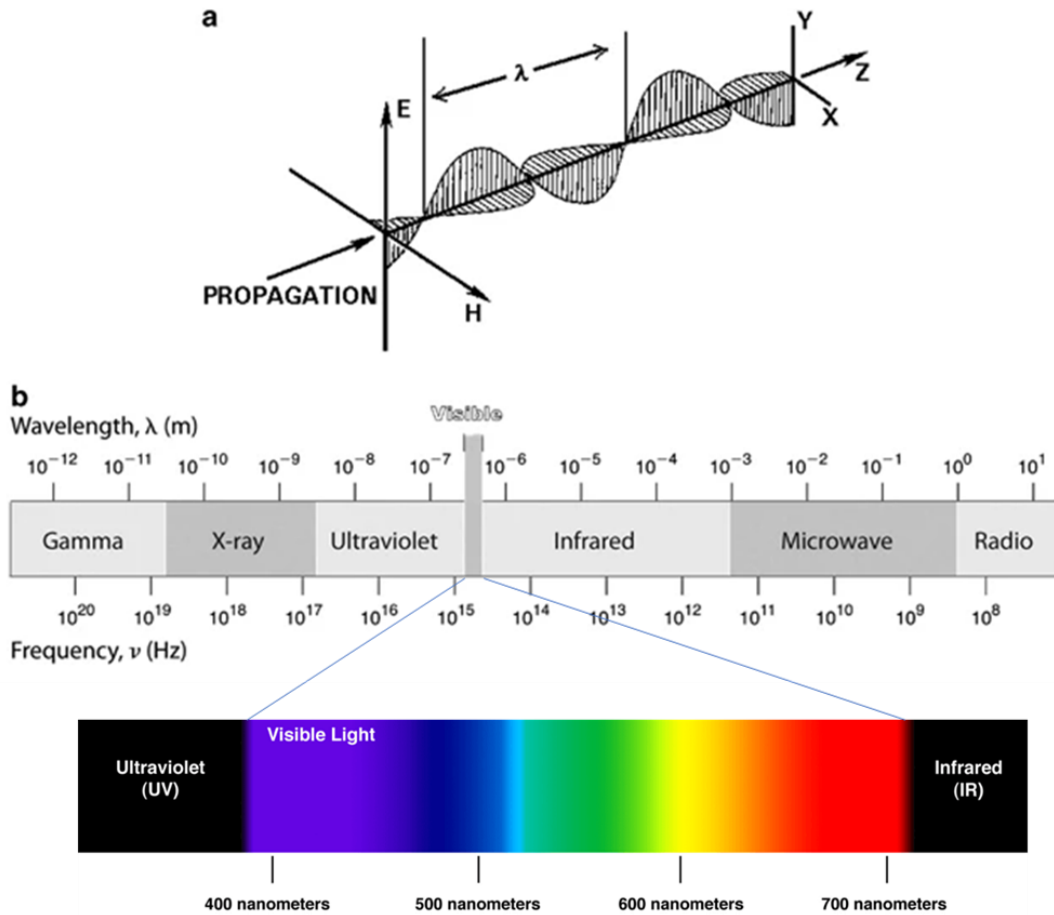
Figure 1. Electromagnetic waves and the electromagnetic (E–M) spectrum (adapted from Sliney)(Sliney, 2016). (a) (top) A geometrical representation of an oscillating E–M wave with E (electric) and H (magnetic) fields. (b) (below) Familiar regions of the E–M spectrum.

The human eye contains more rod photoreceptors than cone photoreceptors. Approximately 6 million cones are located mostly in the fovea, a pit-like structure located in the center of the retina that allows one to perceive more details of images. While more than 100 million rod cells are present in the retina, they are absent from the fovea (Chen et al., 1997, 2005).
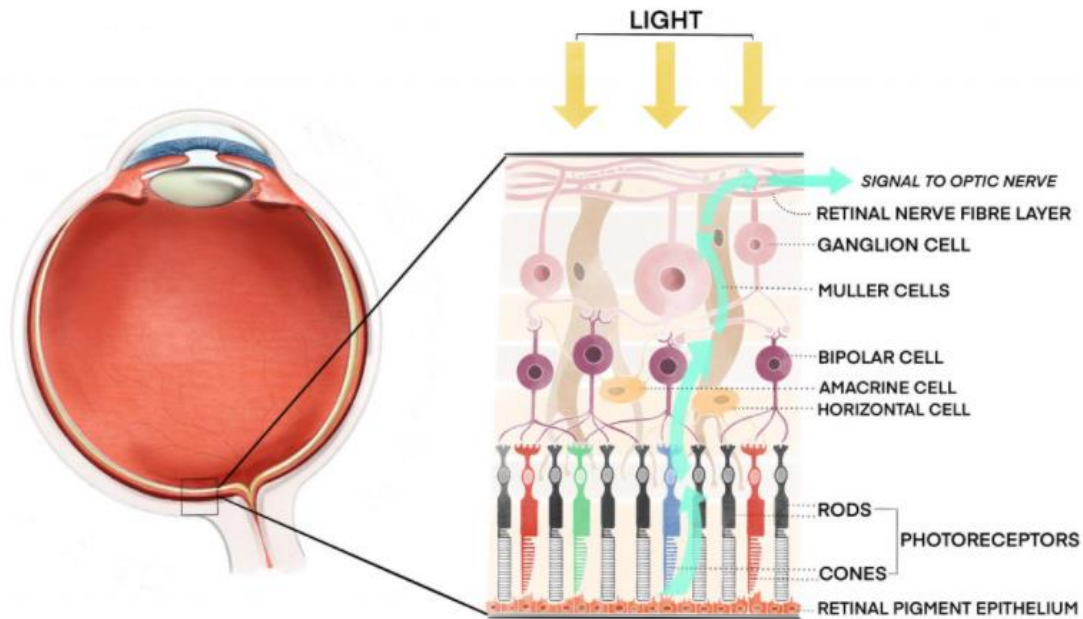
Figure 2. Microscopic view of the cells in the retina. The rod and cone photoreceptors are at the bottom supported by the retinal pigment epithelium. The other cell types above the photoreceptors, in particular the ganglion cells, relay electrical signals to the brain. Taken from https://gene.vision/retina/

Human eyes possess three types of cone pigments that mediate color vision in the retina, which have absorption maxima at approximately 420 nm (the blue-sensitive pigment), 530 nm (the green-sensitive pigment), and 560 nm (the red-sensitive pigment) (Nathans et al., 1986). A fourth pigment, present in a different class of photoreceptors, known as rod photoreceptors, mediates vision in dim light and absorbs maximally at 495 nm (Nathans et al., 1986). Importantly, blue, green and red-sensitive pigments are not just maximally sensitive to the wavelengths described above but respond also, although to a lesser extent to other wavelengths, depending on the form of their spectral sensitivity curve.
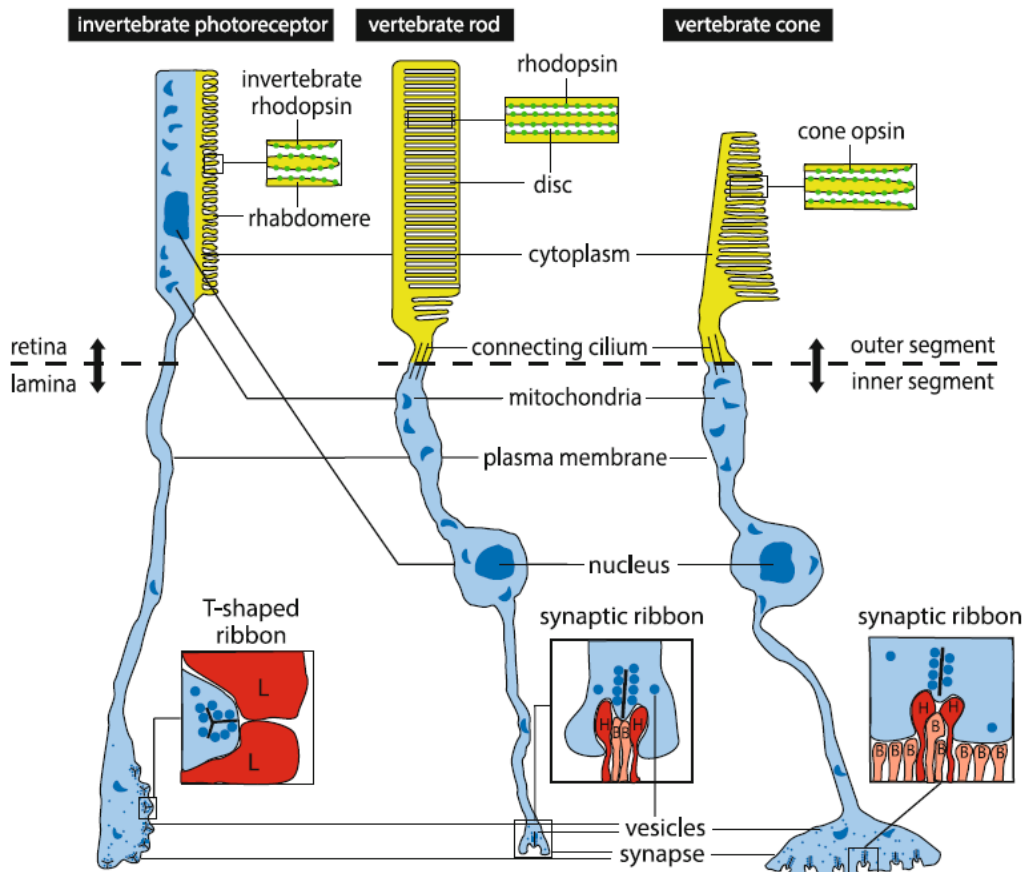
Figure 3. Photoreceptors in vertebrate and invertebrate. Sketch of insect microvillar photoreceptor (left), and vertebrate ciliar receptors rod (middle) and cone (right). Specialized photosensitive membrane regions with embedded opsins (see upper insets) are shown in yellow. Lower insets show highly specialized ribbon synapses transferring signals to postsynaptic neurons, e.g., to lamina cells (L) in flies and to horizontal cells (H) and bipolar cells (B) in vertebrates (Galizia and Lledo, 2013).

1.2 The nature of color stimulation

Color is a psychophysical sensation as it has a physical basis (see above, and Fig. 1a) but also depends on perceptual (psychological) processes. In physical terms, color has three main dimensions in the case of human perception: 1) *tone* (or hue), which corresponds to the specific wavelength processed (violet, blue, green, yellow, red, etc.); 2) *saturation*, which corresponds to the amount of a neutral color (e.g., white) that is added to a pure tone; 3) *intensity* (or luminance), which corresponds to the amount of light that passes through, is emitted from, or is reflected from a particular area. The luminance dimension is achromatic as photoreceptors evaluating light intensity simply respond to the amount of light reflected, irrespective of its color. While humans integrate the three dimensions in their color perception, thus building a 3D space for color vision,

animals may differ in the way they evaluate colors. For instance, in honey bees many experiments have reported that color vision is bidimensional (including hue and saturation) as it excludes the intensity dimension. In other words, bees respond to differences in color and saturation but do not detect differences between colors with the same hue and saturation, but rather those differing in intensity (Daumer, 1956; von Helversen, 1972; Backhaus et al., 1987; Chittka et al., 1992).

Compared to visual judgments based on luminance differences, color vision can help animals to detect and better discriminate objects based on the wavelength composition of their light reflection (Osorio et al., 2004). For example, a red fruit between green leaves can be hard to detect based solely on luminance, but it clearly stands out for observers able to perceive color differences.

Color perception is based on the responses of photoreceptors, which respond specifically in a certain range of light wavelengths (Fig. 4). Some vertebrate species are tetrachromats. They have four different types of cones, which usually cover the spectral range from ~350 to ~650 nm (Bowmaker, 2008). Other vertebrate species and many insects are trichromats (with three types of photoreceptors in their retina) with stronger sensitivity in the short wavelength range (UV light, 300– 400 nm), mid wavelength range (400- 550 nm) and long-wavelength range (550 – 700 nm) (Warrant and Nilsson, 2006; Kretzberg and Ernst, 2013). Some mammals have lost two of the four vertebrate photoreceptor types during evolution (Lamb et al., 2007). Hence, they are dichromats with only one type of green/red-sensitive cone and a lower number (~10 %) of blue cones (Kretzberg and Ernst, 2013). Only a few mammals, like Old-World primates and Humans, have regained the third photoreceptor type during evolution, leading to the unusually similar absorption maxima of the L- (long wavelength) and M- (medium wavelength) cones (in human 564 and 533 nm) in addition to the S- (short-wavelength) cone (absorption maximum 437 nm) (Jameson and Hurvich, 1968; Zelinger and Swaroop, 2018).

For color perception and discrimination, it is necessary to combine the responses of photoreceptor types with overlapping spectral sensitivity curves via neural elements that are downstream of photoreceptors. These neural elements are characterized by a combination of photoreceptor signals termed "*opponent processing*", as it involves subtraction of photoreceptor signals, i.e., while some photoreceptor class may excite/inhibit these opponent neurons, another photoreceptor class may induce the reverse response (Gegenfurtner and Kiper, 2003). Color opponent neurons have been characterized both in vertebrates and invertebrates, thus providing

the basis for color vision. Some of these neurons have color-opponent receptive fields responding in their center to one wavelength with excitation, and to another wavelength in the periphery with inhibition, or vice versa.

Animals endowed with a single photoreceptor type have only access to color-blind vision. For instance, a medium response amplitude of a cone could be elicited either by a relatively low intensity of the optimal wavelength or by a high intensity of a suboptimal wavelength. Dichromats, on the contrary, can perceive colors but are not able to discriminate between many colors, because many different mixtures of wavelengths lead to the same activation pattern of the two types of photoreceptors.
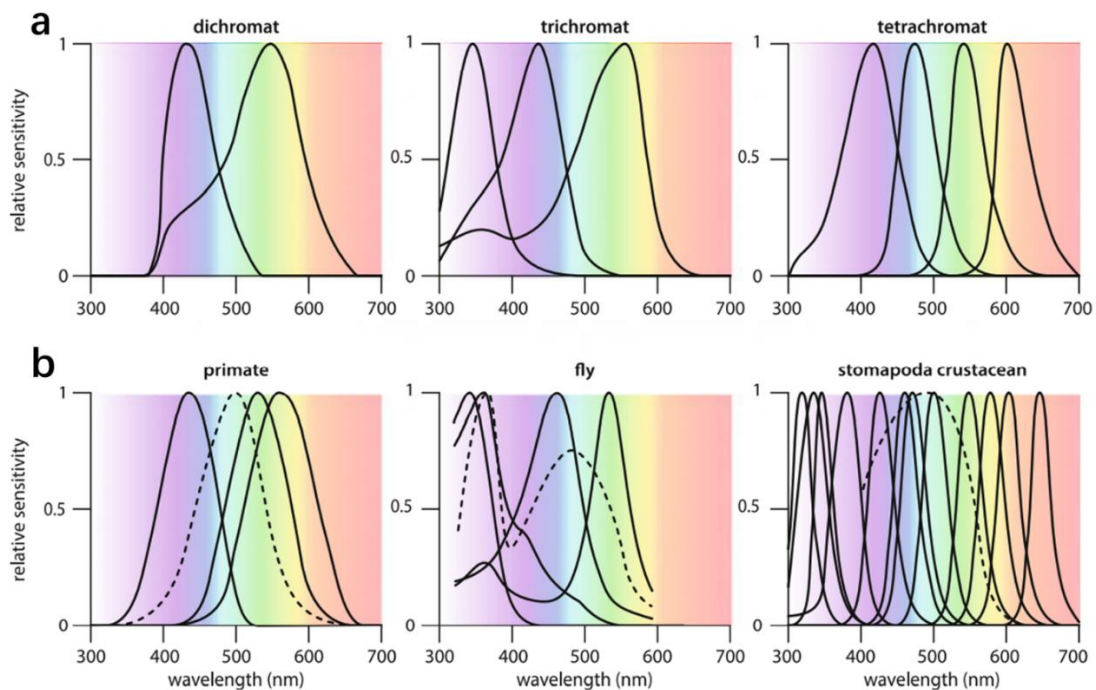
Figure 4. Color vision. (a) Typical sensitivity curves of dichromats, trichromats and tetrachromats. (b) Three specific examples of spectral sensitivity of different photoreceptors involved in color vision (black lines, in primate cones), together with the spectral sensitivity of a wavelength-unspecific photoreceptor type (dashed lines, in primate rod).

2. The case of insects

Insects possess two main kinds of visual organs, the ocelli, which are typically located on the vertex and/or the frontal part of the head, and the compound eyes, integrated by many functional units termed ommatidia, which are located laterally to the head. In some cases, photoreceptors have been identified in unusual parts of the insect body (such as in the genitalia of butterflies (Arikawa et al., 1980), but these are exceptions that will not be considered here.

2.1 Ocelli

Most flying insects possess three simple eyes known as ocelli (Berry et al., 2007; Mizunami, 1995; Warrant et al., 2006). Typically, these simple eyes are placed in a triangular formation on the dorsal surface of the head. They do not build images from the external world but allow detecting light-intensity differences, which are important in several navigation and orientation contexts. Each ocellus consists of a lens, an iris, a corneageous cell layer, and a retina (Mobbs et al., 1981). In dragonflies and locusts, the ocelli play a crucial role in horizon detection for the stabilization of displacements (Berry et al., 2007; Stange et al., 2002), altitude control during flight (Stange, 1981; Taylor, 1981), flight time initiation (Eaton et al., 1983; Wellington, 1974), optomotor responses (Honkanen et al., 2018) and phototactic responses (Barry and Jander, 1968). In addition, the ocelli are able to resolve some spatial information in wasps and dragonflies (Berry et al., 2007; Stange et al., 2002; Warrant et al., 2006). In desert ants, they can also derive compass information from celestial cues (Schwarz et al., 2011a, 2011b), especially from the pattern of polarized skylight (Fent and Wehner, 1985; Mote and Wehner, 1980). By covering the compound eyes or the ocelli separately, researchers found that ocelli mediate a distinct directional system and unlike the dorsal rim area (DRA) of the compound eyes (see below), they cannot mediate path integration by themselves (Schwarz et al., 2011b). There is a different ocellar structure in four sympatric species of *Myrmecia* ants that differ in their activity rhythms along the day: ants active in dim light have larger ocellar lenses and wider rhabdoms than ants active during bright-light conditions (Narendra and Ribi, 2017). Short- and long-wavelength spectral receptor types are commonly found in insect ocelli (Henze et al., 2012; Futahashi et al., 2015; Mizunami, 1995).

Honey bees also possess three ocelli located on top of their head (Fig. 5). The ocellar retina of honey bees is divided into a ventral and a dorsal part, with their ventral retina looking skywards and their dorsal retina looking at the horizon (Ribi et al., 2011). Each ocellus in the honeybee has a single flattened spheroidal lens. Each lateral ocellus contains approximately 1100 photoreceptors, while the median ocellus contains 1350 photoreceptors (Ogawa et al., 2017). Using three-dimensional (3-D) reconstructions of the honeybee ocelli and neuroanatomical analyses of filled ocellar descending neurons, Hung and Ibbotson (2014) were able to establish functional principles of honey bee ocelli. In both the median and lateral ocelli, the ocellar retinas can be divided into

dorsal and ventral parts. As mentioned above, the dorsal retinas view the horizon, while the ventral retinas view the sky, suggesting quite different roles in attitude control, consistent with Ribi's observations (Ribi et al., 2011). Moreover, the hanging drop method, which consists in imaging specific patterns (i.e., spatial gratings, concentric or linear patterns) projected by a screen and viewed through the lens of a given ocellus suspended from a water drop attached to a cover slip, allowed one to assess the spatial resolution of the retinas. The lateral ocelli have significantly higher spatial resolution compared to the median ocellus (Hung and Ibbotson, 2014).

There are two classes of ocellar photoreceptors in honeybee workers, which peak at wavelengths of 360 and 500 nm (UV and green receptors, respectively); UV receptors have on average a higher polarization sensitivity compared with green receptors (Ogawa et al., 2017). Five pairs of large ocellar descending neurons were found in the ocellar retinas; four of these neuron pairs have their dendritic fields in the dorsal retinas of the lateral ocelli, while the fifth has fine dendrites in the ventral retina (Hung and Ibbotson, 2014).

Using a cobalt staining technique, Pan and Goodman (Pan and Goodman, 1977) showed that ocellar fibers in the honey bee worker project to different "ocellar association areas" in the central nervous system. Five large fibers in each lateral ocellar nerve and twelve in the median ocellar nerve have wide-field terminal arborizations on either side of the posterior protocerebral bridge (central complex). Nine medium-sized fibers in each lateral nerve and twelve in the median nerve form a second ocellar association area on each side of the perioesophageal foramen. A group of fine fibers arborize just below and anterior to the protocerebral bridge. Ten medium-sized fibers run from the level of the ocellar nerve tracts to the first and second thoracic ganglia, branching into a number of discrete areas within each ganglion. A few fibers run between the higher-order optic centers and the ocellar tract. Thus, ocellar neurons project to multiple areas of the bee brain, including higher-order visual centers and motor-control centers in the thoracic ganglia.
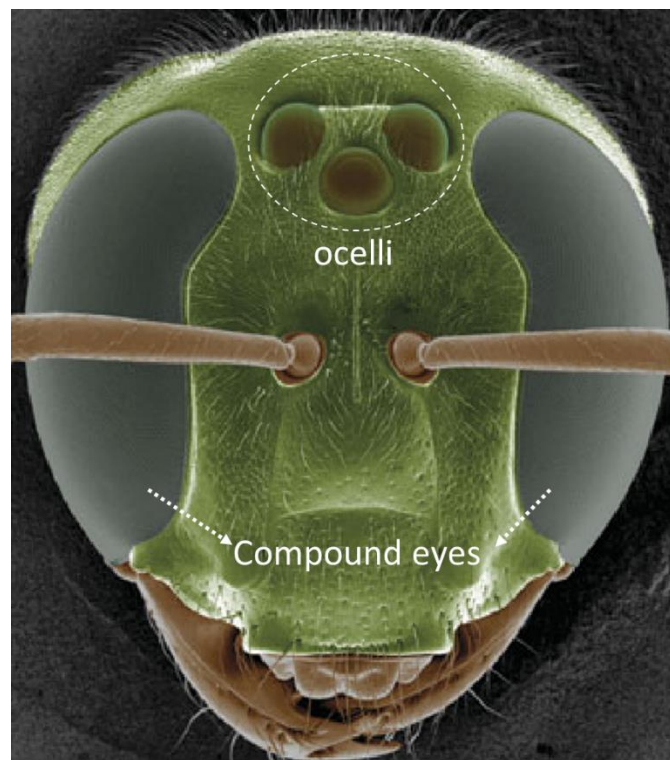
Figure 5. A scanning electron microscope image of the head of a bee, Megalopta genalis, showing the position of the two large compound eyes and the three small ocelli. (Warrant, 2019)

2.2 Compound eyes

Most adult insects have one pair of compound eyes, which are generally composed of many basic structural units named ommatidia (Goldsmith and Bernard, 1974). Each ommatidium typically consists of a dioptric apparatus, a number of primary and secondary pigment cells, and retinular cells also termed photoreceptor cells (Paulus, 1979).

There are two main types of compound eyes in insects: the superposition and the apposition eyes (Exner, 1891) (Fig. 6). The principle of superposition eyes (usually found in nocturnal insects such as moths) is that photoreceptors signals located in different ommatidia are combined according to their optical axes, while in apposition eyes (usually found in diurnal insects) the rhabdomeres of all photoreceptors in one ommatidium are fused (Nilsson, 1989). With a clear zone lacking pigment separating the cornea from rhabdomeres, the superposition eyes are more sensitive to light, because they permit all photoreceptors to use the corneal dioptrical construction, thus increasing light transmittance (Land and Fernald, 1992).

As mentioned above, the superposition eye, also known as the clear-zone eye because of its diagnostic pigment-free gap between dioptric and light-perceiving structures is present in

nocturnal species like moths (Yagi and Koyama, 1963), caddisflies (Nilsson, 1989) and lobsters (Meyer-Rochow, 2001), but it may also be found in some diurnal species like skipper butterflies (Horridge et al., 1972) and other butterflies and moths, such as *Orygia antiqua* (Lau and Meyer-Rochow, 2007) and *Parnassius glacialis* (Matsushita et al., 2012). The apposition compound eyes are present mainly in diurnal insects such as the honey bee (Warrant et al., 1996), locusts (Warrant, 1999) and damselflies (Meyer and Labhart, 1993).
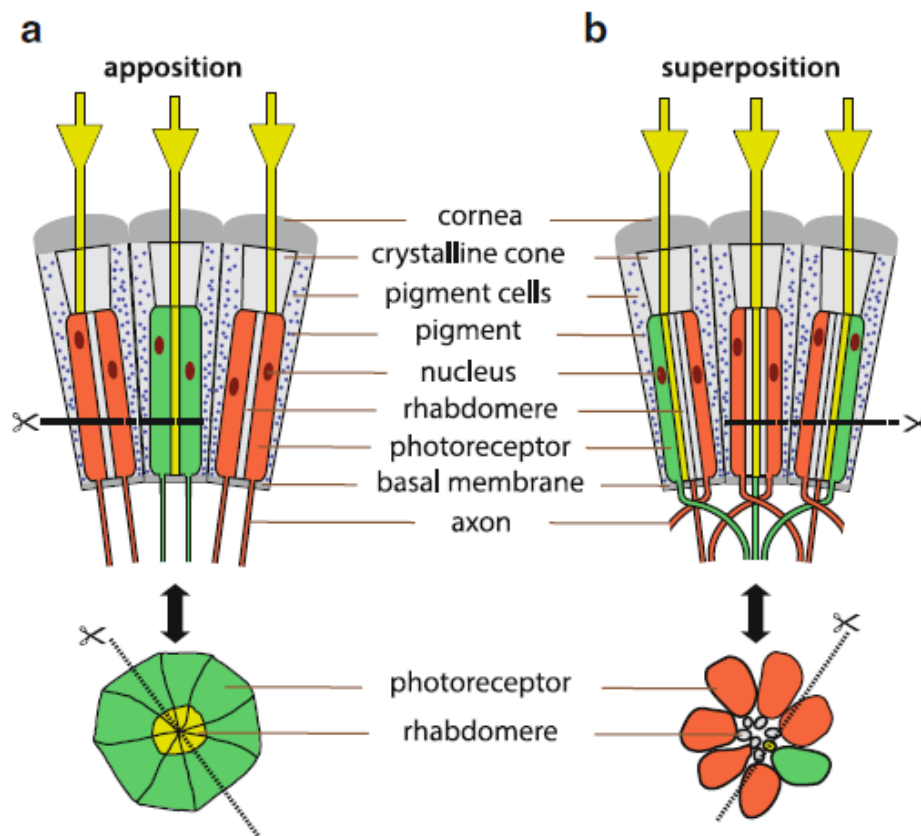
Figure 6. Scheme of apposition and neural superposition eyes (shown in two dissection planes). Rhabdomeres are shown in yellow when activated and in gray when inactivated; activated somata and axons are shown in green, inactivated in orange. (a) In apposition eyes (e.g., of honeybees), the rhabdomeres of all photoreceptors are fused, leading to combined activation of all photoreceptors of one ommatidium. (b) In neural superposition eyes of flies, activation is restricted to individual photoreceptors. Photoreceptors signals from different ommatidia are combined post-synaptically. Photoreceptor R8 is not shown, because it is located underneath R7 and both photoreceptors form the central rhabdomere of the ommatidium (Kretzberg and Ernst, 2013).

3. The case of honeybee

3.1 The peripheral visual system: photoreceptors in the compound eyes

Honeybees possess compound eyes of the apposition type (Fig. 6a). Each compound eye of a worker bee comprises approximately 5500 ommatidia, which are the modular anatomical structures and functional units of compound eyes (Gribakin, 1975). Anatomically, each ommatidium is an elongated structure, equipped with a transparent cuticular lens covering a conic crystalline. The crystalline is surrounded by principal pigment cells, which shield light diffusion across ommatidia while guiding it towards the underlying photoreceptor cells. Each ommatidium is equipped with nine photoreceptor cells, R1-9. In the proximal portion of the ommatidia, photoreceptor cells are elongated and isolated from one another by glial and pigment cells and project to second order neurons in the optic lobes, the primary visual regions in the bee brain (Varela and Porter, 1969).

The photoreceptors R1-8 contribute the microvilli to the entire length of the rhabdom while the R9 photoreceptor, located close to the basal membrane, contributes microvilli only at the base of the ommatidium (Wakakuwa et al., 2005). Towards the center of each ommatidium, photoreceptor cells extend a dense array of microvilli, forming together an ordered structure known as the rhabdom (Fig. 7), with each microvillar contribution by a given photoreceptor cell being termed rhabdomere. Rhabdomeres contain densely packed opsins, which are members of the rhodopsin family of the superfamily of G-protein-coupled receptors (GPCRs), coupled to Vitamin A-derived chromophores, thus forming visual pigments that are light sensitive (Brody and Cravchik, 2000; Hill et al., 2002). While the main chromophore of both vertebrates and insects is retinal, the aldehyde of vitamin A1, many insect species such as flies and butterflies, have a different chromophore called 3-hydroxy-retinal, the aldehyde of vitamin A3 (Vogt, 1989). These visual pigments mediate the first step in the visual signaling pathway, the conversion of light into an electrical response (Henze et al., 2012), a process termed phototransduction.

3.2. The phototransduction process

As mentioned above, the light-sensitive pigment molecules are densely packed in the microvilli of rhabdomeres. Rhabdomeres act, therefore, as the place to stock opsins at high density and as a light-guide, conveying the incident light along their axis. Upon capturing a photon, the chromophore of the rhodopsin molecule undergoes isomerization from the 11-*cis* to the all-*trans*

form. This transition is accompanied by a conformational change of the protein, from rhodopsin to meta-rhodopsin (Fain et al., 2010). In vertebrates, meta-rhodopsin is degraded and separated into the opsin and the chromophore. Yet, in insects, meta-rhodopsin is stable and, without separation of the opsin and the chromophore, can reconvert into the resting state upon absorption of a photon of another wavelength (Kretzberg and Ernst, 2013). When considering the peak wavelength of rhodopsin absorption spectra, a large range is found, from 320 up to 600 nm, depending on the insect species. In most cases, the rhodopsin and the meta-rhodopsin forms differ in their absorption spectra (Stavenga, 1992; Warrant and Nilsson, 2006).

In *Drosophila*, where the steps of phototransduction have been well characterized (Hardie and Raghu, 2001), after absorption of a photon, rhodopsin turns into metarhodopsin and activates a trimeric G-protein. This leads to dissociation of an active GTP-bound Gα subunit of the G-protein. In turn, Gα activates a phospholipase C (PLC), which cleaves phosphatidyl inositol (PIP_2) to generate diacylglycerol (DAG) and inositol-3-phosphate (IP_3) (Hardie and Raghu, 2001; Borst, 2009). Subsequent intermediates lead to the opening of calcium-permeable channels, which results in calcium influx and concomitant depolarization of the photoreceptor.

Opsins are proteins formed from amino acids. The physico-chemical properties of the chromophore may be modified, based on slight changes in amino acid composition. Photoreceptors differ in spectral sensitivity, precisely because the opsins they contain in their corresponding rhabdomeres differ in their amino acid composition (Shichida and Matsuyama, 2009). Thus, by providing a different opsin to the retinal, light of different wavelengths or colors can be sensed by different photoreceptor types. Small changes near the chromophore are enough to change the absorbance maxima of a photoreceptor.
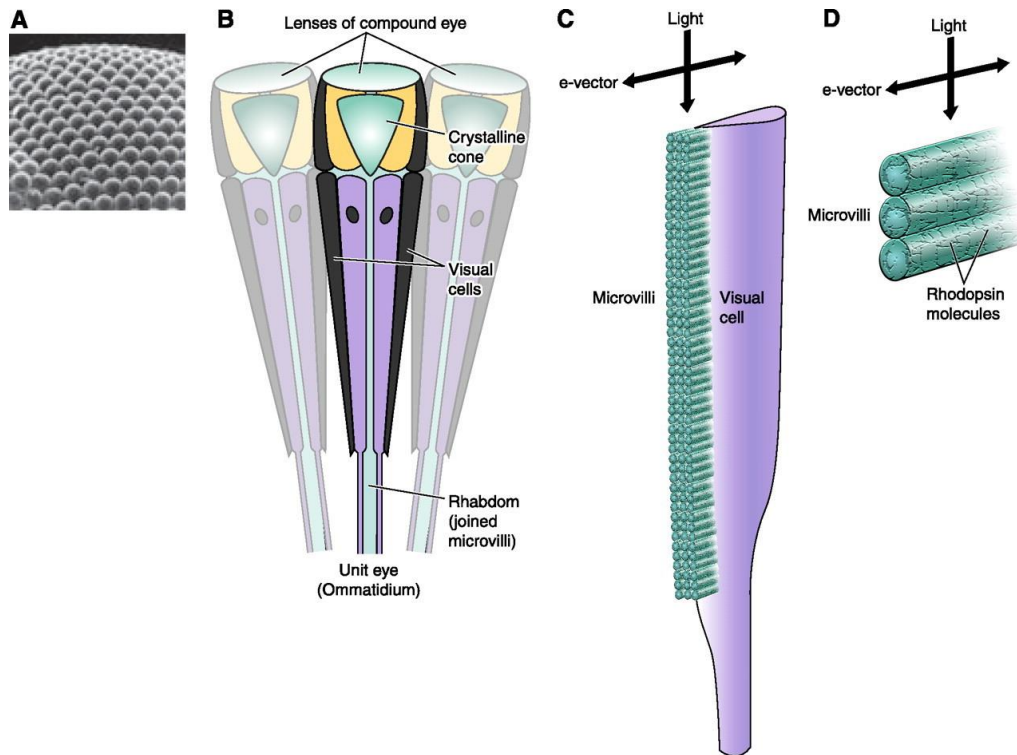
Figure 7. Schematic illustration of the compound insect eye. A: compound eye surface, showing the facet lenses. **B:** longitudinal cross section of an ommatidium. **C:** structure of one of the photoreceptor cells within an ommatidium, showing the microvilli, containing the photopigment that contributes to the structure of the rhabdom. **D:** detail of microvillar structure, illustrating the location and inferred alignment of the photopigment (rhodopsin) molecules. (Srinivasan, 2011)
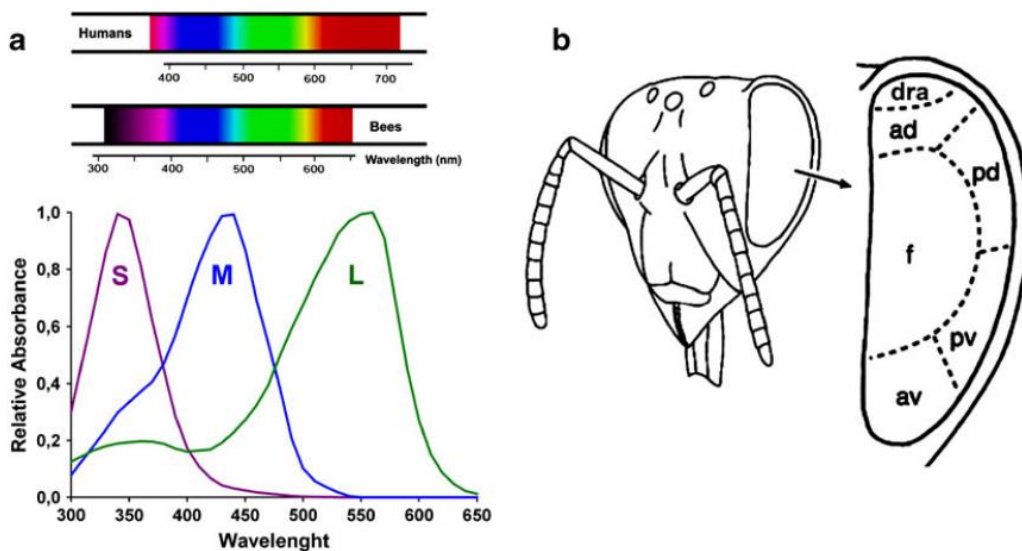
Figure 8. The compound eye and the photoreceptors in the bee retina (Avarguès-Weber et al., 2012). **a)** The spectral range of honey bee vision is shifted toward the ultraviolet when compared to that of humans. Three types of photoreceptors, S, M, and L (for short-, mid-, and long-range wavelength) peaking in the UV, blue and green regions of the spectrum, respectively, have been identified in the honey bee retina (Peitsch et al., 1992). **b)** The compound eye of Apis mellifera and its different eye regions (Wakakuwa et al., 2005): dorsal rim area (dra), anterior dorsal (ad), posterior dorsal (pd), frontal (f), anterior ventral (av), posterior ventral (pv).

Honey bees have trichromatic color vision, just as we do, although their visible spectrum is

shifted towards shorter wavelengths compared to ours, as they see from the UV region to the orange region of the spectrum (Menzel, 1979). Red colors are achromatic to them. Their color vision is based on the existence of three types of photoreceptors, tuned to detect short (S, UV), medium (M, blue) and long (L, green) wavelengths (Fig. 8). These photoreceptors have sensitivities peaking in the UV, blue and green parts of the spectrum; they are termed S (short-wavelength sensitive, λ_{max} = 344 nm), M (middle-wavelength sensitive, λ = 436 nm) and L (long-wavelength sensitive; λ_{max} = 544 nm) receptor types, respectively (Menzel and Backhaus, 1991; Wakakuwa et al., 2005), although they are commonly called UV, blue and green receptor types. While all three types of receptors contribute to color coding, the achromatic dimension of luminance is predominantly mediated by the latter, i.e., the L-receptor type (Srinivasan and Lehrer, 1988; Giurfa et al., 1996). This mechanism of luminance encoding relies on a single photoreceptor channel and differs therefore from the summation mechanism involving the signals of all three photoreceptor types present in humans. Summation at the level of "brightness neurons" is what confers our ability to distinguish surfaces differing in light intensity or luminance (white-black scale). In the case of bees, the proposed mechanism is the quantification of light intensity at the level of higher-order neurons receiving exclusive input from L-receptors. These neurons do not perceive color (i.e. no green color sensation), as color opponent neurons are required; they simply quantify luminance differences, thus providing an achromatic evaluation channel (Giurfa et al., 1996).

Early evidence suggested that photoreceptors might not have an even distribution across the retina (Gribakin, 1975). Menzel and Snyder (Menzel and Snyder, 1974) used an electrophysiological approach to characterize photoreceptor responses in ommatidia of the bee compound eyes and showed that green sensitive (G or L) photoreceptor cells were the majority within individual ommatidia, while blue sensitive (B or M) and ultraviolet-sensitive (UV or S) cells were rare. While L- and M- receptors showed little polarized light sensitivity, S receptors were the only ones showing polarized light sensitivity, in particular the ninth photoreceptor type, which is located deeper in the ommatidia, close to the basal membrane, and whose chromatic sensitivity remains obscure, even if Menzel and Snyder (1974) suggested that it is a UV receptor, based on its polarization sensitivity. Further investigation showed that polarized light detection

mainly happens in specialized ommatidia located in the most dorsal part of the compound eye, the dorsal rim area (DRA), which has the particularity of presenting photoreceptors with no twist along the photoreceptor longitudinal axis, thus allowing consistent responses to specific directions of polarized light vibration. Beyond the DRA, photoreceptors twist all along their longitudinal axis, thus canceling responses to specific directions of polarized light vibration (Labhart and Meyer, 1999; Wehner and Labhart, 2006).

The predominant view arising from these studies, based on electrophysiological analyses of photoreceptor responses within ommatidia of the bee compound eye, was that they were relatively homogeneous in their photoreceptor composition. Except for the DRA, exhibiting a high presence of S-photoreceptors for skylight processing, the rest of the compound eye was thought to have ommatidia integrated by 4 L, 2 M and 2 S photoreceptors; the ninth photoreceptor was also thought to be sensitive to UV light, as mentioned above, and thus belonging to the S-receptor class.

Yet subsequent *in situ* hybridization experiments (Wakakuwa et al., 2005), which attempted to characterize precisely the nature of the photoreceptors present within single ommatidia of the compound eye of bees, corrected this long-standing view. This study targeted the three types of opsins known for the honey bee at that time and revealed the existence of three types of ommatidia: type 1 including 1 UV + 1 B + 6 G receptors, type 2 including 2 UV + 6 G receptors and type 3 including 2 B + 6 G receptors. The opsin type of the ninth receptor could not be clearly identified in these *in situ* hybridization studies. Although Menzel and Snyder (Menzel and Snyder, 1974) assumed that it was likely to be a UV receptor (see above), Wakakuwa et al. (2005) could neither label it with the UV nor with the B probe, suggesting that it could instead be a G receptor, although this point remains to be determined. Concerning the distribution of the ommatidial types across the different regions of the compound eye, they are relatively homogeneous, although with a higher percentage of UV receptors in the dorsal rim area and of the blue receptors in the anterior ventral region. This distribution possibly evolved to better cope with sky (polarized light) and ground (colored flowers and contrasted objects) information (Wakakuwa et al., 2005). It is particularly notable that the number of L receptors is larger than what was originally assumed (6 per ommatidium instead of 4); this underlines the importance of the L channel not only for chromatic vision but also for achromatic vision. In particular, numerous studies (Lehrer et al., 1990; Si et al., 2003) have indicated that movement perception and parallax contrasts occur via the L channel.

3.3 From photoreceptors to the primary visual neuropils in the bee brain

The bee retina appears therefore as a random mesh of photoreceptor classes whose axons project to the visual neuropils or optic lobes of the bee brain. These optic lobes are organized sequentially and are termed the lamina, the medulla and the lobula (Fig. 9). From there, information is conveyed to higher-order centers such as the central complex and the mushroom bodies.
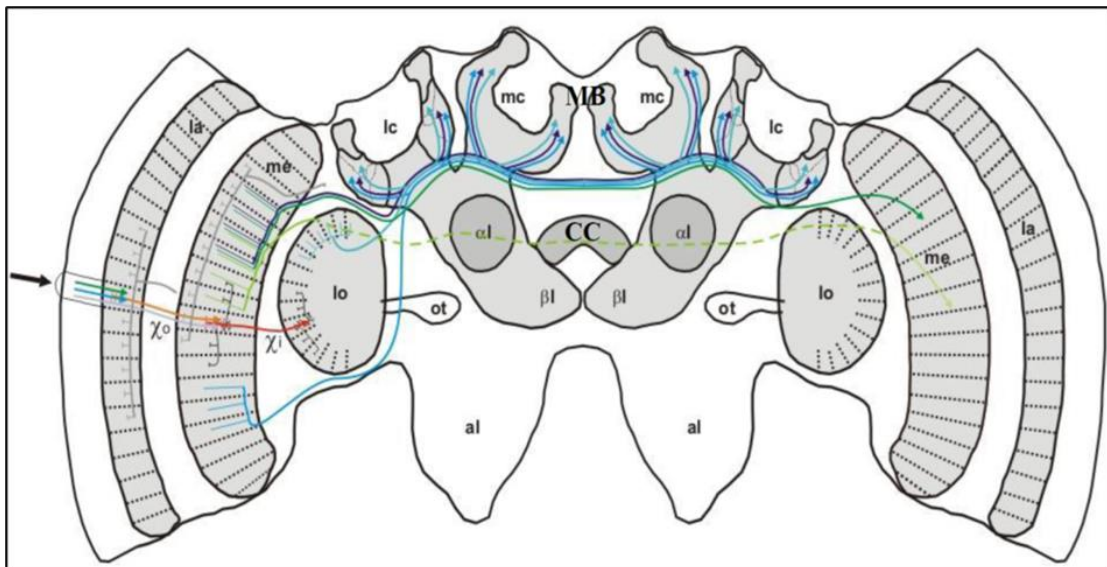
.
Figure 9. The different visual neuronal populations and pathways of the honeybee brain. The black arrow indicates color stimulation. La = lamina, χo = outer chiasm, me = medulla, χl = inner chiasm, lo = lobula, le = lateral calyx of the mushroom bodies, me = median calyx, α = alpha-lobe, β = beta-lobe, al = antennal lobe, ot = anterior optic tuberculum. MB: mushroom bodies; CC: central complex. Courtesy of M. Giurfa

3.3.1. The lamina

The lamina is the first visual center, where the axons of photoreceptor cells are connected to first-order processing interneurons, the lamina monopolar cells (LMC) (Fig. 9). It is structured in modular cartridges, each corresponding to one ommatidium. Each cartridge is crossed by the axons of the 9 photoreceptors of the corresponding ommatidium. In insects with fused rhabdoms, all the photoreceptor axons of one ommatidium project to the same synaptic region (the cartridge) in the first optic ganglion (the lamina), where they synapse with the first interneurons (Menzel and

Snyder, 1974). The lamina consists of thousands of optical columns, each receiving an axon bundle from the overlying ommatidium, as well as the axons of four different types of monopolar cells (Mota et al., 2011). Additionally, tangential, centrifugal and horizontal fibers can be found within each cartridge. The spatial arrangement of photoreceptor axons and the lamina monopolar cells within a cartridge remain constant throughout the lamina, thus retaining the retinotopic organization (Avargues-Weber et al., 2012).

3.3.2. The medulla

A structure called the outer chiasm forms the connection between the lamina and the second visual neuropile, the *medulla*. Fiber bundles in the outer chiasm cross horizontally, i.e., fibers coming from the anterior part of the lamina project to the posterior medulla, while posterior fibers from the lamina project to the anterior medulla. The second visual neuropil is the medulla, a structure that contains most of the neurons of the bee visual system. Axons from lamina monopolar cells and S- M- photoreceptors (that bypass the lamina) proceed to the medulla by way of the outer chiasm that forms the connection between the lamina and medulla (Ribi and Scheel, 1981). Fibers coming from the anterior part of the lamina project to the posterior medulla, while posterior fibers from the lamina project to the anterior medulla. Thus, a reversed (anteroposterior) retinotopic representation of the visual input is found at this level (Mota et al., 2011). Many horizontal fibers (serotoninergic or GABAergic) are in the medulla, in contrast to the few horizontal connections in the lamina (Rehder et al., 1987). Neurons in the distal medulla respond with spectral opponency (Kien and Menzel, 1977). Two types of color opponency were characterized by means of electrophysiological recordings: S+M-L- & S+M-L+ and their mirror image forms S-M+L+ & S-M+L- (Kien and Menzel, 1977). These two types have been the basis of opposing models of color vision (Menzel and Backhaus, 1991), which ignored the existence of other types of opponent neurons that have been reported (Hertel, 1980; Hertel et al., 1987; Hertel and Maronde, 1987; Yang et al., 2004). So that although neural opponency clearly exists in the central visual system, the types and number of opponent neuron types remain unclear.

3.3.3. The lobula

The third visual neuropil is the lobula, where the columnar stratification and the retinotopic

organization are preserved, mainly in the outer part (Hertel and Maronde, 1987; Hertel et al. 1987). An internal chiasm forms the junction between the medulla and the lobula, so that the retinotopical organization reverses again. Chromatic properties of neurons in the medulla are preserved and amplified in the lobula, which was also shown to contain distinct color-opponent neurons (Kien and Menzel, 1977; Hertel and Maronde, 1987). Furthermore, different types of contralateral spatial neurons have been described in the lobula (Hertel and Maronde, 1987).

In vivo intracellular recordings from 105 morphologically identified neurons in the lobula of bumblebees (*Bombus impatiens*) (Fig. 10) (Paulk et al., 2008) show that these cells have anatomically segregated dendritic inputs confined to one or two of the six lobula layers. Lobula neurons exhibit physiological characteristics common to their respective input layer. Cells with arborizations in layers 1–4 are generally indifferent to color but sensitive to motion, whereas layer 5–6 neurons often respond to both color and motion cues (Paulk et al., 2008). Furthermore, the temporal characteristics of these responses differ systematically with dendritic branching patterns. Some layers are more temporally precise, whereas others are less precise but more reliable across trials. Because different layers send projections to different regions of the central brain, these results show that the anatomical layers of the lobula are the structural basis for segregation of visual information into color, motion and stimulus timing (Paulk et al., 2008).

Different pathways connect the visual lobes to higher-order centers such as the mushroom bodies, involved in multimodal sensory integration and cognitive phenomena (Menzel, 1999; Giurfa, 2007), and to the central complex. These regions are reviewed briefly below, with respect to visual processing.
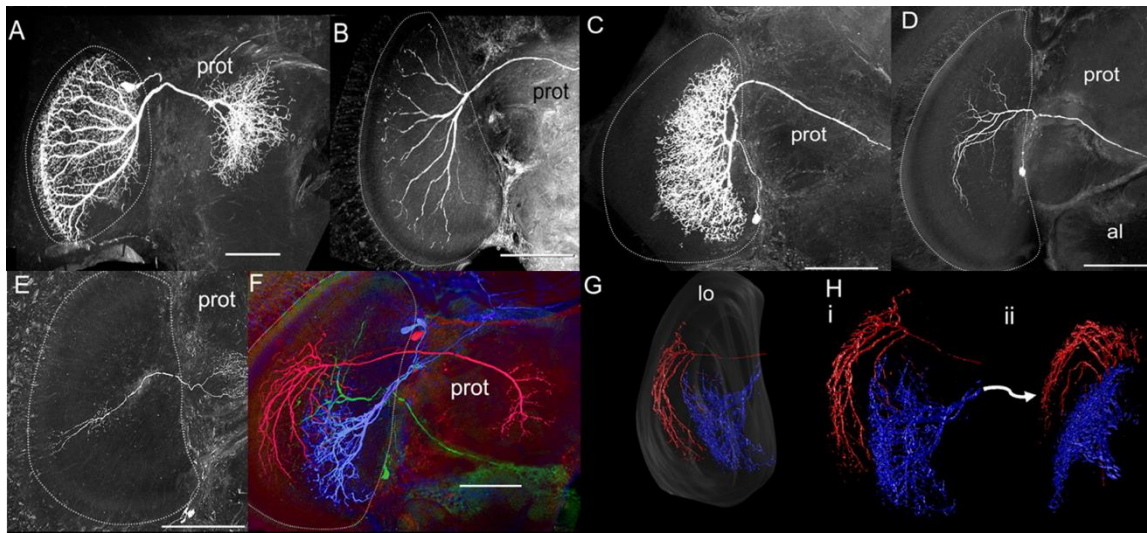
Figure 10. Lobula neuron morphology (Paulk et al., 2008). A, B, Reconstructed layer 1–4 neurons filled with fluorescent dye. Note that the neurons project to the rim of the lobula and have highly regular projections. C, D, Reconstructed layer 5–6 neurons. These neurons do not project to the rim of the lobula and have less regular branching patterns. E, an example of the six recorded and filled columnar neurons. F, Multiple neurons filled in the same brain. The blue- and green-labeled neurons project to layers 5 and 6, whereas the red-labeled neuron projects to layers 3 and 4. G, H, some of these neurons were reconstructed in three dimensions to examine their branching pattern relationships to the layers. Note how the layer 1–4 neuron (red) forms a rim around the layer 5–6 neuron (blue). A–F, the lobula is outlined with white dotted line. Scale bars, 100 µm.

3.4 Higher-order processing of color information in the bee brain

3.4.1 Central complex (CX)

The photoreceptors in the DRA terminate in the lamina or the medulla in the optic lobe, and, from there, polarized light signals primarily project into the central complex through a pathway involving the lower unit of the anterior optic tubercle and lower division of the central body (Homberg, 2008). The central complex, one of the higher centers of the insect brain, is considered to host an internal navigation compass, in particular for polarized light available in the sky, although it is still unclear how it controls the animal's steering during navigation (Heinze, 2017; Homberg et al., 2011).

The central complex mainly receives indirect visual input (Pfeiffer and Homberg, 2014). Two parallel visual pathways have been identified in locusts (Homberg et al., 2003; Pfeiffer et al., 2005), bees (Mota et al., 2011; Pfeiffer and Kinoshita, 2012) and butterflies (Heinze et al., 2013). The anterior pathway originates in the visual neuropils and does not directly enter the lower division of the central body lower (CBL), but enters indirectly via the anterior lobe of the lobula, the anterior optic tubercle and the median and lateral bulb (Fig. 11). In the locust polarized light input is conveyed to the CX via this pathway, and this is assumed to be the case for bees and butterflies as well (Mota et al., 2011; Pfeiffer and Kinoshita, 2012; Heinze et al., 2013).
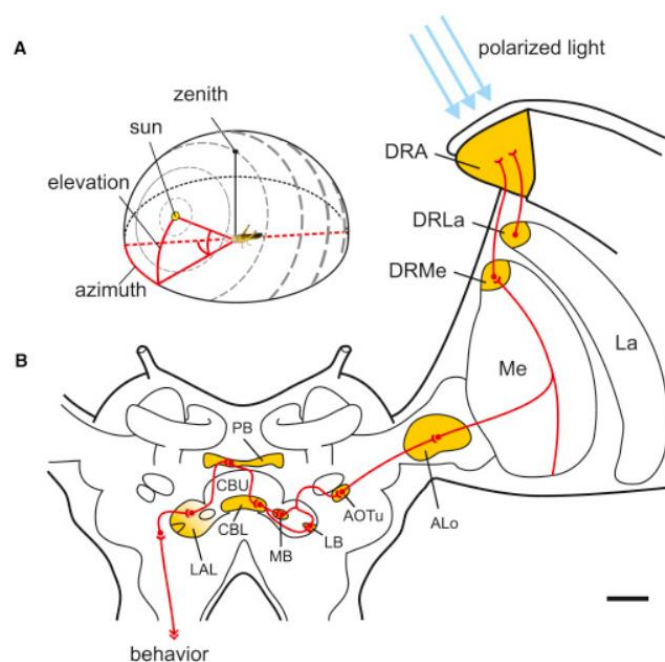
Figure 11. Polarization Pattern in the Sky, Polarization Vision Pathways in the Locust Brain (Bech et al., 2014) (A) The planes of polarization in the sky (gray bars) are oriented perpendicularly to the solar position and thus form concentric circles around the sun. Degrees of polarization are indicated by the thickness of the bars. The position of the sun is defined by its elevation (vertical component) and its azimuth (horizontal component). (B) Frontal schematic view of the brain of Schistocerca gregaria showing the polarization-vision pathway (red). Polarized light is perceived by the dorsal rim area (DRA) of the compound eye. Subsequently, polarized-light information passes the dorsal rim areas of the lamina (DRLa) and medulla (DRMe), the anterior lobe of the lobula (ALo), the lower unit of the anterior optic tubercle (AOTu), the lateral bulb (LB), and medial bulb (MB) near the lateral accessory lobe (LAL) and is, finally, processed in the central complex, consisting of the protocerebral bridge (PB) and the upper (CBU) and lower (CBL) divisions of the central body. Output neurons of the central complex transmit polarized-light information to descending neurons, which contribute to appropriate orientation behavior. La, lamina; Me, medulla. Scale bar, 200 μm.

Other functions have been ascribed to the central complex, such as being the site for short-term visual memories (Liu et al., 2006) and for mediating path integration in Drosophila (Neuser et al., 2008). Its role in visual information processing for the sake of orientation, navigation and different forms of spatial learning (Ofstad et al., 2011) seems to be clear in several insect species

(Honkanen et al., 2019).

3.4.2 Mushroom bodies

Mushroom bodies are central, prominent structures occupying approximately one-third of the brain (see Fig. 9). Each mushroom body consists of approximately 170,000 tightly packed neurons, the Kenyon cells, and consists of two subunits, a lateral and a median calyx. The calyces constitute the input region of the mushroom bodies. Each calyx is subdivided into three regions: the lip, the collar and the basal ring. Each region receives a specific sensory input: the lip, olfactory input, the collar, visual input and the basal ring, olfactory and mechanosensory input (Mobbs, 1982). Visual input neurons connecting to the collar of the mushroom bodies are divided into medulla-mushroom body neurons and lobula-mushroom body neurons, which are segregated in the calyx (Mobbs, 1984; Gronenberg, 2001; Ehmer and Gronenberg, 2002).

The output regions of the mushroom bodies are in the alpha- and beta-lobes, which are structures resulting from the fusion of both the median and the lateral calyces. The output neurons respond to different kinds of sensory stimulation (Grünewald, 1999). As the input is sensory-specific and separated by modality, while the output is not, the mushroom bodies are centers in which sensory integration has to take place. In other words, they are a potential substrate for transfer between different sensory modalities and for complex, non-elemental forms of learning. The mushroom bodies are intimately related to olfactory learning and memory (Menzel, 1999; Giurfa and Sandoz, 2012). Their connectivity allows one to suppose that the same kind of involvement could exist for visual learning and memory, but experiments addressing this point are missing. This may be due to the fact that visual learning has been traditionally studied in free-flying bees, thus precluding parallel access to neural supports mediating this capacity.

Mushroom bodies increase their volume in honey bee foragers, a variation that has been related to the needs imposed by spatial learning and navigation (Withers et al., 1993). The necessity of mushroom bodies for navigation tasks has been recently shown by two studies performed in ants (Buehlmann et al., 2020; Kamhi et al., 2020). In one case, ants with anesthetized vertical lobes, by means of procaine injections, cannot retrieve familiar visual landmark memories to navigate home (Kamhi et al., 2020). In the other case, using similar methods, it was shown that mushroom bodies are required for visual navigation to a learned location, but not for innate orientation toward

a visual cue. The dissociation between innate and learned visual responses provides direct evidence for a specific role of mushroom bodies in navigational memory in ants (Buehlmann et al., 2020). However, spatial learning and navigation could be only a small fraction of a more general function, which could be supporting complex forms of learning, including visual ones.

4. The advent of the honey bee genome

In 2002, the honey bee *Apis mellifera* was selected by the NIH's National Human Genome Research Institute to be among the organisms with a sequenced genome (Check, 2002). Apis mellifera was the third insect to have its genome sequenced (after the fruit fly *Drosophila melanogaster* and the malaria vector mosquito *Anopheles gambiae*) (Robinson, 2002).

In 2006, the sequence of the Honey Bee Genome based on whole-genome shotgun sequencing with Sanger technology was published (Weinstock and Robinson, 2006), thus opening a series of new perspectives for understanding functional and mechanistic aspects of bee behavior. For instance, bee researchers can directly query single nucleotide polymorphisms (Whitfield et al. 2006, Zayed and Whitfield 2008) and carry out molecular evolution analyses on interesting genes (Fig. 12) (Harpur and Zayed, 2013; Hasselmann et al., 2008; Kent et al., 2011).
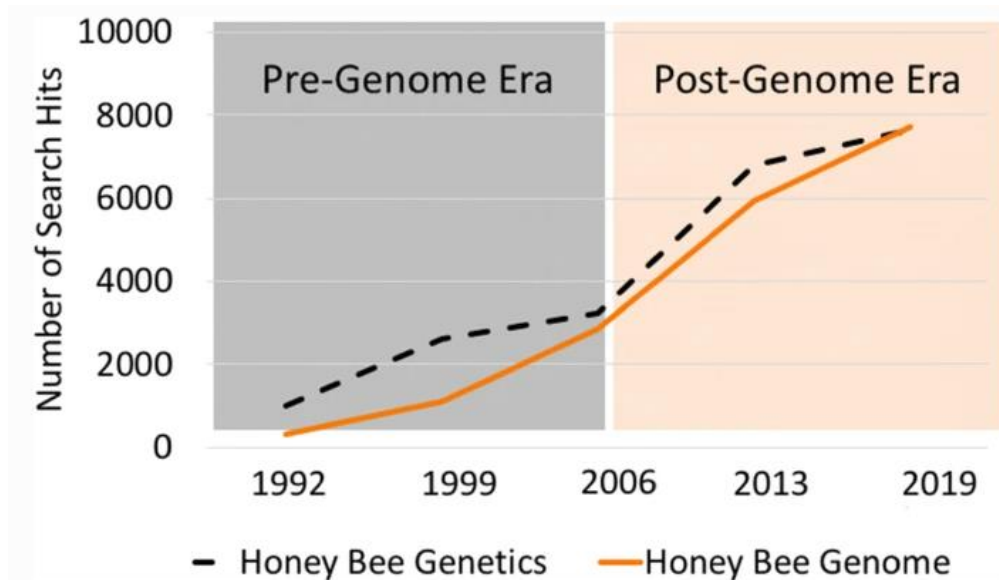
Figure 12. Research on both honey bee genetics and genomics has grown in the past three decades. The honey bee genome's publication in 2006 has fueled an increase in molecular studies (as determined by a number of search hits on Google Scholar within a given publication year). In fact, studies that incorporate genomics have recently overtaken studies that mention only "genetics", demonstrating that the honey bee genome has become an integral part of honey bee research (Toth and Zayed, 2021).

Many transcriptomic studies are based on honey bee genome-derived gene sequence information. For example, researchers conducted large-scale transcriptomic profiling of selected regions of the central nervous system (CNS) across three species of dancing honey bees, in order to determine the extent of regional specialization in gene expression and to explore the molecular basis of dance communication. The results of this analysis showed brain region-specific gene expression in dancing *Apis mellifera*, *A. florea* and *A. dorsata*, which differed greatly in aspects of their dance behavior (Sarma et al., 2009). In addition, regions of the honey bee brain involved in visual processing and learning and memory, were found to have a specific genomic response to distance information (Sen Sarma et al., 2010). With the help of transcriptomic studies, one study also showed that miRNAs are substantially different between the foraging and dancing stages, and suggest that miRNAs might play important roles in regulating dancing behaviors in honey bees (Li et al., 2012).

Other studies have focused on Immediate Early Genes (IEG) in the bee brain, as these genes are considered as neural activity markers (see below). For instance, IEG expression was analyzed in response to isopentyl acetate (IPA), a releaser pheromone that communicates alarm in honey bees. Exposure to IPA affected behavioral responsiveness to subsequent exposures to IPA and induced the expression of the immediate early gene and transcription factor *c-Jun* in the antennal lobes (Alaux and Robinson, 2007).

Most studies on IEG expression in brain areas of the honey bee have been performed in broader foraging and navigation contexts (see below for examples), thus trying to correlate changes in IEG expression with changes in foraging behavior, orientation close to the hive or circadian rhythms (Lutz and Robinson, 2013; Shah et al., 2018; Singh et al., 2018; Ugajin et al., 2018; Iino et al., 2020).

Interestingly, no study has been performed up to now in which similar analyses at a molecular scale are performed in the framework of controlled laboratory protocols for the analysis of visual learning. Despite the fact that such protocols exist and could be easily coupled to molecular approaches, such as the ones mentioned above, no attempt to link genomic signatures and visual learning and memory has been undertaken in controlled laboratory conditions.

The Honey Bee Genome Sequencing also enabled new approaches for gene disruption via the

development of tools such as RNAi or CRISPR/Cas9 knockout, which allow one to confirm directly causal relationships between genes and phenotypes.

In the following sections, I will focus on the molecular approaches that I have implemented in my work to answer questions related to visual learning and visual processing in honey bees. Having explained these approaches, I will outline the questions at the origin of my thesis and the goals of my PhD work.

4.1 IEG expression in the bee brain

One way to detect activated brain regions and neural pathways is the quantification of the expression of IEGs in neural tissues (Clayton, 2000). IEGs are transcribed transiently and rapidly in response to specific stimulation inducing neural activity without *de novo* protein synthesis (Bahrami and Drablos, 2016). In mammals, IEGs such as *c-fos, zif268* and *Arc* are regularly used as markers of neural activity during learning, memory and other forms of cellular plasticity such as long-term potentiation (Gallo et al., 2018; He et al., 2019; Minatohara et al., 2015). In insects, the use of IEGs as neural markers is less expanded, as the number of candidate genes serving this goal is still reduced and the reliable detection of their expression is sometimes difficult (Sommerlandt et al., 2019). Besides research using IEGS to quantify neural activation in response to olfactory stimuli (e.g. Alaux and Robinson, 2007, see above), three of the IEGs reported for the honey bee are interesting, as they have been related to a foraging context in which visual learning may play a fundamental role. The first one, termed *Kakusei* (which means "awakening" in Japanese) is a nuclear non-coding RNA transiently and strongly induced in the brain of European worker bees, by seizures occurring upon awakening from anesthesia (Kiya et al., 2007). It is also activated after the experience of dancing in the hive, following a foraging flight, and in pollen foragers, so that it seems related to the neural excitation resulting from foraging activities (Kiya and Kubo, 2011). This IEG is activated within a subtype of Kenyon cells, the constitutive neurons of the mushroom bodies, which are a higher-order center in the insect brain (Kiya et al., 2008). A second IEG is the hormone receptor 38 gene (*Hr38*), which is a transcription factor conserved among insects and other species including humans (Fujita et al., 2013), and which is upregulated by foraging experiences in honey bees (Singh et al., 2018) and bumblebees (Iino et al., 2020), and

by orientation activities upon hive displacement (Ugajin et al., 2018). Consequently, a role for this IEG in honey bee learning and memory has been proposed but not demonstrated so far (Iino et al., 2020; Singh et al., 2018). The third gene is the early growth response gene-1 (*Egr1*), whose expression is induced in the brain of honey bees and bumble bees upon foraging (Iino et al., 2020; Singh et al., 2018) and orientation flights (Lutz and Robinson, 2013), and which seems to be controlled by circadian timing of foraging (Shah et al., 2018). This gene has received several names (e.g., *ngf1-a, zif268, krox-24* and *zenk*), thus rendering its homology with respect to equivalent genes in *Drosophila* difficult. Yet, it seems that *Egr-1* is a homologue of the Drosophila *stripe* (*str*). Given its implication in a foraging context, a role in learning and memory is also presumed. However, none of these IEGs has been studied so far in the context of controlled protocols for associative learning and memory formation in the honey bee.

4.2 CRISPR/Cas9, a novel technique for gene knock-out in honey bees

4.2.1 CRISPR/Cas9 system

CRISPR (clustered regularly interspaced short palindromic repeats)/Cas adaptive immune system was first discovered in Bacteria and Archaea (Ishino et al., 1987; Jansen et al., 2002). Compared to zinc finger nucleases (ZFNs) and transcription activator-like effector nucleases (TALENs) that rely on protein-based systems with DNA-binding specificities, the CRISPR/Cas system uses RNA as the moiety that targets the nuclease to a desired DNA sequence (Sander and Joung, 2014). The ease of designing and generating these reagents at the bench, has opened the door for studies on gene function in many organisms. Since the CRIPSR/Cas9 system was shown to cut foreign DNAs *in vitro* and induce a double-strand break (DSB) in target site in human and mouse cells (Jinek et al., 2012; Cong et al., 2013), this system has been successfully applied in many species, such as yeast (Tsarmpopoulos et al., 2016), the nematode *Caenorhabditis elegans* (Friedland et al., 2013), rats (Hu et al., 2013), *Drosophila* (Gratz et al., 2013), the silk worm *Bombyx mori* (Ma et al., 2014), zebrafish (Hwang et al., 2013), ants (Trible et al., 2017; Yan et al., 2017), honeybees (Kohno et al., 2016) and many plant species (Jiang et al., 2013).

The CRISPR-Cas system has three major types called type I, type II and type III CRISPR–Cas systems. Type II CRISPR-Cas system has been used widely in gene editing and genetic screening applications (Makarova et al., 2011; Tang and Fu, 2018). Typically, CRISPRs are preceded by a leader sequence (Fig. 13 black box) that is AT-rich but otherwise not conserved. The number of repeats can vary substantially, from a minimum of two to a few hundred.

Repeat length, however, is restricted to 23 to 50 nucleotides. Repeats are separated by similarly sized, non-repetitive spacers (Fig. 13 colored boxes) that share sequence identity with fragments of plasmids and bacteriophage genomes and specify the targets of CRISPR interference.
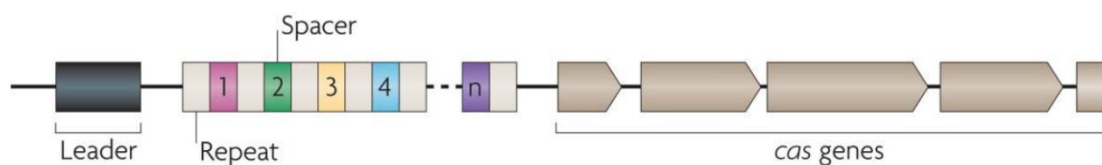
Figure 13. Features of CRISPR loci

A set of CRISPR-associated (*cas*) genes immediately precedes or follows the repeats. These genes are conserved, can be classified into different families and subtypes, and encode the protein machinery responsible for CRISPR activity (Marraffini and Sontheimer, 2010). CRISPR/Cas9-mediated adaptive immunity proceeds in three distinct stages: acquisition of foreign DNA, CRISPR RNA (crRNA) biogenesis, and target interference. The first stage is to identify the invading nucleic acid and scan the potential PAM (NGG sequence) of the exogenous DNA, and use the sequence adjacent to the PAM as a candidate protospacer (Fig. 14); then cut the invading nucleic acid to obtain a new spacer. These spacers form complexes with synthetic repeats at the 5' end of the CRISPR locus; they are finally integrated between the two repeats of CRISPR loci encoded in the bacterial genome (Makarova et al., 2011). In the second stage, when the phage invades the bacteria again, the CRISPR cluster is first transcribed into pre-crRNA, which is then gradually processed into small mature crRNA (Brouns et al., 2008). When the phage invades bacteria, it also promotes up-regulation of the CRISPR locus expression level (Lillestøl et al., 2009). In the third stage, the mature crRNA binds to the relevant Cas protein to form a crRNA-Cas protein complex, and then precisely binds to the target DNA through base complementation and PAM. Finally, the crRNA-Cas protein complex binds to the target site and degrades the target DNA (Marraffini, 2015; Wilkinson and Wiedenheft, 2014).
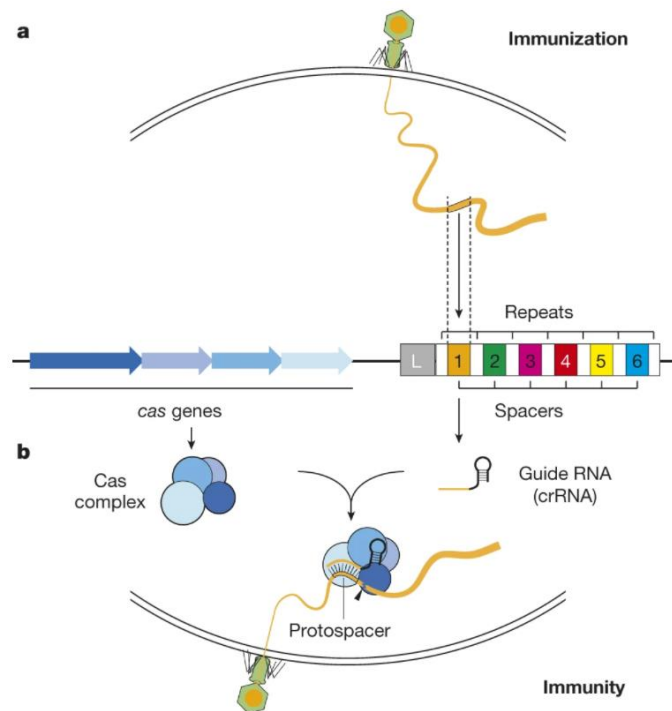
Figure 14. The principle of CRISPR/Cas9 (Marraffini, 2015). a, In the first stage, spacer sequences are captured upon entry of the foreign DNA into the cell and integrated into the first position of the CRISPR array. b, In the second and third immunity stage the spacer is used to target invading DNA that carries a cognate sequence for destruction. Spacers are transcribed and processed into small CRISPR RNAs (crRNAs) in the 'crRNA biogenesis' phase. These small RNAs act as antisense guides for Cas RNA-guided nucleases (which usually form a complex) that locate and cleave the target sequence (black arrowhead) in the invader's genome during the 'targeting' phase.

4.2.2 Gene editing in the honeybee

In the honey bee, there has been a lack of effective genetic tools (Robinson et al., 2000), which is probably related to the complexity of the reproductive cycle (female queens and workers are diploid, while male drones are haploids), and the impossibility of raising honey bees completely in the laboratory, without access to the external world. Although the new gene-editing tool technology, in particular, CRISPR/Cas9 has been used in many species, CRISPR/Cas9 research in honey bees faces two major difficulties. First, collecting honeybee embryos, in particular 2 hour old honeybee eggs, for microinjection constitutes a challenging task, given the highly aggressive behavior displayed by worker bees towards experimenters willing to collect honey bee eggs from the beehive. Then, the transfer of eggs can result in mortality or abnormal development, since eggs are not adaptable to harsh environments and are very sensitive to changes in temperature (Groh et

al., 2004). Moreover, the egg shell is thin and flexible, and it is difficult to manipulate when it sticks to the bottom of the cells. Even if the eggs can be taken out and transferred by an egg retrieval tool, it is difficult to guarantee a high hatching rate. Observing these unhatched bee eggs under a stereo microscope reveals that such handling may induce mechanical wounds on the surface of the eggs, which are invisible to the naked eye. However, gene editing requires collection of younger eggs, preferably within 2 hours. Thus, the difficulty is how to get eggs within 1.5 hours post oviposition. Forcing queen bees to lay eggs in a fixed area of the comb, by using a queen-limiting ovipositor, makes the colony irritable and prone to attack the experimenter. Moreover, the queen is reluctant to lay eggs in such an environment. Second, ensuring the transition from honey bee embryos to adults, is also a challenging task. Any manipulated honey bee embryo cannot be replaced back into the hive, because during close contact between eggs and larvae, nurses may detect perturbations in normal development and thus destroy the larvae or the treated eggs (Fahrbach and Robinson, 1995; Robinson et al., 1992). Although artificially rearing manipulated embryos is possible (Rembold and Lackner, 1981), there is no method available to rear fully functional reproductive queens outside a natural colony environment. Rearing manipulated honey bee embryos into worker bees implies a considerable workload, but so far, it is the only protocol that is currently possible (Büchler et al., 2013; Crailsheim et al., 2013; Kaftanoglu et al., 2010).

In the honeybee, the first report on genetic editing showed that the sperm-mediated transformation method allows one to introduce foreign DNA constructs into the bee genome (Robinson et al., 2000). Then, Schulte et al. reported on highly efficient integration and expression of piggyBac-derived cassettes that could be stably transmitted by certain queens (between 20 and 30 %) to their offspring (Schulte et al., 2014). The cassettes stably and efficiently expressed marker genes in progeny, under either an artificial or an endogenous promoter, which led the authors to suggest that this system could be used to inhibit gene functions through RNAi in specific tissues and developmental stages by using various promoters.

The first report of CRISPR/Cas9 used in honey bees was produced by the group of Takeo Kubo in 2016 (Kohno et al., 2016). To test the feasibility of the protocol in honeybees, the researchers selected target genes that were unlikely to affect honeybee development. A knock out of the *mrjp1* gene (*major royal jelly proteins*) was achieved by injecting sgRNA and Cas9 mRNA

into fertilized embryos. Then, the same group published another study using a CRISPR/Cas9 approach to knock out the *mKast* gene (*middle-type Kenyon cell-preferential arrestin-related protein*) in drones. This gene is preferentially expressed in a certain class of Kenyon cells (Class I), the constitutive neurons of the mushroom bodies (see above). The results showed that *mKast* is dispensable for normal development and sexual maturation in drone honeybees (Kohno and Kubo, 2018). Although the two studies showed successful knock out of the targeted genes, the gene editing rate was not very high (40% - 50%) (Kohno et al., 2016; Kohno and Kubo, 2018). Hu et al. (2019) improved CRISPR/Cas9 gene-editing efficiency to more than 70%, in a study that targeted the *Mrjp1* gene (see above) and the *Pax6* gene, a transcription factor involved in developmental processes.

The first morphological honey bee mutants induced via CRISPR/Cas9 showed that the response to nutrition relies on a genetic program that is switched "on" by the feminizer (*fem*) gene (Roth et al., 2019). Diploid mutant males can also be produced, by injecting the mixture of complementary sex determiner (*csd*) gene sgRNA and Cas9 protein into the fertilized honeybee eggs (Wang et al., 2021). In addition, the first visible homozygous mutant drones were produced by the CRISPR/Cas9 edited queen, in which the *Amyellow-y* gene, which controls melanin synthesis and thus eye/body pigmentation, was targeted. The results of this work showed that the second generation of mutant drones have a dramatic body pigmentation defect, visible to the naked eyes (Nie et al., 2021).

CRISPR/Cas9 has also been used recently in honey bees to check for the specificity of antibodies developed against the insect GABAA receptor subunit Resistance to Dieldrin (RDL) and a metabotropic glutamate receptor mGlutR1 (mGluRA) (Sinakevitch et al., 2020). The corresponding genes *Rdl* and *mGlutR1 w*ere knocked out by injecting corresponding CRISPR/Cas9 in the brain of adult honey bees via the ocellar tract. The distribution of the receptors was analyzed in honeybee brains 48h after injection. For both (anti-RDL and anti-mGlutR1), when the uptake of mGlutR1 CRISPR/Cas9 or RDL CRISPR/Cas9 was successful, the level of corresponding antibody staining was also reduced significantly, thus showing that the knock out procedure was successful (yet perfectible) in adult bees.

Sensory receptor genes have been recent targets of recent studies that used the CRISPR/Cas9 technology. The *AmGr3* gustatory receptor gene, which was originally described as a sugar

receptor based on its homology with *Drosophila* sweet-tastant receptors (Robertson and Wanner, 2006), was characterized combining CRISPR/Cas9, electrophysiology and behavioral studies (Değirmenci et al., 2020). It was shown that *AmGr3* is highly specific for fructose and besides gustatory detection could also participate in internal fructose sensing for metabolic needs. Another study targeted the *orco* gene, which is a conserved, canonical olfactory co-receptor gene accompanying olfactory receptor genes in olfactory neurons. This gene can have a neurodevelopmental function, in addition to its role in olfaction (Chen et al., 2021). The *orco*-gene mutants induced via CRISPR/Cas9 had significant changes at the level of the antennal lobe, the primary olfactory center of the insect brain. In this region, mutants exhibited fewer glomeruli (the functional units of the antennal lobe), smaller total volume of all the glomeruli, and higher mean individual glomerulus volume compared to wild-type controls. RNA-Sequencing revealed that *orco* knockout also caused differential expression of hundreds of genes in the antenna, including genes related to neural development and genes encoding odorant receptors but no other receptor types, thus showing an odor-specific knockout (Chen et al., 2021).

Overall, a dozen genes, including *mrjp1*, *mKast*, *pax6*, *doublesex*, *fruitless*, *feminizer*, *loc552773*, *csd*, *Rdl*, *mGlutR1*, *Amyellow*, *Amgr3* and *Orco*, have been knocked out using a CRISPR/Cas9 technology, showing thereby the suitability of this approach for the study of gene functions (Kohno et al., 2016; Kohno and Kubo, 2018; Hu et al., 2019; Roth et al., 2019; Sinakevitch et al., 2020; Değirmenci et al., 2020; Chen et al., 2021; Nie et al., 2021; Wang et al., 2021). So far, no study has focused on vision-related genes. Our goal was precisely to address the role of opsin genes (see above) *via* the CRISPR/Cas9 approach. As many of the cited studies lacked a behavioral phenotype, our goal was to induce opsin mutations and determine the effect of these mutations in controlled behavioral protocols for the study of visual perception and learning. To this end, we benefited from substantial developments achieved in our laboratory for the behavioral characterization of visually-related behaviors.

5. Behavioral protocols for the study of color vision and color learning in non-flying honeybees in laboratory conditions

Although it is well known that freely-flying honey bees learn efficiently color cues in discrimination problems of variable complexity (Avargues-Weber et al., 2011), traditional protocols for the study of visual abilities in honey bees cannot be used if CRISPR/Cas9 mutants have to be generated, for several reasons. First, if visually-related genes are targeted, it is highly probable that the generated mutants will not be able to fly properly and therefore will not visit the feeding place in which the training setup (for instance, a Y-maze) has been set. Training and testing with visual cues will be impossible in these conditions, as normal and regular free-flight between the hive and the experimental site is required. Second, if visually-related genes such as opsin genes are targeted, it will be impossible to determine if mutations occurred by simple external observation. Under these circumstances, losing an experimental bee, because it did not return to the training setup, will leave the experimenter with the unsolved question of whether the lost animal was a mutant or a wild type. Finally, and more importantly, genetically modified organisms cannot be used in conventional experiments on visual learning performed with free-flying bees, because of legal issues. Thus, other protocols are required, in which visual learning and visually-guided behaviors can be studied in animals that are either harnessed or enclosed, without escape possibilities in the laboratory.

In my work, I have used two such protocols. In one of them, bees learn to inhibit phototactic attraction induced by a colored light in a two-compartment enclosure, via the association of light with electric shock (Icarus protocol; Marchal et al., 2019). I used this protocol to test CRISPR/Cas9 opsin mutants. In another protocol, I studied IEG activation in the bee brain following different forms of color associative learning. In this case, I used a virtual reality (VR) setup in which tethered bees walking stationary on a treadmill, learn to respond to virtual color stimuli displayed in front of them, based on their different reinforcements (Geng et al., 2022; Lafon et al., 2022). These protocols are described below.

5.1 The ICARUS setup: learned phototactic inhibition in enclosed bees

Avoidance learning is a form of operant learning that allows animals to anticipate and elude noxious events in their environment (Krypotos et al., 2015; LeDoux et al., 2017). Several protocols have been conceived to study the animals' capacity to learn that the emission or omission of a specific behavior, results in the presence or absence of an aversive stimulus (typically an electric shock). In honey bees, a form of passive-avoidance learning can be studied using the Icarus setup and procedure (Marchal et al., 2019). In passive-avoidance learning, a specified response needs to be suppressed to avoid the delivery of a negative reinforcement, such as an electric shock (Venable and Kelly, 1990; Kaminsky et al., 2001). For instance, rats, which spontaneously avoid bright illuminated areas to seek refuge in dark compartments, learn that entering the dark compartment results in electric shock delivery. Learning results, therefore, in longer latencies to reenter the dark compartment, as the animal inhibits its spontaneous response. In bees, a similar principle was adopted by pairing the spontaneous attraction to light exhibited by bees in a dark compartment (Menzel and Greggers, 1985) with the delivery of an electric shock (Marchal et al., 2019). We thus established a learning paradigm in which bees learn to inhibit this spontaneous behavior based on punishing their phototactic responses. Bees are enclosed in a two-chamber compartment, connected via a small opening in the middle and presenting metallic grids on the floor and ceiling, thus allowing for the delivery of an electric shock to the walking animal commuting between the two compartments (Fig. 15). The height of the chambers is very small, so that animals can only walk within this setup. Surrounding lights allow illuminating or not the chambers, thereby inducing spontaneous phototaxis, which is paired, or not, with shock. Bees efficiently learn to inhibit their spontaneous attraction to the illuminated compartment and consequently increase their latency before reentering it during successive trials (Marchal et al., 2019) (Fig. 16). In my work, I have used this experimental setup to study the response of opsin-gene mutants generated via CRISPR/Cas 9 technology (Experimental Chapter 1). Moreover, I also contributed to an *ex vivo* analysis of aminergic gene expression in the bee brain following successful phototactic inhibitory learning (Appendix).
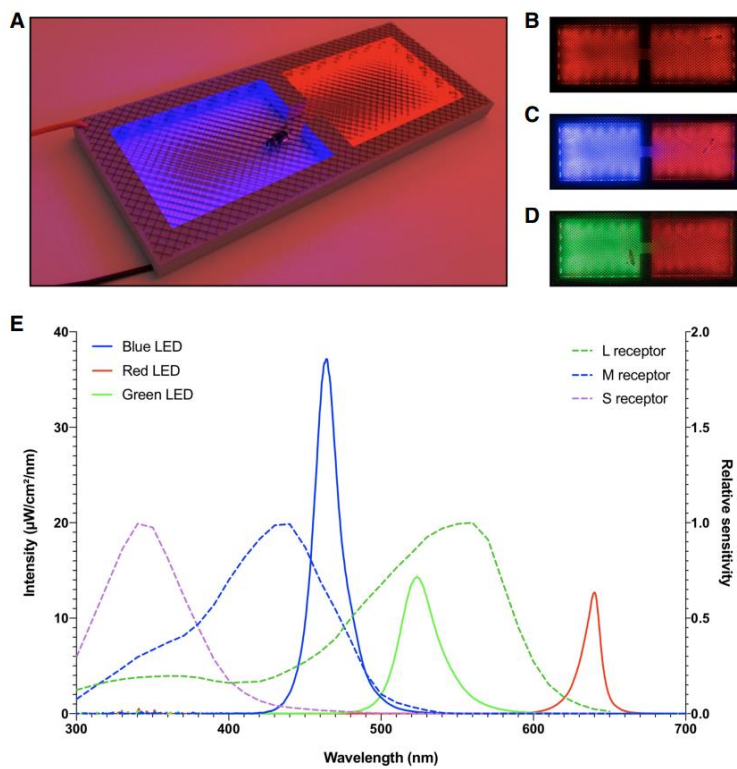
Figure 15. ICARUS - a passive-avoidance setup for inhibitory conditioning of phototaxis in honeybees. (A) The ICARUS setup under red light. Red and black cables represent the electrodes connected to upper and lower metal grids by which the shock is delivered. (B–D) Top view images of the ICARUS setup taken with the camera used for video recording the experiments. (B) Background stimulation with red LEDs only. (C) Illumination of one compartment with blue LEDs. (D) Illumination of one compartment with green LEDs. (E) Spectral emittance (continuous lines; left ordinate) of the three types of LEDs used in the setup (blue, green, and red) and spectral sensitivity (dashed lines; right ordinate) of the three types of honeybee photoreceptors (S, M, and L, for short, mid, and long wavelengths, respectively) as a function of wavelength. Spectral analysis of quantum catches—the proportion of incident photons that are captured by the photo-pigments—showed that red LEDs induced negligible activation of photoreceptors (QS = 0.6, QM = 0.64, QL = 1.84) while green LEDs activated mainly the L photoreceptors (QS = 0.84, QM = 3.25, QL = 44.22) and blue LEDs activated both L and M photoreceptors (QS = 0.36, QM = 21.42, QL = 23.19). Quantum-catch values depend on the spectrum of the stimulating light and the spectral sensitivity of the photoreceptor considered; they are used to infer the signal generated at the photoreceptor level.

Figure 16. Multiple conditioning trials in a passive-avoidance task induce strong phototactic inhibitory learning and a memory retrievable 24 h after conditioning. (A) Schematic representation of the experimental protocol. After a familiarization period of 5 min in the setup under red light, three groups of bees (paired, unpaired, and no-chock) were subjected to three conditioning protocols in which the latency to enter a blue-lit compartment was measured as a proxy of learning and memory. The paired group received eight conditioning trials in which the action of entering the blue-lit compartment was paired with a mild electric shock. The unpaired group received eight trials consisting of stimulations with attractive blue light and mild electric shock separated by 30 sec. The no-shock group received eight trials consisting of only the stimulation with the attractive blue light. In all groups, trials were separated by an intertrial interval of 1 min. Memory retention was tested 24 h after conditioning. The test session consisted of a familiarization period, and two tests separated by 1 min. In the first test, one of the compartments was illuminated with blue light; in the second test, one compartment was illuminated with green light. No-shock was delivered during

tests. (B) Learning curves represented in terms of the latency (s) to enter the blue-lit compartment during conditioning trials for the three experimental groups. (C) Memory scores represented in terms of the latency (s) to enter the blue-lit and green-lit compartments. They are displayed in a logarithmic scale for better visualization. Each box extends from the 25th to 75th percentiles; the line in the middle of the box shows the median. Tukey's method was used for plotting whiskers and outliers.

5.2 The virtual reality (VR) setup: color associative learning in tethered bees

Virtual-reality (VR) environments constitute a novel tool to overcome the limitation of using bees that either fly freely between the hive and the laboratory, or walk freely in a specific setup (e.g., Icarus, see above). The free movement granted to animals in both cases precludes the use of invasive techniques to study neural activity in the bee brain in parallel with behavioral recordings. VR environments can be displayed to animals that are partially immobilized (e.g., tethered by the thorax) and that walk stationarily on a treadmill (Fig. 17). This virtual scenario is coupled and modified according to the animal's movement, thus creating an immersive situation that allows studying decision making based on visual cues (Buatois et al., 2018, 2017; Lafon et al., 2021; Rusch et al., 2021, 2017; Schultheiss et al., 2017; Zwaka et al., 2018a). Under these conditions, bees learn and memorize simple and higher-order visual discrimination problems, which enables coupling the study of this visual learning with mechanistic analyses of brain activity (Rusch et al., 2021; Zwaka et al., 2018b). VR setups may differ according to the degree of variation introduced by the bee movement into the visual environment. In open-loop conditions, the animal has no control on stimulus displacements, which are defined by the experimenter. In closed-loop conditions, on the contrary, the animal controls stimulus displacements, which are made contingent on the movements of a tethered bee, thus creating a more immersive environment. Our team has, so far, established two forms of closed-loop conditions in our VR system, conceived for honey bees: in a 2D VR environment, stimulus displacements are only possible in a single frontal plane (i.e., from left to right and vice versa) with no 3D sensation (Buatois et al., 2020, 2018, 2017). In a 3D VR, a more realistic environment is achieved, as stimulus expansions and retractions are possible depending on forward or backward movements, respectively. In both cases, bees learn to discriminate colors, but their degree of stimulus control changes considerably (Fig. 17).

In my work, I used *ex vivo* analysis of IEG expression in different areas of the honey bee brain following color discrimination learning in these two forms of closed-loop VR (Experimental

Chapters 2 and 3, respectively).
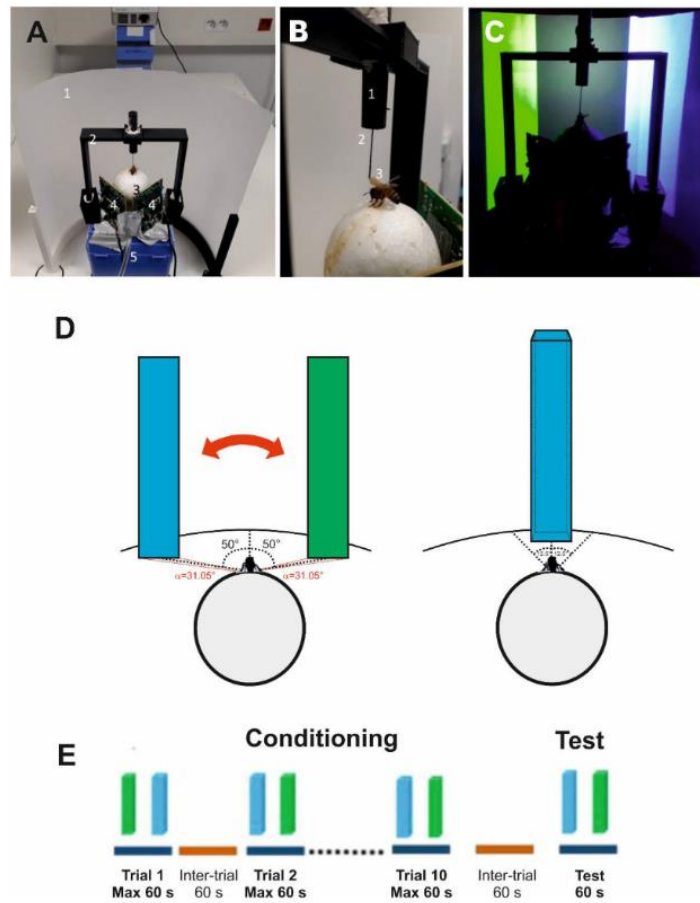
Figure 17. 2D Experimental setup, choice criterion and conditioning procedure. (A) Global view of the setup. 1, semicircular projection screen made of tracing paper; 2, holding frame to place the tethered bee on the treadmill; 3, the treadmill was a Styrofoam ball positioned within a cylindrical support (not visible) floating on an air cushion; 4, infrared mouse optic sensors allowing to record the displacement of the ball and to reconstruct the bee's trajectory; 5, air arrival. The video projector displaying images on the screen from behind can be seen on top of the image. (B) The tethering system. 1, plastic cylinder held by the holding frame; the cylinder contained a glass cannula into which a steel needle was inserted; 2, the needle was attached to the thorax of the bee; 3, its curved end was fixed to the thorax by means of melted bee wax. (C) Color discrimination learning in the VR setup. The bee had to learn to discriminate two vertical bars based on their different color and their association with reward and punishment. Bars were green and blue on a dark background. Color intensities were adjusted to avoid phototactic biases independent of learning. Displacement of the bars was restricted to the 2D plane in front of the bee. (D) Left: view of the stimuli at the start of a trial or test. The green and the blue virtual bars were a presented at $-50°$ and $+50°$ of the bee's longitudinal axis of the bee. Stimuli could be only displaced by the bee from left to right and vice versa (double red arrow). The red angles on the virtual surface indicate the visual angle subtended by each bar at the bee position ($\alpha = 31.05°$). Right: Choice of a bar. A choice was recorded when the bee kept the center of the object between $-12.5°$ and $+12.5°$ in front of it for 1 s. The bar image was then frozen during 8 s and the corresponding reinforcement (US) was delivered. (E) Conditioning protocol. Bees were trained along 10 conditioning trials that lasted a maximum of 1 min and that were spaced by 1 min (intertrial interval). After the end of conditioning, and following an additional interval of 1 min, bees were tested in extinction conditions during 1 min.

6. Goals and Questions of the Thesis

In my thesis, I aimed at exploring the molecular aspects of honey bee visual perception and learning, using a combination of molecular analyses and behavioral approaches. The originality of this work resides in the coupling of these two levels in controlled laboratory conditions, a totally novel endeavor. My overall goal was to characterize the molecular mechanisms underlying color vision and learning in honey bees, an insect in which a significative amount of knowledge on these functions has been gained through behavioral tests, yet with scarce information on the molecular underpinnings of these performances.

The goals and questions that I addressed are the following:

1) **Addressing the role of honey bee opsin genes via a CRISPR/Cas9 approach in phototactic inhibitory learning (Experimental Chapter 1):**

In this chapter, I aimed at establishing a CRISPR/Cas9 approach to knock out opsin genes characterized for the honey bee visual system. I first focused, as a proof of concept, on the *white* gene, which controls the external coloration of the compound eyes, because mutants can be easily detected, due to the whitish coloration of the external surface of compound eyes. I then targeted opsin genes, and I focused in particular on the two forms of green opsin that have been reported for the honey bee, *Amlop1* and *Amlop2*. I verified via *in situ* hybridization that these two opsins are spatially segregated, with *Amlop1* confined to the ommatidia of the compound eyes and *Amlop2* to the ocelli, and then I studied their functional implication in phototactic inhibitory learning. *White, Amlop1* and *Amlop2* mutants were studied in the Icarus setup to determine their capacity to inhibit phototactic attraction, via pairing of an attractive light with electric shock.

2) **Studying IEG expression in the bee brain as a consequence of color discrimination learning in VR conditions (Experimental Chapters 2 and 3)**

I aimed at characterizing neural activation in the bee brain following associative color learning in a VR environment and using an IEG-quantification approach. As studies on neural activity during associative color learning are scarce, I used *ex vivo* analyses of IEG expression in the case

of three IEGs characterized for honey bees, *kakusei, Hr38* and *Erg1*, to determine which areas of the bee brain mediate color associative learning, and if changes in activity patterns are observed according to the way in which bees learn to solve the same color discrimination. To answer this last question, I compared IEG expression under 3D (Experimental Chapter 2) and 2D VR conditions (Experimental Chapter 3), as these two scenarios impose different constraints on the control that the experimental bee can have on the stimuli to be discriminated.

3) Studying aminergic gene expression in phototactic inhibitory learning (Appendix)

Finally, I contributed to an analysis of aminergic gene expression in the context of phototactic inhibitory learning in the Icarus setup. I aimed at determining if inhibitory learning of phototaxis induces transcriptional changes immediately post learning; these might participate either in memory consolidation or in amplifying the representation of shock reinforcement and/or the light used as discriminative stimulus. To this end, I quantified expression levels of the three dopamine receptor genes *Amdop1, Amdop2 and Amdop3* (Kyle T Beggs et al., 2011), given the essential role of dopamine for aversive-reinforcement signaling in honey bees (Tedjakumala et al., 2014; Tedjakumala and Giurfa, 2013; Vergoz et al., 2007). I also quantified expression of the main octopamine receptor gene *AmoctαR1* (Kyle T. Beggs et al., 2011; Farooqui et al., 2004, 2003; Sinakevitch et al., 2011), due to the inverse relationship found between octopamine levels in the optic lobes of bee foragers and their phototactic responses (Scheiner et al., 2014). Finally, I measured levels of the serotonin receptor gene *Am5-ht1a*, which has been shown to be highly expressed in brain regions involved in visual information processing and which has a strong impact on phototactic behavior (Thamm et al., 2010).

7. Publication Outcome

- **Experimental Chapter 1** is still under preparation for submission. Additional experiments may be added, as they were not possible during my PhD thesis due to COVID-19 confinements, which coincided with the period of egg injection and thus impacted severely my CRISPR/Cas 9 experiments. I performed all the experiments presented in this chapter, from the molecular ones to the behavioral ones.

- **Experimental Chapter 2** was published in ***Communications Biology***. My role as co-first author (*) was to contribute all the molecular analyses presented in this work:

  Geng H*, Lafon G*, Avarguès-Weber A, Buatois A, Massou I, Giurfa M. (2022) Visual learning in a virtual reality environment upregulates immediate early gene expression in the mushroom bodies of honey bees. Commun Biol. 14;5(1):130. doi: 10.1038/s42003-022-03075-8.
  (*) 1ˢᵗ authorship shared

- **Experimental Chapter 3** was published in ***Frontiers in Behavioral Neuroscience***. My role as co-first author (*) was to contribute all the molecular analyses presented in this work:

  Lafon G(*), Geng H(*), Avarguès-Weber A, Buatois A, Massou I, Giurfa M. (2022) The neural signature of visual learning under restrictive virtual-reality conditions. Front Behav Neurosci. 16:846076. doi: 10.3389/fnbeh.2022.846076.
  (*) 1ˢᵗ authorship shared

- The work presented in **Appendix** was part of an article published in *Learning and Memory*. My role was to contribute the aminergic-gene analysis in areas of the bee brain following inhibitory phototactic learning.

  Marchal P, Villar ME, Geng H, Arrufat P, Combe M, Viola H, Massou I, Giurfa M. (2019) Inhibitory learning of phototaxis by honeybees in a passive-avoidance task. Learn Mem. 26(10):1-12. doi: 10.1101/lm.050120.119.

8. References

Alaux, C., Robinson, G.E., 2007. Alarm Pheromone Induces Immediate–Early Gene Expression and Slow Behavioral Response in Honey Bees. J Chem Ecol 33, 1346–1350. https://doi.org/10.1007/s10886-007-9301-6

Arikawa, K., Eguchi, E., Yoshida, A., Aoki, K., 1980. Multiple extraocular photoreceptive areas on genitalia of butterfly Papilio xuthus. Nature 288, 700–702. https://doi.org/10.1038/288700a0

Avargues-Weber, A., Deisig, N., Giurfa, M., 2011. Visual cognition in social insects. Annu Rev Entomol 56, 423–43. https://doi.org/10.1146/annurev-ento-120709-144855

Avarguès-Weber, A., Mota, T., Giurfa, M., 2012. New vistas on honey bee vision. Apidologie 43, 244–268. https://doi.org/10.1007/s13592-012-0124-2

Backhaus, W., Menzel, R., Kreißl, S., 1987. Multidimensional scaling of color similarity in bees. Biol. Cybernetics 56, 293–304. https://doi.org/10.1007/BF00319510

Bahrami, S., Drablos, F., 2016. Gene regulation in the immediate-early response process. Adv Biol Regul 62, 37–49. https://doi.org/10.1016/j.jbior.2016.05.001

Barry, C.K., Jander, R., 1968. Photoinhibitory Function of the Dorsal Ocelli in the Phototactic Reaction of the Migratory Locust Locusta migratoria L. Nature 217, 675–677.

Bech, M., Homberg, U., Pfeiffer, K., 2014. Receptive fields of locust brain neurons are matched to polarization patterns of the sky. Current Biology 24, 2124–2129. https://doi.org/10.1016/j.cub.2014.07.045

Beggs, Kyle T, Tyndall, J.D., Mercer, A.R., 2011. Honey bee dopamine and octopamine receptors linked to intracellular calcium signaling have a close phylogenetic and pharmacological relationship. PLoS One 6, e26809. https://doi.org/10.1371/journal.pone.0026809

Berry, R., van Kleef, J., Stange, G., 2007. The mapping of visual space by dragonfly lateral ocelli. Journal of Comparative Physiology A: Neuroethology, Sensory, Neural, and Behavioral Physiology 193, 495–513. https://doi.org/10.1007/s00359-006-0204-8

Borst, A., 2009. Drosophila's View on Insect Vision. Current Biology 19, R36–R47. https://doi.org/10.1016/j.cub.2008.11.001

Bowmaker, J.K., 2008. Evolution of vertebrate visual pigments. Vision Research 48, 2022–2041. https://doi.org/10.1016/j.visres.2008.03.025

Brody, T., Cravchik, A., 2000. Drosophila melanogaster G Protein–Coupled Receptors. J Cell Biol 150, 83–88. https://doi.org/10.1083/jcb.150.2.F83

Brouns, S.J.J., Jore, M.M., Lundgren, M., Westra, E.R., Slijkhuis, R.J.H., Snijders, A.P.L., Dickman, M.J., Makarova, K.S., Koonin, E.V., van der Oost, J., 2008. Small CRISPR RNAs Guide Antiviral Defense in Prokaryotes. Science 321, 960–964. https://doi.org/10.1126/science.1159689

Buatois, A., Flumian, C., Schultheiss, P., Avargues-Weber, A., Giurfa, M., 2018. Transfer of visual learning between a virtual and a real environment in honey bees: the role of active vision. Frontiers in behavioral neuroscience 12, 139. https://doi.org/10.3389/fnbeh.2018.00139

Buatois, A., Laroche, L., Lafon, G., Avargues-Weber, A., Giurfa, M., 2020. Higher-order discrimination learning by honeybees in a virtual environment. Eur J Neurosci 51, 681–694. https://doi.org/10.1111/ejn.14633

Buatois, A., Pichot, C., Schultheiss, P., Sandoz, J.-C., Lazzari, C.R., Chittka, L., Avarguès-Weber,

A., Giurfa, M., 2017. Associative visual learning by tethered bees in a controlled visual environment. Sci Rep 7, 12903. https://doi.org/10.1038/s41598-017-12631-w

Büchler, R., Andonov, S., Bienefeld, K., Costa, C., Hatjina, F., Kezic, N., Kryger, P., Spivak, M., Uzunov, A., Wilde, J., 2013. Standard methods for rearing and selection of Apis mellifera queens. Journal of Apicultural Research 52, 1–30. https://doi.org/10.3896/IBRA.1.52.1.07

Buehlmann, C., Wozniak, B., Goulard, R., Webb, B., Graham, P., Niven, J.E., 2020. Mushroom bodies are required for learned visual navigation, but not for innate visual behavior, in ants. Current Biology 30, 3438–3443.

Check, E., 2002. Priorities for genome sequencing leave macaques out in the cold. Nature 417, 473–475.

Chen, J., Rattner, A., Nathans, J., 2005. The Rod Photoreceptor-Specific Nuclear Receptor Nr2e3 Represses Transcription of Multiple Cone-Specific Genes. J. Neurosci. 25, 118–129. https://doi.org/10.1523/JNEUROSCI.3571-04.2005

Chen, S., Wang, Q.-L., Nie, Z., Sun, H., Lennon, G., Copeland, N.G., Gilbert, D.J., Jenkins, N.A., Zack, D.J., 1997. Crx, a novel Otx-like paired-homeodomain protein, binds to and transactivates photoreceptor cell-specific genes. Neuron 19, 1017–1030.

Chen, Z., Traniello, I.M., Rana, S., Cash-Ahmed, A.C., Sankey, A.L., Yang, C., Robinson, G.E., 2021. Neurodevelopmental and transcriptomic effects of CRISPR/Cas9-induced somatic *orco* mutation in honey bees. Journal of Neurogenetics 35, 320–332. https://doi.org/10.1080/01677063.2021.1887173

Chittka, L., Beier, W., Hertel, H., Steinmann, E., Menzel, R., 1992. Opponent colour coding is a universal strategy to evaluate the photoreceptor inputs in Hymenoptera. J Comp Physiol A 170, 545–563. https://doi.org/10.1007/BF00199332

Clayton, D.F., 2000. The genomic action potential. Neurobiology of learning and memory 74, 185–216. https://doi.org/10.1006/nlme.2000.3967

Cong, L., Ran, F.A., Cox, D., Lin, S., Barretto, R., Habib, N., Hsu, P.D., Wu, X., Jiang, W., Marraffini, L.A., Zhang, F., 2013. Multiplex genome engineering using CRISPR/Cas systems. Science 339, 819–823. https://doi.org/10.1126/science.1231143

Crailsheim, K., Brodschneider, R., Aupinel, P., Behrens, D., Genersch, E., Vollmann, J., Riessberger-Gallé, U., 2013. Standard methods for artificial rearing of Apis mellifera larvae. Journal of Apicultural Research 52, 1–16. https://doi.org/10.3896/IBRA.1.52.1.05

Daumer, K., 1956. Reizmetrische Untersuchung des Farbensehens der Bienen. Zeitschrift fü vergleichende Physiologie 38, 413–478. https://doi.org/10.1007/BF00340456

Değirmenci, L., Geiger, D., Rogé Ferreira, F.L., Keller, A., Krischke, B., Beye, M., Steffan-Dewenter, I., Scheiner, R., 2020. CRISPR/Cas9 mediated mutations as a new tool for studying taste in honeybees (preprint). Genetics. https://doi.org/10.1101/2020.03.26.009696

Eaton, J.L., Tignor, K., Holtzman, G., 1983. Role of moth ocelli in timing flight initiation at dusk. Physiological entomology 8, 371–375.

Ehmer, B., Gronenberg, W., 2002. Segregation of visual input to the mushroom bodies in the honeybee (Apis mellifera). Journal of Comparative Neurology 451, 362–373.

Exner, S., 1891. Die Physiologie der facettirten Augen von Krebsen und Insecten: eine Studie. Franz Deuticke.

Fahrbach, S.E., Robinson, G.E., 1995. Behavioral development in the honey bee: Toward the study of learning under natural conditions. Learning & Memory 2, 199–224. https://doi.org/10.1101/lm.2.5.199

Fain, G.L., Hardie, R., Laughlin, S.B., 2010. Phototransduction and the Evolution of Photoreceptors. Current Biology 20, R114–R124. https://doi.org/10.1016/j.cub.2009.12.006

Farooqui, T., Robinson, K., Vaessin, H., Smith, B.H., 2003. Modulation of early olfactory processing by an octopaminergic reinforcement pathway in the honeybee. The Journal of Neuroscience 23, 5370–80.

Farooqui, T., Vaessin, H., Smith, B.H., 2004. Octopamine receptors in the honeybee (Apis mellifera) brain and their disruption by RNA-mediated interference. Journal of Insect Physiology 50, 701–713. https://doi.org/10.1016/j.jinsphys.2004.04.014

Fent, K., Wehner, R., 1985. Ocelli: a celestial compass in the desert ant Cataglyphis. Science 228, 192–194.

Friedland, A.E., Tzur, Y.B., Esvelt, K.M., Colaiácovo, M.P., Church, G.M., Calarco, J.A., 2013. Heritable genome editing in C. elegans via a CRISPR-Cas9 system. Nat Methods 10, 741–743. https://doi.org/10.1038/nmeth.2532

Fujita, N., Nagata, Y., Nishiuchi, T., Sato, M., Iwami, M., Kiya, T., 2013. Visualization of neural activity in insect brains using a conserved immediate early gene, Hr38. Curr Biol 23, 2063–70. https://doi.org/10.1016/j.cub.2013.08.051

Futahashi, R., Kawahara-Miki, R., Kinoshita, M., Yoshitake, K., Yajima, S., Arikawa, K., Fukatsu, T., 2015. Extraordinary diversity of visual opsin genes in dragonflies. Proc Natl Acad Sci USA 112, E1247. https://doi.org/10.1073/pnas.1424670112

Galizia, C.G., Lledo, P.-M. (Eds.), 2013. Neurosciences - From Molecule to Behavior: a university textbook. Springer Berlin Heidelberg, Berlin, Heidelberg. https://doi.org/10.1007/978-3-642-10769-6

Gallo, F.T., Katche, C., Morici, J.F., Medina, J.H., Weisstaub, N.V., 2018. Immediate early genes, memory and psychiatric disorders: focus on *c-Fos, Egr1* and *Arc*. Frontiers in behavioral neuroscience 12, 79. https://doi.org/10.3389/fnbeh.2018.00079

Gegenfurtner, K.R., Kiper, D.C., 2003. Color vision. Annual review of neuroscience 26, 181–206.

Geng, H., Lafon, G., Avarguès-Weber, A., Buatois, A., Massou, I., Giurfa, M., 2022. Visual learning in a virtual reality environment upregulates immediate early gene expression in the mushroom bodies of honey bees. Commun Biol 5, 1–11. https://doi.org/10.1038/s42003-022-03075-8

Giurfa, M., 2007. Behavioral and neural analysis of associative learning in the honeybee: a taste from the magic well. J Comp Physiol A 193, 801–824. https://doi.org/10.1007/s00359-007-0235-9

Giurfa, M., Sandoz, J.-C., 2012. Invertebrate learning and memory: Fifty years of olfactory conditioning of the proboscis extension response in honeybees. Learn. Mem. 19, 54–66. https://doi.org/10.1101/lm.024711.111

Giurfa, M., Vorobyev, M., Kevan, P., Menzel, R., 1996. Detection of coloured stimuli by honeybees: minimum visual angles and receptor specific contrasts. J Comp Physiol A 178, 699–709. https://doi.org/10.1007/BF00227381

Goldsmith, T.H., Bernard, G.D., 1974. Chapter 5 - The visual system of insects, in: Rockstein, M.

(Ed.), The Physiology of Insecta (Second Edition). Academic Press, pp. 165–272. https://doi.org/10.1016/B978-0-12-591602-8.50012-6

Gratz, S.J., Cummings, A.M., Nguyen, J.N., Hamm, D.C., Donohue, L.K., Harrison, M.M., Wildonger, J., O'Connor-Giles, K.M., 2013. Genome engineering of Drosophila with the CRISPR RNA-guided Cas9 nuclease. Genetics 194, 1029–1035. https://doi.org/10.1534/genetics.113.152710

Gribakin, F., 1975. Functional morphology of the compound eye of the bee. Oxford, UK: Clarendon Press.[Google Scholar].

Groh, C., Tautz, J., Rössler, W., 2004. Synaptic organization in the adult honey bee brain is influenced by brood-temperature control during pupal development. Proc Natl Acad Sci U S A 101, 4268–4273. https://doi.org/10.1073/pnas.0400773101

Gronenberg, W., 2001. Subdivisions of hymenopteran mushroom body calyces by their afferent supply. Journal of Comparative Neurology 435, 474–489. https://doi.org/10.1002/cne.1045

Grünewald, B., 1999. Physiological properties and response modulations of mushroom body feedback neurons during olfactory learning in the honeybee, Apis mellifera. Journal of Comparative Physiology A 185, 565–576.

Hardie, R.C., Raghu, P., 2001. Visual transduction in Drosophila. Nature 413, 186–193. https://doi.org/10.1038/35093002

Harpur, B.A., Zayed, A., 2013. Accelerated evolution of innate immunity proteins in social insects: adaptive evolution or relaxed constraint? Mol Biol Evol 30, 1665–1674. https://doi.org/10.1093/molbev/mst061

Hasselmann, M., Gempe, T., Schiøtt, M., Nunes-Silva, C.G., Otte, M., Beye, M., 2008. Evidence for the evolutionary nascence of a novel sex determination pathway in honeybees. Nature 454, 519–522. https://doi.org/10.1038/nature07052

He, Q., Wang, J., Hu, H., 2019. Illuminating the activated brain: emerging activity-dependent tools to capture and control functional neural circuits. Neuroscience bulletin 35, 369–377. https://doi.org/10.1007/s12264-018-0291-x

Heinze, S., 2017. Unraveling the neural basis of insect navigation. Current opinion in insect science 24, 58–67.

Heinze, S., Florman, J., Asokaraj, S., El Jundi, B., Reppert, S.M., 2013. Anatomical basis of sun compass navigation II: the neuronal composition of the central complex of the monarch butterfly. Journal of Comparative Neurology 521, 267–298.

Henze, M.J., Dannenhauer, K., Kohler, M., Labhart, T., Gesemann, M., 2012. Opsin evolution and expression in Arthropod compound Eyes and Ocelli: Insights from the cricket Gryllus bimaculatus. BMC Evol Biol 12, 1–16. https://doi.org/10.1186/1471-2148-12-163

Hertel, H., 1980. Chromatic properties of identified interneurons in the optic lobes of the bee. Journal of comparative physiology 137, 215–231.

Hertel, H., Maronde, U., 1987. The physiology and morphology of centrally projecting visual interneurones in the honeybee brain. Journal of Experimental Biology 133, 301–315.

Hertel, H., Schafer, S., Maronde, U., 1987. The physiology and morphology of visual commissures in the honeybee brain. Journal of Experimental Biology 133, 283–300.

Hill, C.A., Fox, A.N., Pitts, R.J., Kent, L.B., Tan, P.L., Chrystal, M.A., Cravchik, A., Collins, F.H., Robertson, H.M., Zwiebel, L.J., 2002. G Protein-Coupled Receptors in Anopheles gambiae.

Science 298, 176–178. https://doi.org/10.1126/science.1076196

Homberg, U., 2008. Evolution of the central complex in the arthropod brain with respect to the visual system. Arthropod structure & development 37, 347–362.

Homberg, U., Heinze, S., Pfeiffer, K., Kinoshita, M., El Jundi, B., 2011. Central neural coding of sky polarization in insects. Philosophical Transactions of the Royal Society B: Biological Sciences 366, 680–687.

Homberg, U., Hofer, S., Pfeiffer, K., Gebhardt, S., 2003. Organization and neural connections of the anterior optic tubercle in the brain of the locust, Schistocerca gregaria. Journal of Comparative Neurology 462, 415–430.

Honkanen, A., Adden, A., da Silva Freitas, J., Heinze, S., 2019. The insect central complex and the neural basis of navigational strategies. Journal of Experimental Biology 222, jeb188854.

Honkanen, A., Saari, P., Takalo, J., Heimonen, K., Weckström, M., 2018. The role of ocelli in cockroach optomotor performance. Journal of Comparative Physiology A 204, 231–243.

Horridge, G.A., Giddings, C., Stange, G., 1972. The superposition eye of skipper butterflies. Proceedings of the Royal Society of London. Series B. Biological Sciences 182, 457–495.

Hu, X., Chang, N., Wang, X., Zhou, F., Zhou, X., Zhu, X., Xiong, J.-W., 2013. Heritable gene-targeting with gRNA/Cas9 in rats. Cell Res 23, 1322–1325. https://doi.org/10.1038/cr.2013.141

Hu, X.F., Zhang, B., Liao, C.H., Zeng, Z.J., 2019. High-Efficiency CRISPR/Cas9-Mediated Gene Editing in Honeybee (Apis mellifera) Embryos. G3 Genes|Genomes|Genetics 9, 1759–1766. https://doi.org/10.1534/g3.119.400130

Hung, Y.-S., Ibbotson, M., 2014. Ocellar structure and neural innervation in the honeybee. Frontiers in Neuroanatomy 8, 6. https://doi.org/10.3389/fnana.2014.00006

Hwang, W.Y., Fu, Y., Reyon, D., Maeder, M.L., Tsai, S.Q., Sander, J.D., Peterson, R.T., Yeh, J.-R.J., Joung, J.K., 2013. Efficient genome editing in zebrafish using a CRISPR-Cas system. Nat Biotechnol 31, 227–229. https://doi.org/10.1038/nbt.2501

Iino, S., Shiota, Y., Nishimura, M., Asada, S., Ono, M., Kubo, T., 2020. Neural activity mapping of bumble bee (Bombus ignitus) brains during foraging flight using immediate early genes. Scientific reports 10, 7887. https://doi.org/10.1038/s41598-020-64701-1

Ishino, Y., Shinagawa, H., Makino, K., Amemura, M., Nakata, A., 1987. Nucleotide sequence of the iap gene, responsible for alkaline phosphatase isozyme conversion in Escherichia coli, and identification of the gene product. J Bacteriol 169, 5429–5433.

Jameson, D., Hurvich, L.M., 1968. Opponent-response functions related to measured cone photopigments. JOSA 58, 429_1-430.

Jansen, R., Embden, J.D.A. van, Gaastra, W., Schouls, L.M., 2002. Identification of genes that are associated with DNA repeats in prokaryotes. Mol Microbiol 43, 1565–1575. https://doi.org/10.1046/j.1365-2958.2002.02839.x

Jiang, W., Zhou, H., Bi, H., Fromm, M., Yang, B., Weeks, D.P., 2013. Demonstration of CRISPR/Cas9/sgRNA-mediated targeted gene modification in Arabidopsis, tobacco, sorghum and rice. Nucleic Acids Res 41, e188. https://doi.org/10.1093/nar/gkt780

Jinek, M., Chylinski, K., Fonfara, I., Hauer, M., Doudna, J.A., Charpentier, E., 2012. A programmable dual-RNA-guided DNA endonuclease in adaptive bacterial immunity. Science 337, 816–821. https://doi.org/10.1126/science.1225829

Kaftanoglu, O., Linksvayer, T.A., Page, R.E., 2010. Rearing honey bees (Apis mellifera L.) in vitro:

effects of feeding intervals on survival and development. Journal of Apicultural Research 49, 311–317. https://doi.org/10.3896/IBRA.1.49.4.03

Kamhi, J.F., Barron, A.B., Narendra, A., 2020. Vertical lobes of the mushroom bodies are essential for view-based navigation in Australian Myrmecia ants. Current Biology 30, 3432–3437.

Kaminsky, O., Klenerova, V., Stöhr, J., Sida, P., Hynie, S., 2001. Differences in the behaviour of Sprague–Dawley and Lewis rats during repeated passive avoidance procedure: effect of amphetamine. Pharmacological Research 44, 117–122.

Kent, C.F., Issa, A., Bunting, A.C., Zayed, A., 2011. Adaptive evolution of a key gene affecting queen and worker traits in the honey bee, Apis mellifera. Molecular Ecology 20, 5226–5235. https://doi.org/10.1111/j.1365-294X.2011.05299.x

Kien, J., Menzel, R., 1977. Chromatic properties of interneurons in the optic lobes of the bee. Journal of comparative physiology 113, 17–34.

Kiya, T., Kubo, T., 2011. Dance type and flight parameters are associated with different mushroom body neural activities in worker honeybee brains. PloS ONE 6, e19301. https://doi.org/10.1371/journal.pone.0019301

Kiya, T., Kunieda, T., Kubo, T., 2008. Inducible- and constitutive-type transcript variants of kakusei , a novel non-coding immediate early gene, in the honeybee brain. Insect molecular biology 17, 531–6. https://doi.org/10.1111/j.1365-2583.2008.00821.x

Kiya, T., Kunieda, T., Kubo, T., 2007. Increased neural activity of a mushroom body neuron subtype in the brains of forager honeybees. PloS ONE 2, e371. https://doi.org/10.1371/journal.pone.0000371

Kohno, H., Kubo, T., 2018. mKast is dispensable for normal development and sexual maturation of the male European honeybee. Sci Rep 8, 11877. https://doi.org/10.1038/s41598-018-30380-2

Kohno, H., Suenami, S., Takeuchi, H., Sasaki, T., Kubo, T., 2016. Production of Knockout Mutants by CRISPR/Cas9 in the European Honeybee, Apis mellifera L. Zoological Science 33, 505. https://doi.org/10.2108/zs160043

Kretzberg, J., Ernst, U., 2013. Vision, in: Galizia, C.G., Lledo, P.-M. (Eds.), Neurosciences - From Molecule to Behavior: A University Textbook. Springer, Berlin, Heidelberg, pp. 363–407. https://doi.org/10.1007/978-3-642-10769-6_18

Krypotos, A., Effting, M., Kindt, M., Beckers, T., 2015. Avoidance learning: a review of theoretical models and recent developments. Frontiers in Behavioral Neuroscience 9. https://doi.org/10.3389/fnbeh.2015.00189

Labhart, T., Meyer, E.P., 1999. Detectors for polarized skylight in insects: a survey of ommatidial specializations in the dorsal rim area of the compound eye. Microscopy research and technique 47, 368–379.

Lafon, G., Geng, H., Avarguès-Weber, A., Buatois, A., Massou, I., Giurfa, M., 2022. The Neural Signature of Visual Learning Under Restrictive Virtual-Reality Conditions. Frontiers in Behavioral Neuroscience 16.

Lafon, G., Howard, S.R., Paffhausen, B.H., Avarguès-Weber, A., Giurfa, M., 2021. Motion cues from the background influence associative color learning of honey bees in a virtual-reality scenario. Sci Rep 11, 21127. https://doi.org/10.1038/s41598-021-00630-x

Lamb, T.D., Collin, S.P., Pugh, E.N., 2007. Evolution of the vertebrate eye: opsins, photoreceptors,

retina and eye cup. Nature Reviews Neuroscience 8, 960–976.

Land, M.F., Fernald, R.D., 1992. The evolution of eyes. Annual review of neuroscience 15, 1–29.

Lau, T.F.S., Meyer-Rochow, V.B., 2007. The compound eye of Orgyia antiqua (Lepidoptera: Lymantriidae): Sexual dimorphism and light/dark adaptational changes. European Journal of Entomology 104, 247.

LeDoux, J., Moscarello, J., Sears, R., Campese, V., 2017. The birth, death and resurrection of avoidance: a reconceptualization of a troubled paradigm. Molecular Psychiatry 22, 24–36. https://doi.org/10.1038/mp.2016.166

Lehrer, M., Srinivasan, M.V., Zhang, S.W., Horridge, G.A., 1990. Visual edge detection in the honeybee and its chromatic properties. Proceedings of the Royal Society of London. B. Biological Sciences 238, 321–330. https://doi.org/10.1098/rspb.1990.0002

Li, L., Liu, F., Li, W., Li, Z., Pan, J., Yan, L., Zhang, S., Huang, Z.Y., Su, S., 2012. Differences in microRNAs and their expressions between foraging and dancing honey bees, Apis mellifera L. J Insect Physiol 58, 1438–1443. https://doi.org/10.1016/j.jinsphys.2012.08.008

Lillestøl, R.K., Shah, S.A., Brügger, K., Redder, P., Phan, H., Christiansen, J., Garrett, R.A., 2009. CRISPR families of the crenarchaeal genus Sulfolobus: bidirectional transcription and dynamic properties. Molecular Microbiology 72, 259–272. https://doi.org/10.1111/j.1365-2958.2009.06641.x

Liu, G., Seiler, H., Wen, A., Zars, T., Ito, K., Wolf, R., Heisenberg, M., Liu, L., 2006. Distinct memory traces for two visual features in the Drosophila brain. Nature 439, 551–556.

Lutz, C.C., Robinson, G.E., 2013. Activity-dependent gene expression in honey bee mushroom bodies in response to orientation flight. The Journal of experimental biology 216, 2031–8. https://doi.org/10.1242/jeb.084905

Ma, S., Chang, J., Wang, X., Liu, Y., Zhang, J., Lu, W., Gao, J., Shi, R., Zhao, P., Xia, Q., 2014. CRISPR/Cas9 mediated multiplex genome editing and heritable mutagenesis of BmKu70 in Bombyx mori. Sci Rep 4, 4489. https://doi.org/10.1038/srep04489

Makarova, K.S., Haft, D.H., Barrangou, R., Brouns, S.J.J., Charpentier, E., Horvath, P., Moineau, S., Mojica, F.J.M., Wolf, Y.I., Yakunin, A.F., van der Oost, J., Koonin, E.V., 2011. Evolution and classification of the CRISPR–Cas systems. Nat Rev Microbiol 9, 467–477. https://doi.org/10.1038/nrmicro2577

Marchal, P., Villar, M.E., Geng, H., Arrufat, P., Combe, M., Viola, H., Massou, I., Giurfa, M., 2019. Inhibitory learning of phototaxis by honeybees in a passive-avoidance task. Learn. Mem. 26, 412–423. https://doi.org/10.1101/lm.050120.119

Marraffini, L.A., 2015. CRISPR-Cas immunity in prokaryotes. Nature 526, 55–61. https://doi.org/10.1038/nature15386

Marraffini, L.A., Sontheimer, E.J., 2010. CRISPR interference: RNA-directed adaptive immunity in bacteria and archaea. Nat Rev Genet 11, 181–190. https://doi.org/10.1038/nrg2749

Matsushita, A., Awata, H., Wakakuwa, M., Takemura, S., Arikawa, K., 2012. Rhabdom evolution in butterflies: insights from the uniquely tiered and heterogeneous ommatidia of the Glacial Apollo butterfly, Parnassius glacialis. Proceedings of the Royal Society B: Biological Sciences 279, 3482–3490. https://doi.org/10.1098/rspb.2012.0475

Menzel, R., 1999. Memory dynamics in the honeybee. J Comp Physiol A 185, 323–340.

Menzel, R., Backhaus, W., 1991. Colour Vision in Insects, in: Gouras, P. (Ed.), Vision and Visual

Dysfunction. The Perception of Colour. MacMillan Press, London, pp. 262–288.

Menzel, R., Greggers, U., 1985. Natural phototaxis and its relationship to colour vision in honeybees. Journal of Comparative Physiology A 157, 311–321.

Menzel, R., Snyder, A.W., 1974. Polarised light detection in the bee, Apis mellifera. Journal of comparative physiology 88, 247–270.

Menzel, Randolf, 1979. Spectral Sensitivity and Color Vision in Invertebrates, in: Autrum, H., Bennett, M.F., Diehn, B., Hamdorf, K., Heisenberg, M., Järvilehto, M., Kunze, P., Menzel, R., Miller, W.H., Snyder, A.W., Stavenga, D.G., Yoshida, M., Autrum, H. (Eds.), Comparative Physiology and Evolution of Vision in Invertebrates: A: Invertebrate Photoreceptors, Handbook of Sensory Physiology. Springer, Berlin, Heidelberg, pp. 503–580. https://doi.org/10.1007/978-3-642-66999-6_9

Meyer, E.P., Labhart, T., 1993. Morphological specializations of dorsal rim ommatidia in the compound eye of dragonflies and damselfies (Odonata). Cell and tissue research 272, 17–22.

Meyer-Rochow, V.B., 2001. The crustacean eye: dark/light adaptation, polarization sensitivity, flicker fusion frequency, and photoreceptor damage. Zoological science 18, 1175–1197.

Minatohara, K., Akiyoshi, M., Okuno, H., 2015. Role of immediate-early genes in synaptic plasticity and neuronal ensembles underlying the memory trace. Frontiers in molecular neuroscience 8, 78. https://doi.org/10.3389/fnmol.2015.00078

Mizunami, M., 1995. Functional diversity of neural organization in insect ocellar systems. Vision research 35, 443–452. https://doi.org/10.1016/0042-6989(94)00192-O

Mobbs, P., 1982. The brain of the honeybee Apis mellifera. I. The connections and spatial organization of the mushroom bodies. Philosophical Transactions of the Royal Society of London. B, Biological Sciences 298, 309–354.

Mobbs, P., Guy, R., Goodman, L., Chappell, R., 1981. Relative spectral sensitivity and reverse Purkinje shift in identified L neurons of the ocellar retina. Journal of comparative physiology 144, 91–97.

Mobbs, P.G., 1984. Neural networks in the mushroom bodies of the honeybee. Journal of Insect Physiology 30, 43–58. https://doi.org/10.1016/0022-1910(84)90107-0

Mota, T., Yamagata, N., Giurfa, M., Gronenberg, W., Sandoz, J.C., 2011. Neural organization and visual processing in the anterior optic tubercle of the honeybee brain. The Journal of neuroscience : the official journal of the Society for Neuroscience 31, 11443–11456. https://doi.org/10.1523/jneurosci.0995-11.2011

Mote, M.I., Wehner, R., 1980. Functional characteristics of photoreceptors in the compound eye and ocellus of the desert ant, Cataglyphis bicolor. Journal of comparative physiology 137, 63–71.

Narendra, A., Ribi, W.A., 2017. Ocellar structure is driven by the mode of locomotion and activity time in Myrmecia ants. Journal of Experimental Biology 220, 4383–4390. https://doi.org/10.1242/jeb.159392

Nathans, J., 1999. The Evolution and Physiology of Human Color Vision: Insights from Molecular Genetic Studies of Visual Pigments. Neuron 24, 299–312. https://doi.org/10.1016/S0896-6273(00)80845-4

Nathans, J., Thomas, D., Hogness, D.S., 1986. Molecular genetics of human color vision: the genes

encoding blue, green, and red pigments. Science 232, 193–202.

Neuser, K., Triphan, T., Mronz, M., Poeck, B., Strauss, R., 2008. Analysis of a spatial orientation memory in Drosophila. Nature 453, 1244–1247.

Nie, H.-Y., Liang, L.-Q., Li, Q.-F., Li, Z.-H.-Q., Zhu, Y.-N., Guo, Y.-K., Zheng, Q.-L., Lin, Y., Yang, D.-L., Li, Z.-G., Su, S.-K., 2021. CRISPR/Cas9 mediated knockout of Amyellow-y gene results in melanization defect of the cuticle in adult Apis mellifera. Journal of Insect Physiology 132, 104264. https://doi.org/10.1016/j.jinsphys.2021.104264

Nilsson, D.-E., 1989. Optics and Evolution of the Compound Eye, in: Stavenga, D.G., Hardie, R.C. (Eds.), Facets of Vision. Springer, Berlin, Heidelberg, pp. 30–73. https://doi.org/10.1007/978-3-642-74082-4_3

Ofstad, T.A., Zuker, C.S., Reiser, M.B., 2011. Visual place learning in Drosophila melanogaster. Nature 474, 204–207.

Ogawa, Y., Ribi, W., Zeil, J., Hemmi, J.M., 2017. Regional differences in the preferred e-vector orientation of honeybee ocellar photoreceptors. Journal of Experimental Biology 220, 1701–1708. https://doi.org/10.1242/jeb.156109

Osorio, D., Smith, A.C., Vorobyev, M., Buchanan-Smith, H.M., 2004. Detection of Fruit and the Selection of Primate Visual Pigments for Color Vision. The American Naturalist 164, 696–708. https://doi.org/10.1086/425332

Pan, K.C., Goodman, L.J., 1977. Ocellar projections within the central nervous system of the worker honey bee, Apis mellifera. Cell Tissue Res 176, 505–527. https://doi.org/10.1007/BF00231405

Paulk, A.C., Phillips-Portillo, J., Dacks, A.M., Fellous, J.M., Gronenberg, W., 2008. The processing of color, motion, and stimulus timing are anatomically segregated in the bumblebee brain. The Journal of Neuroscience 28, 6319–6332. https://doi.org/10.1523/jneurosci.1196-08.2008

Paulus, H. von, 1979. Eye structure and the monophyly of the arthropod eye. Arthropod phylogeny 299–383.

Peitsch, D., Fietz, A., Hertel, H., de Souza, J., Ventura, D.F., Menzel, R., 1992. The spectral input systems of hymenopteran insects and their receptor-based colour vision. J Comp Physiol A 170, 23–40. https://doi.org/10.1007/BF00190398

Pfeiffer, K., Homberg, U., 2014. Organization and functional roles of the central complex in the insect brain. Annual review of entomology 59, 165–184.

Pfeiffer, K., Kinoshita, M., 2012. Segregation of visual inputs from different regions of the compound eye in two parallel pathways through the anterior optic tubercle of the bumblebee (Bombus ignitus). Journal of Comparative Neurology 520, 212–229. https://doi.org/10.1002/cne.22776

Pfeiffer, K., Kinoshita, M., Homberg, U., 2005. Polarization-sensitive and light-sensitive neurons in two parallel pathways passing through the anterior optic tubercle in the locust brain. Journal of neurophysiology 94, 3903–3915.

Rehder, V., Bicker, G., Hammer, M., 1987. Serotonin-immunoreactive neurons in the antennal lobes and suboesophageal ganglion of the honeybee. Cell and tissue research 247, 59–66.

Rembold, H., Lackner, B., 1981. Rearing of Honeybee Larvae in Vitro: Effect of Yeast Extract on Queen Differentiation. Journal of Apicultural Research 20, 165–171. https://doi.org/10.1080/00218839.1981.11100492

Ribi, W., Warrant, E., Zeil, J., 2011. The organization of honeybee ocelli: Regional specializations and rhabdom arrangements. Arthropod Structure & Development 40, 509–520. https://doi.org/10.1016/j.asd.2011.06.004

Ribi, W.A., Scheel, M., 1981. The second and third optic ganglia of the worker bee. Cell and tissue research 221, 17–43.

Robertson, H.M., Wanner, K.W., 2006. The chemoreceptor superfamily in the honey bee, Apis mellifera: expansion of the odorant, but not gustatory, receptor family. Genome research 16, 1395–1403.

Robinson, G.E., 2002. Sociogenomics Takes Flight. Science 297, 204–205. https://doi.org/10.1126/science.1074493

Robinson, G.E., Page Jr., R.E., Strambi, C., Strambi, A., 1992. Colony Integration in Honey Bees: Mechanisms of Behavioral Reversion. Ethology 90, 336–348. https://doi.org/10.1111/j.1439-0310.1992.tb00844.x

Robinson, K.O., Ferguson, H.J., Cobey, S., Vaessin, H., Smith, B.H., 2000. Sperm-mediated transformation of the honey bee, Apis mellifera. Insect Molecular Biology 9, 625–634. https://doi.org/10.1046/j.1365-2583.2000.00225.x

Rodieck, R.W., Rodieck, R.W., 1998. The first steps in seeing. Sinauer Associates Sunderland, MA.

Roth, A., Vleurinck, C., Netschitailo, O., Bauer, V., Otte, M., Kaftanoglu, O., Page, R.E., Beye, M., 2019. A genetic switch for worker nutrition-mediated traits in honeybees. PLoS Biol 17, e3000171. https://doi.org/10.1371/journal.pbio.3000171

Rusch, C., Alonso San Alberto, D., Riffell, J.A., 2021. Visuo-motor feedback modulates neural activities in the medulla of the honeybee, *Apis mellifera*. The Journal of neuroscience : the official journal of the Society for Neuroscience 41, 3192–3203. https://doi.org/10.1523/jneurosci.1824-20.2021

Rusch, C., Roth, E., Vinauger, C., Riffell, J.A., 2017. Honeybees in a virtual reality environment learn unique combinations of colour and shape. The Journal of experimental biology 220, 3478–3487. https://doi.org/10.1242/jeb.164731

Sander, J.D., Joung, J.K., 2014. CRISPR-Cas systems for editing, regulating and targeting genomes. Nat Biotechnol 32, 347–355. https://doi.org/10.1038/nbt.2842

Sarma, M.S., Rodriguez-Zas, S.L., Hong, F., Zhong, S., Robinson, G.E., 2009. Transcriptomic Profiling of Central Nervous System Regions in Three Species of Honey Bee during Dance Communication Behavior. PLoS ONE 4, e6408. https://doi.org/10.1371/journal.pone.0006408

Scheiner, R., Toteva, A., Reim, T., Søvik, E., Barron, A.B., 2014. Differences in the phototaxis of pollen and nectar foraging honey bees are related to their octopamine brain titers. Frontiers in Physiology 5, 1–8. https://doi.org/10.3389/fphys.2014.00116

Schulte, C., Theilenberg, E., Müller-Borg, M., Gempe, T., Beye, M., 2014. Highly efficient integration and expression of piggyBac-derived cassettes in the honeybee (Apis mellifera). PNAS 111, 9003–9008. https://doi.org/10.1073/pnas.1402341111

Schultheiss, P., Buatois, A., Avarguès-Weber, A., Giurfa, M., 2017. Using virtual reality to study visual performances of honeybees. Curr Opin Insect Sci 24, 43–50. https://doi.org/10.1016/j.cois.2017.08.003

Schwarz, S., Albert, L., Wystrach, A., Cheng, K., 2011a. Ocelli contribute to the encoding of celestial compass information in the Australian desert ant Melophorus bagoti. Journal of Experimental Biology 214, 901–906.

Schwarz, S., Wystrach, A., Cheng, K., 2011b. A new navigational mechanism mediated by ant ocelli. Biology letters 7, 856–858.

Sen Sarma, M., Rodriguez-Zas, S.L., Gernat, T., Nguyen, T., Newman, T., Robinson, G.E., 2010. Distance-responsive genes found in dancing honey bees. Genes Brain Behav 9, 825–830. https://doi.org/10.1111/j.1601-183X.2010.00622.x

Shah, A., Jain, R., Brockmann, A., 2018. Egr-1: A candidate transcription factor involved in molecular processes underlying time-memory. Frontiers in Psychology 9. https://doi.org/10.3389/fpsyg.2018.00865

Shichida, Y., Matsuyama, T., 2009. Evolution of opsins and phototransduction. Philosophical Transactions of the Royal Society B: Biological Sciences 364, 2881–2895.

Si, A., Srinivasan, M.V., Zhang, S., 2003. Honeybee navigation: properties of the visually driven `odometer'. Journal of Experimental Biology 206, 1265–1273. https://doi.org/10.1242/jeb.00236

Sinakevitch, I., Kurtzman, Z., Choi, H.G., Pardo, D.A.R., Dahan, R.A., Klein, N., Bugarija, B., Wendlandt, E., Smith, B.H., 2020. Anti-RDL and Anti-mGlutR1 Receptors Antibody Testing in Honeybee Brain Sections using CRISPR-Cas9. JoVE (Journal of Visualized Experiments) e59993.

Sinakevitch, I., Mustard, J.A., Smith, B.H., 2011. Distribution of the octopamine receptor AmOA1 in the honey bee brain. PLoS ONE 6, e14536. https://doi.org/10.1371/journal.pone.0014536

Singh, A.S., Shah, A., Brockmann, A., 2018. Honey bee foraging induces upregulation of early growth response protein 1, hormone receptor 38 and candidate downstream genes of the ecdysteroid signalling pathway. Insect molecular biology 27, 90–98. https://doi.org/10.1111/imb.12350

Sliney, D.H., 2016. What is light? The visible spectrum and beyond. Eye 30, 222–229. https://doi.org/10.1038/eye.2015.252

Sommerlandt, F.M.J., Brockmann, A., Roessler, W., Spaethe, J., 2019. Immediate early genes in social insects: a tool to identify brain regions involved in complex behaviors and molecular processes underlying neuroplasticity. Cellular and molecular life sciences : CMLS 76, 637–651. https://doi.org/10.1007/s00018-018-2948-z

Srinivasan, M.V., 2011. Honeybees as a Model for the Study of Visually Guided Flight, Navigation, and Biologically Inspired Robotics. Physiological Reviews 91, 413–460. https://doi.org/10.1152/physrev.00005.2010

Srinivasan, M.V., Lehrer, M., 1988. Spatial acuity of honeybee vision and its spectral properties. J. Comp. Physiol. 162, 159–172. https://doi.org/10.1007/BF00606081

Stange, G., 1981. The ocellar component of flight equilibrium control in dragonflies. Journal of Comparative Physiology 141, 335–347. https://doi.org/10.1007/BF00609936

Stange, G., Stowe, S., Chahl, J., Massaro, A., 2002. Anisotropic imaging in the dragonfly median ocellus: a matched filter for horizon detection. Journal of Comparative Physiology A 188, 455–467.

Stavenga, D.G., 1992. Eye regionalization and spectral tuning of retinal pigments in insects.

Trends in Neurosciences 15, 213–218. https://doi.org/10.1016/0166-2236(92)90038-A

Tang, Y., Fu, Y., 2018. Class 2 CRISPR/Cas: an expanding biotechnology toolbox for and beyond genome editing. Cell & Bioscience 8, 59. https://doi.org/10.1186/s13578-018-0255-x

Taylor, C., 1981. Contribution of compound eyes and ocelli to steering of locusts in flight: I. Behavioural analysis. Journal of Experimental Biology 93, 1–18.

Tedjakumala, S.R., Aimable, M., Giurfa, M., 2014. Pharmacological modulation of aversive responsiveness in honey bees. Frontiers in Behavioral Neuroscience 7. https://doi.org/10.3389/fnbeh.2013.00221

Tedjakumala, S.R., Giurfa, M., 2013. Rules and mechanisms of punishment learning in honey bees: the aversive conditioning of the sting extension response. The Journal of Experimental Biology 216, 2985–97. https://doi.org/10.1242/jeb.086629

Thamm, M., Balfanz, S., Scheiner, R., Baumann, A., Blenau, W., 2010. Characterization of the 5-HT1A receptor of the honeybee (Apis mellifera) and involvement of serotonin in phototactic behavior. Cellular and Molecular Life Sciences 67, 2467–2479. https://doi.org/10.1007/s00018-010-0350-6

Toth, A.L., Zayed, A., 2021. The honey bee genome-- what has it been good for? Apidologie 52, 45–62. https://doi.org/10.1007/s13592-020-00829-3

Trible, W., Olivos-Cisneros, L., McKenzie, S.K., Saragosti, J., Chang, N.-C., Matthews, B.J., Oxley, P.R., Kronauer, D.J.C., 2017. orco Mutagenesis Causes Loss of Antennal Lobe Glomeruli and Impaired Social Behavior in Ants. Cell 170, 727-735.e10. https://doi.org/10.1016/j.cell.2017.07.001

Tsarmpopoulos, I., Gourgues, G., Blanchard, A., Vashee, S., Jores, J., Lartigue, C., Sirand-Pugnet, P., 2016. In-Yeast Engineering of a Bacterial Genome Using CRISPR/Cas9. ACS Synth Biol 5, 104–109. https://doi.org/10.1021/acssynbio.5b00196

Ugajin, A., Uchiyama, H., Miyata, T., Sasaki, T., Yajima, S., Ono, M., 2018. Identification and initial characterization of novel neural immediate early genes possibly differentially contributing to foraging-related learning and memory processes in the honeybee. Insect molecular biology 27, 154–165. https://doi.org/10.1111/imb.12355

Varela, F.G., Porter, K.R., 1969. Fine structure of the visual system of the honeybee (Apis mellifera): I. The retina. Journal of Ultrastructure Research 29, 236–259. https://doi.org/10.1016/S0022-5320(69)90104-X

Venable, N., Kelly, P.H., 1990. Effects of NMDA receptor antagonists on passive avoidance learning and retrieval in rats and mice. Psychopharmacology 100, 215–221.

Vergoz, V., Roussel, E., Sandoz, J.-C., Giurfa, M., 2007. Aversive learning in honeybees revealed by the olfactory conditioning of the sting extension reflex. PLoS ONE 2, e288. https://doi.org/10.1371/journal.pone.0000288

Vogt, K., 1989. Distribution of insect visual chromophores: functional and phylogenetic aspects, in: Facets of Vision. Springer, pp. 134–151.

von Helversen, O., 1972. Zur spektralen Unterschiedsempfindlichkeit der Honigbiene. J. Comp. Physiol. 80, 439–472. https://doi.org/10.1007/BF00696438

Wakakuwa, M., Kurasawa, M., Giurfa, M., Arikawa, K., 2005. Spectral heterogeneity of honeybee ommatidia. Naturwissenschaften 92, 464–467. https://doi.org/10.1007/s00114-005-0018-5

Wang, X., Lin, Y., Liang, L., Geng, H., Zhang, M., Nie, H., Su, S., 2021. Transcriptional Profiles

of Diploid Mutant Apis mellifera Embryos after Knockout of csd by CRISPR/Cas9. Insects 12, 704. https://doi.org/10.3390/insects12080704

Warrant, E., 2019. Invertebrate vision.

Warrant, E., Kelber, A., Wallen, R., Wcislo, W., 2006. Ocellar optics in nocturnal and diurnal bees and wasps. Arthropod Structure & Development 35, 293–305. https://doi.org/10.1016/j.asd.2006.08.012

Warrant, E., Nilsson, D.-E., 2006. Invertebrate vision. Cambridge University Press.

Warrant, E., Porombka, T., Kirchner, W.H., 1996. Neural image enhancement allows honeybees to see at night. Proceedings of the Royal Society of London. Series B: Biological Sciences 263, 1521–1526. https://doi.org/10.1098/rspb.1996.0222

Warrant, E.J., 1999. Seeing better at night: life style, eye design and the optimum strategy of spatial and temporal summation. Vision Research 39, 1611–1630. https://doi.org/10.1016/S0042-6989(98)00262-4

Wehner, R., Labhart, T., 2006. Polarization vision. Invertebrate vision 291, 348.

Weinstock, G.M., Robinson, G.E., 2006. Insights into social insects from the genome of the honeybee Apis mellifera. Nature 443, 931–949. https://doi.org/10.1038/nature05260

Wellington, W., 1974. Bumblebee Ocelli and Navigation at Dusk. Science 183, 550–551. https://doi.org/10.1126/science.183.4124.550

Wilkinson, R., Wiedenheft, B., 2014. A CRISPR method for genome engineering. F1000Prime Rep 6, 3. https://doi.org/10.12703/P6-3

Withers, G.S., Fahrbach, S.E., Robinson, G.E., 1993. Selective neuroanatomical plasticity and division of labour in the honeybee. Nature 364, 238–240.

Yagi, N., Koyama, N., 1963. compound eye of Lepidoptera.

Yan, H., Opachaloemphan, C., Mancini, G., Yang, H., Gallitto, M., Mlejnek, J., Leibholz, A., Haight, K., Ghaninia, M., Huo, L., Perry, M., Slone, J., Zhou, X., Traficante, M., Penick, C.A., Dolezal, K., Gokhale, K., Stevens, K., Fetter-Pruneda, I., Bonasio, R., Zwiebel, L.J., Berger, S.L., Liebig, J., Reinberg, D., Desplan, C., 2017. An Engineered orco Mutation Produces Aberrant Social Behavior and Defective Neural Development in Ants. Cell 170, 736-747.e9. https://doi.org/10.1016/j.cell.2017.06.051

Yang, E.-C., Lin, H.-C., Hung, Y.-S., 2004. Patterns of chromatic information processing in the lobula of the honeybee, Apis mellifera L. Journal of Insect Physiology 50, 913–925.

Zelinger, L., Swaroop, A., 2018. RNA Biology in Retinal Development and Disease. Trends in Genetics 34, 341–351. https://doi.org/10.1016/j.tig.2018.01.002

Zwaka, H., Bartels, R., Grunewald, B., Menzel, R., 2018a. Neural Organization of A3 Mushroom Body Extrinsic Neurons in the Honeybee Brain. Frontiers in neuroanatomy 12, 57. https://doi.org/10.3389/fnana.2018.00057

Zwaka, H., Bartels, R., Lehfeldt, S., Jusyte, M., Hantke, S., Menzel, S., Gora, J., Alberdi, R., Menzel, R., 2018b. Learning and its neural correlates in a virtual environment for honeybees. Frontiers in behavioral neuroscience 12, 279. https://doi.org/10.3389/fnbeh.2018.00279

Chapter 1

Addressing the function of opsin genes in the honey bee via a combination of CRISPR/Cas9 and visual conditioning experiments

Haiyang Geng[1,2], Sarah Larnaudie[1], Marco Paoli[1], Gregory Lafon[1], Benjamin Paffhausen[1], Martin Beye[3], Isabelle Massou[1*], Martin Giurfa[1,4*]

[1] *Centre de Recherches sur la Cognition Animale, Centre de Biologie Intégrative (CBI), University of Toulouse, CNRS, UPS, 31062 Toulouse cedex 9, France.*

[2] *College of Animal Sciences (College of Bee Science), Fujian Agriculture and Forestry University, Fuzhou, 350002, China.*

[3] *Institute of Evolutionary Genetics, Heinrich-Heine University Düsseldorf, Düsseldorf, Germany.*

[4] *Institut Universitaire de France (IUF), Paris, France.*

*: shared senior authorship

Abstract

Honey bee color vision relies on the existence of three types of spectral photoreceptor types in compound-eye ommatidia, which are maximally sensitive to UV, blue and green light due to the presence of three different types of opsins termed *Amuvop, Amblop and Amlop1*, respectively. An additional green-sensitive opsin (*Amlop2*) was identified in the ocellar system. Whether *Amlop1* and *Amlop2* differ in their capacity to mediate different visually-guided behaviors remain unknown. Here, we characterized *Amlop1* and *Amlop2* distribution in the honey bee visual system and confirmed that *Amlop1* is present in compound-eye ommatidia but not in the ocelli, while *Amlop2* is confined to the ocelli. We then developed a CRISPR/Cas9 approach to knockout opsin genes and determine, in this way, functional differences between *Amlop1* and *Amlop2*. We successfully created *Amlop1* and *Amlop2* adult mutant bees as well as *white-gene* mutants as a control for the efficiency of our method. Mutants were studied using a conditioning protocol in which bees learn to inhibit attraction towards chromatic light based on electric-shock punishment. *White* and *Amlop2* mutants learned to inhibit spontaneous attraction to blue light while *Amlop1* mutants failed to do so. Thus, responses to blue light, which is also sensed by green receptors, are mediated mainly by compound-eye photoreceptors containing *Amlop1* but not by the ocellar system containing *Amlop2*. Accordingly, 24 hours later, *white* and *Amlop2* mutants exhibited an aversive memory for the punished color that was comparable to control bees but *Amlop1* mutants exhibited no memory. We discuss these findings in terms of chromatic vision vs. achromatic vision and in terms of the efficiency of our CRISPR/Cas9 method.

Keywords: Vision, Visual Learning, Honey bee, Photoreceptor Sensitivity, Opsins, *Amlop1*, *Amlop2, White gene*, CRISPR/Cas9, Aversive Learning

Introduction

Color vision is defined as the capacity to distinguish colored surfaces based on their different chromatic contents, independently of intensity differences [1]. Humans and numerous animal species see the world in colors, which provides unique advantages for detecting food sources, partners, and predators, among others [2]. Among the species with a well-characterized color vision, honey bees have played a fundamental role to uncover behavioral and neural mechanisms underlying this capacity. The color vision of bees was officially demonstrated by Nobel Prize winner Karl von Frisch [3] 118 years ago. Before him, several scientists suggested that bees may see colors [4–6] but did not provide robust experimental evidence proving this capacity.

Von Frisch showed that bees can be trained to associate different color cardboards with a reward of sucrose solution, which he placed on an experimental table to which foragers were regularly coming. Following repeated visits to a rewarded color, he presented a test situation in which the color cardboard was shown adjacent to achromatic grey cardboards with different levels of intensity. All cardboards had on top of them an empty feeder. The results of von Frisch showed conclusively that in choosing a rewarded color, bees distinguished it from different levels of achromatic grey cardboards, some of which displayed an intensity similar to that of the color trained (Fig. 1a). He used 16 colored cardboards varying from violet to red and purple (as seen by humans). This method proved that bees could see the majority of his cardboards as colored surfaces, except in the case of red, which was confused with a black cardboard [3]. Later, Kühn extended the demonstration to the ultraviolet range using spectral lights produced by a mercury lamp [7]. In this way, it was demonstrated that bees can see and discriminate colors in the range of 300 nm (ultraviolet) to orange-reddish (650 nm).

At the peripheral level, the physiological basis for this capacity resides in the existence of three types of spectral photoreceptor types contained in the ommatidia, the functional units of compound eyes. Ommatidia contain 9 photoreceptors arranged concentrically, one of which (the 9th photoreceptor cell) is located distally, close to the basal membrane of the retina. The different sensitivity of these photoreceptors was demonstrated by means of behavioral experiments based on color matching [8–10] and, more conclusively, by electrophysiological recordings [11–13]. The three spectral photoreceptor types present in the bee retina exhibit sensitivity peaks at 344 nm in the short-wave (ultra violet) region of the spectrum (S receptor), at 436 nm in the middle-wave (blue) region (M receptor), and at 544 nm in the long-wave (green)

region of the spectrum (L receptor), respectively (Fig. 1b). The different spectral sensitivity of these photoreceptor types is conferred by photopigments densely packed within an inner region of the photoreceptors termed 'rhabdomere' consisting of microvilli (i.e., cellular membrane protrusions that increase considerably the membrane area). The light sensitive photopigments are made of proteins termed *opsins* coupled to Vitamin A-derived chromophores [14]. Opsins are members of the rhodopsin family of the superfamily of G-protein-coupled receptors (GPCRs). These visual pigments mediate the phototransduction process, i.e., the conversion of light into an electrical response [15]. Opsins may differ in their amino acid composition, thus leading to different spectral sensitivities [16].

In honey bees, three types of opsins correspond to UV, blue and green absorbing visual pigments were first characterized in molecular studies, consistently with the reported existence of three types of photoreceptors in the retina [17,18]. They were termed *Amuvop, Amblop and Amlop*, respectively. The distribution of these opsins within ommatidia of the compound eye was studied by means of *in situ* hybridization studies, which identified three types of ommatidia in the compound eye of honey bee workers [19]. Each ommatidium type contains six green photoreceptor cells, and in addition, either one UV and one blue photoreceptor (type I), two UV photoreceptors (type II), or two blue photoreceptors (type III) [19]. The sensitivity of the short distal photoreceptor is still unknown [19]. Further analyses took advantage of the sequencing of the bee genome and identified an additional green-sensitive opsin, which seemed confined to the ocellar system and which was termed *Amlop2* to differentiate it from the one present in compound-eye ommatidia, which was then termed *Amlop1* [20]. Whether *Amlop1* and *Amlop2* differ in their capacity to mediate different visually-guided behaviors remain unknown.

Here we characterized opsin distribution in the honey bee visual system, focusing on *Amlop1* and *Amlop2*. We confirmed that *Amlop1* is present in ommatidia of the compound eye but not in the ocelli, while *Amlop2* is confined to the ocelli. We then developed a CRISPR/Cas9 approach to knockout opsin genes and determine, in this way, functional differences between *Amlop1* and *Amlop2*. The CRISPR/Cas9 knock-out technique has been employed successfully in numerous insects such as *Drosophila melanogaster* [21], *Aedes aeqypti* [22], *Bombyx mori* [23], *Spodoptera littoralis* [24] and recently in the honeybee [25–35]. In this insect, no CRISPR/Cas9 study addressed the visual modality so far. We successfully created *Amlop1* and *Amlop2* adult mutant bees by means of the CRISPR/Cas9 technology and we also produced *white-gene* mutants [36,37] as a control for the efficiency of our method. The white gene controls the external coloration of compound eyes, thus providing a direct readout of mutation efficiency.

We tested our mutants using a conditioning protocol in which bees learn to inhibit phototaxis towards blue light based on electric-shock punishment (Icarus protocol) [38]. *White* and *Amlop2* mutants learned to inhibit spontaneous phototaxis to blue light while *Amlop1* mutants failed to do so. These results indicate that responses to blue light, which is also sensed by green receptors, are mediated mainly by compound-eye photoreceptors containing *Amlop1* but not by the ocellar system, i.e., by *Amlop2*. Accordingly, 24 hours later, *white* and *Amlop2* mutants exhibited an aversive memory for the punished color that was comparable to control bees but *Amlop1* mutants exhibited no memory. We discuss these findings in terms of chromatic vision and in terms of the consequences that the induced mutation might have on other mechanisms of neural signaling.

Results

Different patterns of expression of green-sensitive opsins *Amlop1* and *Amlop2* in the visual system of the worker honey bee

We first designed primers for *Amlop1* and *Amlop2* to characterize their pattern of spatial distribution in the peripheral visual system. Figure 2a shows the sequences of these two opsin genes, highlighting common in black and different nucleotide sequences in green. Primers were designed based on the reported sequences of these opsin genes [17,39] using Primer BLAST (NCBI, Bethesda, USA). Two-step PCR amplification was used to ensure high fidelity in the synthesis of special DNA sequences and the T7 RNA polymerase promoter.

Our results confirmed that these two opsins are strictly segregated, with *Amlop1* being confined to the compound eyes and *Amlop2* to the ocellar system. *Amlop1* mRNA was found to be expressed exclusively in compound-eye ommatidia with a within-ommatidium pattern that was described previously [19], i.e. the *Amlop1* probe labelled 6 photoreceptor cells per ommatidium in the entire compound eye (Fig. 2b). Conversely, no trace of *Amlop2* was detected in compound-eye ommatidia while it was clearly expressed in the ocellar system [20]. No trace of *Amlop1* expression was detected in the ocelli (Fig. 2d). These results thus suggest that different visual processes are mediated by the two types of green-sensitive photoreceptors located in the ocelli and in the compound eyes, respectively.

CRISPR/Cas9 generation of *Amlop1, Amlop2* and *white gene* mutants in the honey bee

We next used a CRISPR/Cas9 approach to produce adult honey bee workers with insertions or deletions leading to nonfunctional proteins of *Amlop1*, *Amlop2* and of the *white gene*, which controls the external coloration of compound-eye facets. The latter thus provided a control visible to the naked eye for the efficiency of our CRISPR/Cas9 procedure. Freshly laid eggs were injected with a mixture of 100 ng/μl of sgRNA and 300 ng/μl of Cas9 protein within 1 h post laying. Control animals were injected with control sgRNA which doesn't target any gene in the honeybee genome (see material section). In our control group, around 82% of all eggs injected survived the injection. The treatment showed a 72% (*Amlop2*) and 21% (*Amlop1*) hatching rate and a survival rate to the adult stage of 63% and 30% (see Table 1), which is above average of reported values for other CRISPR/Cas9 studies on honey bees[25,26,28,29].

White-gene mutants could be easily detected due to the presence of white spots in different regions of the compound eyes (Fig. 3b,3c), thus showing that the CRISPR/Cas9 procedure was effective to induce mosaic mutants. In the case of the *Amlop1* and *Amlop2* mutants, the presence of mutations could be only determined *a posteriori* of visual-conditioning (i.e., in 7-day old adult bees having being subjected to conditioning and to a 24-h retention test; see below). Genomic analyses performed on *white-gene*, *Amlop1* and *Amlop2* mutants showed that impurity peaks (base pair mismatch) occurred in the target region (Figs. 3d-3f). Only bees containing multiple base-pair mismatches in the target region were identified as mutant bees as these mismatches would lead to reading frameshifts (nonsense code) and produce non-functional proteins. These results show that our CRISPR/Cas9 was successful, which was confirmed by the percentage of adult mutants obtained, after verification following behavioral experiments (see Table 1).

Visual avoidance learning and retention performances of CRISPR/Cas9 *Amlop1, Amlop2* and *white gene* mutants

All 7 days-old adult bees were tested for their learning and retention responses in a passive-avoidance task in which they had to suppress positive phototaxis. After behavior experiments and genomic analyses, we first verified that mutants did not differ in size from normal control bees, as otherwise the contact with the grids establishing the floor and ceiling of the setup through which electric shock is delivered would be reduced and the efficiency of the punishment reduced. The inter-wing distance (dorsal thorax) of mutants and control bees was quantified as it provides a good proxy of bee size. No significant differences were found between control group and mutant bees' groups (Fig. 4; one-way ANOVA for Dunnett's multiple

comparisons test, $F_{(3, 45)} = 1.765$; P=0.1675), thus showing that the CRISPR/Cas9 procedure did not induce morphological variations in mutant bees.

Bees were placed in a two-compartment box (Icarus Setup) [38] in which they had to learn to inhibit spontaneous attraction to a compartment illuminated with blue light paired with electric shock delivery upon entering in that compartment [38] (Fig. 4A, left). In this setup, learning is visible through an increase in the latency (s) to enter the blue compartment due to its association with shock. Despite the fact that we generated *Amlop1* and *Amlop2* mutants, green light could not be used to train them as preliminary experiments showed that normal bees cannot learn to inhibit their attraction towards green light despite repeated shock experiences although they do it in the case of blue light (see Supplementary Fig. S2). Indeed, the latency (s) to enter the green-lit compartment did not change along trials both in a paired group that experienced green light associated with shock and in an unpaired group that experienced non-contingent green light and shock (Two-way repeated measurement ANOVA; Interaction Trials*Groups: $F_{(7, 217)} = 0.80$, P=0.59). The latency in the paired group was slightly higher than that in the unpaired Group (Factor Groups: $F_{(1,31)} = 4.57$, $P < 0.05$). In agreement with this absence of learning, a 24-h retention test in the absence of shock showed no significant differences in the latency (s) to enter the green-lit compartment vs. a novel blue-lit compartment both in the paired group and in the unpaired group (Wilcoxon Signed Rank test; paired: W= 31, P = 0.44; unpaired: W= -41, P=0.35). In consequence, we trained bees with a blue-lit compartment paired with shock because bees learn efficiently to avoid blue light paired with shock in this setup and because green-light perception engages also the green photoreceptor (see Fig. 1b).

Figure (5B, 5C, 5D, 5E, left) shows that the control group, *white* group, and *Amlop2* group increased progressively the latency to enter the blue-illuminated compartment during trials while no change in latency was found in the *Amlop1* group (ANOVA for repeated measurements; Groups: $F_{(3,45)} = 3.51$, P = 0.02). Moreover, we found a significant effect for the interaction of the two factors (Trials × Groups: $F_{(21,315)} = 1.67$, P = 0.03), confirming a difference in the dynamic of responses during trials between groups. A Dunnett's post-hoc test ratified the significant variation of latency between trials 1 and 8 for the control group, *White* group, and *Amlop2* group (control: mean diff = −133.7, P < 0.05; *White*: mean diff = −118.0, P < 0.05; *Amlop2*: mean diff = −115.5, P < 0.05) and the absence of difference for the *Amlop1* group (*Amlop1*: mean diff = −9.37, P = 0.14). Thus, control bees, *White* bees and *Amlop2* bees learned to avoid the blue light because of its association with shock punishment. Bees from the *Amlop1* group did not change their performance along with trials.

All groups were tested for 24-h memory retention following conditioning. Figure (5B, 5C, 5D,

5E, right) shows the test performances of the different groups in the absence of shock and in terms of the latency to enter the blue-lit and a green-lit compartment, which was offered to test memory specificity. The latency to enter the blue-illuminated compartment remained higher than the latency to enter the green-illuminated compartment in the control group, *White* group, and *Amlop2* group (Wilcoxon signed-rank test; control: W = -171.0, P < 0.01; *White*: W = −52, P = 0.04; *Amlop2*, W = -55, P < 0.01) while no significant difference was found in the *Amlop1* group (*Amlop1*, W = -29, P = 0.10), thus confirming the presence of a 24-h memory in control bees, *White* bees, and *Amlop2* bees but not in *Amlop1* bees, which did not learn and had no memory in consequence. These results indicate that inhibitory responses to blue light, which is also sensed by green receptors (see Fig. 1), are mediated mainly by compound-eye photoreceptors containing *Amlop1* but not by the ocellar system in which photoreceptors contain *Amlop2*.

To verify this conclusion, we performed an additional experiment in which we trained and tested control forager bees having either the compound eyes or the ocelli covered by acrylic black paint. We reasoned that covering the ocelli should not affect inhibitory learning of the blue light in the Icarus setup, while covering the compound eyes would suppress learning, consistently with the performances of our *Amlop2* and *Amlop1* mutants.

Three groups of bees were established: Control group, uncovered bees (n = 16); Ocelli Covered group, bees with covered ocelli (n = 19); Compound Eyes Covered group, bees with covered compound eyes (n = 17). Figure (6B, 6C, 6D, left) shows that the Control group and Ocelli Covered group increased progressively the latency to enter the blue-illuminated compartment during trials while no change in latency was found in the Compound Eyes Covered group (ANOVA for repeated measurements; Groups: $F_{(2,49)} = 5.56$, P < 0.01). This different pattern of responses resulted in a significant interaction of the two factors (Trials × Groups: $F_{(14,343)} = 2.71$, P < 0.01). A Dunnett's post-hoc test confirmed that the latency increased significantly along trials in the Control group and the Ocelli Covered group (Control: mean diff = −47.87, P = 0.03; Ocelli Covered: mean diff = −44.59, P = 0.03) but not in the Compound Eyes Covered group (mean diff = −7.26, P = 0.17). Thus, having free, functional compound eyes (Control bees and Ocelli Covered bees) allowed to solve the learning task while covering them with light-proof black paint suppressed learning even if the ocelli were available.

Figure (6B, 6C, 6D, right) confirmed these findings for the 24-h retention test. The latency to enter the blue-illuminated compartment remained higher than the latency to enter the green-illuminated compartment both in the Control group and in the Ocelli Covered group (Wilcoxon

signed-rank test; Control: W = -122, P < 0.01; Ocelli Covered: W = −178, P < 0.01), thus confirming the presence of a color memory in these bees. In the Compound Eyes Covered group, a significant difference was also found but due in the opposite direction, i.e., the covered-eye bees had a higher latency to enter the green compartment than the blue one (W = 127, P < 0.01). Although this result may appear counterintuitive given that blue light was paired with shock it can be understood by considering that with only the ocelli available, these bees did not perceive colors (ocellar photoreceptors do not feed onto color opponent neurons) but just different light intensities. As they have only UV-sensitive and green photoreceptors in the ocelli, the blue light may have stimulated green photoreceptors and to a lower extent (see spectral sensitivity curves) the UV receptors. These bees may have therefore learned that high-light intensity perceived via the green-receptor channel was associated with punishment irrespective of its chromatic quality. They therefore tended to avoid green light more than the blue light itself. These results thus confirm that the discrimination task learned by the bees in the ICARUS setup was a chromatic discrimination requiring the compound eyes and their associated photoreceptors (here *Amlop1*) but not the ocelli and their associated photoreceptors (i.e., n*ot Amlop2*), a conclusion that is in line with the results obtained from the mutants we generated *via* the CRISPR/Cas9 procedure.

Discussion

Our results confirm the spatial separation of *Amlop1* and *Amlop2*, with the former being confined to the compound eyes and the latter to the ocelli [20]. The reasons for this divergence are unclear and when the presence of two green-sensitive opsin genes was first reported in other Hymenopterans (*Bombus impatiens, B. terrestris, Diadasia afflicta, D. rinconis, and Osmia rufa,*) it was argued that the second gene, unknown until then contrary to the retinal one, evolved at a lower rate [40]. Yet, this report did not analyze where these genes were expressed in the visual system. One year later, Velarde et al [20], reported for the first time the presence of *Amlop2* in worker honey bees and referred its expression to the ocellar system. We confirmed this finding (Fig. 2) and developed a CRISPR/Cas9 procedure to knock out alternatively these opsin genes and determine the impact of this knock-out on an aversive visual conditioning task [38]. In parallel we applied the same procedure to the *white* gene to obtain a visible readout of CRISPR/Cas9 efficiency.

Mutants and control bees kept in a dark compartment were conditioned to avoid a blue-lit compartment to which they were initially attracted following its association with electric shock

[38]. Blue light had to be used for this task despite the fact that green light would be in principle ideal to determine a possible loss of sensitivity in *Amlop1* and *Amlop2* mutants. This choice was due to the fact that our preliminary experiments showed an incapacity of normal bees to learn the association between green light and electric shock. Despite receiving repeated the electric shock upon entering a green-illuminated compartment, normal bees did not increase their latency and continued entering the punished compartment as if they were incapable of learning (Fig. S2). Reducing the intensity of the green light did not change this response pattern (not shown), thus suggesting that the massive presence of green-sensitive photoreceptors in the compound eyes of bees, which exceeds largely that of ultraviolet and blue-sensitive photoreceptors (6 from 9 photoreceptors available per compound-eye ommatidium are green-sensitive), was responsible for an enhanced sensitivity and responsiveness to green light, inducing spontaneous attraction. It seems, therefore, that attraction to green light was too strong to be inhibited via aversive learning. Thus, we chose to stimulate the bees with blue light as in this case normal bees learn the association between light and electric shock and increase progressively their avoidance of the blue compartment and because blue light is also sensed via the green-sensitive photoreceptors; this is due to the relatively large and high spectral sensitivity of green photoreceptors in the blue domain (see Fig. S1) but essentially to the color opponent processes that are responsible for creating color sensations and which occur in the brain via the antagonizing responses of color opponent neurons [41–43]. Input to these neurons, and thus color sensations, were intact in normal bees but would suffer profound modifications in mutants missing the green-sensitive channel.

The CRISPR/Cas9 procedure applied to *white* and *opsin* genes

Our results indicate that our CRISPR/Cas9 procedure was effective and yielded mosaic mutants for the genes we targeted. Although the CRISPR/Cas9 knock-out technique has already been employed successfully in the honey bee[25–34], few studies have focused on sensory receptors, for instance, gustatory receptor *AmGr3* [26] and olfactory co-receptor gene [25]. The results of Laura Değirmenci demonstrate that *AmGr3* is a highly specific fructose receptor in the honeybee [26]. The results of Chen zhenqing suggest that neurodevelopmental effects of *orco* are related to specific insect life histories [25]. In addition, no CRISPR/Cas9 study had addressed the visual modality of honey bees so far. Our procedure allowed us to create *Amlop1* and *Amlop2* adult mutant bees and *white* mutants[36,37] as a control for the efficiency of our method. The *white* gene

controls the external coloration of compound eyes, thus providing a direct readout of mutation efficiency.

In the honeybee, the first report on genetic editing showed that the sperm-mediated transformation method allows to introduce foreign DNA constructs into the bee genome [44]. Then, Schulte et al. reported that highly efficient integration and expression of piggyBac-derived cassettes that could be stably transmitted by certain queens (between 20% and 30%) to their offspring [45]. The first report of CRISPR/Cas9 use in honey bees was produced by the group of Takeo Kubo in 2016 [28]. Hu et al (2019) improved CRISPR/Cas9 gene-editing efficiency in more than 70% in a study that targeted the *Mrjp1* gene and the *Pax6* gene, a transcription factor involved in developmental processes[27]. The first morphological honey bee mutants induced via CRISPR/Cas9 showed that the response to nutrition relies on a genetic program that is switched "on" by the feminizer (*fem*) gene [33]. Laura Değirmenci firstly performed behavior experiment using mutant adult bees [26].

Here, we summarized three major improvements in our honeybee gene editing system as follows:

First, optimize the protocol to collect bee egg. The bee researchers have done a lot of work on bee egg collection [46–51]. The current more mature method is to establish multiple small nuclear colonies, and the queen bee is caged in a special queen-limited plastic box that allowed worker bees to enter freely. The back of this plastic frame is a removable wax cup. After limiting the queen bee to lay eggs for 2 hours, remove the wax cup to collect bee eggs. This method was used in several articles [45,27,33,26,25]. The limitation of this method is that the queen bees do not like to lay eggs in the plastic frame [26]. And due to seasonal conditions, this method can only be carried out in the breeding season of the bee colony (about 3 months). Moreover, it cost a lot of manpower and material resources. In order to solve such problems, we adopt new bee frames and cage the queen bee on the fresh frames to lay eggs. Usually, the queen bee can lay thousands of eggs in 24 hours. We then remove the eggs from the restricted area and leave some of the marked eggs as bait to lure the queen to lay eggs. This method can ensure that the queen bee can lay eggs when the outdoor temperature is above 20°. For instance, we can collect honeybee eggs every day for up to 7 months. In addition, an average of hundreds of bee eggs can be harvested every day from one or two normal bee colonies.

Second, optimize microinjection of bee eggs. On the basis of previous research [45,33,26,25], we have further optimized. The previous research used a manual syringe, which can adjust the injection angle 360°. Since the color of the bee eggs is close to the color of the injection needle,

it is difficult to control the depth of injection, which brings great difficulties to the novice injecting bee eggs. Without thousands of practices of injecting bee eggs, it would be difficult to do the job [26]. By fixing the injection angle, we also fixed the arrangement angle of the bee eggs to avoid inconsistent injection angles caused by manual syringes. In other words, we standardize the injection process. Lowered the learning threshold for injection. We have up to a 95% hatching rate after injecting water.

Third, optimize *in vitro* rearing protocol of injected honey bee larvae. There are currently many protocols for *in vitro* rearing of injected honey bee larvae [52,53]. But so far, no laboratory protocol has been seen from bee eggs after microinjection to adult bees. The difficulty is mainly in the transition from bee eggs to small larvae. Normally, bee eggs after injecting a mixture of sgRNA and Cas9 protein have a certain degree of delayed hatching [27,26]. The transfer of eggs after hatching inflicts a great deal of death and injury. Researchers inject thousands of bee eggs to get a small number of adult bees [26]. In order to prevent the hatched larvae from starving to death, we put a layer of food on the bottom of the small larvae to be hatched that day, so that the hatched small larvae will fall on the food. This solves the problem of high mortality from bee eggs to larvae.

Sensory processes mediated by *Amlop1* and *Amlop2*

The present results show that the aversive conditioning supposed to induce phototaxis inhibition is mediated exclusively by visual information from the compound eyes and not from the ocelli, i.e., by *Amlop1* and not by *Amlop2* photoreceptors. This conclusion was confirmed by the control group in which these structures were covered by black paint. Suppressing the ocelli did not affect visual learning and memory retention in the aversive task assayed. This result is interesting as ocellar photoreceptors are considered as light-intensity sensors participating in the phototactic response of bees in addition to the compound eyes-. Moreover, phototaxis has been characterized as a color blind behavior, which relies exclusively on light intensity irrespective of its chromatic context[44]. The fact that bees discriminated the punished blue light from a novel green light despite their equivalent intensity shows that bees were in fact not learning to inhibit phototaxis but learned to associate a chromatic cue with punishment. Their increased latency to enter the blue-lit compartment was not extended to the green light, thus showing that the visual process engaged in our ICARUS setup was one of true color vision. As such, it makes sense that the integrity of the compound eyes, which are responsible for color

vision processes, is required to learn and memorize the task. It can be therefore suggested that while *Amlop1* photoreceptors mediate both phototaxis and color vision, *Amlop2* photoreceptors mediate only pure phototactic responses. This last conclusion is confirmed by retention performances of the bees with the compound eyes covered by black paint which had access to visual information only through the ocelli. Ocelli specific opsin genes are present in almost all insect species possessing three ocelli [54] (e.g. dragonflies [55], bumblebees [40], scorpionflies [56], cricket [15], cockroach [57], Drosophila [58]). Many studies reported that ocelli have important roles in celestial navigation [59–61], light polarization [61], circadian rhythm [62,63], and detection of variation in light intensity that mediates flight activity [64] but they do not mediate color vision. In bees with compound eyes, which had access only to information conveyed by the ocelli, a significantly higher avoidance of green light was observed in the test, even if blue light was paired with shock (see Fig. 6). As only UV-sensitive and *Amlop2* photoreceptors exist in the ocelli, it is possible that light intensity may have been processed mostly by *Amlop2* receptors, thus leading to an association of light intensity perceived through the green channel and electric shock. This scenario may explain the green light avoidance observed in the tests in bees with only the ocelli available.

Knockout of *Amlop1* photoreceptors had a dramatic effect almost comparable to that attained via covering of the entire compound eyes with black paint. This may be due to the massive presence of green-sensitive photoreceptors in the compound eyes of bees which, as mentioned above, is three to six times larger than that of ultraviolet and blue-sensitive photoreceptors. Genomic analyses performed *a posteriori* of conditioning and memory retention tests revealed the clear presence of mutations (see Fig. 3). Yet, these analyses did not reveal extent of the knock out, i.e., the percentage of green-sensitive receptors exhibiting mutations. However, the performance of *Amlop1* mutants was very similar to that of normal bees with compound eyes covered, i.e., with a total absence of visual input, thus suggesting that the quantitative impact of the mutations induced was significant. An important difference existed, nevertheless, between these two cases: even assuming a significant knockout of green-sensitive photoreceptors, *Amlop1* mutants disposed of UV and blue-sensitive photoreceptors and were not, nevertheless, more efficient at learning to avoid the blue light than full blind bees. This result may appear counterintuitive but one should keep in mind that color vision, which guided the bees in this task, is not mediated exclusively by photoreceptor input, but arises at the central level from color-opponent neurons, which combine photoreceptor input in an antagonistic manner. As color sensations are the product of these opponent processes, even with intact blue

photoreceptors the sensation produced by the green light in *Amlop1* mutants would be drastically different due to the massive absence of the green-sensitive input to color-opponent neurons.

Perspectives

In diamondback moths *Plutella xylostella,* CRISPR/Cas9 knockout of the long-wavelength-sensitive opsin (LW-opsin), which is green-sensitive, with a peak absorbance between 500 and 600 nm, resulted in deficits in phototaxis and locomotion which varied according to the sex [65]. In our case, only female worker mutant bees were generated and tested behaviorally. It would be interesting to achieve similar experiments with drones (males) in order to determine if sex-specific differences can also be observed in our behavioral assays. Previous results have suggested that opsin distribution in the compound eyes of drones may be drastically different from that of bees [20]. Considering this difference, behavioral performances in the ICARUS setup are expected to differ between both intact and mutant worker and drone bees.

Generation of *Uvop* and *Blop* opsin mutants is now at our reach. This opens attractive perspectives for the functional study of these opsins in multiple behavioral tasks involving chromatic and achromatic vision. Beyond visual studies, the possibility of targeting other sensory receptor genes and other candidate genes is a reality as long as the induced mutations are not lethal. Further studies will allow exploring these possibilities and answering specific questions at the single or multiple gene level.

Materials and Methods

In situ hybridization analyses of *Amlop1* and *Amlop2* expression in the visual system of honey bee workers

Primers for *Amlop1* and *Amlop2* were designed based on the reported sequences of these opsin genes [17,39] using Primer BLAST (NCBI, Bethesda, USA) and ordered from Sigma (See Table 1). Two-step PCR amplification was used to ensure high fidelity in the synthesis of special DNA sequences and the T7 RNA polymerase promoter. The first primer pair was used to obtain the specific complementary DNA sequences. The first PCR products were isolated with 1% agarose gel and separated from the gel with QIAquick PCR Purification Kit. The secondary PCR

amplification was performed with the secondary primer pair which is the same as the first primer but with T3 and T7 promoters attached to the 5′ and 3′ primers, respectively. Purified PCR products were used as the template for *in vitro* transcription. Synthesis of riboprobes and digoxigenin-labeling were performed by means of *in vitro* transcription using Roche RNA Labeling Mix. Probes were around 400 bases in length. For *in vitro* transcription, the reaction solution with a final volume of 20 µl was prepared with the following components: 1 µg purified template DNA, 2 µl 10x NTP labeling mixture, 2 µl 10x Transcription buffer, 1 µl RNase Inhibitor, and 2 µl RNA Polymerase T7 or T3. The reaction was incubated at 37°C for 2 h. The RNA probe was purified with MEGA shortscript™ T7 Transcription Kit and was stored at −80°C before use.

Bee's brains are dissected in a 4% paraformaldehyde (PFA-PBS) and kept in 4% PFA (PBS) for 12 hours. The next day, brains are rinsed in (PBTX). Dehydration step by successive baths of methanol/PBTX (25%, 50%, 75%, 50%, 25%) for 20 min each is performed. The proteinase K should be diluted to 1/2000 in the PBTX and incubated for 105s at 20 °C. After rinsed, bee brains were incubated with a total volume of 500 µl hybridization buffer (50% Formamide, 5X SSC, 2% Blocking Reagent, 0.1% Triton, 0.5% CHAPS, 1 mg/ml yeast RNA, 5 mM EDTA, 50 g/ml Heparin) at 62°C for 12 h. 3 µl (50 ng) of antisense and sense probes (control) are diluted in 30 µl of hybridization buffer. They are denatured at 95°C for 5 min, then placed immediately on ice and added to 500 µl of pre-heated hybridization buffer. The brains are then added to the 530 µl of the solution containing the probe and left at 62°C for 48 h. post-hybridization washes were performed with 2× SSC for 30 min, 1× SSC for 30 min, and 0.1× SSC for 60 min at 37 °C. The brains were washed with 4 washes of 5 min at 62°C in a wash solution (Formamide 50%, 5X SSC, 0.1% Triton, 0.5% CHAPS), then a mixture of wash solution with 2X SSC (with a volumes ratio of 3:1, 1:1, 1:3, in total a volume of 500 µl). Finally, samples are washed in (2X SSC + 0.1% CHAPS) at 62°C followed by another solution (0.2X SSC +0.1% CHAPS) at 62°C and were in PBTX at room temperature. Then the blocking solution (PBTX + 10% goat serum + 2% BSA) was added at 4°C for 3 hours followed by the Anti-DIG antibody at a dilution of 1:2500 in the blocking solution. After 5 washes for 1 hour each at 4°C, the samples were kept in the same wash solution (PBTX+ 0.1% BSA) at 4°C for 12 hours. The next day, 2 washes in PBTX were performed at room temperature followed by three 30 min washes in NTMT (100 mM NaCl, 100 mM Tris-HCl (PH 9.5), 50 mM MgCl2, 0.1% Tween-20). Then, the brains were in the revelation solution (4 µl of 1.45M levamisole, 30 µl of NBT (50 mg/ml) and 21 µl of BCIP (stock 50 mg/ml) are added to 6 ml of NTMT) for 48 hours. Then they were embedded in a GAM (a mix of gelatin and BSA proteins) and glutaraldehyde (25%) matrix for sectioning,

and a vibrating-blade microtome is used (Leica VT1000S) with a speed of 6, frequency of 7-9, and a thickness of 30 μm. Pictures were taken by the Leica Microscopes (Leica DM2500).

Preparation of sgRNA and Cas9 protein for CRISPR/Cas9 knockout of *Amlop1, Amlop2* and *white* genes of honey bee workers

Three Target-specific oligos (*white, Amlop1,* and *Amlop2* genes) are designed on the ChopChop website (https://chopchop.cbu.uib.no/). All target-specific oligos for sgRNA and for PCR are ordered from Sigma. The target sequence for the control sgRNA is 5'-CATCCTCGGCACCGTCACCC-3'. This sequence is within the prokaryotic tetR gene which there is no similar DNA target sequence in the honeybee genome and offered in EnGen® sgRNA Synthesis Kit. The complete CRISPR-F oligo sequence consists of three parts, one T7 promoter at the 5′ end, one target gene site in the middle, and one overlapping sequence at the 3′ end (the basic general formula is 5′-TTCTAATACGACTCACTATA-G(N)20-GTTTTAGAGCTAGA-3′). The common CRISPR-R oligo sequence is included in EnGen® sgRNA Synthesis Kit (5'-AAAAGCACCGACTCGGTGCCACTTTTTCAAGTTGATAACGGACTAGCCTTATTTTAACTTGCTATTTCTAGCTCTA AAAC-3′). The sgRNAs were synthesized using a EnGen® sgRNA Synthesis Kit (NEB) according to the manufacturer's instructions. sgRNAs were purified using the Monarch® RNA Cleanup Kit (50 μg) (NEB). Cas9 protein (EnGen® Spy Cas9 NLS, 20 μM) was purchased from New England Biolabs.

Microinjection of eggs

Freshly laid eggs (within 1h20 min of oviposition) were collected from the honeybee colony. Then, eggs were arranged and fixed in a line on the edge of a beeswax strip under a stereo microscope. 53-mm injection glass capillaries were used for the microinjection (Hilgenberg). The tips of the pipettes were rigid and beveled at a 37° angle and its inner diameter was 5 μm. A mixture of 100 ng/μl of sgRNA and 300 ng/μl of Cas9 protein was injected into individual eggs using a microinjection device (PLI-100, Medical Systems Corporation). In order to get a higher gene mutation rate, we increased the injection time to 240 ms from 120 ms [45]. The injection pressure and the balance pressure were 60 kPa and 5 kPa [45]. This microinjection step was completed within 40 minutes. Honeybee eggs after injection were put into incubater at 35°C and 95% relative humidity for around 72 hours. Normally, honeybee eggs injected with the mixture of target sgRNA and cas9 protein have a delayed hatching phenomenon of several hours.

Artificial rearing of honey bees

Rearing procedures of honeybees' larvae was followed as previously reported protocol with some modifications [53]. Freshly hatched larvae were transferred to a Petri dish (diameter 3 cm) with 2ml diet A (44.25% royal jelly, 5.3% glucose, 5.3% fructose, 0.9% yeast extract, and 44.25% sterile water) for two days. New fresh diet A was added on the third day. On the fourth day, all larvae were moved in 48-well plates (Thermo Fisher) filled with 30 ul the worker larval diet C (50% royal jelly, 9% glucose, 9% fructose, 2% yeast extract, and 30% sterile water). 40 ul and 50 ul were fed with fresh diet C on the fifth day and sixth day. The closed 48-well plates were placed in a separate box in the incubator at 35 °C with 90% relative humidity for the duration of larval development. Mature larvae will spin silk cocoons to cover themself when they are going to the pupae stage. The condition for the incubation of pupae was 34.5 °C with 75% relative humidity. Once adult's emergence, the adult bees were individually marked with colored number plates using super glue. And they were placed in one frame with honey and pollen from the honeybee colony for one day. The next day, they were placed into a cage with pollen and sugar water (50% sucrose, w/v). The fresh pollen and sugar water should be updated every day until the end of the experiment. The condition for the incubation of adult bees was 28 °C with 50% relative humidity.

Genomic analyses for mutation detection

After finishing the behavioral experiment, Genomic DNA was extracted from abdomen of adult bees using PureLink TM Genomic DNA Mini Kit (Invitrogen). The gene-specific primers (see table 2) were used to amplify the target region. Phusion High-Fidelity DNA Polymerase (Invitrogen) was used for PCR amplification. PCR was performed using 95 °C for 3 min as initial step, followed by 35 cycles of amplification (95 °C for 30 s, 60 °C for 30 s, 72 °C for 60 s) and a final extension at 72 °C for 10 min. And then PCR products were purified with QIAquick PCR Purification Kit (QIAGEN) for sequencing directly or for further sequencing by cloning into a plasmid vector to determine the exact indel types. A stretch of typical multiple peaks of PCR products is the representative character of mutated G0 individuals. Mutagenic events were detected by sequencing the amplification products. Impurity peaks in the target region mean base pair mismatch. Only the bees containing base pair mismatch in the target region were identified as mutant bees.

Aversive visual conditioning experiments

The behavioral experiments followed the procedure previous used in a study that established the aversive conditioning used in our work [38]. The conditioning apparatus, termed ICARUS, consisted in a plastic rectangular box (14 cm × 7 cm × 0.8 cm, on the inside) made of two chambers connected by a small passage (1 cm width) (see Fig. S1). The floor and ceiling were two metallic grids connected to a hightension generator that allowed delivering an electric shock (1.3 kV, 65 μA, 200 msec) to the bee. The space between them was reduced so that the bee could only walk but not fly within the setup. Each chamber was surrounded by a set of 19 RGB LEDs (λ^{blue} = 464 nm, λ^{green} = 523 nm, and λ^{red} = 640 nm; Fig. S1) controlled by an Arduino Mega. In this way, both chambers could be lit in the same color, or in different colors. Red color was chosen to provide the equivalent of a dark surrounding to the bees given the absence of chromatic sensitivity in this range of the spectrum [66].

During a phase of familiarization, the bee was allowed to explore freely the two chambers of the setup (under dark conditions, red-illuminated) for 5 min before the beginning of the first conditioning trial. A conditioning trial began when the compartment opposite to the one occupied by the bee was illuminated with a blue light. This only happened when the bee was located facing the wall opposite to the passage connecting the two compartments. This procedure allowed standardizing the position and distance to cross between bees. When the blue light was turned on, the bee driven by its innate positive phototaxis entered into the blue-illuminated compartment and received the electric shock during 200 msec. Two seconds after shock offset, the light was switched to red (only red-light illumination remains). If 5 min after blue-light onset the bee did not enter the blue-illuminated chamber, the light was turned off and the trial finished without electric shock. This means that every trial had a possible maximal latency of 5 min. The intertrial interval was 1 min during which only red illumination was present. Overall, training consisted of familiarization and eight trials spaced by seven intertrial intervals. In all cases, we quantified the latency to enter into the blue-lit compartment, which is a proxy of learning and memory. At the end of the training session, each bee was placed inside a 5 mL pierced plastic syringe and immediately fed with 5 μL of 50% (w/w) sugar solution. The solution was renewed every 3 h until the last feeding of the day, which took place at around6 p.m. and which consisted of 20 μL of 50% sugar solution to overcome the night. The syringes containing the bees were placed in an incubator at 28°C and 50% until the 24 h test session. In the morning of the test-session day, bees were fed with 10 μL of 50% sugar solution, and if the test session occurred more than 3 h later, 5 μL of 50% sugar solution was further supplied. Two memory-retention tests were performed 24 h after the end of conditioning. The test session

included a familiarization period of 5 min inside the setup under red-light conditions, which was followed by the first test. This test was identical to a conditioning trial with the difference that no-shock was delivered upon entering the blue-lit compartment. Once the test 1 finished, and after an intertest interval of 1 min under red-light conditions, the second test was performed in which green light was used. The main goal of the test with the green light was to demonstrate that the innate phototactic tendency was still present and that the potential increase in the latency to enter the blue- lit compartment in the first test was only due to the previous aversive experience, instead of being due to motor fatigue or loss of light sensitivity, among others. Therefore, the test with green light was performed always after the test with blue light. The intensity of blue light is always equal to the green light in the test.

Statistical analysis

One-way ANOVA for Dunnett's multiple comparisons test was used for comparing the difference in the inter-wing distance (dorsal thorax) of mutants and control bees. Learning curves were analyzed by performing two-way repeated measure analyses of variance (ANOVA) followed by post-hoc analysis using Dunnett's multiple comparisons test when necessary. If the sphericity criterion was not met for the repeated-measurement ANOVA, the GeisserGreenhouse's correction was applied, thus resulting in corrected degrees of freedom for some Fischer statistics. Memory tests were analyzed by performing Wilcoxon signed-rank test on the difference between the latencies to cross toward blue and green-illuminated compartments followed by post-hoc analysis using Dunn's multiple comparisons test when necessary. Statistical analyses were performed using GraphPad Prism 9 software.

Acknowledgements

Contributions

I.M. and M.G. conceived this project. H.G. and S.L performed *in situ* hybridization experiment. H.G. performed CRISPR/Cas9 experiments and behavioral experiments. Statistical analyses on behavioral data were performed by H.G., G.L, and M.P. M.P. and B.P. were involved in behavioral memory experiments. M.B. contributed to the manuscript revision. The manuscript

was written by M.G. who also obtained the funding. All authors reviewed and approved the final version of the manuscript.

Ethics declarations

Competing interests

The authors declare no competing interests.

References

1. Wyszecki, G. & Stiles, W. S. Color science: concepts and methods, quantitative data and formulas. (1982).

2. Osorio, D. & Vorobyev, M. A review of the evolution of animal colour vision and visual communication signals. *Vision Research* **48**, 2042–2051 (2008).

3. Frisch, K. v. Der farbensinn und formensinn der biene. *Zool. J. Physiol.* **37**, 1–238 (1914).

4. Lubbock, J. *Ants, bees, and wasps: a record of observations on the habits of the social Hymenoptera*. vol. 40 (Kegan Paul, Trench, 1882).

5. psychischen Fähigkeiten, D. der Ameisen und einiger anderer Insekten. *mit einem Anhang über die Eigentümlichkeiten des Geruchsinnes bei jenen Tieren.. München* **8**, 57 (1901).

6. Turner, C. H. Experiments on color-vision of the honey bee. *The Biological Bulletin* **19**, 257–279 (1910).

7. Kühn, A. Zum Nachweis des Farbenunterscheidungsvermögens der Bienen. *Naturwissenschaften* **12**, 116–118 (1924).

8. Daumer, K. Reizmetrische Untersuchung des Farbensehens der Bienen. *Zeitschrift fü vergleichende Physiologie* **38**, 413–478 (1956).

9. Menzel, R. Untersuchungen zum Erlernen von Spektralfarben durch die Honigbiene (Apis mellifica). *Zeitschrift für vergleichende Physiologie* **56**, 22–62 (1967).

10. von Helversen, O. Zur spektralen Unterschiedsempfindlichkeit der Honigbiene. *J. Comp. Physiol.* **80**, 439–472 (1972).

11. Autrum, H. Die spektrale empfindlichkeit einzelner Sehzellen des Bienenauges. *Zeitschrift für vergleichende Physiologie* **48**, 357–384 (1964).

12.   Menzel, R. & Blakers, M. Colour receptors in the bee eye— Morphology and spectral sensitivity. *Journal of Comparative Physiology A* **108**, 11–13 (1976).

13.   Peitsch, D. *et al.* The spectral input systems of hymenopteran insects and their receptor-based colour vision. *J Comp Physiol A* **170**, 23–40 (1992).

14.   Brody, T. & Cravchik, A. Drosophila melanogaster G Protein–Coupled Receptors. *J Cell Biol* **150**, 83–88 (2000).

15.   Henze, M. J., Dannenhauer, K., Kohler, M., Labhart, T. & Gesemann, M. Opsin evolution and expression in Arthropod compound Eyes and Ocelli: Insights from the cricket Gryllus bimaculatus. *BMC Evol Biol* **12**, 1–16 (2012).

16.   Shichida, Y. & Matsuyama, T. Evolution of opsins and phototransduction. *Philosophical Transactions of the Royal Society B: Biological Sciences* **364**, 2881–2895 (2009).

17.   Chang, B. S., Ayers, D., Smith, W. C. & Pierce, N. E. Cloning of the gene encoding honeybee long-wavelength rhodopsin: a new class of insect visual pigments. *Gene* **173**, 215–219 (1996).

18.   Townson, S. M. *et al.* Honeybee blue-and ultraviolet-sensitive opsins: cloning, heterologous expression in Drosophila, and physiological characterization. *Journal of Neuroscience* **18**, 2412–2422 (1998).

19.   Wakakuwa, M., Kurasawa, M., Giurfa, M. & Arikawa, K. Spectral heterogeneity of honeybee ommatidia. *Naturwissenschaften* **92**, 464–467 (2005).

20.   Velarde, R. A., Sauer, C. D., O. Walden, K. K., Fahrbach, S. E. & Robertson, H. M. Pteropsin: A vertebrate-like non-visual opsin expressed in the honey bee brain. *Insect Biochemistry and Molecular Biology* **35**, 1367–1377 (2005).

21.   Bassett, A. R., Tibbit, C., Ponting, C. P. & Liu, J.-L. Highly efficient targeted mutagenesis of Drosophila with the CRISPR/Cas9 system. *Cell Rep* **4**, 220–228 (2013).

22.   Basu, S. *et al.* Silencing of end-joining repair for efficient site-specific gene insertion after TALEN/CRISPR mutagenesis in Aedes aegypti. *Proceedings of the National Academy of Sciences* **112**, 4038–4043 (2015).

23.   Baci, G.-M. *et al.* Advances in Editing Silkworms (Bombyx mori) Genome by Using the CRISPR-Cas System. *Insects* **13**, 28 (2021).

24.   Koutroumpa, F. A. *et al.* Heritable genome editing with CRISPR/Cas9 induces anosmia in a crop pest moth. *Sci Rep* **6**, 29620 (2016).

25.   Chen, Z. *et al.* Neurodevelopmental and transcriptomic effects of CRISPR/Cas9-induced somatic *orco* mutation in honey bees. *Journal of Neurogenetics* **35**, 320–332 (2021).

26.   Değirmenci, L. *et al.* CRISPR/Cas 9-Mediated Mutations as a New Tool for Studying Taste in Honeybees. *Chemical Senses* **45**, 655–666 (2020).

27.   Hu, X. F., Zhang, B., Liao, C. H. & Zeng, Z. J. High-Efficiency CRISPR/Cas9-Mediated Gene Editing in Honeybee (*Apis mellifera*) Embryos. *G3 Genes|Genomes|Genetics* **9**, 1759–1766 (2019).

28.   Kohno, H., Suenami, S., Takeuchi, H., Sasaki, T. & Kubo, T. Production of Knockout Mutants by CRISPR/Cas9 in the European Honeybee, Apis mellifera L. *Zoological Science* **33**, 505 (2016).

29.   Kohno, H. & Kubo, T. mKast is dispensable for normal development and sexual maturation of the male European honeybee. *Sci Rep* **8**, 11877 (2018).

30.   Liang, L. *et al.* Expansion of CRISPR Targeting Sites Using an Integrated Gene-Editing System in Apis mellifera. *Insects* **12**, 954 (2021).

31.   Nie, H.-Y. *et al.* CRISPR/Cas9 mediated knockout of Amyellow-y gene results in melanization defect of the cuticle in adult Apis mellifera. *Journal of Insect Physiology* **132**, 104264 (2021).

32.   Otte, M. *et al.* Improving genetic transformation rates in honeybees. *Sci Rep* **8**, 16534 (2018).

33.   Roth, A. *et al.* A genetic switch for worker nutrition-mediated traits in honeybees. *PLoS Biol* **17**, e3000171 (2019).

34.   Sinakevitch, I. *et al.* Anti-RDL and Anti-mGlutR1 Receptors Antibody Testing in Honeybee Brain Sections using CRISPR-Cas9. *JoVE (Journal of Visualized Experiments)* e59993 (2020).

35.   Wang, X. *et al.* Transcriptional Profiles of Diploid Mutant Apis mellifera Embryos after Knockout of csd by CRISPR/Cas9. *Insects* **12**, 704 (2021).

36.   Laidlaw, H., Green, M. & Kerr, W. Genetics of several eye color mutants in the honey bee. *Journal of Heredity* **44**, 246–250 (1953).

37.   Laidlaw, H., El Banby, M. & Tucker, K. Five new eye-color mutants in the honey bee. *Journal of Heredity* **55**, 207–210 (1964).

38.   Marchal, P. *et al.* Inhibitory learning of phototaxis by honeybees in a passive-avoidance task. *Learn. Mem.* **26**, 412–423 (2019).

39.   Leboulle, G. *et al.* Characterisation of the RNA interference response against the long-wavelength receptor of the honeybee. *Insect Biochemistry and Molecular Biology* **43**, 959–969 (2013).

40.   Spaethe, J. & Briscoe, A. D. Early duplication and functional diversification of the opsin gene family in insects. *Molecular Biology and Evolution* **21**, 1583–1594 (2004).

41.   Kien, J. & Menzel, R. Chromatic properties of interneurons in the optic lobes of the bee. *Journal of comparative physiology* **113**, 17–34 (1977).

42.   Backhaus, W. Color opponent coding in the visual system of the honeybee. *Vision research* **31**, 1381–1397 (1991).

43.   Chittka, L., Beier, W., Hertel, H., Steinmann, E. & Menzel, R. Opponent colour coding is a universal strategy to evaluate the photoreceptor inputs in Hymenoptera. *J Comp Physiol A* **170**, 545–563 (1992).

44.   Robinson, K. O., Ferguson, H. J., Cobey, S., Vaessin, H. & Smith, B. H. Sperm-mediated transformation of the honey bee, Apis mellifera. *Insect Molecular Biology* **9**, 625–634 (2000).

45.   Schulte, C., Theilenberg, E., Müller-Borg, M., Gempe, T. & Beye, M. Highly efficient integration and expression of piggyBac-derived cassettes in the honeybee (Apis mellifera). *PNAS* **111**, 9003–9008 (2014).

46.   Taber, S., III. Forceps Design for Transferring Honey Bee Eggs. *Journal of Economic Entomology* **54**, 247–250 (1961).

47.   Milne Jr, C. P., Phillips, J. P. & Krell, P. J. Microinjection of early honeybee embryos. *Journal of apicultural research* **27**, 84–89 (1988).

48.   Omholt, S., Hagen, A., Elmholdt, O. & Rishovd, S. A laboratory hive for frequent collection of honeybee eggs. *Apidologie* **26**, 297–304 (1995).

49.   Collins, A. M. Collection of honey bee eggs for cryopreservation. *Journal of apicultural research* **41**, 89–95 (2002).

50.   Evans, J. D., Boncristiani, H. & Chen, Y. Scientific note on mass collection and hatching of honey bee embryos. *Apidologie* **41**, 654–656 (2010).

51.   Lee, J. & Lee, S. H. Development of a film-assisted honeybee egg collection system (FECS). *Apidologie* **50**, 804–810 (2019).

52.   Kaftanoglu, O., Linksvayer, T. A. & Page, R. E. Rearing Honey Bees, Apis mellifera, *in vitro*: Effects of Sugar Concentrations on Survival and Development. *Journal of Insect Science* **11**, 1–10 (2011).

53.   Schmehl, D. R., Tomé, H. V., Mortensen, A. N., Martins, G. F. & Ellis, J. D. Protocol for the *in vitro* rearing of honey bee (Apis mellifera L.) workers. *Journal of Apicultural Research* **55**, 113–129 (2016).

54.   Guignard, Q., Allison, J. D. & Slippers, B. The evolution of insect visual opsin genes

with specific consideration of the influence of ocelli and life history traits. *BMC Ecol Evo* **22**, 1–9 (2022).

55. Futahashi, R. *et al.* Extraordinary diversity of visual opsin genes in dragonflies. *Proc Natl Acad Sci USA* **112**, E1247 (2015).

56. Böhm, A., Meusemann, K., Misof, B. & Pass, G. Hypothesis on monochromatic vision in scorpionflies questioned by new transcriptomic data. *Scientific reports* **8**, 1–8 (2018).

57. French, A. S., Meisner, S., Liu, H., Weckstrom, M. & Torkkeli, P. H. Transcriptome analysis and RNA interference of cockroach phototransduction indicate three opsins and suggest a major role for TRPL channels. *Frontiers in physiology* **6**, 207 (2015).

58. Pollock, J. A. & Benzer, S. Transcript localization of four opsin genes in the three visual organs of Drosophila; RH2 is ocellus specific. *Nature* **333**, 779–782 (1988).

59. Schwarz, S., Albert, L., Wystrach, A. & Cheng, K. Ocelli contribute to the encoding of celestial compass information in the Australian desert ant Melophorus bagoti. *Journal of Experimental Biology* **214**, 901–906 (2011).

60. Schwarz, S., Wystrach, A. & Cheng, K. A new navigational mechanism mediated by ant ocelli. *Biology letters* **7**, 856–858 (2011).

61. Taylor, G. J. *et al.* The dual function of orchid bee ocelli as revealed by X-ray microtomography. *Current Biology* **26**, 1319–1324 (2016).

62. RENCE, B. G., LISY, M. T., GARVES, B. R. & QUINLAN, B. J. The role of ocelli in circadian singing rhythms of crickets. *Physiological entomology* **13**, 201–212 (1988).

63. Wang, B. *et al.* Evolution and expression plasticity of opsin genes in a fig pollinator, Ceratosolen solmsi. *PLoS One* **8**, e53907 (2013).

64. Eaton, J. L., Tignor, K. & Holtzman, G. Role of moth ocelli in timing flight initiation at dusk. *Physiological entomology* **8**, 371–375 (1983).

65. Chen, S.-P. *et al.* CRISPR/Cas9-mediated knockout of LW-opsin reduces the efficiency of phototaxis in the diamondback moth Plutella xylostella. *Pest Management Science* **77**, 3519–3528 (2021).

66. Reisenman, C. E. & Giurfa, M. Chromatic and achromatic stimulus discrimination of long wavelength (red) visual stimuli by the honeybee Apis mellifera. *Arthropod-Plant Interactions* **2**, 137–146 (2008).
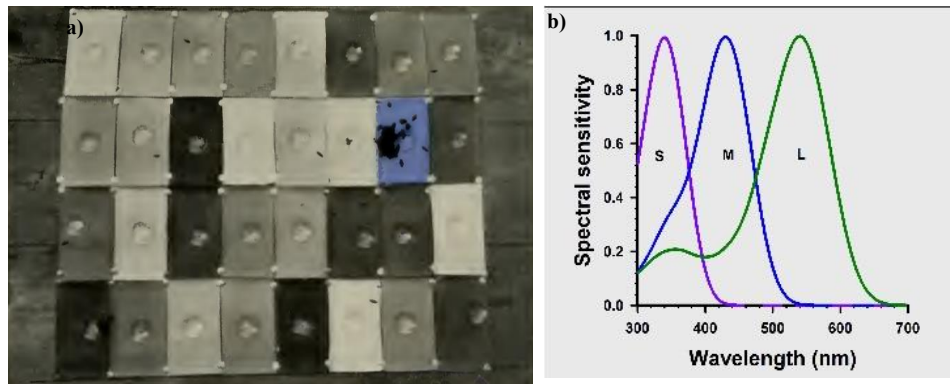
Fig. 1. a) Karl von Frisch's basic experimental design to demonstrate color vision in honey bees [from 19]. Bees were trained to collect sucrose solution on a dish placed on a blue cardboard. Bees chose the trained color and did not confuse it with achromatic alternatives presenting, in some cases, similar intensity. **b)** Spectral sensitivity curves of honey bee photoreceptors, peaking in the UV (S photoreceptor), blue (M photoreceptor) and green range of the spectrum (L photoreceptor).

a)

Compound eye   ocelli
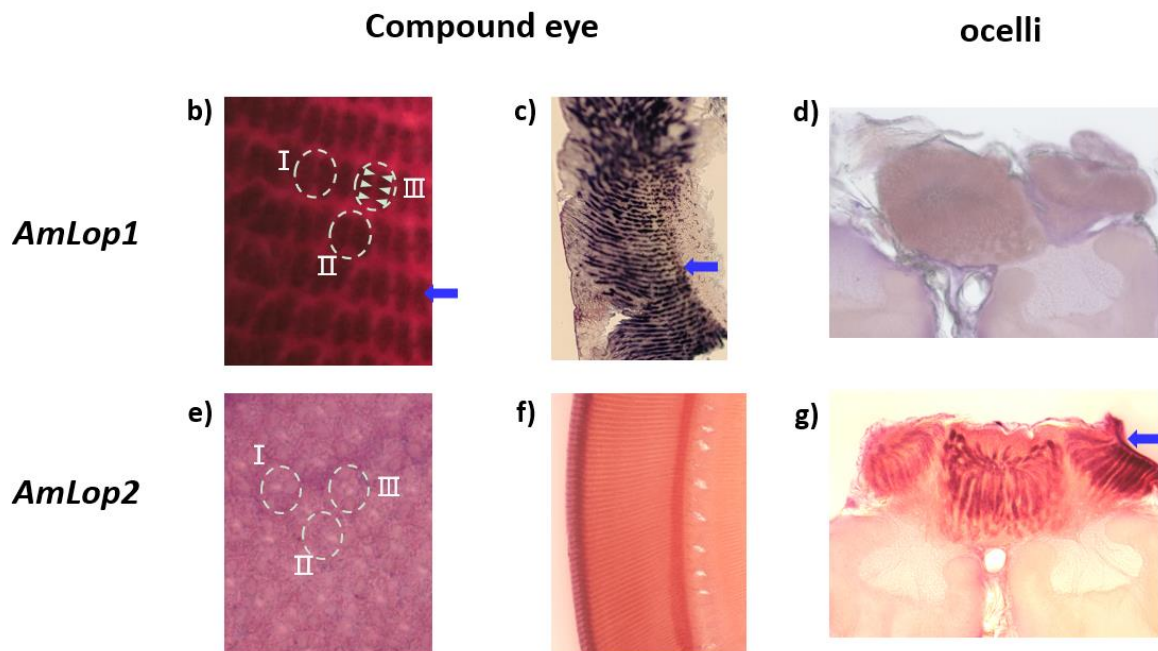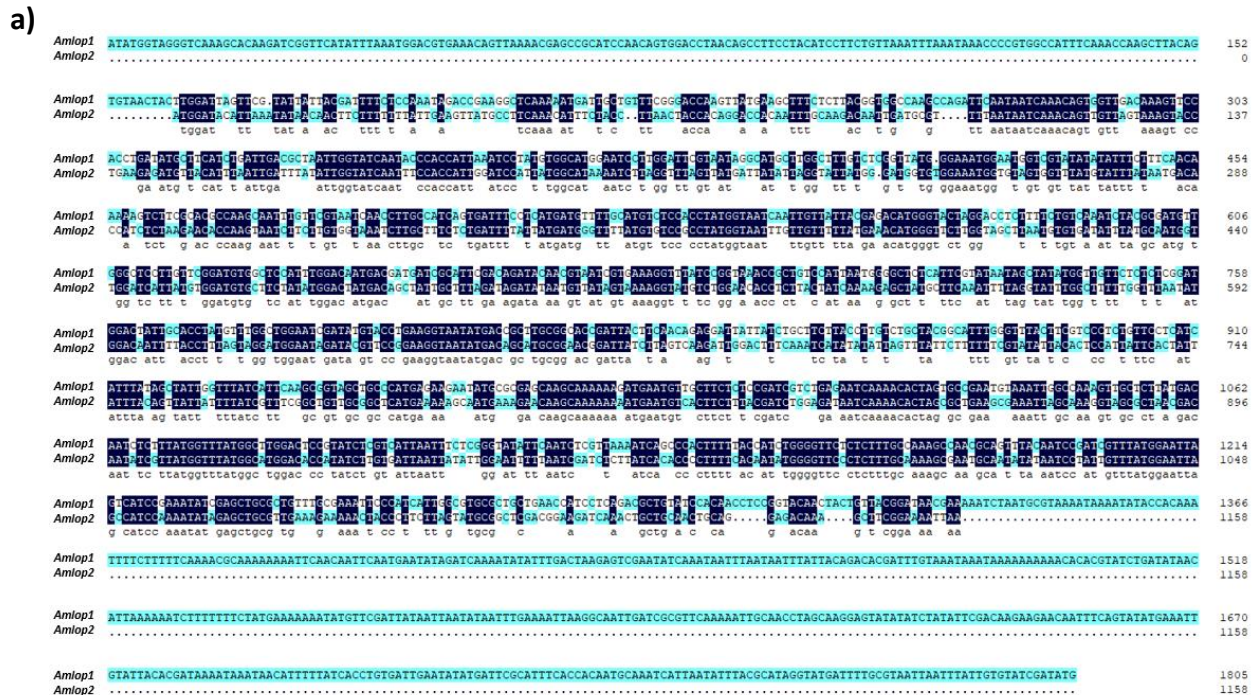
Figure 2. a) The sequences of *Amlop1* and *Amlop2* opsin genes, highlighting common in black and different nucleotide sequences in sky blue. **b)-g)** Distribution of mRNAs encoding *Amlop1* and *Amlop2* in the peripheral visual system of worker honey bees (retina of the compound eye and in ocellar system). Blue arrows show signals obtained via ISH. **(b, e)** show that there are six *Amlop1* photoreceptors in one ommatidia while there is no signal in the ommatidia for *Amlop2*. **(c, f)** show that *Amlop1,* but not *Amlop2,* was present in the retina. **(d, g)** show a reversed pattern in the ocelli. **(b, c, d)** Labelling with *Amlop1 probe*. **(e, f, g)** Labelling with *Amlop2* probe.
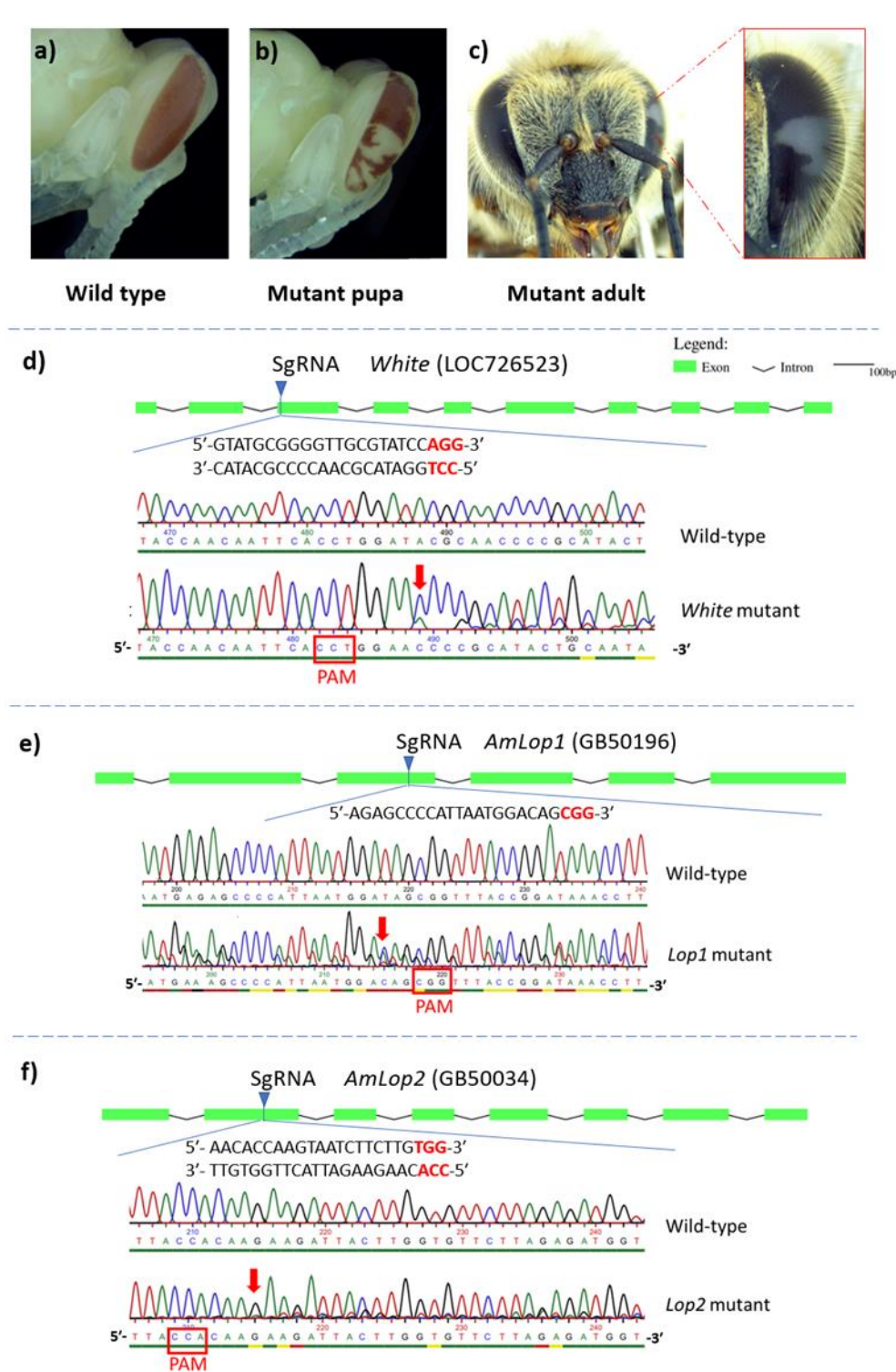
Figure 3. Targeted mutation of honeybee *white* gene and *Amlop1* and *Amlop2* genes by means of CRISPR/Cas9 procedure. Upper row: Targeted mutation of *White* gene induced by CRISPR/Cas9. **a)** wild type in bee pupa. **b)**, **c)** mosaic white compound eyes of *White* gene mutant in bee pupa and adult bee. **d-f)** Position and design of sgRNA target site in *white* gene and the two green-sensitive opsin genes. Schematic diagrams of the gene structure of target genes are shown in the upper part. **d)** *White*. **e)** *Amlop1*. **f)** *Amlop2*. The red box, red arrow, and black arrowhead indicate PAM, the cleavage sites, and the position of the sgRNA target site, respectively. A stretch of typical multiple peaks of PCR products directing sequencing is the representative character of mutated G0 individuals.

Figure 4. Bee body size in control group and mutant groups. The inter-wing distance (dorsal thorax) of bees was quantified for representing bee body size. Error bars correspond to SEM. Same letters on top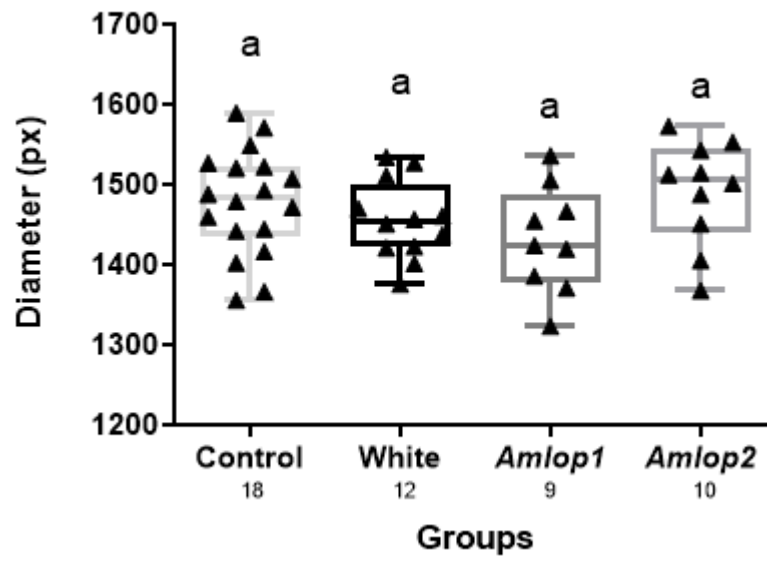 of box plots indicate no significate differences in all groups (one-way ANOVA for Dunnett's multiple comparisons test, $F_{(3, 45)} = 1.765$; P=0.1675).
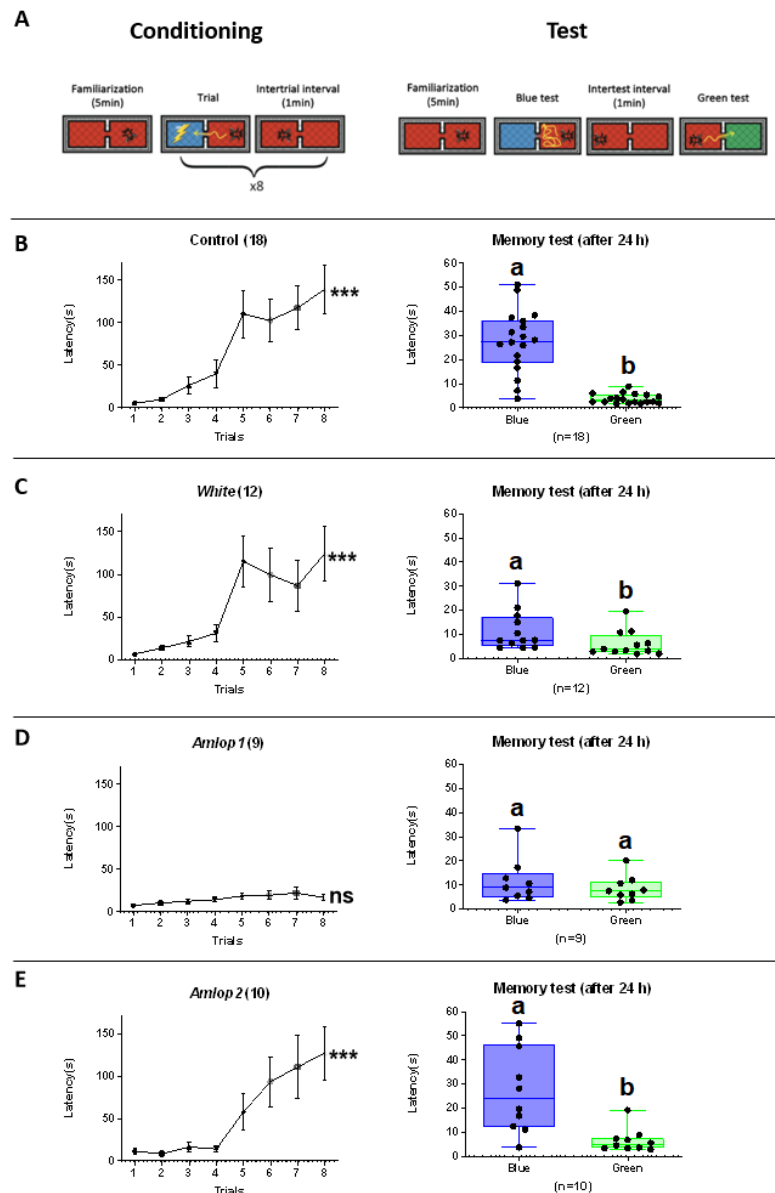
Figure 5. Inhibitory learning of phototaxis in control and mutant bees for the *white* gene and the genes *Amlop1* and *Amlop2*. **(A)** Schematic representation of the experimental protocol. After a familiarization period of 5 min under red light in the setup, bees were subjected to two conditioning protocols in which the latency (s) to enter a blue-lit compartment was measured as a proxy of learning and memory. Each group received eight conditioning trials during which the action of entering the blue-lit compartment was paired with a mild electric shock (1.3 kV, 65 μA, 200 msec). In all groups, trials were separated by intervals of 1 min. Memory retention was tested 24 h after conditioning. The test session consisted of a familiarization period, and two tests separated by 1 min. In the first test, one of the compartments was illuminated with blue light; in the second test, one compartment was illuminated with green light. No shock was delivered during tests. **(B-E)** Left: Learning curves are represented in terms of the latency (s) to enter the blue-lit compartment during conditioning trials for all groups (**B:** Control, **C:** *White*, **D:** *Amlop1*, **E:** *Amlop2*). Right: Memory scores are represented in terms of the latency (s) to enter the blue-lit and green-lit compartments. Error bars correspond to SEM. Different letters on top of box plots indicate significance differences (Paired t-test, two-tailed; p < 0.05).
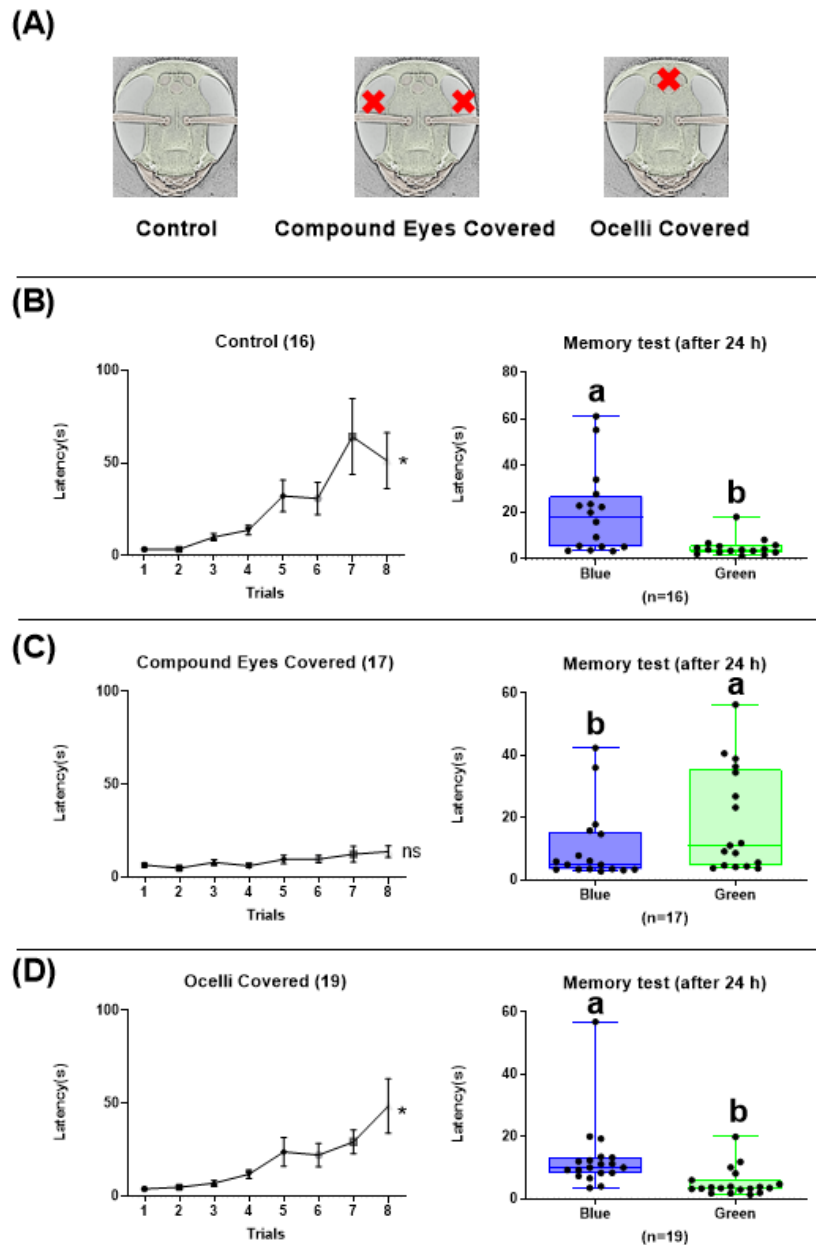
Figure 6. Inhibitory learning and memory of phototaxis in control, Compound Eyes Covered group and Ocelli Covered group. (A) Schematic representation of the three groups' experimental protocol. (B-D) Left: Learning curves are represented in terms of the latency (s) to enter the blue-lit compartment during conditioning trials for all groups (B: Control group, C: Compound Eyes Covered group, D: Ocelli Covered group). Right: Memory scores are represented in terms of the latency (s) to enter the blue-lit and green-lit compartments. Error bars correspond to SEM. Different letters on top of box plots indicate significance differences (Paired t-test, two-tailed; $p < 0.05$)

Table 1. Successive steps in the CRISPR/Cas9 procedure used to produce mosaic worker bees and survival values (absolute and in %) corresponding to each step.

| Groups	Injecting content	Injecting number	Hatching number	Larva number after transfer	Pupa number	Emerging Workers	Adult bees' number after transfer	7 days old adult bees	Learning curve and test	After PCR sequencing
Control	sgRNA+Cas9 protein	161	132(82%)	98	63	48(49%)	33	18	18	18
White	sgRNA+Cas9 protein	232	126(54%)	60	45	36(60%)	22	12	12	12
Amlop1	sgRNA+Cas9 protein	582	120(21%)	69	30	21(30%)	21	14	10	9
Amlop2	sgRNA+Cas9 protein	113	82(73%)	60	43	38(63%)	32	15	10	10

Supplementary Materials
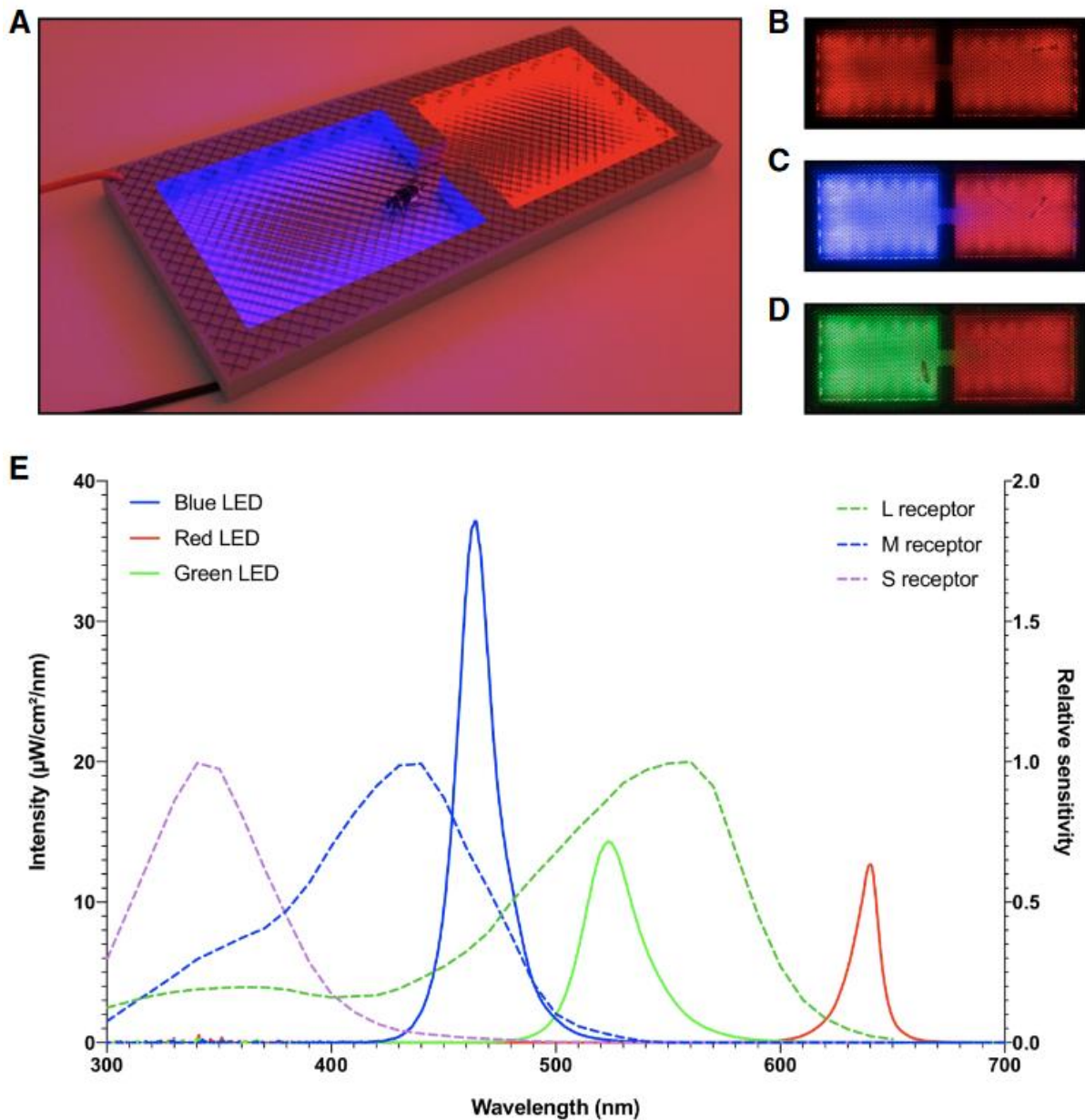
Figure S1. ICARUS—a passive-avoidance setup for inhibitory conditioning of phototaxis in honeybees. **(A)** The ICARUS setup under red light. Red and black cables represent the electrodes connected to upper and lower metal grids by which the shock is delivered. **(B–D)** Top view images of the ICARUS setup taken with the camera used for video recording the experiments. (B) Background stimulation with red LEDs only. **(C)** Illumination of one compartment with blue LEDs. **(D)** Illumination of one compartment with green LEDs. (E) Spectral emittance (continuous lines; left ordinate) of the three types of LEDs used in the setup (blue, green, and red) and spectral sensitivity (dashed lines; right ordinate) of the three types of honeybee photoreceptors (S, M, and L, for short, mid, and long wavelengths, respectively) as a function of wavelength. Spectral analysis of quantum catches—the proportion of incident photons that are captured by the photo-pigments—showed that red LEDs induced negligible activation of photoreceptors (QS = 0.6, QM = 0.64, QL = 1.84) while green LEDs activated mainly the L photoreceptors (QS = 0.84, QM = 3.25, QL = 44.22) and blue LEDs activated both L and M photoreceptors (QS = 0.36, QM = 21.42, QL = 23.19). Quantum-catch values depend on the spectrum of the stimulating light and the spectral sensitivity of the photoreceptor considered; they are used to infer the signal generated at the photoreceptor level.

Figure S2. Inhibitory conditioning of phototaxis to green light. **(A)** Schematic representation of the experimental protocol. Bees were conditioned (paired or unpaired to green light with intertrial intervals of 1 minute and their memory tested 24 h later. **(B)** Learning curves represented in terms of the latency (s) to enter the green-lit compartment during conditioning trials for the 2 experimental groups (Two-way repeated measures ANOVA; Groups: $F_{(1,31)}$ =4.57, P < 0.05; Trials: $F_{(1.215,37.67)}$ =0.843, P = 0.386; Trials*Groups: $F_{(7,217)}$ =0.798, P=0.59). **(C)** Memory scores represented in terms of the latency (s) to enter the green-lit compartment and blue-lit compartments (Wilcoxon Signed Rank test; paired: W= 31, P = 0.441; unpaired: W= -41, P=0.353) (Mann Whitney test: U=106, P=0.292). The memory scores are represented in a logarithmic scale for better visualization. Outliers are shown as black dots.

Table S1. Primers used for PCR amplification from cDNA, PCR products were used for *in vitro* transcription to generate sense (T3) and anti-sense (T7) cRNA probes. Letters in bold type correspond to the T3(black) and T7(red) promoter sequences added to the ends of the specific primer sequences.

Gene (ID)	Primer's name	sequence
Lop1	Lop1-F1	CAAAAAGTCTTCGCACGCCA
(413961)	Lop1-R1	CGAGATACGGAGTCCAAGCC
	Lop1-F1(T3)	**ATTAACCCTCACTAAAGGGA**CAAAAAGTCTTCGCACGCCA
	Lop1-R1(T7)	**TAATACGACTCACTATAGGG**CGAGATACGGAGTCCAAGCC
Lop2	Lop2-F1	TGGGATGGTGTGGAAATGGT
(768250)	Lop2-R1	TCGTTAGCGCTACCTTTGCT
	Lop2-F1(T3)	**ATTAACCCTCACTAAAGGGA**TGGGATGGTGTGGAAATGGT
	Lop2-R1(T7)	**TAATACGACTCACTATAGGG**TCGTTAGCGCTACCTTTGCT

Table S2. Primers used for making sgRNA and for doing genomic analyses.

Primer's name	Primer sequence (5' to 3')	Size bp
B-lop1-1 sgRNA	TTCTAATACGACTCACTATA**GAGAGCCCCATTAATGGACAG**GTTTTAGAGCTAGA	
B-lop1 +2 sgRNA	TTCTAATACGACTCACTATA**GCAGATTCAATAATCAAACAG**GTTTTAGAGCTAGA	
B-lop2 -4 sgRNA	TTCTAATACGACTCACTATA**GAACACCAAGTAATCTTCTTG**GTTTTAGAGCTAGA	
B-lop2 +5 sgRNA	TTCTAATACGACTCACTATA**GTGCCATAATGGATCCAATGG**GTTTTAGAGCTAGA	
control oligo sgRNA	TTCTAATACGACTCACTATA**GGCATCCTCGGCACCGTCACCC**GTTTTAGAGCTAGA	
B-W1 sgRNA	TTCTAATACGACTCACTATA**GAGAATAGGGATAACGTCGA**GTTTTAGAGCTAGA	
B-W2 sgRNA	TTCTAATACGACTCACTATA**GTATGCGGGGTTGCGTATCC**GTTTTAGAGCTAGA	
B-W3 sgRNA	TTCTAATACGACTCACTATA**GGTAATTATGGGATCATCAG**GTTTTAGAGCTAGA	
F-P-LOP1+2	TTTCAAATGGTACTCTGGacgtt	
R1-P-LOP1+2	atatacgaccATTCCATTTCCC	425
R2-P-LOP1+2	ATTTCCCATAACCGAGACAAAG	410
F-P-Lop1-1	GAAATTCTTGTTGCTTGACAGG	
R1-P-Lop1-1	CCTCTGTTGAAGTAATCGGTGC	424
R2-P-Lop1-1	TCCTCTGTTGAAGTAATCGGTG	425
F-P-Lop2-4	gcagGTATCAATTTCCACCATT	
R1-P-Lop2-4	AGCACATCCACATAATGATCCA	389
R2-P-Lop2-4	CCACATAATGATCCAACCATTG	382

Chapter 2

Visual learning in a virtual reality environment upregulates immediate early gene expression in the mushroom bodies of honey bees

Haiyang Geng[1,2,5], Gregory Lafon [1,5], Aurore Avarguès-Weber[1], Alexis Buatois[1,4,6], Isabelle Massou[1,6] & Martin Giurfa [1,2,3,6✉]

Free-flying bees learn efficiently to solve numerous visual tasks. Yet, the neural underpinnings of this capacity remain unexplored. We used a 3D virtual reality (VR) environment to study visual learning and determine if it leads to changes in immediate early gene (IEG) expression in specific areas of the bee brain. We focused on *kakusei, Hr38* and *Egr1*, three IEGs that have been related to bee foraging and orientation, and compared their relative expression in the calyces of the mushroom bodies, the optic lobes and the rest of the brain after color discrimination learning. Bees learned to discriminate virtual stimuli displaying different colors and retained the information learned. Successful learners exhibited *Egr1* upregulation only in the calyces of the mushroom bodies, thus uncovering a privileged involvement of these brain regions in associative color learning and the usefulness of *Egr1* as a marker of neural activity induced by this phenomenon.

Visual learning in a virtual reality environment upregulates immediate early gene expression in the mushroom bodies of honey bees

Haiyang Geng*[1,2], Gregory Lafon[1]*, Aurore Avarguès-Weber[1], Alexis Buatois[1,¥,§], Isabelle Massou[1,§], Martin Giurfa[1,2,3§]

[1] Research Centre on Animal Cognition, Center for Integrative Biology, CNRS, University of Toulouse, 118 route de Narbonne, F-31062 Toulouse cedex 09, France.

[2] College of Animal Sciences (College of Bee Science), Fujian Agriculture and Forestry University, Fuzhou 350002, China.

[3] Institut Universitaire de France, Paris, France (IUF).

* Equal contribution

§ Senior authorship shared

¥ Present address: School of Health and Life Sciences, Pontifícia Universidade Católica do Rio Grande do Sul (PUCRS), Porto Alegre, RS, Brasil.

Corresponding author: Dr. Martin Giurfa

Research Centre on Animal Cognition, CNRS – UPS, 31062 Toulouse cedex 9, France

martin.giurfa@univ-tlse3.fr

Subject Areas: Behavior, Neuroscience

Summary

Free-flying bees learn efficiently to solve numerous visual tasks. Yet, the neural underpinnings of this capacity remain unexplored. We used a 3D virtual reality (VR) environment to study visual learning and determine if it leads to changes in immediate early gene (IEG) expression in specific areas of the bee brain. We focused on *kakusei, Hr38* and *Egr1,* three IEGs that have been related to bee foraging and orientation, and compared their relative expression in the calyces of the mushroom bodies, the optic lobes and the rest of the brain after color discrimination learning. Bees learned to discriminate virtual stimuli displaying different colors and retained the information learned. Successful learners exhibited *Egr1* upregulation only in the calyces of the mushroom bodies, thus uncovering a privileged involvement of these brain regions in associative color learning and the usefulness of *Egr1* as a marker of neural activity induced by this phenomenon.

Keywords: Vision – Visual Learning – Virtual Reality – Honey Bee Brain – Immediate Early Genes – *Kakusei – Hr38 – Egr1* – Mushroom Bodies

Introduction

Invertebrate models of learning and memory have proved to be extremely influential to determine where and when such experience-dependent plasticity occurs in the nervous system[1-6]. One of these models is the domestic honey bee *Apis mellifera,* which has been intensively investigated for its visual and olfactory learning capacities[6-8]. Yet, the knowledge gained on the mechanisms of these abilities is disparate. While an extensive body of research has accumulated on the neural bases of olfactory learning and memory in bees[9], practically nothing is known about the neural and molecular underpinnings of their visual learning and memory[10,11]. This asymmetry is due to the fact that olfactory learning protocols use harnessed bees that learn to extend their proboscis to an odorant that has been forward-paired with sucrose water, while visual learning protocols use free-flying bees trained to choose a visual target where they collect sucrose reward[6,10]. Whilst the harnessing situation of olfactory-learning protocols facilitates the use of invasive techniques to record neural activity, the use of bees that commute freely between the hive and the experimental site precludes an equivalent access to visual neural circuits.

Virtual-reality (VR) environments constitute a novel tool to overcome this limitation. In such environments, tethered bees walking stationary on a treadmill are exposed to a controlled visual environment that allows studying decision making based on visual cues[12-17]. Under these conditions, bees learn and memorize simple and higher-order visual discrimination problems, which enables coupling the study of this visual learning with mechanistic analyses of brain activity[16,17]. VR setups may differ according to the degree of variation introduced by the bee movement into the visual environment. In closed-loop conditions, this variation is contingent with the movements of a tethered bee, thus creating a more immersive environment. In prior works, we introduced a 2D VR environment in which a tethered bee could displace laterally (from left to right and vice versa) a color stimulus on a frontal screen according to its association with sucrose reward of absence of reward[12,14,18]. Here we moved towards a more realistic 3D VR environment which allowed, in addition, for stimulus expansions and retractions depending on forward or backward movements, respectively. In this arena, bees may therefore learn to discriminate colors but can also explore in a less restricted way the virtual world proposed to them.

One way to detect brain regions and pathways activated in this scenario is the quantification of

immediate early genes (IEGs) in neural tissues[19]. IEGs are transcribed transiently and rapidly in response to specific stimulations inducing neural activity without *de novo* protein synthesis[20]. In mammals, IEGs such as *c-fos*, *zif268* and *Arc* are regularly used as markers of neural activity during learning, memory and other forms of cellular plasticity such as long-term potentiation[21-23]. In insects, the use of IEGs as neural markers is less expanded as the number of candidate genes serving this goal is still reduced and the reliable detection of their expression is sometimes difficult[24]. Three of the IEGs reported for the honey bee are interesting as they have been related to a foraging context in which learning plays a fundamental role. The first one, termed *kakusei* (which means 'awakening' in Japanese) is a nuclear non-coding RNA transiently and strongly induced in the brain of European workers by seizures that can be induced by awakening them from anesthesia[25]. It is also activated after the experience of dancing in the hive following a foraging flight and in pollen foragers so that it seems related to the neural excitation resulting from foraging activities[26]. This IEG is activated within a subtype of Kenyon cells, the constitutive neurons of the mushroom bodies, which are a higher-order center in the insect brain[27]. A second IEG is the hormone receptor 38 gene (*Hr38*), which is a transcription factor conserved among insects and other species including humans[28], and which has been indirectly related to learning and memory in honey bees and other insects[29,30]. *Hr38* is also upregulated by foraging experiences in honey bees[29] and bumblebees[30] and by orientation activities upon hive displacement[31]. The third gene is the early growth response gene-1 (*Egr1*), whose expression is induced in the brain of honey bees and bumble bees upon foraging[29,30] and orientation flights[32], and which seems to be controlled by circadian timing of foraging[33]. None of these IEGs has been studied so far in the context of associative learning and memory formation in the honey bee.

We thus focused on these IEGs to characterize neural activation induced by visual learning in the brain of bees under 3D VR conditions. Bees had to learn to discriminate a rewarded color from a punished color[34-37] and should retain this information in a short-term retention test. Our goal was to determine if successful learning and retention activate specifically certain regions in the brain, in particular the mushroom bodies, whose importance for olfactory learning and memory has been repeatedly stressed[6,38], yet with a dramatic lack of equivalent evidence in the visual domain.

Results

Color learning under 3D VR conditions

Honey bee foragers were captured at an artificial feeder to which they were previously trained and brought to the laboratory where a tether was glued on their thorax. (Fig. 1A,B). They could be then attached to a holder that allowed adjusting their position on a treadmill, a polystyrene ball floating on a constant airflow produced by an air pump (see Methods for details). The VR setup consisted of this treadmill placed in front of a semi-spherical semi-transparent plastic screen (Fig. 1A). The movements of the walking bee on the treadmill were recorded by two infrared optic-mouse sensors placed on the ball support perpendicular to each other.

Bees were trained to discriminate a green from a blue vertical cuboid presented against a black background during ten conditioning trials (Fig. 1C; see Supplementary Fig. 1 for color characteristics). Training consisted in pairing one of the colored cuboids (CS+) with a rewarding 1 M sucrose solution and the other cuboid (CS-) with an aversive 3M NaCl solution[39,40] (Fig. 2). Conditioned bees were subdivided according to their test performance to distinguish those which showed successful discrimination (i.e. choice of the CS+; "*learners*") from those which did not ("*non-learners*"). This distinction allowed subsequent brain gene analyses according to learning success. Bees that were unable to choose a stimulus in at least 5 trials were excluded from the analysis. Acquisition was significant for *learners* (n=17) during conditioning trials (Fig. 3A; CS*Trial effect: χ^2=33.68, df:2, p<0.0001), confirming the occurrence of learning. Indeed, the percentages of bees responding to the CS+ and to the CS- differed significantly along trials (*CS+ vs. CS-*: CS*Trial; z=-5.46, p<0.0001). Significant differences were also found when comparing the percentages of non-responding bees against the CS+ responding bees and against the CS- responding bees (*NC vs. CS+*: CS*Trial; z=8.14, p<0.0001; *NC vs. CS-*: CS*Trial; z=4.59, p<0.0001). *Non-learners* (n=18) did also show a significant interaction (Fig. 3B; CS*Trial effect: χ^2=7.66, df:2, p=0.02), but this was introduced by the percentage of non-responding bees. These bees differed significantly along trials both from the bees responding to the CS+ (*NC vs. CS+*: CS*Trial; z=6.10, p<0.0001) and from the bees responding to the CS- (*NC vs. CS-*: CS*Trial; z=6.07, p<0.0001). On the contrary, the percentages of bees responding to the CS+ and to the CS-

did not vary along trials (*CS+ vs. CS-*: CS*Trial; z=-0.07, p=1), consistently with the absence of learning.

We next asked if differences between learners and non-learners could be due to differences in motor components. To answer this question, we analyzed for each conditioning trial the total distance walked, the walking speed, and the tortuosity of the trajectories. Tortuosity was calculated as the ratio between the total distance walked and the distance between the first and the last point of the trajectory connected by an imaginary straight line. When the ratio was 1, or close to 1, trajectories were straightforward while higher values corresponded to sinuous trajectories. The distance travelled (Fig. 4A) did neither vary along trials (*Trial:* χ^2=0.24, df:1, p=0.62) nor between *learners* and *non-learners* (*Condition*: χ^2=1.10, df:1, p=0.30; *Condition*Trial*: χ^2=0.71, df:1, p=0.40). Tortuosity (Fig. 4B) varied along trials (*Trial:* χ^2=14.53, df:1, p<0.001) but not between *learners* and *non-learners* (*Condition*: χ^2=0.08, df:1, p=0.80; *Condition*Trial*: χ^2=0.42, df:1, p=0.52). Finally, the walking speed (Fig. 4C) increased significantly along trials (*Trial:* χ^2=30.49, df:1, p<0.0001) but did not vary between *learners* and *non-learners* (*Condition:* χ^2=1.43, df:1, p=0.23); in this case, however, the interaction between *Trial* and *Condition* was significant (χ^2=4.68, df:1, p<0.05). This suggests that *learners* were slower than *non-learners*, which is reminiscent of a speed-accuracy trade off reported in numerous experiments in bees[41-43].

Finally, in the non-reinforced test, per definition *learners* (n=17; Fig. 3C) chose correctly the CS+ (100% of the bees) while *non-learners* (n=18; Fig. 3D) did either chose the CS- (72.22%) or did not perform any choice (27.78%). We thus focused on differences between *learners* and *non-learners* in the subsequent IEG analyses to uncover possible changes in neural activity induced by learning.

IEG analyses in the honey bee brain following color learning under 3D VR conditions

We aimed at determining if visual learning in VR induces post learning transcriptional changes, which might participate in amplifying neural activity reflecting associative color learning. To this end, we performed RT-qPCR in individual brains of *learners* and *non-learners*, which were collected 1h after the retention test and placed in liquid nitrogen until brain dissection. We analyzed relative expression levels of *kakusei*, *Hr38* and *Egr1* (see Table 1) in three main brain regions[44]

(Fig. 5A): the optical lobes (OL), the upper part of the mushroom bodies (i.e. the mushroom-body calyces or MB Ca) and the remaining central brain (CB), which included mainly the central complex, the subesophageal zone and the peduncula and lobes (α and β lobes) of the mushroom bodies. Two reference genes were used for the normalization, $Ef1\alpha$ (E=106%) and *Actin* (E=110%), which proved to be the best choice for the normalization (see Table 1). The Cq values of these reference genes for the different conditions of this experiment are shown in Supplementary Fig. 2. Stability was granted for both genes and experimental groups (*learners* and *non-learners*) for the MB and the CB. In the case of the OL, $Ef1\alpha$ varied significantly between groups. Thus, normalization used the product of the two reference genes for MB and CB while only actin could be used to normalize OL data. No cross-comparisons between brain regions or genes were performed.

Figure 5 B-D shows the relative normalized expression of *kakusei* for the three brain regions considered in the case of *learners and non-learners*. No significant variations of relative expression were found between these two groups for the three regions considered (two-sample t test; Fig. 5B, OL: $t_{29}=0.83$, p=0.42; Fig. 5C, MB: $t_{29}=1.09$, p=0.29; Fig. 5D, CB: $t_{29}=1.04$, p=0.31). Thus, *kakusei* was unable to reveal learning-induced variations in neural activity under our experimental conditions. The normalized expression of *Hr38* (Fig. 5 E-G) was also insufficient to uncover learning related differences between *learners* and *non-learners* (Fig. 5E, OL: $t_{29}=0.37$, p=0.72; Fig. 5F, MB: $t_{29}=0.99$, p=0.33; Fig. 5G, CB: $t_{29}=0.44$, p=0.67). However, a significant upregulation of *Egr1* expression was found in the mushroom bodies of *learners* when compared to *non-learners* (Fig. 5I, $t_{29}=2.40$, p=0.02). Differences in *Egr1* expression between *learners* and *non-learners* were neither found in the OL (Fig. 5H, $t_{29}=1.48$, p=0.15) nor in the CB (Fig. 5J, $t_{29}=0.17$, p=0.86), thus showing that learning-dependent variation in IEG expression was circumscribed to the calyces of the mushroom bodies and that *Egr1* was more sensitive than both *Hr38* and *kakusei* to detect changes in neural activity induced by associative learning.

Discussion

Our work shows that visual discrimination learning under virtual-reality conditions leads to an

enhancement of IEG expression in the case of *Egr1* in the calyces of the mushroom bodies in successful honey bee learners. Learning success did not correlate with differences in distance travelled or tortuosity of trajectories, i.e. with differences in exploratory drive (Fig. 4), but was correlated with differences in walking speed as *learners* tended to be slower than *non-learners*. Although strictly speaking the two categories did not differ with respect to this parameter, the significant interaction between *Trial* and *Condition* suggests a speed-accuracy trade off in which individuals taking more time to decide can improve the accuracy of their decisions[41-43]. Differences in *Egr1* expression were thus related to learning success and not to differences in exploratory components. For the other two IEGs analyzed, *kakusei* and *Hr38,* no learning-dependent changes could be detected in the different brain regions considered, even if prior reports indicated similar levels of expression for the three IEGs in the brain of bees engaged in foraging[29,30,33,45] and orienting around the hive[29-31]. Our work demonstrates therefore that this similarity does not necessarily reflect a relationship with associative learning and memory as only *Egr1* acted as *bona fide* marker of learning success in the bee brain under our experimental conditions and revealed the implication of the calyces of the mushroom bodies in associative visual learning and memory in honey bees.

Differential expression of IEGs in the honey bee brain as related to visual learning

Kakusei did not vary in the brain regions considered, under the experimental conditions defined in our work. This IEG does not have orthologous genes in other taxa and its role in honey bees is unclear. It is induced by seizures following anesthesia[25,27,45,46] and thermal stimulation[46], but also by foraging and reorientation activity following hive displacement[25,31,45]. These experiences increase *kakusei* expression in the mushroom bodies[25] but also in the optic lobes[25,27,45] and the dorsal lobe[27]. Our results suggest that its enhanced expression in foragers or in orienting bees is not necessarily related to learning occurring in these contexts.

Differential expression of *kakusei* with respect to an inducing treatment (typically, an induced seizure) starts around 15 min post treatment[25,31,46] but continues during longer periods which may go beyond 60 min[46]. Thus, the waiting time of 60 min between test and brain freezing in our experiments was appropriate to detect changes in *kakusei* as a result of associative visual learning.

However, as other temporal analyses of *kakusei* expression reported a decay in expression beyond 30 min[25], the possibility that our sampling period was too long to capture changes in *kakusei* expression cannot be excluded.

This concern does not apply to *Hr38* and *Egr1*, for which temporal expression analyses showed a systematical increase at the time chosen for our experiments[30]. As in the case of *kakusei*, no learning-related changes were detected in *Hr38* expression across the brain regions considered. This hormone receptor gene has been indirectly related to learning and memory in honey bees and other insects[29,30] and is also upregulated by foraging experiences in honey bees[29] and bumblebees[30] and by orientation activities upon hive displacement[31]. Despite its involvement in these activities, it did not reveal learning-dependent changes in neural activity in the experimental context defined by our setup and training protocol.

Only *Egr1* reported a significant variation in the mushroom body calyces of *learners* in relation to *non-learners* (Fig. 5). As for the two other IEGs, the expression of this early growth response gene is enhanced in the brain of honey bees and bumble bees upon foraging[29,30] and orientation flights[32]. Yet, in this case, *Egr1* was sensitive enough to report differences in neural activity related to learning success in our experimental conditions. *Learners* and *non-learners* were identical in their experience and handling all along the experiment and they only differed in learning success. Thus, differences in *Egr1* expression demonstrate that associative color learning is accompanied by increased neural activity in the calyces of the mushroom bodies.

The role of mushroom bodies for visual learning and memory

Although the crucial role of mushroom bodies for the acquisition, storage and retrieval of olfactory memories has been extensively documented in bees[7,38,47] and other insect species[3,4,48], less is known about their implication in visual learning and memory. In the honey bee, the fact that visual learning was mainly studied using free-flying bees trained to choose visual targets precluded its study at the cellular level[13]. The neural circuits for color processing are known in the bee brain[49-52] but evidence about plasticity-dependent changes in these circuits remains scarce. Such changes could occur at multiple stages, as is the case in olfactory circuits mediating olfactory learning[9]. Upstream the mushroom bodies, inner-layer lobula and inner medulla neurons project to both the

mushroom bodies and the lateral protocerebrum [49,50,53] and exhibit color sensitivity, color opponency and temporally complex patterns including adaptation and entrainment [49,53,54]. These patterns are important for color coding and discrimination and could be subjected to experience-dependent changes in activity[55].

The implication of mushroom bodies in visual learning and memory in the bee is expected given the parallels between visual and olfactory inputs at the level of the calyces. Whilst afferent projection neurons convey olfactory information to a subdivision of the calyces, the lip[56], afferent neurons from the lobula and the medulla, which are part of the optic lobes, convey visual information to other calyx subdivisions, the collar and the basal ring[50,57]. In spite of this similarity, studies addressing the role of mushroom bodies in honey bee visual learning and memory remain rare. The recent development of protocols for the study of *aversive* visual learning (association between a color light and an electric shock delivered to walking bees enclosed in a box compartment)[44,58] has yielded novel findings on the possible implication of mushroom bodies in this form of learning. In a pharmacological study, in which one half of a chamber was illuminated with one color and paired with shock while the other half was illuminated with a different color not paired with shock, bees learned to escape the shock-paired light and spent more time in the safe light after a few trials[59]. When ventral lobe neurons of the mushroom bodies were silenced by procaine injection, bees were no longer able to associate one light with shock. By contrast, silencing one collar region of the mushroom body calyx did not alter behavior in comparison with that of controls[59]. The latter result does not exclude a role for the calyces in visual learning, as blocking one of four collar regions may not have a significant impact on learning. In a different study, bees were trained to inhibit their spontaneous phototaxis by pairing the attracting light with an electric shock[44]. In this case, learning induced an increase in the dopaminergic receptor gene *Amdop1* in the calyces of the mushroom bodies, consistently with the role of dopaminergic signaling for electric-shock representation in the bee brain[60,61].

In the fruit fly, the study of the role of mushroom bodies for visual learning and memory has yielded contradictory results. Flies suspended within a flight simulator learn to fly towards unpunished visual landmarks to avoid heat punishment delivered to their thorax; mushroom body deficits do not affect learning so that these structures were considered dispensable for visual

learning and memory[62]. Similarly, learning to discriminate colors in a cylindrical container made of a blue-lit and a yellow-lit compartment, one of which was associated with aversive shaking, was not affected in mushroom body mutants[63]. Visual place learning by flies walking within a cylindrical arena displaying landmarks can also take place in the absence of functional mushroom bodies but requires the central complex[64]. Yet, the dispensability of mushroom bodies for visual learning and memory in fruit flies has been questioned by experiments in which appetitive and aversive color learning and discrimination were studied in an arena in which blue and green colors were presented from below. Walking flies learned both the appetitive (based on pairing one color with sugar) and the aversive discrimination (based on pairing one color with electric shock) but failed if mushroom body function was blocked using neurogenetic tools[65]. Thus, the role of mushroom bodies for visual learning and memory in fruit flies may be both task- and learning specific. In addition, the dominance of olfactory inputs to the mushroom bodies may overshadow their role for visual learning in *Drosophila*.

IEG expression within the mushroom bodies in relation to visual learning

Kenyon cells are the constitutive neurons of the mushroom bodies. Their somata are located both within the mushroom-body calyces and adjacent to them. Thus, our brain sectioning (see Fig. 4A) collected them massively. Detection of IEG activation in the mushroom bodies upon visual learning may be particularly difficult as learning-dependent changes in neural activity may be subtle and lower than in other brain centers due to the characteristic sparse neural activity observed at the level of the calyces. This reduced activity, which has been revealed in studies on olfactory coding[66-68] and odor-related learning[69], can also be a hallmark of visual processing and visual learning. Sparse neural coding of odorants is in part due to GABAergic inhibition by feedback extrinsic mushroom-body neurons acting on Kenyon cells[70,71], the constitutive neurons of the mushroom bodies. These GABAergic neurons (APL neurons in the fruit fly and A-3 neurons in the honey bee[70,72,73]) suppress Kenyon cell activity to maintain sparse, neural coding, and may, therefore, account for the lower levels of IEG expression detected in the calyces. In fact, it could be even expected that under certain learning conditions inhibitory feedback in the calyces is particularly relevant, thus leading to IEG *downregulation* as a hallmark of learning success. This

could be the case of non-linear discriminations, in which subjects have to inhibit response summation to the simultaneous presentation of stimuli A and B, which are rewarded when presented alone but non-rewarded when presented together; bees learn to solve this discrimination in the olfactory domain and require inhibitory GABA-ergic feedback in the calyces of the mushroom bodies to this end[47]. Such a requirement could translate into IEG downregulation in this brain region as a consequence of discrimination learning.

Recent work on gene expression in the Kenyon-cells of honey bees revealed the existence of various cell subtypes/populations with unique gene expression profiles and cell body morphology[74]. Among these populations, small Kenyon cells (sKC)[75], formerly called inner Kenyon cells[76], are found in the central, inner core of the MB calyces and express preferentially three genes, *EcR*, *E74* and *Hr38*, the latter being higher in the brain of foragers than in nurses[74]. Unfortunately, no information on *Egr1* was reported in this analysis. Yet, another study that did not distinguished between Kenyon-cell subtypes reported that the expression of *Egr1*is enriched in Kenyon cells compared to the rest of the brain[32] and that this enrichment might be related to learning and memory given its association with the orientation flights of bees[32] and with foraging activities[29,30,77]. However, the sensory cues and behavioral programs participating in both foraging and orientation are multiple so that it is difficult to sustain such a claim in the absence of a controlled learning experiment. For instance, *Egr1* is also upregulated in the brain of honey bees upon seizure induction[78], with no relation to foraging or orientation. Only specific experiments like the one performed in this work can reveal whether increases in this and other IEGs reflect neural activity induced by associative learning.

Consistently with the notion that sKCs may be particularly relevant for learning and memory formation, phosphorylated (activated) cAMP-response element binding protein (pCREB) is enriched in these sKCs in the honey bee[79]. CREB is a nuclear protein that modulates the transcription of genes required for the cellular events underlying long-term memory (LTM) formation in both invertebrates and vertebrates[80-83] and its activation leads also to the expression of IEGs. It is thus possible that the increased expression of *Egr1* induced by visual learning and memory formation is localized within sKCs, and that this increase results from CREB activation. In our experiments, the reinforced tests were done shortly after the last conditioning trial and only

one hour elapsed since the end of the test and the collection of brains for IEG analysis (a time necessary for the expression of the IEGs selected). This period does not correspond with the temporal requirements for olfactory LTM formation in the standard view of memory dynamics in the honey bee, where a protein-synthesis dependent LTM is expected after 24-h post conditioning[84]. However, recent work on olfactory memory formation has shown that protein-synthesis dependent memories arise much earlier and with less conditioning trials than previously thought[85]. Whether our visual conditioning leads to protein-synthesis dependent LTM, mediated by CREB activation, remains to be determined.

Conclusion and Outlook

Taken together, our results show both the implication of mushroom bodies in appetitive visual learning in honey bees and the usefulness of *Egr1* as a marker of neural activity induced by these phenomena under our experimental conditions. The learning success in our VR setup was 50%, which contrasts with the higher learning rates observable for similar color discriminations in the case of free-flying bees. This decrease may be due to several reasons such as the impossibility to return to the hive between rewarded experiences, the tethering conditions and the resulting reduction in active vision. As the tethering impedes, in part, free movements, it may affect the possibility of actively scanning the images perceived, impairing thereby the possibility of extracting target information and learning. In spite of these restrictions, our setup allowed to segregate between *learners* and *non-learners* and achieve relevant analyses to answer questions on the neural and molecular underpinnings of associative visual learning. It constitutes therefore a valuable tool for further studies on the mechanisms of visual cognition in bees.

The protocol used to train the bees in our work consisted in an elemental discrimination between a rewarded and non-rewarded color. Yet, bees are well known for remarkable visual performances, which include the non-elemental learning of concepts and relational rules[86-88]. It is therefore possible that different forms of learning, which recruit different brain regions[47], may reveal experience-dependent neural activation through different IEGs and with different temporal dynamics. Moreover, IEG upregulation may not always be the hallmark of successful learning as in some cases inhibition of neural activity may be crucial for plastic changes in behavior. Thus,

addressing if IEG expression varies qualitatively and quantitatively according to learning type and complexity is of fundamental importance. Furthermore, including different intervals post conditioning is important to characterize possible activity changes related to the formation of different memory phases in different regions of the bee brain. Last, but not least, our results highlight the value of virtual-reality conditions for further explorations of the neural and molecular underpinnings of visual learning and memory in bees.

Methods

Honey bees (*Apis mellifera*) were obtained from our apiary located at the campus of the University Paul Sabatier – Toulouse III. Only foragers caught upon landing on a gravity feeder filled with a 0.9 M sucrose solution were used in our experiments to ensure high appetitive motivation. Captured bees were brought to the laboratory where they were placed on ice for five minutes to anesthetize them and facilitate the fixation of a tether glued to their thorax by means of melted wax (Fig. 1A). After being attached to the tether, each bee was placed on a small (49 mm diameter) Styrofoam ball for familiarization with the treadmill situation and for evaluating its walking behavior. Bees were provided with 5 μl of 1.5 M sucrose solution and kept for 3 h in this provisory setup in the dark. Bees that walked under these conditions were moved to the VR arena and used for the experiments.

Once in the VR setup, the bee was attached to a holder that allowed adjusting its position on the treadmill (Fig. 1B), a polystyrene ball (diameter: 10 cm, weight: 8 g) held by a 3D-printed support and floating on a constant airflow produced by an air pump (airflow: 555ml/s; Aqua Oxy CWS 2000, Oase, Wasquehal, France).

VR setup

The VR setup consisted of the treadmill and of a half-cylindrical vertical screen made of semi-transparent tracing paper, which allowed presentation of a 180° visual environment to the bee (diameter: 268 mm, height: 200 mm, distance to the bee: 9 cm Fig. 1AB) and which was placed in

front of the treadmill. The visual environment was projected from behind the screen using a video projector connected to a laptop (Fig. 1A). The video projector was an Acer K135 (Lamp: LED, Maximum Vertical Sync: 120 Hz, Definition: 1280 x 800, Minimum Vertical Sync: 50 Hz, Brightness: 600 lumens, Maximum Horizontal Sync: 100.10^3 Hz, Contrast ratio: 10 000:1, Minimum Horizontal Sync: 30.10^3 Hz)[14]. The movements of the walking bee on the treadmill were recorded by two infrared optic-mouse sensors (Logitech M500, 1000 dpi, Logitech, Lausanne, Switzerland) placed on the ball support perpendicular to each other.

Experiments were conducted under 3D closed-loop conditions, i.e. rotations of the ball displaced the visual stimuli not only laterally but also towards the bee. To this end, we used a custom software developed using the Unity engine (version 2018.3.11f1), open-source code available at https://github.com/G-Lafon/BeeVR. The software updated the position of the bee within the VR every 0.017 s. A displacement of 1 cm on the ball corresponds to an equivalent displacement in the VR landscape. Moving 1 cm on the ball towards an object increased the visual angle of the object by ca. 1.7°. Based on the ball movements, our software calculated the position of the walking bee and its heading, and determined which object was centered on the screen.

Visual stimuli

Bees had to discriminate two vertical cuboids (Fig. 1C) based on their different colors and association with reward and punishment. The colors of the cuboids (see supplementary Fig. S1) were blue (RGB: 0, 0, 255, with a dominant wavelength of 450 nm and an irradiance of 161,000 µW) and green (RGB: 0, 100, 0, with a dominant wavelength of 530 nm and an irradiance of 24 370 µW/cm2). They were displayed on a black background (RGB: 0, 0, 0). These colors were chosen based on previous work showing their successful learning in the VR setup[14].

Each cuboid had a 5×5 cm base and 1 m height so that it occupied the entire vertical extent of the screen irrespective of the bee's position. The cuboids were positioned at -50° and +50° from the bee's body axis at the beginning of each trial. Approaching a cuboid within an area of 3 cm surrounding its virtual surface followed by direct fixation of its center was recorded as a choice (Fig. 2A).

Conditioning and testing at the treadmill

Bees were trained using a differential conditioning, which promotes better learning performances owing to the presence of penalized incorrect color choice that result in an enhancement of visual attention[36].

Bees were trained during 10 consecutive trials using a differential conditioning procedure (Fig. 2B) in which one of the cuboids (i.e. one of the two colors, green or blue) was rewarded with 1.5 M sucrose solution (the appetitive conditioned stimulus or CS+) while the other cuboid displaying the alternative color (the aversive conditioned stimulus or CS-) was associated with 3 M NaCl solution. The latter was used to increase the penalty of incorrect choices[40,89,90]. To avoid directional biases, the rewarded and the punished color cuboids were swapped between the left and the right side of the virtual arena in a pseudo random manner along trials. Moreover, a reconstruction of the trajectories of the bees analyzed did not show side biases.

At the beginning of the experiment, bees were presented with a dark screen. During training trials, each bee faced the two cuboids. The bee had to choose the CS+ cuboid by walking towards it and centering it on the screen. Training was balanced in terms of color contingencies (i.e. blue and green equally rewarded across bees) based on a random assignment by the VR software. If the bee reached the CS+ within an area of 3 cm in the virtual environment (i.e. the chosen cuboid subtended a horizontal visual angle of 53°) and centered it in its front, the screen was locked on that image for 8 s. This allowed the delivery of sucrose solution in case of a correct choice, or of quinine or NaCl in case of an incorrect choice. Solutions were delivered for 3 s by the experimenter who sat behind the bee and used a toothpick to this end. The toothpick contacted first the antennae and then the mouthparts while the screen was locked on the visual image fixated by the bee. Each training trial lasted until the bee chose one of both stimuli or until a maximum of 60 s (no choice). Trials were separated by an inter-trial interval of 60 s during which the dark screen was presented. Bees that were unable to choose a stimulus (i.e. that did not fulfill the criterion of a choice defined above) in at least 5 trials were excluded from the analysis. From 216 bees trained, 75 were kept for analysis (~35%).

After the last training trial, each bee was subjected to a non-reinforced test that lasted 60 s (Fig. 2B). Test performance allowed distinguishing *learners* (i.e. bees that chose the CS+ as their first

choice in the test) from *non-learners* (i.e. bees that either chose the CS- in their first test choice or that did not make any choice during the test). IEG expression was compared between these two groups, which had the same sensory experience in the VR setup and which differed only in their learning success.

Brain dissection

 One hour after the test, bees were decapitated, and the head was instantly frozen in a nitrogen solution. The period between post-test and brain collection was chosen to allow induction of the three IEGS studied (typically, 15 or more min in the case of kakusei[25,46] and 30-60 min in the case of *Hr38*[31] *and Egr1*[30]). The frozen bee head was dissected on dry ice under a microscope. First, the antennae were removed and a window was cut in the upper part of the head capsule, removing the cuticle between the compound eyes and the ocelli. Second, the glands and tracheae around the brain were removed. Third, the retinas of the compound eyes were also removed.

The frozen brain was cut in three main parts for IEG analyses (Fig. 4A): the optic lobes (OL), the upper part of the mushroom bodies (the mushroom-body calyces, MB Ca) and the remaining central brain (CB), which included mainly the central complex (CC), the subesophageal zone (SEZ) and the peduncula of the mushroom-bodies (α and β lobes). Samples were stored at -80 °C before RNA extraction. During the dissection process, 4 brains of the 18 non-learner bees were lost, which explains the difference in sample sizes between the behavioral and the molecular analyses.

RNA extraction and reverse transcription

The RNAs from the three sections mentioned above (OL, MB Ca and CB) were extracted and purified using the RNeasy Micro Kit (Qiagen). The final RNA concentration obtained was measured by spectrophotometry (NanoDrop™ One, Thermo Scientific). A volume of 10 µl containing 100 ng of the RNA obtained was used for reverse transcription following the procedure recommended in the Maxima H Minus First Strand cDNA Synthesis kit (Thermoscientific, 0.25 µl of random hexamer primer, 1 µl of 10 mM dNTP mix, 3.75 µl of nuclease free H_2O, 4 µl 5X RT Buffer and 1 µl Maxima H Minus Enzyme Mix).

Quantitative Polymerase Chain Reaction (RT-qPCR)

All the primers used for target and reference genes generated amplification products of approximately 150 pb. The efficiencies of all reactions with the different primers used were between 95 and 110 % (Table 1). Their specificity was verified by analyzing melting curves of the qRT-PCR products (see Supplementary Fig. S2). Two reference genes (*Ef1 α* and *Actin*) were used for normalization.

Expression was quantified using a SYBR Green real-time PCR method. Real-time PCR were carried out in 384-Well PCR Plates (Bio-Rad) cover with Microseal 'B' PCR Plate Sealing Film (Bio-Rad). The PCR reactions were performed using the SsoAdvancedTM Universal SYBR® Green Supermix (Bio-Rad) in a final volume of 10 μl containing 5 μl of 2X SsoAdvancedTM Universal SYBR® Green Supermix, 2 μl of cDNA template (1:3 dilution from the reverse transcription reaction), 0.5 μl of 10 μmol of each primer and 2 μl of ultrapure water. The reaction conditions were as follows: 95 °C for 30 s followed by 40 cycles of 95 °C for 10 s, 55 °C for 30 s and a final step at 95 °C for 10 s followed by a melt curve from 55 °C to 95 °C with 0.5 °C per second. The reaction was performed in a CFX384 Touch Real-Time PCR Detection System (Bio-Rad) and analyzed with the software Bio-Rad CFX Manager.

Each sample was run in triplicates. If the triplicates showed too much variability (SD > 0.3), the furthest triplicate was discarded. If the two remaining triplicates still showed too much variability (SD > 0.3) the sample was discarded. The samples were subjected to a relative quantification and normalization. First for each sample and for each reference gene per brain region, the relative quantity (Qr) was computed using the difference between the mean Ct value of each sample and the highest mean Ct value (ΔCt), using the following formula: $Qr = (1+E)^{\Delta Ct}$ (with E= efficiency of the reaction). Then a normalization factor for each sample was obtained computing the geometric mean of the relative quantities obtained for the reference genes in the corresponding samples (ΔΔCt).

Data analysis and statistics

Behavioral data

The first choice of the bees was recorded during the conditioning trials and the non-reinforced test. In this way, we established for each trial and test the percentages of bees choosing first each of the stimuli displayed or not choosing any stimulus. Data were bootstrapped to plot choice percentages ± their corresponding 95% confidence interval.

Test percentages were analyzed within groups by means of a generalized linear mixed model (GLMM) for binomial family in which the individual identity (Bee) was considered as a random factor (individual effect) while the choice category (CS+, CS-, NC) was fitted as a fixed effect; z values with corresponding degrees of freedom are reported throughout for this kind of analysis. Statistical analyses were performed using with R 3.5.1[91] using the packages lme4 and lsmeans were used for GLMMs.

For the acquisition trials, we recorded motor variables such as the total distance walked during a trial, the walking speed, and the tortuosity of the trajectories. Tortuosity was calculated as the ratio between the total distance walked and the distance between the first and the last point of the trajectory connected by an imaginary straight line. When the ratio was 1, or close to 1, trajectories were straightforward while higher values corresponded to sinuous trajectories. The analysis of these continuous variables was done using a linear mixed model (lmer function) in which the individual identity (*Bee ID*) was a random factor and the experimental condition (*Condition*) and trial number (*Trial*) were fixed factors.

Gene expression data

Statistical differences in gene expression were assessed for reference genes to check for stability and for target genes within a given brain region using One-Factor ANOVA for independent groups in the case of multiple comparisons or two-sample T test in the case of dual comparisons. Pots hoc comparisons between groups were performed by means of a Tukey test following ANOVA. No cross-comparisons between brain regions or genes were performed due to within-area normalization procedures. Statistical analyses were done either with R 3.5.1 software[91] or with Statistica 13 Software (TIBCO® Data Science).

REPORTING SUMMARY

Further information on research design is available in the Nature Research Reporting Summary linked to this article.

DATA AND CODE AVAILABILITY

The datasets generated during this study are available at figshare.com with the following accession ID: https://figshare.com/s/1e868800d08a17dc300e

ACKNOWLEDGMENTS

CONTRIBUTIONS

GL performed the behavioral experiments. HG dissected and sectioned the brains of the bees trained in the VR setup and performed all the molecular analyses. Behavioral experiments were supervised by AB, AAW and MG. Molecular experiments were supervised by IM and MG Statistical analyses on behavioral data were performed by GL and MG. Statistical analyses on gene-expression data were performed by HG and MG. The manuscript was written by MG who also obtained the funding. All authors reviewed and approved the final version of the manuscript.

ETHICS DECLARATIONS

Competing interests

The authors declare no competing interests.

References

1   Giurfa, M. Cognition with few neurons: higher-order learning in insects. *Trends Neurosci* **36**, 285-294 (2013).

2   Kandel, E. R. Neuroscience - The molecular biology of memory storage: A dialogue between genes and synapses. *Science* **294**, 1030-1038 (2001).

3   Heisenberg, M. Mushroom body memoir: from maps to models. *Nat Rev Neurosci* **4**, 266-275 (2003).

4   Cognigni, P., Felsenberg, J. & Waddell, S. Do the right thing: neural network mechanisms of memory formation, expression and update in *Drosophila*. *Curr Opin Neurobiol* **49**, 51-58 (2018).

5   Benjamin, P. R., Kemenes, G. & Kemenes, I. Non-synaptic neuronal mechanisms of learning and memory in gastropod molluscs. *Front Biosci* **13**, 4051-4057 (2008).

6   Giurfa, M. Behavioral and neural analysis of associative learning in the honeybee: a taste from the magic well. *J Comp Physiol A* **193**, 801-824 (2007).

7   Menzel, R. Memory dynamics in the honeybee. *J Comp Physiol A* **185**, 323-340 (1999).

8   Menzel, R. The honeybee as a model for understanding the basis of cognition. *Nature Rev Neurosci* **13**, 758-768 (2012).

9   Giurfa, M. & Sandoz, J. C. Invertebrate learning and memory: Fifty years of olfactory conditioning of the proboscis extension response in honeybees. *Learn Mem* **19**, 54-66 (2012).

10   Avargues-Weber, A., Deisig, N. & Giurfa, M. Visual cognition in social insects. *Annu Rev Entomol* **56**, 423-443 (2011).

11   Avargues-Weber, A., Mota, T. & Giurfa, M. New vistas on honey bee vision. *Apidologie* **43**, 244-268 (2012).

12   Buatois, A. *et al.* Associative visual learning by tethered bees in a controlled visual environment. *Sci Reports* **7**, 127903 (2017).

13   Schultheiss, P., Buatois, A., Avarguès-Weber, A. & Giurfa, M. Using virtual reality to study visual performances of honeybees. *Curr Opin Insect Sci* **24**, 43–50 (2017).

14   Buatois, A., Flumian, C., Schultheiss, P., Avargues-Weber, A. & Giurfa, M. Transfer of visual learning between a virtual and a real environment in honey bees: the role of active vision. *Front Behav Neurosci* **12**, 139 (2018).

15   Rusch, C., Roth, E., Vinauger, C. & Riffell, J. A. Honeybees in a virtual reality environment learn unique combinations of colour and shape. *J Exp Biol* **220**, 3478-3487 (2017).

16   Zwaka, H. *et al.* Learning and its neural correlates in a virtual environment for honeybees. *Front Behav Neurosci* **12**, 279 (2018).

17   Rusch, C., Alonso San Alberto, D. & Riffell, J. A. Visuo-motor feedback modulates neural activities in the medulla of the honeybee, *Apis mellifera*. *J Neurosci* **41**, 3192-3203 (2021).

18   Buatois, A., Laroche, L., Lafon, G., Avargues-Weber, A. & Giurfa, M. Higher-order discrimination learning by honeybees in a virtual environment. *Eur J Neurosci* **51**, 681-694 (2020).

19   Clayton, D. F. The genomic action potential. *Neurobiol Learn Mem* **74**, 185-216 (2000).

20   Bahrami, S. & Drablos, F. Gene regulation in the immediate-early response process. *Adv Biol Regul* **62**, 37-49 (2016).

21   Minatohara, K., Akiyoshi, M. & Okuno, H. Role of immediate-early genes in synaptic plasticity and neuronal ensembles underlying the memory trace. *Front Mol Neurosci* **8**, 78 (2015).

22   Gallo, F. T., Katche, C., Morici, J. F., Medina, J. H. & Weisstaub, N. V. Immediate early genes, memory

and psychiatric disorders: focus on *c-Fos, Egr1* and *Arc. Front Behav Neurosci* **12**, 79 (2018).

23   He, Q., Wang, J. & Hu, H. Illuminating the activated brain: emerging activity-dependent tools to capture and control functional neural circuits. *Neurosci Bull* **35**, 369-377 (2019).

24   Sommerlandt, F. M. J., Brockmann, A., Roessler, W. & Spaethe, J. Immediate early genes in social insects: a tool to identify brain regions involved in complex behaviors and molecular processes underlying neuroplasticity. *Cell Mol Life Sci* **76**, 637-651 (2019).

25   Kiya, T., Kunieda, T. & Kubo, T. Increased neural activity of a mushroom body neuron subtype in the brains of forager honeybees. *PLoS One* **2**, e371 (2007).

26   Kiya, T. & Kubo, T. Dance type and flight parameters are associated with different mushroom body neural activities in worker honeybee brains. *PLoS One* **6**, e19301 (2011).

27   Kiya, T., Kunieda, T. & Kubo, T. Inducible- and constitutive-type transcript variants of kakusei , a novel non-coding immediate early gene, in the honeybee brain. *Insect Mol Biol* **17**, 531-536 (2008).

28   Fujita, N. *et al.* Visualization of neural activity in insect brains using a conserved immediate early gene, Hr38. *Curr Biol* **23**, 2063-2070 (2013).

29   Singh, A. S., Shah, A. & Brockmann, A. Honey bee foraging induces upregulation of early growth response protein 1, hormone receptor 38 and candidate downstream genes of the ecdysteroid signalling pathway. *Insect Mol Biol* **27**, 90-98 (2018).

30   Iino, S. *et al.* Neural activity mapping of bumble bee (*Bombus ignitus*) brains during foraging flight using immediate early genes. *Sci Rep* **10**, 7887 (2020).

31   Ugajin, A. *et al.* Identification and initial characterization of novel neural immediate early genes possibly differentially contributing to foraging-related learning and memory processes in the honeybee. *Insect Mol Biol* **27**, 154-165 (2018).

32   Lutz, C. C. & Robinson, G. E. Activity-dependent gene expression in honey bee mushroom bodies in response to orientation flight. *J Exp Biol* **216**, 2031-2038 (2013).

33   Shah, A., Jain, R. & Brockmann, A. Egr-1: A candidate transcription factor involved in molecular processes underlying time-memory. *Frontiers in Psychology* **9** (2018).

34   Giurfa, M. Conditioning procedure and color discrimination in the honeybee *Apis mellifera*. *Naturwissenschaften* **91**, 228-231 (2004).

35   Dyer, A. G. & Chittka, L. Fine colour discrimination requires differential conditioning in bumblebees. *Naturwissenschaften* **91**, 224-227 (2004).

36   Avarguès-Weber, A. & Giurfa, M. Cognitive components of color vision in honey bees: how conditioning variables modulate color learning and discrimination. *J Comp Physiol A* **200**, 449-461 (2014).

37   Avarguès-Weber, A., de Brito Sanchez, M. G., Giurfa, M. & Dyer, A. G. Aversive reinforcement improves visual discrimination learning in free-flying honeybees. *PLoS One* **5**, e15370 (2010).

38   Menzel, R. The insect mushroom body, an experience-dependent recoding device. *J Physiol Paris* **108**, 84-95 (2014).

39   de Brito Sanchez, M. G., Serre, M., Avarguès-Weber, A., Dyer, A. G. & Giurfa, M. Learning context modulates aversive taste strength in honey bees. *J Exp Biol* **218**, 949-959 (2015).

40   Aguiar, J., Roselino, A. C., Sazima, M. & Giurfa, M. Can honey bees discriminate between floral-fragrance isomers? *J Exp Biol* **221** (2018).

41   Dyer, A. G. & Chittka, L. Bumblebees (*Bombus terrestris*) sacrifice foraging speed to solve difficult colour discrimination tasks. *J Comp Physiol A* **190**, 759-763 (2004).

42   Ings, T. C. & Chittka, L. Speed-accuracy tradeoffs and false alarms in bee responses to cryptic

predators. *Curr Biol* **18**, 1520-1524 (2008).

43   Burns, J. G. & Dyer, A. G. Diversity of speed-accuracy strategies benefits social insects. *Curr Biol* **18**, R953-R954 (2008).

44   Marchal, P. *et al.* Inhibitory learning of phototaxis by honeybees in a passive-avoidance task. *Learn Mem* **26**, 412-423 (2019).

45   Kiya, T. & Kubo, T. Analysis of GABAergic and non-GABAergic neuron activity in the optic lobes of the forager and re-orienting worker honeybee (*Apis mellifera* L.). *PLoS One* **5**, e8833 (2010).

46   Ugajin, A. *et al.* Detection of neural activity in the brains of Japanese honeybee workers during the formation of a "hot defensive bee ball". *PLoS One* **7**, e32902 (2012).

47   Devaud, J. M. *et al.* Neural substrate for higher-order learning in an insect: Mushroom bodies are necessary for configural discriminations. *Proc Natl Acad Sci U S A* **112**, E5854-5862 (2015).

48   Guven-Ozkan, T. & Davis, R. L. Functional neuroanatomy of *Drosophila* olfactory memory formation. *Learn Mem* **21**, 519-526 (2014).

49   Paulk, A. C., Phillips-Portillo, J., Dacks, A. M., Fellous, J. M. & Gronenberg, W. The processing of color, motion, and stimulus timing are anatomically segregated in the bumblebee brain. *J Neurosci* **28**, 6319-6332 (2008).

50   Paulk, A. C., Dacks, A. M., Phillips-Portillo, J., Fellous, J. M. & Gronenberg, W. Visual processing in the central bee brain. *J Neurosci* **29**, 9987-9999 (2009).

51   Menzel, R. & Backhaus, W. in *Vision and Visual Dysfunction. The Perception of Colour.*   (ed P. Gouras) 262-288 (MacMillan Press, 1991).

52   Mota, T., Yamagata, N., Giurfa, M., Gronenberg, W. & Sandoz, J. C. Neural organization and visual processing in the anterior optic tubercle of the honeybee brain. *J Neurosci* **31**, 11443-11456 (2011).

53   Paulk, A. C., Dacks, A. M. & Gronenberg, W. Color processing in the medulla of the bumblebee (Apidae: *Bombus impatiens*). *J Comp Neurol* **513**, 441-456 (2009).

54   Paulk, A. C. & Gronenberg, W. Higher order visual input to the mushroom bodies in the bee, *Bombus impatiens*. *Arthropod Struct Dev* **37**, 443-458 (2008).

55   Dyer, A. G., Paulk, A. C. & Reser, D. H. Colour processing in complex environments: insights from the visual system of bees. *Proc Biol Sci* **278**, 952-959 (2011).

56   Kirschner, S. *et al.* Dual olfactory pathway in the honeybee, *Apis mellifera*. *J Comp Neurol* **499**, 933-952 (2006).

57   Ehmer, B. & Gronenberg, W. Segregation of visual input to the mushroom bodies in the honeybee (*Apis mellifera*). *J Comp Neurol* **451**, 362-373 (2002).

58   Kirkerud, N. H., Schlegel, U. & Giovanni Galizia, C. Aversive learning of colored lights in walking honeybees. *Front Behav Neurosci* **11**, 94 (2017).

59   Plath, J. A. *et al.* Different roles for honey bee mushroom bodies and central complex in visual learning of colored lights in an aversive conditioning assay. *Front Behav Neurosci* **11**, 98 (2017).

60   Vergoz, V., Roussel, E., Sandoz, J. C. & Giurfa, M. Aversive learning in honeybees revealed by the olfactory conditioning of the sting extension reflex. *PLoS One* **2**, e288 (2007).

61   Tedjakumala, S. R., Aimable, M. & Giurfa, M. Pharmacological modulation of aversive responsiveness in honey bees. *Front Behav Neurosci* **7** (2014).

62   Wolf, R. *et al. Drosophila* mushroom bodies are dispensable for visual, tactile, and motor learning. *Learn Mem* **5**, 166-178 (1998).

63   Heisenberg, M., Borst, A., Wagner, S. & Byers, D. *Drosophila* mushroom body mutants are deficient in olfactory learning. *J Neurogenet* **2**, 1-30 (1985).

64   Ofstad, T. A., Zuker, C. S. & Reiser, M. B. Visual place learning in *Drosophila melanogaster*. *Nature* **474**, 204-U240 (2011).

65   Vogt, K. *et al.* Shared mushroom body circuits underlie visual and olfactory memories in *Drosophila*. *eLife* **3**, e02395 (2014).

66   Szyszka, P., Ditzen, M., Galkin, A., Galizia, C. G. & Menzel, R. Sparsening and temporal sharpening of olfactory representations in the honeybee mushroom bodies. *J Neurophysiol* **94**, 3303-3313 (2005).

67   Perez-Orive, J. *et al.* Oscillations and sparsening of odor representations in the mushroom body. *Science* **297**, 359-365 (2002).

68   Laurent, G. J. *et al.* Odor encoding as an active, dynamical process: experiments, computation, and theory. *Annu Rev Neurosci* **24**, 263-297 (2001).

69   Lin, A. C., Bygrave, A. M., de Calignon, A., Lee, T. & Miesenbock, G. Sparse, decorrelated odor coding in the mushroom body enhances learned odor discrimination. *Nat Neurosci* **17**, 559-568 (2014).

70   Froese, A., Szyszka, P. & Menzel, R. Effect of GABAergic inhibition on odorant concentration coding in mushroom body intrinsic neurons of the honeybee. *J Comp Physiol A* **200**, 183-195 (2014).

71   Papadopoulou, M., Cassenaer, S., Nowotny, T. & Laurent, G. Normalization for sparse encoding of odors by a wide-field interneuron. *Science* **332**, 721-725 (2011).

72   Rybak, J. & Menzel, R. Anatomy of the mushroom bodies in the honey bee brain: The neuronal connections of the alpha-lobe. *J Comp Neurobiol* **334**, 444-465 (1993).

73   Zwaka, H., Bartels, R., Grunewald, B. & Menzel, R. Neural Organization of A3 Mushroom Body Extrinsic Neurons in the Honeybee Brain. *Front Neuroanat* **12**, 57 (2018).

74   Suenami, S., Oya, S., Kohno, H. & Kubo, T. Kenyon cell subtypes/populations in the honeybee mushroom bodies: possible function based on their gene expression profiles, differentiation, possible evolution, and application of genome editing. *Front Psychol* **9** (2018).

75   Kaneko, K. *et al.* Novel middle-type Kenyon cells in the honeybee brain revealed by area-preferential gene expression analysis. *PLoS One* **8**, e71732 (2013).

76   Strausfeld, N. J. Organization of the honey bee mushroom body: representation of the calyx within the vertical and gamma lobes. *J Comp Neurol* **450**, 4-33 (2002).

77   Shah, A., Jain, R. & Brockmann, A. Egr-1: A Candidate transcription factor involved in molecular processes underlying time-memory. *Front Psychol* **9** (2018).

78   Ugajin, A., Kunieda, T. & Kubo, T. Identification and characterization of an Egr ortholog as a neural immediate early gene in the European honeybee (*Apis mellifera* L.). *FEBS Letters* **587**, 3224-3230 (2013).

79   Gehring, K. B., Heufelder, K., Kersting, I. & Eisenhardt, D. Abundance of phosphorylated *Apis mellifera* CREB in the honeybee's mushroom body inner compact cells varies with age. *J Comp Neurol* **524**, 1165-1180 (2016).

80   Silva, A. J., Kogan, J. H., Frankland, P. W. & Kida, S. CREB and memory. *Annu Rev Neurosci* **21**, 127-148 (1998).

81   Kandel, E. R. The molecular biology of memory: cAMP, PKA, CRE, CREB-1, CREB-2, and CPEB. *Mol Brain* **5**, 14 (2012).

82   Yin, J. C. P. & Tully, T. CREB and the formation of long-term memory. *Curr Opin Neurobiol* **6**, 264-268 (1996).

83   Alberini, C. M. Transcription factors in long-term memory and synaptic plasticity. *Physiol Rev* **89**,

121-145 (2009).

84   Wüstenberg, D., Gerber, B. & Menzel, R. Long- but not medium-term retention of olfactory memory in honeybees is impaired by actinomycin D and anisomycin. *Eur J Neurosci* **10**, 261-261 (1998).

85   Villar, M. E., Marchal, P., Viola, H. & Giurfa, M. Redefining single-trial memories in the honey bee. *Cell Reports* **30**, 2603-2613 (2020).

86   Avarguès-Weber, A. & Giurfa, M. Conceptual learning by miniature brains. *Proc Biol Sci* (2013).

87   Giurfa, M. An Insect's Sense of Number. *Trends Cogn Sci* **23**, 720-722 (2019).

88   Giurfa, M. Learning of sameness/difference relationships by honey bees: performance, strategies and ecological context. *Curr Opin Behav Sci* **37**, 1-6 (2021).

89   de Brito Sanchez, M. G., Serre, M., Avargues-Weber, A., Dyer, A. G. & Giurfa, M. Learning context modulates aversive taste strength in honey bees. *J Exp Biol* **218**, 949-959 (2015).

90   Bestea, L. *et al.* Peripheral taste detection in honey bees: what do taste receptors respond to? *Eur J Neurosci* (2021).

91   R Development Core Team. *R: A Language and Environment for Statistical Computing*.   (The R Foundation for Statistical Computing, 2016).
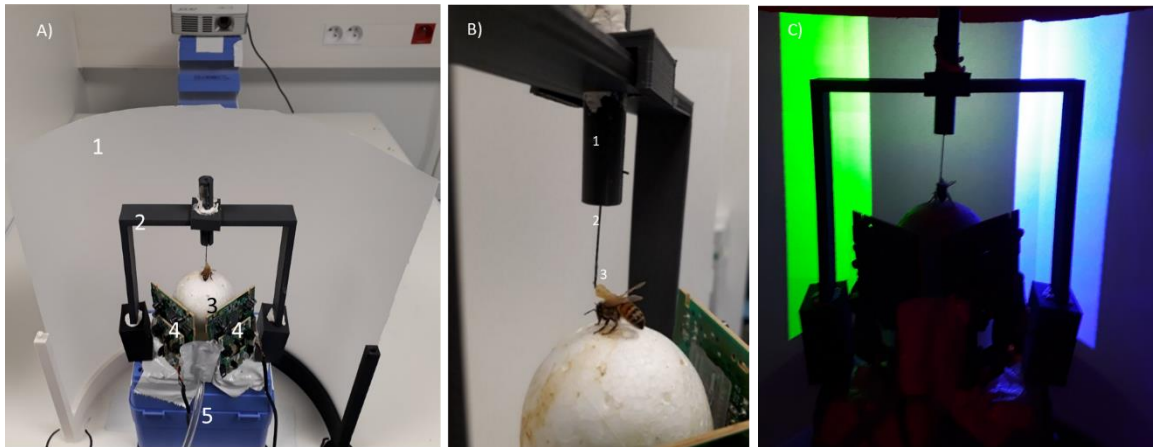
Figure 1. Experimental setup and 3D environment. A) Global view of the VR system. 1: Semicircular projection screen made of tracing paper. 2: Holding frame to place the tethered bee on the treadmill. 3: The treadmill was a Styrofoam ball positioned within a cylindrical support (not visible) floating on an air cushion. 4: Infrared mouse optic sensors allowing to record the displacement of the ball and to reconstruct the bee's trajectory. 5: Air arrival. The video projector displating images on the screen from behind can be seen on top of the image. **B) The tethering system.** 1: Plastic cylinder held by the holding frame; the cylinder contained a glass cannula into which a steel needle was inserted. 2: The needle was attached to the thorax of the bee. 3: Its curved end was fixed to the thorax by means of melted bee wax. **C) Color discrimination learning in the VR setup.** The bee had to learn to discriminate two vertical cuboids based on their different color and their association with reward and punishment. Cuboids were green and blue on a dark background. Color intensities were adjusted to avoid phototactic biases independent of learning.
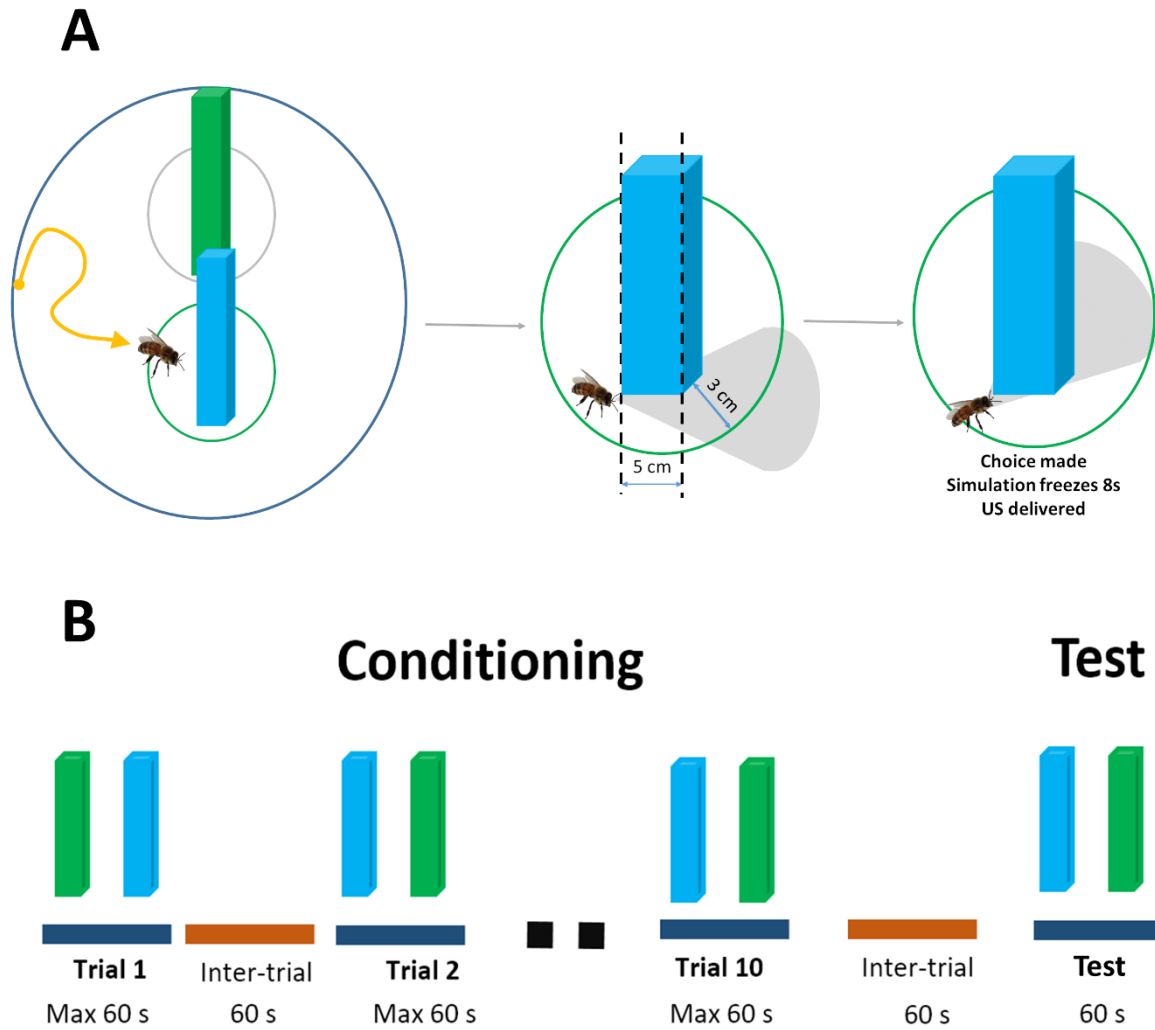
Figure 2. Choice criterion and conditioning protocol for color discrimination learning. A) Choice criterion. A choice was recorded when the bee reached an area of a radius of 3 cm centered on the cuboid and fixed it frontally. The cuboid image was then frozen during 8 s and the corresponding reinforcement (US) was delivered. **B) Conditioning protocol.** Bees were trained along 10 conditioning trials that lasted a maximum of 1 min and that were spaced by 1 min (intertrial interval). After the end of conditioning, and following an additional interval of 1 min, bees were tested in extinction conditions with the two colored cuboids during 1 min.
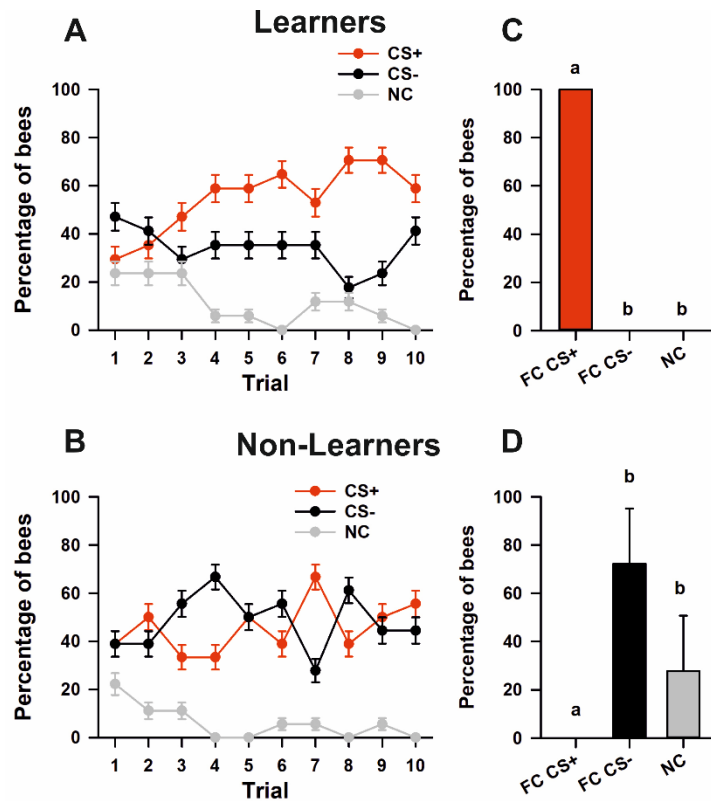
Figure 3. Discrimination learning in the VR setup. A) Acquisition performance of *learners* (i.e. bees that chose the CS+ in the non-reinforced test; n=17). The red, black and grey curves show the percentages of bees choosing the CS+, the CS- or not making a choice (NC), respectively. Bees learned the discrimination between CS+ and CS-. **B) Acquisition performance of *non-learners*** (i.e. bees that chose the CS- or did not make a choice in the non-reinforced test; n=18). These bees did not learn to discriminate the CS+ from the CS-. **C) Test performances of *learners*.** Per definition, these bees were the ones choosing first the CS+ (FC CS+). FC CS-: first choice of the CS-; NC: bees not making a choice. Different letters on top of bars indicate significant differences (p<0.05). **D). Test performances of *non-learners*.** Different letters on top of bars indicate significant differences (p<0.05).
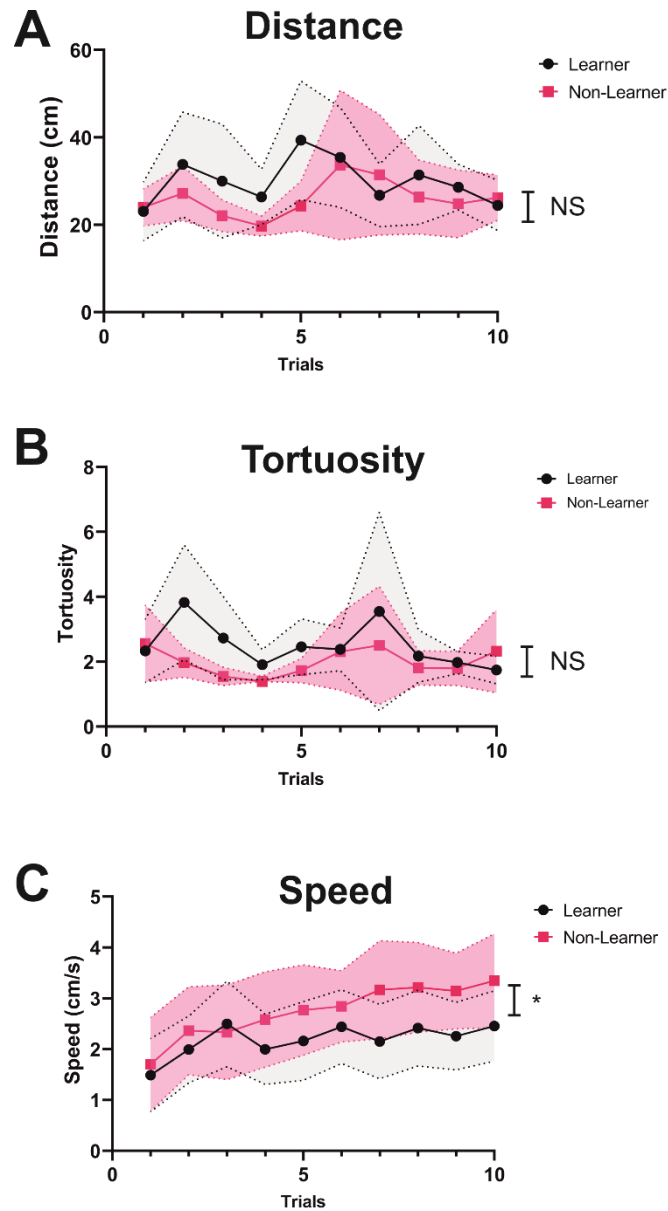
Figure 4. Motor components of learners (n=17) and non-learners (n = 18) in the VR setup during conditioning. A) Distance travelled (cm) during each conditioning trial. **B) Tortuosity** of the trajectories (see text for explanation) during each conditioning trial. **C) Walking speed** (cm/s) during each conditioning trial. The dashed lines above and below the curves represent the 95% confidence interval. Comparisons between curves refer to the significance of the interaction between the factors *Trial* (1 to 10) and *Condition* (*learners* vs. *non-learners*). All comparisons referring to *Condition* alone were non-significant. NS: non-significant. *: p<0.05.
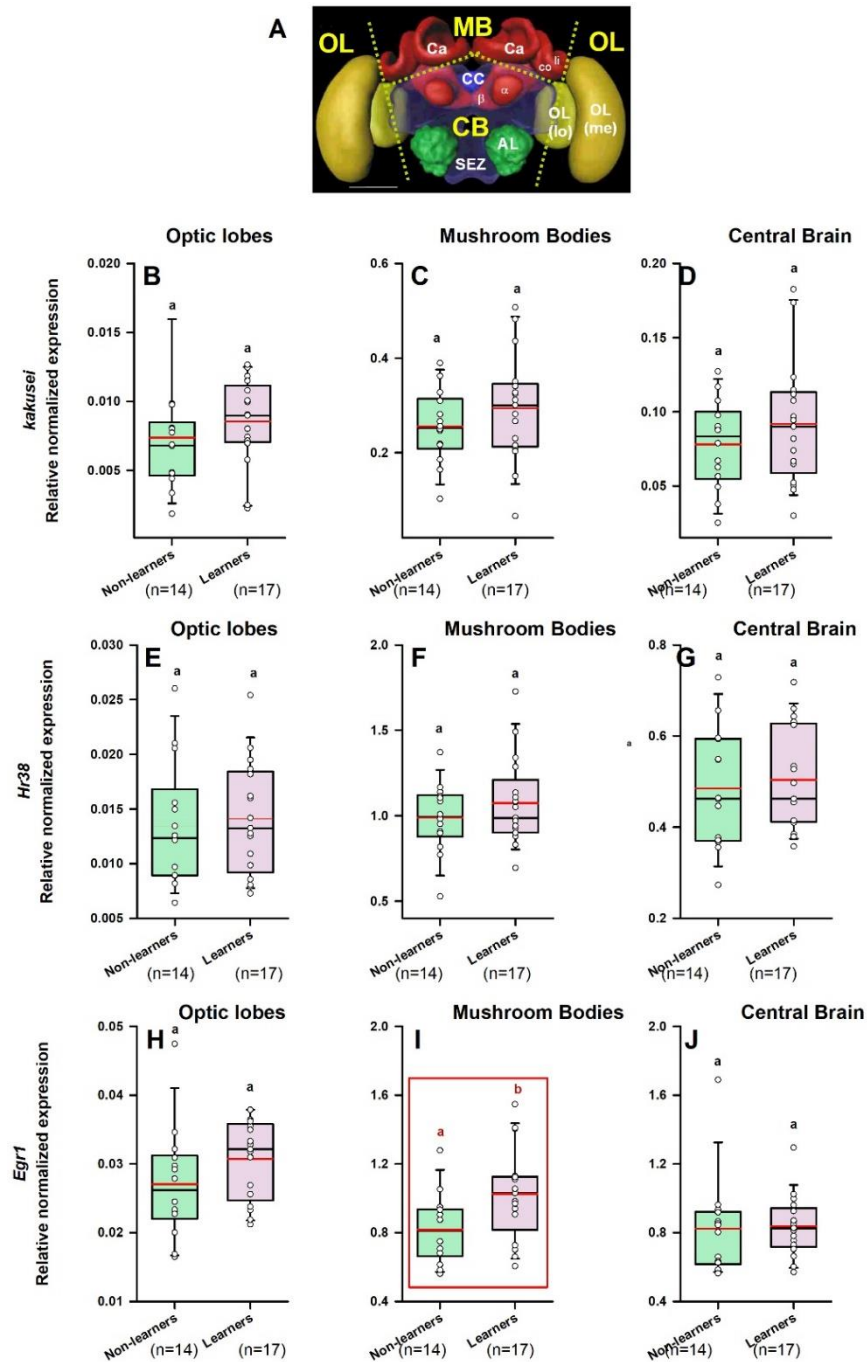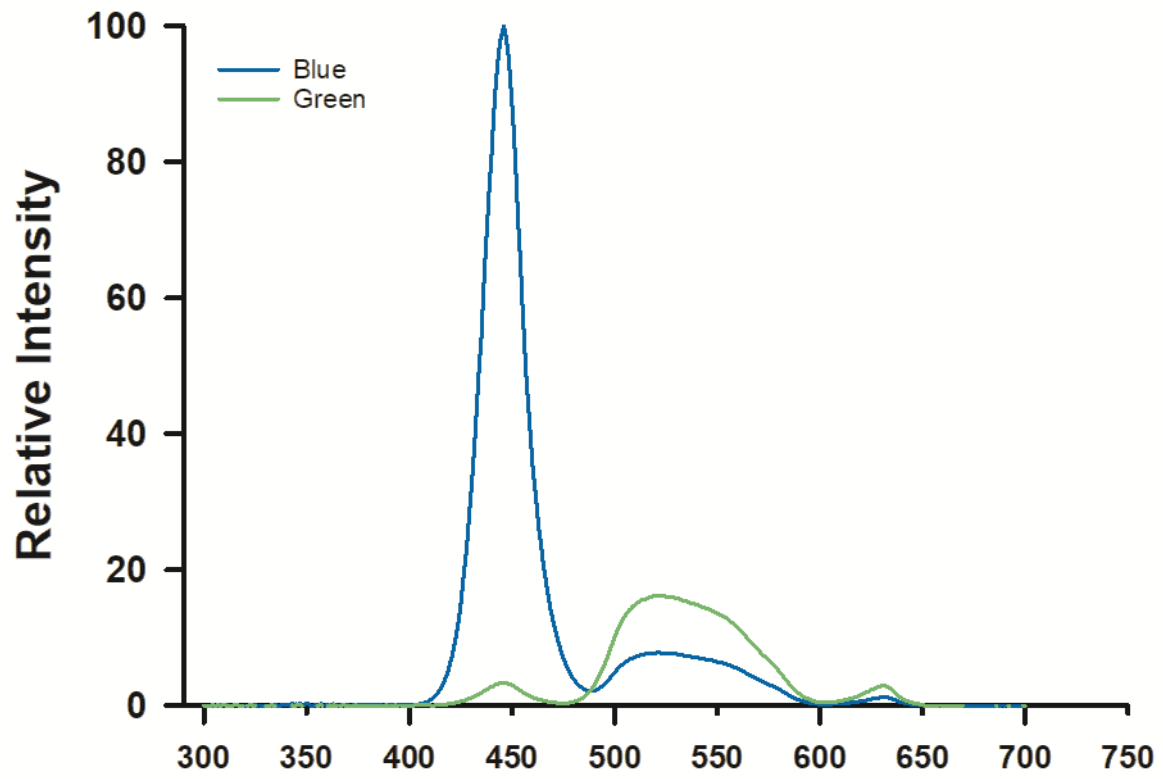
Figure 5. *Egr1*, **but neither** *kakusei* **nor** *Hr38,* **shows significant variation of relative expression in the mushroom bodies following visual associative learning in a 3D VR environment. A) Honey bee brain with sections used for quantifying IEG expression.** Yellow labels indicate the brain regions used for the analysis: MB: mushroom body; CB: central brain; OL: optic lobes. The dashed lines indicate the sections performed. Ca: calyx of the mushroom body; li: lip; co: collar; α and β: α and β lobes of the mushroom body; CC: central complex; AL: antennal lobe; SEZ: subesophagic zone; OL: optic lobe; Me: medulla; lo: lobula. **(B-D) Relative normalized expression of** *kakusei*, **of** *Hr38* **(E-G) and of** *Egr1* **(H-J) in three main regions of**

the bee brain, the optic lobes (B, E, H), the calyces of the mushroom bodies (C, F, I) and the central brain (D, G, J). The expression of each IEG was normalized to the expression of two genes of reference (*Actin and Ef1α*) in the case of the MB and the CB, and of *Actin* alone in the case of the OL (see Supplementary Figure 2). The range of ordinates was varied between target genes to facilitate appreciation of data scatter. IEG expression was analyzed in individual brains of bees belonging to two categories: *learners* (conditioned bees that responded correctly and chose the CS+ in their first choice during the non-reinforced test) and *non-learners* (conditioned bees that did not choose the CS+ in their first choice during the non-reinforced test). The range of ordinates was varied between target genes to facilitate appreciation of data scatter. Numbers within parentheses indicate the number of brains used for each analysis. Box plots show the mean value in red. Error bars define the 10th and 90th percentiles. Red boxes indicate cases in which significant variations were detected. Different letters on top of box plots indicate significate differences ($p < 0.05$).
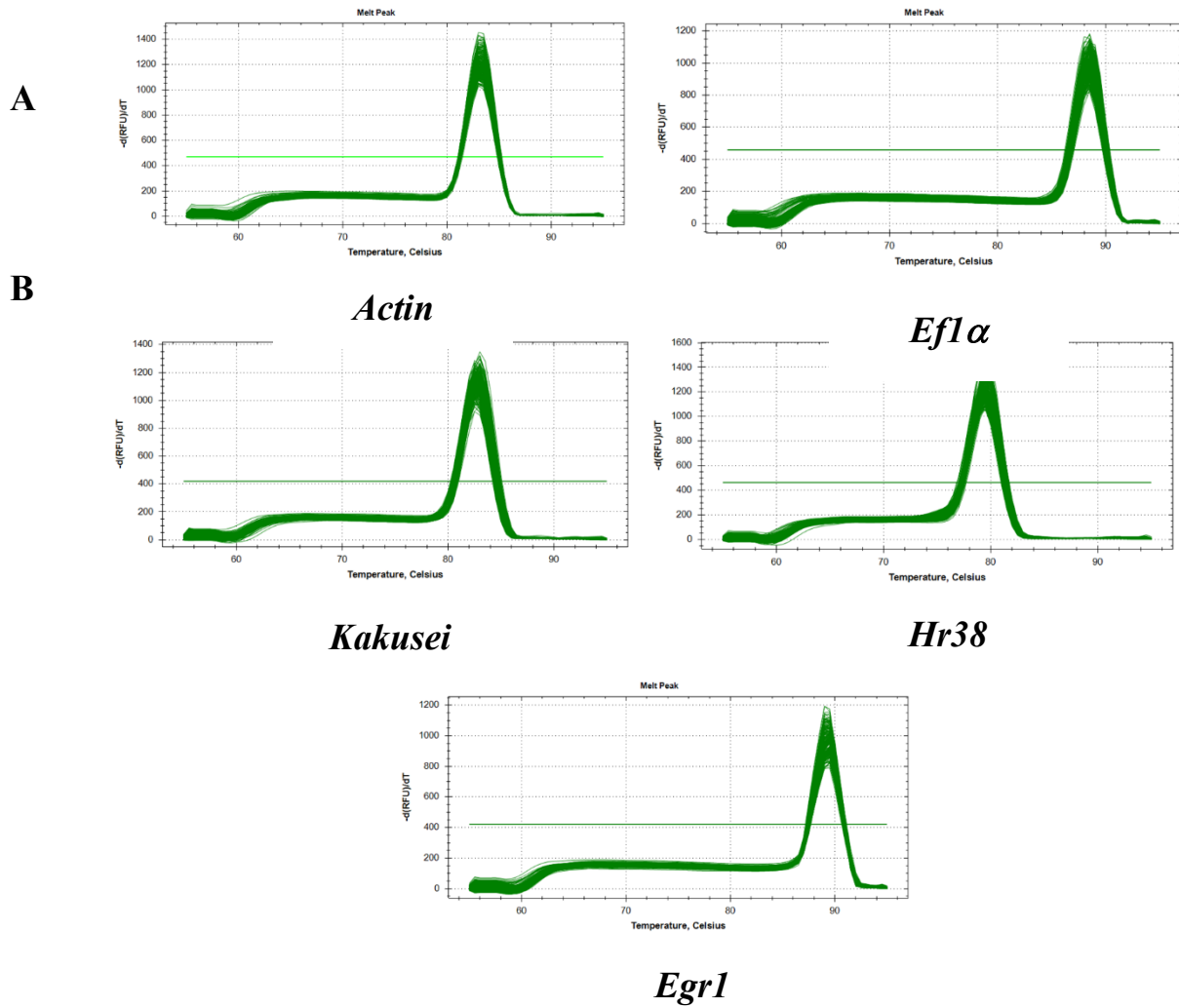
Table 1. Primer sequences used to quantify RNA expression of genes of interest and reference genes by RT-qPCR. Amplicon length (bp), efficiency (E, %) and the coefficient of correlation obtained for the standard curve (R^2) are also shown.

| Type of gene	Target	Primer sequence 5' ➤3'	Amplicon length (bp)	E (%)	R^2
Target genes	*Kakusei*	CTACAACGTCCTCTTCGATT (forward)	149	96.4	0.991
		CCTACCTTGGTATTGCAGTT (reverse)			
	Hr38	TGAGATCACCTGGTTGAAAG (forward)	118	106	0.995
		CGTAGCAGGATCAATTTCCA (reverse)			
	Egr1	GAGAAACCGTTCTGCTGTGA (forward)	138	109	0.991
		GCTCTGAGGGTGATTTCTCG (reverse)			
Reference genes	*Ef1α*	AAGAGCATCAAGAGCGGAGA (forward)			
		CACTC TTAATGACGCCCACA (reverse)	148	106	0.993
	Actin	TGCCAACACTGTCCTTTCTG (forward)			
		AGAATTGACCCACCAATCCA (reverse)	156	110	0.995

Supplementary Materials

Supplementary Figure 1. Spectral distribution (relative intensity as a function of wavelength) of the blue light (dominant wavelength 446 nm) and the green light (dominant wavelength 528 nm) used to train the bees in the color discrimination task.

A

Actin

Ef1α

B

Kakusei

Hr38

Egr1

Supplementary Figure 2. Validation selectivity of gene-specific primers. Melting peaks of qRT-PCR. **(A)** Reference genes. *(B)* Target genes.
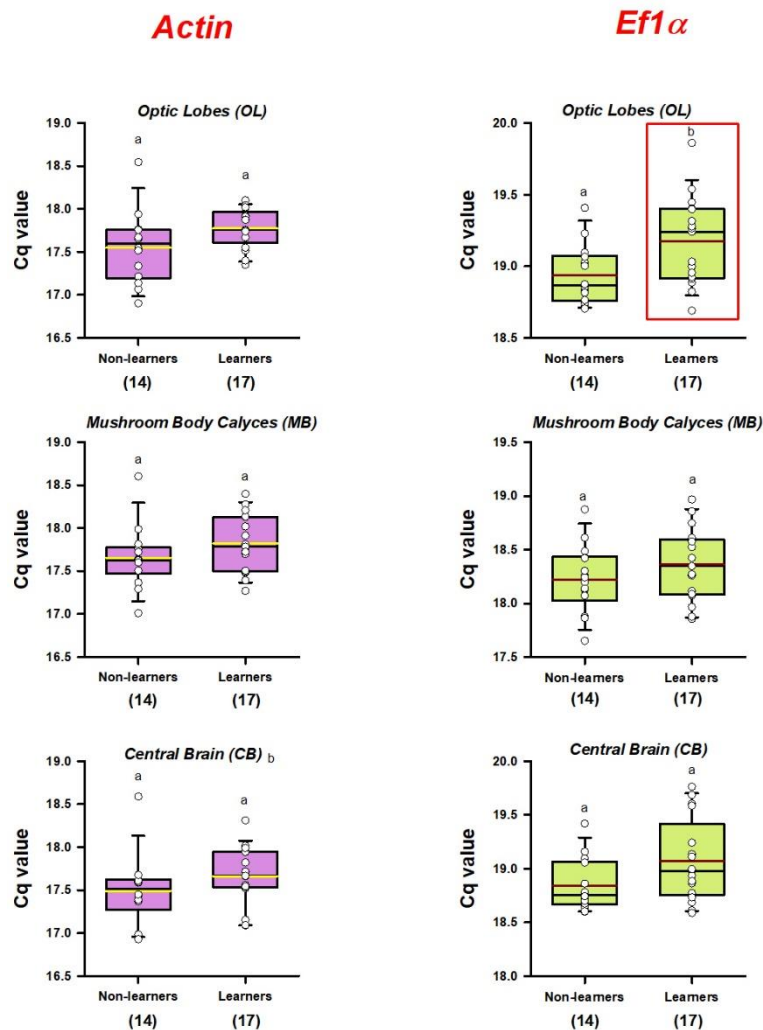
Supplementary Figure 3. Expression levels (Cq values) of the reference genes *Actin* and *Ef1α*. Expression levels are reported for the experimental groups (*Learners* and *Non-learners*) and the brain regions considered (optic lobes, mushroom body calyces and central brain). The range of ordinates was varied between graphs to facilitate appreciation of data scatter. Box plots show the mean value in yellow (*Actin*) or red (*Ef1α*). Sample sizes are indicated within parentheses below each group. Error bars define the 10th and 90th percentiles. Red boxes indicate cases in which significant variations were detected. These cases were excluded in the subsequent target analyses. For instance, for the optic lobes only *Actin* was used as reference gene, while the two reference genes were used for the other brain regions. Different letters on top of box plots indicate significate differences ($p < 0.05$).

Chapter 3

The Neural Signature of Visual Learning Under Restrictive Virtual-Reality Conditions

Gregory Lafon[1‡], Haiyang Geng[1,2‡], Aurore Avarguès-Weber[1], Alexis Buatois[1†§], Isabelle Massou[1§] and Martin Giurfa[1,2,3*§]

[1] Research Center on Animal Cognition, Center for Integrative Biology, CNRS, University of Toulouse, Toulouse, France, [2] College of Animal Sciences (College of Bee Science), Fujian Agriculture and Forestry University, Fuzhou, China, [3] Institut Universitaire de France, Paris, France

Honey bees are reputed for their remarkable visual learning and navigation capabilities. These capacities can be studied in virtual reality (VR) environments, which allow studying performances of tethered animals in stationary flight or walk under full control of the sensory environment. Here, we used a 2D VR setup in which a tethered bee walking stationary under restrictive closed-loop conditions learned to discriminate vertical rectangles differing in color and reinforcing outcome. Closed-loop conditions restricted stimulus control to lateral displacements. Consistently with prior VR analyses, bees learned to discriminate the trained stimuli. *Ex vivo* analyses on the brains of learners and non-learners showed that successful learning led to a downregulation of three immediate early genes in the main regions of the visual circuit, the optic lobes (OLs) and the calyces of the mushroom bodies (MBs). While *Egr1* was downregulated in the OLs, *Hr38* and *kakusei* were coincidently downregulated in the calyces of the MBs. Our work thus reveals that color discrimination learning induced a neural signature distributed along the sequential pathway of color processing that is consistent with an inhibitory trace. This trace may relate to the motor patterns required to solve the discrimination task, which are different from those underlying pathfinding in 3D VR scenarios allowing for navigation and exploratory learning and which lead to IEG upregulation.

Keywords: vision, visual learning, virtual reality, honey bee (*Apis mellifera*), brain, IEG expression, mushroom bodies, optic lobes

INTRODUCTION

Learning relies on changes in neural activity and/or connectivity in the nervous system, which underlie the acquisition of new, durable information based on individual experience. Invertebrate models have proved to be extremely influential to characterize learning and memory at multiple levels, not only because they allow determining where and when such changes occur in the nervous system (Kandel, 2001; Heisenberg, 2003; Giurfa, 2007, 2013, 2015; Benjamin et al., 2008; Cognigni et al., 2018) but also because their behavioral performances can be studied in standardized laboratory protocols that allow full control over the sensory variables that animals should learn and memorize. A paradigmatic example is provided by the honey bee *Apis mellifera*, where the study of olfactory learning and memory experienced significant progresses thanks to the availability of a

The neural signature of visual learning under restrictive virtual-reality conditions

Gregory Lafon[1]*, Haiyang Geng*[1,2], Aurore Avarguès-Weber[1], Alexis Buatois[1,¥,§], Isabelle Massou[1,§], Martin Giurfa[1,2,3§]

[1] Research Centre on Animal Cognition, Center for Integrative Biology, CNRS, University of Toulouse, 118 route de Narbonne, F-31062 Toulouse cedex 09, France.

[2] College of Animal Sciences (College of Bee Science), Fujian Agriculture and Forestry University, Fuzhou 350002, China.

[3] Institut Universitaire de France, Paris, France (IUF).

* Equal contribution

§ Senior authorship shared

¥ Present address: Institute of Neuroscience and Physiology, Department of Neurochemistry and Psychiatry, University of Gothenburg, Su Sahlgrenska, 41345 Göteborg, Sweden.

Corresponding author: Dr. Martin Giurfa

Research Centre on Animal Cognition, CNRS – UPS, 31062 Toulouse cedex 9, France

martin.giurfa@univ-tlse3.fr

Abstract

Honey bees are reputed for their remarkable visual learning and navigation capabilities. These

capacities can be studied in virtual reality (VR) environments, which allow studying performances of tethered animals in stationary flight or walk under full control of the sensory environment. Here we used a 2D VR setup in which a tethered bee walking stationary under restrictive closed-loop conditions learned to discriminate vertical rectangles differing in color and reinforcing outcome. Closed-loop conditions restricted stimulus control to lateral displacements. Consistently with prior VR analyses, bees learned to discriminate the trained stimuli. Ex vivo analyses on the brains of learners and non-learners showed that successful learning led to a downregulation of three immediate early genes in the main regions of the visual circuit, the optic lobes (OLs) and the calyces of the mushroom bodies (MBs). While *Egr1* was downregulated in the OLs, *Hr38* and *kakusei* were coincidently downregulated in the calyces of the MBs. Our work thus reveals that color discrimination learning induced a neural signature distributed along the sequential pathway of color processing that is consistent with an inhibitory trace. This trace may relate to the motor patterns required to solve the discrimination task, which are different from those underlying pathfinding in 3D VR scenarios allowing for navigation and exploratory learning and which lead to IEG upregulation.

Keywords

Vision – Visual Learning – Virtual Reality – Honey Bee Brain – Immediate Early Genes – Mushroom Bodies – Optic Lobes

Introduction

Learning relies on changes in neural activity and/or connectivity in the nervous system, which underlie the acquisition of new, durable information based on individual experience. Invertebrate models have proved to be extremely influential to characterize learning and memory at multiple levels, not only because they allow determining where and when such changes occur in the nervous system [1-7] but also because their behavioral performances can be studied in standardized laboratory protocols that allow full control over the sensory variables that animals should learn and memorize. A paradigmatic example is provided by the honey bee *Apis mellifera,* where the study of olfactory learning and memory experienced significant progresses thanks to the availability of a Pavlovian conditioning protocol that offers the possibility of acquiring consistent behavioral data coupled with the simultaneous use of invasive methods to record neural activity [5, 8-10]. In this protocol, termed the olfactory conditioning of the proboscis extension reflex (PER), harnessed bees learn to associate an odorant with a reward of sucrose solution [10, 11]. The immobility imposed to the trained bees and the Pavlovian nature of the association learned (the odorant acts as the conditioned stimulus and the sucrose reward as the unconditioned stimulus) allows a full control over the stimulations provided and thus a fine characterization of behavioral changes due to learning and memory.

In the case of visual learning by honey bees, this possibility is reduced as performances are mostly studied in free-flying foragers [5, 12] under semi-natural conditions. Yet, virtual-reality (VR) environments have been recently developed to overcome this limitation [13] as they provide not only a full control over the visual surrounding of an experimental subject, be it tethered or not, but also the delivery of physically impossible ambiguous stimuli, which give conflicting visual information [14]. In one type of VR that we developed in the last years, a tethered bee walks stationary on a treadmill while being exposed to a controlled visual environment displayed by a video projector. Bees can then be trained with virtual targets that are paired with gustatory reward or punishment [13, 15-19]. To create an immersive environment, closed-loop visual conditions are used in which the variations of the visual panorama are determined by the walking movements of the bee on the treadmill. Under these conditions, bees learn and memorize simple [15, 19] and higher-order [20] visual discriminations, which offers the potential for mechanistic analyses of visually-oriented

performances [17, 18].

We have used two different types of closed loop situation so far: a restrictive 2D situation, in which bees can displace conditioned targets only frontally (i.e. from left to right and vice versa)[15, 19, 20], and a more realistic 3D situation which includes a depth dimension so that targets expand upon approach and retract upon distancing[21]. Although bees learn to discriminate color stimuli in both conditions, the processes underlying such learning may differ given the different conditions imposed to the bees in terms of stimulus control. Indeed, while in 3D scenarios movement translates into a displacement and a recognizable change in the visual scene, which can then be computed against the available internal information about the displacement, 2D scenarios are restricted to the execution of actions that are dependent on reinforcement contingency. These two conditions may give rise to different mechanisms of information acquisition.

In a recent work, we studied color learning in the 3D scenario and quantified immediate early genes (IEGs) in the brain of learners and non-learners to uncover the regions that are involved in this discrimination learning[22]. IEGs are efficient markers of neural activity as they are transcribed transiently and rapidly in response to specific stimulations inducing neural activity without *de novo* protein synthesis[23-25]. Three IEGs were quantified on the basis of numerous reports that associated them with foraging and orientation activities[26-30]: *kakusei*, a nuclear non-coding RNA[31], the hormone receptor 38 gene (*Hr38*), a component of the ecdysteroid signalling pathway[32], and the early growth response gene-1 (*Egr1*), which is a major mediator and regulator of synaptic plasticity and neuronal activity[33]. We found that color learning in the 3D VR environment was associated with an *upregulation* of *Egr1* in the calyces of the mushroom bodies[22], a main structure of the insect brain repeatedly associated with the storage and retrieval of olfactory memories[2, 9]. No other changes of IEG expression were detected in other regions of the brain, thus underlining the relevance of mushroom bodies for color learning and retention[22].

Here we asked if color learning in the more restrictive 2D VR environment induces changes in IEG expression, both at the gene level and at the brain region level, similar to those detected in the 3D VR system. Asking this question is important to determine if changes in IEG expression differ according to the degrees of freedom of the VR system and the distinct motor patterns that are engaged in either case. Despite the similarity in behavioral performance (bees learn to discriminate

colors in both scenarios), we reasoned that the processes underlying learning may be different given the restrictive conditions of the 2D VR, which demand a tight stimulus control while the 3D VR enables exploration of the virtual environment. We thus studied color learning in the 2D VR environment and performed *ex vivo* analyses to map IEG expression in brain areas of learners and non-learners, which had the same sensory experience and only differed in terms of learning success.

Results

Behavioral analyses

Honey bee foragers from a hive located in our apiary were captured at an artificial feeder to which they were previously trained. They were enclosed in individual glass vials and brought to the laboratory where they were prepared for the VR experiments. A tether was glued on their thorax (Fig. 1A,B), which allowed to attach them to a holder to adjust their position on a treadmill. The treadmill was a polystyrene ball that was suspended on an air cushion produced by an air pumping system (see Methods for details). The bee suspended from its tether could walk stationary on the treadmill; its movements were recorded by two infrared optic-mouse sensors placed on the ball support perpendicular to each other, which allowed to reconstruct the trajectories and quantify motor parameters. A semi-cylindrical screen made of semitransparent tracing paper was placed in front of the treadmill (i.e. of the walking bee; Fig. 1A). Images were projected onto this screen by a video projector placed behind it.

Bees were trained to discriminate a green from a blue vertical bar against a black background during ten conditioning trials (Fig. 1C; see Supplementary Fig. 1 for color characteristics). Experiments were performed under 2D closed-loop conditions so that the movements of the walking bee displaced the bars laterally on the screen to bring them towards or away from front of the bee. During training, one of the bars (CS+) was rewarded with 1 M sucrose solution while the other bar (CS-) was punished with an aversive 3M NaCl solution[34-36]. A choice was recorded when the bee moved one rectangle to the center of the screen (i.e., between -12.5° and +12.5° of the bee's central axis; see Fig. 1D, right).

We segregated learners and non-learners according to the bees' performance in a dedicated

unrewarded test at the end of the training. Learners (n=23) were those bees that showed successful discrimination in the test (i.e. which chose the CS+). Non-learners (n=17), were those bees that did not succeed in the test (i.e. they either chose the CS- or did not make a choice). Importantly, these bees have the same sensory experience in terms of exposure to the color stimuli and reinforcements as our training procedure froze the CS+ or the CS- stimuli in front of the bee during 8 s upon a choice and delivered the reinforcements accordingly. Bees that did neither choose the CS+ nor the CS- in at least 5 trials were excluded from the analysis.

Acquisition was significant for learners during conditioning trials (Fig. 2A; CS*Trial effect: $\chi2=47.746$, df:2, p<0.0001), thus showing that the categorization made based on test performance reflected well learning success. The percentages of bees responding to the CS+ and to the CS- differed significantly along trials (CS+ vs. CS-: CS*Trial; z=6.845, p<0.0001). Significant differences were also found between the bees responding to the CS- and the non-responders (CS- vs NC: CS*Trial; z=3.541, p=0.0004) but not between bees responding to the CS+ and non-responders (CS+ vs. NC: CS*Trial; z=-1.201, p=0.23). Non-learners (n=17) did also show a significant CS*Trial effect (Fig. 2B; $\chi2=9.8383$, df:2, p=0.007), but this effect was introduced by the non-responders. These bees differed significantly along trials both from the bees responding to the CS+ (CS+ vs. NC: CS*Trial; z=2.356, p=0.019) and from the bees responding to the CS- (CS- vs. NC: CS*Trial; z=3.068, p=0.002). On the contrary, the percentages of bees responding to the CS+ and to the CS- did not vary along trials (CS+ vs. CS-: CS*Trial; z=1.437, p=0.2), consistently with the absence of learning.

Learners and non-learners did not differ in their motor activity during training, thus excluding this factor as determinant of possible changes in neural activity. When walking speeds and the distances travelled were compared between groups, no significant differences were detected (*Distance*: Group; $\chi2=1.93$, df:1, p=0.16; *Speed*: Group; $\chi2=1.78$, df:1, p=0.18).

In the non-reinforced test, per definition learners (Fig. 2C) chose correctly the CS+ (100% of the bees) while non-learners (Fig. 2D) did either chose the CS- (35%) or did not perform any choice (65%). Learners spent more time fixating the CS+ than the CS- consistently with the choice made during the test (Wilcoxon signed rank exact test: V=17, p<0.0001) while non-learners did not differ in their fixation time for both stimuli in spite of a tendency to fixate more the CS- (V=26,

p= 0.05).

Molecular analyses

We aimed at determining if visual learning in the 2D VR induces transcriptional changes revealing the neural trace of the associative learning described in the previous section. To this end, we performed RT-qPCR in individual brains of learners (n=22; one learner brain was lost during the dissection process) and non-learners (n=17), focusing on three main brain sections (Fig. 3A): the optic lobes (OLs), the calyces of the mushroom bodies (MB) and the remaining central brain (CB), which included mainly the central complex, the subesophageal zone and the peduncula of the mushroom-bodies (α and β lobes). Brains were collected one hour after the retention test, which ensures that expression of all three genes was already induced (typically, from 15 to 90 min in the case of kakusei[31, 37] and 30-60 min in the case of *Hr38* and *Egr1*[28, 29]).

Two reference genes were used for the normalization (see Table 1): *Ef1a* (E=106%) and *Actin* (E=110%)[38]. Within-brain structure analyses showed that reference genes did not vary between learners and non-learners (t test; all comparisons NS; see Suppl Fig. 3) thus enabling further comparisons between these two categories with respect to the three target IEGs. To this end, the normalization procedure used the geometric mean of the two reference genes. No cross-comparisons between brain regions or genes were performed.

Figures 3 B-D, E-G, and H-J show the relative normalized expression of *kakusei, Hr38* and *Egr1*, respectively, for the three brain regions considered in the case of *learners and non-learners.* (*Egr1:* Fig. 3H; t = -2.32; df:37; p=0.03). All other within-structure comparisons between learners and non-learners were not significant (p>0.05). Notably, in the three cases in which significant variations of IEG expression were found, learners exhibited a *downregulation* of IEG expression with respect of non-learners. In addition, from the three cases, two referred to the MB calyces, which indicates the important role of this region for visual learning and memory.

Discussion

The present work studied visual learning under a restrictive 2D VR environment and confirmed that bees can learn to discriminate visual stimuli based on their color under these artificial conditions. Walking parameters did not differ between learners and non-learners so that changes

in IEG expression could be ascribed to learning success. We showed that associative color learning leads to a downregulation of the three IEGs considered in different areas of the visual circuit. While *Egr1* was downregulated in the optic lobes, *Hr38* and *kakusei* were coincidently downregulated in the MB calyces. Our work thus reveals that the neural trace of associative color learning in the bee brain is distributed along the sequential pathway of color processing and highlights the importance of MBs for color learning in bees.

IEG downregulation in the bee brain

We observed an IEG *downregulation* both in the optic lobes and the calyces of the MBs. This phenomenon is interesting as increased neural activity resulting from experience-dependent phenomena is usually reflected by an *upregulation* of IEG expression[24]. Typically, upon neural responses, a relatively rapid and transient pulse of gene expression may occur, which corresponds to an experience-dependent activation of the underlying synaptic circuitry[23, 39]. In our case, however, the downregulation observed indicates that a different form of experience-dependent change in neural activity occurred as a consequence of learning. A possible explanation for this phenomenon may put the accent on an inhibition of neural activity in key visual areas – optic lobes and mushroom bodies - of the learner group.

In the optic lobes, *Erg1* downregulation may correspond to an increased GABAergic inhibitory activity associated with learning. The optic lobes exhibit multiple GABAergic fibers distributed principally in the medulla and the lobula[40] so that neural activity in these regions is subjected to intense GABAergic inhibitory signaling. Higher GABAergic activity has been reported in the optic lobes of forager bees *via* quantification of *Amgad*, the honey bee homolog of the gene responsible for synthesizing the enzyme GAD[41], which catalyzes the decarboxylation of glutamate to *GABA*. This increase was accompanied by an increase in *kakusei*[41]*,* which we did not observe. Yet, we did not study foraging behavior in a natural context, but associative learning in a controlled laboratory context. Natural foraging may involve multiple behavioral components and stimulations that may be responsible for the increase of *kakusei* that was absent in our study. The interesting finding is, however, that *Amgad* expression revealed higher GABAergic neuron activity in the optic lobes of foragers, confirming the importance of inhibitory feedback for sustaining

experience-dependent visual responses. This conclusion is supported by observed increases of GABA titers in the honey bee optic lobes upon restart of foraging activities[42] and by findings in fruit flies indicating that GABA-ergic neurons in the optic lobes are involved in tuning the sensitivity and selectivity of different visual channels[43, 44].

In the calyces of the MBs, where coincident downregulation of *kakusei* and *Hr38* was found, neural inhibition is provided by GABAergic feedback neurons (the so-called Av3 neurons)[45], which are responsible for the sparse coding responses exhibited by Kenyon cells, the constitutive neurons of the MBs. Similar GABAergic neurons exist in fruit flies, which provide inhibitory feedback to the MBs. These neurons, termed APL (anterior paired lateral) neurons, are necessary for discrimination learning of similar odorants. When flies are trained to discriminate odorants in a simple differential conditioning, disrupting the Kenyon cell-APL feedback loop decreases the sparseness of Kenyon cell odor responses, increases inter-odor correlations and prevents flies from learning to discriminate similar, but not dissimilar, odors[46]. Inhibitory feedback onto the calyces of honey bees is needed for solving patterning tasks in which insects have to suppress summation of responses to single elements previously rewarded when they are presented in an unrewarded compound[47] (i.e. animals have to learn to respond to the elements and not to the compound) or for reversal learning[48]. A similar conclusion applies to fruit flies as GABAergic input to the MBs provided by APL neurons also mediates the capacity to solve patterning tasks[49]. Increased feedback inhibition at the level of the MBs may therefore appear as a hallmark of certain learning phenomena, which require enhanced neural sparseness to decorrelate stimulus representations and thus memory specificity. In our experiments, both *kakusei* and *Hr38* were subjected to downregulation in the MBs as a consequence of learning, a phenomenon that may be due to plastic changes in GABAergic signaling in the calyces of the MBs. Importantly, other visual areas such as the central complex[50] or the anterior optic tuberculum[51, 52], among others, could exhibit similar variations undetectable for our methods as sectioning the frozen bee brain for molecular analyses does not allow a fine dissection of these areas.

IEG downregulation is not a common phenomenon as upregulation is usually reported to indicate the presence of neural activation[22]. Our hypothesis on neural inhibition being the cause for this downregulation requires, therefore, to be considered with caution. Further experiments are necessary to validate it, using – for instance – electrophysiological recordings in key areas of the

visual circuits of learners to verify that neural activity is indeed sparser therein compared to non-learners. In addition, quantifying IEG expression in preparations in which neural inhibition has been characterized extensively at the cellular level such as in the case of hippocampal and cerebellum slices exhibiting long-term depression (LTD)[53] could be also important.

The neural signature of associative learning differs between different forms of VR

While the main finding in our experiments refer to a downregulation of IEG genes in key regions of the visual circuit, our previous work using a different 3D VR system yielded a different result[22]. In this 3D VR, bees could explore the virtual surroundings around the stimuli to be learned (not bars, but cuboids that expanded upon forward movements of the bee) and could displace these stimuli laterally and in depth. They explored and learned to discriminate the color stimuli proposed to them and their learning success was comparable, yet slightly lower than that observed in the 2D VR arena (50% vs. 55%, respectively). IEG analyses comparing learners and non-learners in the 3D VR reported an *upregulation* of *Egr1* expression in the MB calyces of learners but not of non-learners. No other change was detected for *kakusei* and *Hr38* in the same three brain regions considered in the present work[22].

These differences are difficult to interpret as the 2D and the 3D VR experiments were not done simultaneously but in different years, though in similar seasons. In both cases, motivated foragers captured at a feeder were used for the experiments. The previous visual experience of these foragers may have differed across individual and between years, thus leading to differences in performances. This explanation seems, however, rather implausible given that in bees rely on the most recent appetitive learning as the one guiding predominantly actual choices. In addition, irrespective of differences in the VR environments and the resulting difference in VR immersivity, the experiments were done under similar handling conditions and using strictly the same behavioral criteria. Gene analyses were also performed under the same conditions and using the same materials and methods. Thus, the contrasting results obtained in the two VR scenarios may be due to the distinct constraints they imposed to achieve discrimination learning and to the fact that the two scenarios may engage different acquisition mechanisms for learning visual information. In the 3D scenario, bees explored both the stimuli – the vertical color cuboids – and

the imaginary empty surroundings; they could return to the stimuli if they missed them and walk around them, which added an important exploratory component that was absent in the 2D arena. In the latter case, although bees could also bring back the stimuli if they missed them by walking too fast, such a control was restricted to the frontal plane and did not allow for three-dimensional inspection. *Erg1* upregulation in the 3D VR upon learning may thus reflect the convergent effects of an exploratory drive and learning in a non-constrained environment. It cannot be due to a pure exploration of the environment as non-learners exhibited the same motor performances and did not show *Egr1* upregulation.

In the 2D VR, bees were forced to control tightly the lateral displacements of the stimuli – the color rectangles – without any further change allowed. This environment and task may thus impose a higher stimulus and movement control and force the bee to focus exclusively and artificially on lateral stimulus movements to gain access to sucrose reward and avoid aversive saline solution. Although in both VR scenarios the background was empty and only the training stimuli were visible, the 2D VR missed the expansion of the images upon approach and thus lacked of immersivity. In this context, GABA-mediated inhibition may act as a gain control mechanism that enhances response efficiency and stimulus control. In the primary visual cortex (V1) of vertebrates, GABA inhibition has been proposed to play a fundamental role in establishing selectivity for stimulus orientation and direction of motion[54-56]. As the latter is particularly important in the 2D VR, enhanced GABA inhibition could be associated with learning to master the visual discrimination in this context.

In addition, a different, yet compatible explanation for the different patterns of IEG expression found in the 3D and the 2D VR refers to a possible difference in the visual acquisition mechanisms recruited by these two scenarios. In a navigation task, body movement translates into a displacement and a recognizable change in the visual scene, which can then be computed against the available internal information about the displacement[57]. These pathfinding, closed-loop actions can be viewed as different from motor actions that are contingent on reinforcement such as operant behaviors produced when a visual discriminative stimulus is present[58]. In the latter case, vision is also engaged in discrimination learning but in a context that is not navigational. Visual learning in the 2D VR could be seen as a form of operant learning in which colors define the action to be produced to obtain the appropriate reinforcement. Thus, the observed difference in IEG expression

between the two types of VR may reflect a difference in the mechanisms used to reach the rewarded stimulus.

The role of mushroom bodies for visual learning and memory

Our work highlights the participation of mushroom bodies in visual learning and short-term visual retention. Numerous works have demonstrated the necessity of these brain structures for the acquisition, storage and retrieval of olfactory memories in bees[8, 59, 60] and other insects[2, 3, 61]. Yet, less is known about their implication in visually-driven behavioral and neural plasticity[62, 63]. In our study, the full control over sensory stimulation offered by the VR system allowed a sound comparison between the brain of learners and non-learners, which revealed a neural signature for visual learning that included the mushroom bodies.

The implication of mushroom bodies in visual learning and memory in the bee is expected given the parallels between visual and olfactory inputs at the level of the calyces. While afferent projection neurons convey olfactory information to the lip, a subdivision of the calyces[64], afferent neurons from the lobula and the medulla, which are part of the optic lobes, convey visual information to other calyx subdivisions, the collar and the basal ring[65, 66]. In spite of this similarity, studies addressing the role of mushroom bodies in honey bee visual learning and memory remain rare.

Bees learning to associate color lights with the presence or absence of an electric shock in a double-compartment box [38, 67] require the ventral lobe of the mushroom bodies to learn to avoid the punished color and spend more time in the safe color[68]. In the same study, pharmacological blockade of one of the four collars (two per MB) had no effect on discrimination learning[68], which does not exclude a participation of this MB region in this visual learning given that the remaining three calyces could compensate for the loss of the blocked one. In a different study, upregulation of the dopamine receptor *Amdop1* was found in the calyces of the MBs when bees were trained to inhibit positive phototaxis towards a colored light[38].

More recently, the implication of MBs in visual navigation was shown in wood ants *Formica rufa*, which are innately attracted to large visual cues (i.e. a large vertical black rectangle) and which can nevertheless be trained to locate and travel to a food source placed at a specific angle

away from the attractive black rectangle[69]. When their MB calyces were blocked by injection of procaine[70, 71], ants reverted their trajectories towards the attractive rectangle, which suggests a role for mushroom bodies in the dissociation between innate and learned visual responses, and in navigational memory[69]. In another study involving the ant *Myrmecia midas,* procaine was again used to block MB function *via* delivery into the vertical lobes and evaluate the impact of this blockade in orientation in a familiar environment[72]. Experienced forager with procaine-inactivated VLs had tortuous paths and were unable to find their nest, whereas control ants were well directed and successful at returning home[72]. Overall, these two studies on ant navigation indicate that the vertical lobes of MBs are necessary for retrieving visual memories for successful view-based navigation.

Studies on the role of MBs for visual learning and memory in fruit flies have yielded contradictory findings. Mushroom body deficits do not affect learning success in the flight simulator, a setup in which tethered flies in stationary flight learn to avoid quadrants associated with specific visual landmarks based on the presence of an aversive heat beam pointed towards their thorax[73]. Similarly, learning to discriminate colors in a cylindrical container made of a blue-lit and a yellow-lit compartment, one of which was associated with aversive shaking of the flies, was not affected in mushroom body mutants[74]. Spatial learning of a non-heated spot in an otherwise heated cylindrical arena displaying surrounding visual landmarks is possible in the absence of functional mushroom bodies but not of the central complex[75]. Although these various results points toward a dispensability of MBs for visual learning in fruit flies[73], experiments comparing appetitive and aversive color learning and discrimination question this view[76]. When blue and green colors were presented from below in an arena, walking flies learned both the appetitive (based on pairing one color with sugar) and the aversive discrimination (based on pairing one color with electric shock) but failed if MB function was blocked using neurogenetic tools[76]. Furthermore, MBs are required for visual context generalization (e.g. generalizing landmark discrimination in a flight simulator in which contextual light was switched from blue to green between training and test)[77-79]. Thus, MBs participate in different forms of visual learning in fruit flies, although their involvement in these phenomena seems to be less clear than in other insects.

Taken together, our results revealed that learning a visual discrimination under a 2D VR, in

which closed-loop conditions restricted stimulus control to lateral displacements, induced a neural signature that spanned the optic lobes and MB calyces and that was characterized by IEG downregulation, consistent with an inhibitory trace. This trace may vary and become excitatory in more permissive VR conditions in which closed-loop conditions allow for 3D exploration during discrimination learning[22].

Materials and Methods

Honey bees (Apis mellifera) were obtained from our apiary located at the campus of the University Paul Sabatier – Toulouse III during September 2021. Only foragers caught upon landing on a gravity feeder filled with a 0.9 M sucrose solution were used in our experiments to ensure high appetitive motivation. Captured bees were enclosed in individual glass vials and then transferred to small cages housing ten bees in average; caged bees had access to *ad libitum* water and to 300 μl of 1.5 M sucrose solution. They were kept overnight in an incubator at 28 °C and 80% humidity. On the next day, they were placed on ice for five minutes to anesthetize them and facilitate the gluing of a tether to their thorax by means of melted wax (Fig. 1A). After being attached to the tether, each bee was placed on a small (5 cm diameter) Styrofoam ball for familiarization with the treadmill situation. Bees were provided with 5 μl of 1.5 M sucrose solution and kept for 3 h in this provisory setup in the dark. They were then moved to the VR arena and used for the experiments.

Once in the VR setup, the bee was attached to a holder that allowed adjusting its position on the treadmill (Fig. 1B), a polystyrene ball (diameter: 5 cm, weight: 1.07 g) held by a 3D-printed support and floating on a constant airflow produced by an air pump (airflow: 555ml/s; Aqua Oxy CWS 2000, Oase, Wasquehal, France).

VR setup

The VR setup consisted of the treadmill and of a half-cylindrical vertical screen made of semi-transparent tracing paper, which allowed presentation of a 180° visual environment to the bee (diameter: 268 mm, height: 200 mm, distance to the bee: 9 cm Fig. 1ABC) and which was placed in front of the treadmill. The visual environment was projected from behind the screen using a

video projector connected to a laptop (Fig. 1A). The video projector was an Acer K135 (Lamp: LED, Maximum Vertical Sync: 120 Hz, Definition: 1280 x 800, Minimum Vertical Sync: 50 Hz, Brightness: 600 lumens, Maximum Horizontal Sync: 100.103 Hz, Contrast ratio: 10 000:1, Minimum Horizontal Sync: 30.103 Hz)15. The movements of the walking bee on the treadmill were recorded by two infrared optic-mouse sensors (Logitech M500, 1000 dpi, Logitech, Lausanne, Switzerland) placed on the ball support perpendicular to each other.

Experiments were conducted under 2D closed-loop conditions, i.e. rotations of the ball displaced the visual stimuli only laterally. To this end, we used a custom software developed using the Unity engine (version 2018.3.11f1), open-source code available at https://github.com/G-Lafon/BeeVR[21]. The software updated the position of the bee within the VR every 0.017 s.

Visual stimuli

Bees had to discriminate two vertical rectangles (Fig. 1C) based on their different colors and association with reward and punishment. The colors of the rectangles (see supplementary Fig. S1) were blue (RGB: 0, 0, 255, with a dominant wavelength of 450 nm and an irradiance of 161000 μW) and green (RGB: 0, 100, 0, with a dominant wavelength of 530 nm and an irradiance of 24370 μW/cm2). They were displayed on a black background (RGB: 0, 0, 0). These colors were chosen based on previous work showing their successful learning in the VR setup[15, 21].

Each rectangle had a 5 cm base and occupied the entire vertical extent of the screen. The rectangles were positioned at -50° and +50° from the bee's body axis at the beginning of each trial (Fig. 1D, left). Keeping the object within -12.5° and +12.5° in front of the central axis of the bee continuously for 1 s was recorded as a choice (Fig. 1D, right).

Conditioning and testing at the treadmill

Bees were trained using a differential conditioning, which promotes better learning performances owing to the presence of penalized incorrect color choice that result in an enhancement of visual attention[80].

Bees were trained during 10 consecutive trials using a differential conditioning procedure (Fig. 1E) in which one of the rectangles (i.e. one of the two colors, green or blue) was rewarded with 1.5 M

sucrose solution (the appetitive conditioned stimulus or CS+) while the other rectangle displaying the alternative color (the aversive conditioned stimulus or CS-) was associated with 3 M NaCl solution. The latter was used to increase the penalty of incorrect choices[34-36, 81]. To avoid directional biases, the rewarded and the punished color rectangles were swapped between the left and the right side of the virtual arena in a pseudo random manner along trials.

At the beginning of the experiment, bees were presented with a dark screen. During training trials, each bee faced the two rectangles (Fig. 1D, left). Choice of the CS+ rectangle was recorded if the bee kept it at the center of the screen (between -12.5° and +12.5° of the bee's central axis) during 1 s (Fig. 1D, right). Training was balanced in terms of color contingencies (i.e. blue and green equally rewarded across bees) based on a random assignment by the VR software. If the bee kept the CS+ in the center of the screen continuously during 1 s (i.e. if it chose it), the screen was locked on that image for 8 s. This allowed the delivery of sucrose solution in case of a correct choice, or of NaCl in case of an incorrect choice. Solutions were delivered for 3 s by the experimenter who sat behind the bee and used a toothpick to this end. The toothpick contacted first the antennae and then the mouthparts while the screen was locked on the visual image fixated by the bee. A different toothpick was used for each tastant. Each training trial lasted until the bee chose one of the two stimuli or until a maximum of 60 s (no choice). Trials were separated by an inter-trial interval of 60 s during which the dark screen was presented. Bees that were unable to choose a stimulus (i.e. that did not fulfill the criterion of a choice defined above) in at least 5 trials were excluded from the analysis. From 50 bees trained, 40 were kept for analysis (~80%).

After the last training trial, each bee was subjected to a non-reinforced test that lasted 60 s (Fig. 1E). Test performance allowed distinguishing *learners* (i.e. bees that chose the CS+ as their first choice in the test) from *non-learners* (i.e. bees that either chose the CS- in their first test choice or that did not make any choice during the test). IEG expression was compared between these two groups, which had the same sensory experience in the VR setup and which differed only in their learning success.

Brain dissection

One hour after the test, the bee was sacrificed and its head was instantly frozen in a nitrogen

solution. The frozen head was dissected on dry ice under a binocular microscope. First, the antennae were removed and a window was cut in the upper part of the head capsule, removing the cuticle between the compound eyes and the ocelli. Second, the glands and tracheae around the brain were removed. Third, the retinas of the compound eyes were also removed.

The frozen brain was cut in three main parts for IEG analyses (Fig. 3A): the optic lobes (OL), the upper part of the mushroom bodies (the mushroom-body calyces, MB Ca) and the remaining central brain (CB), which included mainly the peduncula of the mushroom-bodies (α and β lobes), the central complex (CC), the antennal lobes (AL) and the subesophageal zone (SEZ). Samples were stored at -80 °C before RNA extraction. During the dissection process, one *learner* brain was lost so that learner sample sizes differ between the behavioral (n=23) and the molecular analyses (n=22).

RNA extraction and reverse transcription

The RNAs from the three sections mentioned above (OL, MB Ca and CB) were extracted using the RNeasy Micro Kit (Qiagen). The final RNA concentration obtained was measured by spectrophotometry (NanoDrop™ One, Thermo Scientific). A volume of 10 µl containing 100 ng of the RNA obtained was used for reverse transcription following the procedure recommended in the Maxima H Minus First Strand cDNA Synthesis kit (Thermo Scientific, 0.25 µl of random hexamer primer, 1 µl of 10 mM dNTP mix, 3.75 µl of nuclease free H_2O, 4 µl 5X RT Buffer and 1 µl Maxima H Minus Enzyme Mix).

Quantitative Polymerase Chain Reaction (RT-qPCR)

All the primers used for target and reference genes generated amplification products of approximately 150 bp. The efficiencies of all reactions with the different primers used were between 95% and 110 % (Table 1). Their specificity was verified by analyzing melting curves of the RT-qPCR products (see Supplementary Fig. S2). Two reference genes (*Ef1α* and *Actin*) were used for normalization.

Expression was quantified using a SYBR Green real-time PCR method. Real-time PCR were carried out in 384-Well PCR Plates (Bio-Rad) cover with Microseal 'B' PCR Plate Sealing Film

(Bio-Rad). The PCR reactions were performed using the SsoAdvancedTM Universal SYBR® Green Supermix (Bio-Rad) in a final volume of 10 μl containing 5 μl of 2X SsoAdvancedTM Universal SYBR® Green Supermix, 2 μl of cDNA template (1:3 dilution from the reverse transcription reaction), 0.5 μl of 10 μmol of each primer and 2 μl of ultrapure water. The reaction conditions were as follows: 95 °C for 30 s followed by 40 cycles of 95 °C for 10 s, 55 °C for 30 s and a final step at 95 °C for 10 s followed by a melt curve from 55 °C to 95 °C with 0.5 °C per second. The reaction was performed in a CFX384 Touch Real-Time PCR Detection System (Bio-Rad) and analyzed with the software Bio-Rad CFX Manager.

Each sample was run in triplicates. If the triplicates showed too much variability (SD > 0.3), the furthest triplicate was discarded. If the two remaining triplicates still showed too much variability (SD > 0.3) the sample was discarded. The samples were subjected to a relative quantification and normalization. First for each sample and for each reference gene per brain region, the relative quantity (Qr) was computed using the difference between the mean Ct value of each sample and the highest mean Ct value (ΔCt), using the following formula: $Qr = (1+E)^{\Delta Ct}$ (with E= efficiency of the reaction). Then a normalization factor for each sample was obtained computing the geometric mean of the relative quantities obtained for the reference genes in the corresponding samples (ΔΔCt).

Data analysis and statistics

Behavioral data

The first choice of the bees was recorded during the conditioning trials and the non-reinforced test. In this way, we established for each trial and test the percentages of bees choosing first each of the stimuli displayed or not choosing a stimulus (± 95% confidence interval).

Test percentages were analyzed within groups by means of a generalized linear mixed model (GLMM) for binomial family in which the individual identity (Bee) was considered as a random factor (individual effect) while the choice category (CS+, CS-, NC) was fitted as a fixed effect; z values with corresponding degrees of freedom are reported throughout for this kind of analysis. For the acquisition trials, we recorded motor variables such as the total distance walked during a trial, and the walking speed. The analysis of these continuous variables was done using a linear

mixed model (lmer function) in which the individual identity (*Bee ID*) was a random factor and the factors *Group* (i.e. learner or non-learner) and *Trial* were fixed.

Statistical analyses were performed using with R 3.5.1[82]. The package lme4 was used for GLMMs and LMMs.

Gene expression data

Statistical differences in gene expression were assessed for reference genes to check for stability and for target genes within a given brain region using One-Factor ANOVA for independent groups in the case of multiple comparisons or two-sample T test in the case of dual comparisons. Pots hoc comparisons between groups were performed by means of a Tukey test following ANOVA. No cross-comparisons between brain regions or genes were performed due to within-area normalization procedures. Statistical analyses were done either with R 3.5.1 software[82] or with Statistica 13 Software (TIBCO® Data Science).

Acknowledgements

Contributions

The project was conceived by AB, AAW, IM and MG. GL performed all the behavioral experiments. HG dissected and sectioned the brains of the bees trained in the VR setup and performed all the molecular analyses. Behavioral experiments were supervised by AAW and MG. Molecular experiments were supervised by IM and MG. Statistical analyses on behavioral data

were performed by GL. Statistical analyses on gene-expression data were performed by HG and MG. The manuscript was written by MG and was corrected and discussed by all authors. MG obtained the funding necessary for this work. All authors reviewed and approved the final version of the manuscript.

Ethics declarations

Competing interests

The authors declare no competing interests.

References

1. Giurfa, M., Cognition with few neurons: higher-order learning in insects. *Trends Neurosci* **2013,** *36* (5), 285-294.

2. Heisenberg, M., Mushroom body memoir: from maps to models. *Nat. Rev. Neurosci.* **2003,** *4* (4), 266-275.

3. Cognigni, P.; Felsenberg, J.; Waddell, S., Do the right thing: neural network mechanisms of memory formation, expression and update in *Drosophila*. *Curr Opin Neurobiol* **2018,** *49*, 51-58.

4. Benjamin, P. R.; Kemenes, G.; Kemenes, I., Non-synaptic neuronal mechanisms of learning and memory in gastropod molluscs. *Front Biosci* **2008,** *13*, 4051-7.

5. Giurfa, M., Behavioral and neural analysis of associative learning in the honeybee: a taste from the magic well. *J. Comp. Physiol. A* **2007,** *193* (8), 801-824.

6. Giurfa, M., Learning and cognition in insects. *Wiley Interdiscip. Rev. Cogn. Sci.* **2015,** *6* (4), 383-395.

7. Kandel, E. R., The molecular biology of memory storage: a dialogue between genes and synapses. *Science* **2001,** *294* (5544), 1030-8.

8. Menzel, R., Memory dynamics in the honeybee. *J. Comp. Physiol. A* **1999,** *185*, 323-340.

9. Menzel, R., The honeybee as a model for understanding the basis of cognition. *Nature Rev Neurosci* **2012,** *13*, 758-768.

10. Giurfa, M.; Sandoz, J. C., Invertebrate learning and memory: fifty years of olfactory conditioning of the proboscis extension response in honeybees. *Learn Mem* **2012,** *19* (2), 54-66.

11. Bitterman, M. E.; Menzel, R.; Fietz, A.; Schäfer, S., Classical conditioning of proboscis extension in honeybees (*Apis mellifera*). *Journal of comparative psychology (Washington, D.C. : 1983)* **1983,** *97* (2), 107-119.

12. Avargues-Weber, A.; Deisig, N.; Giurfa, M., Visual cognition in social insects. *Annu Rev Entomol* **2011,** *56*, 423-43.

13. Schultheiss, P.; Buatois, A.; Avargues-Weber, A.; Giurfa, M., Using virtual reality to study visual performances of honeybees. *Curr Opin Insect Sci* **2017,** *24*, 43-50.

14. Frasnelli, E.; Hempel de Ibarra, N.; Stewart, F. J., The dominant role of visual motion cues in bumblebee flight control revealed through virtual reality. *Front. Physiol.* **2018,** *9*, 1038.

15. Buatois, A.; Flumian, C.; Schultheiss, P.; Avargues-Weber, A.; Giurfa, M., Transfer of visual learning between a virtual and a real environment in honey bees: the role of active vision. *Front. Behav. Neurosci.* **2018,** *12*, 139.

16. Rusch, C.; Roth, E.; Vinauger, C.; Riffell, J. A., Honeybees in a virtual reality environment learn unique combinations of colour and shape. *J Exp Biol* **2017,** *220* (Pt 19), 3478-3487.

17. Zwaka, H.; Bartels, R.; Lehfeldt, S.; Jusyte, M.; Hantke, S.; Menzel, S.; Gora, J.; Alberdi, R.; Menzel, R., Learning and its neural correlates in a virtual environment for honeybees. *Front. Behav. Neurosci.* **2018,** *12*, 279.

18. Rusch, C.; Alonso San Alberto, D.; Riffell, J. A., Visuo-motor feedback modulates neural activities in the medulla of the honeybee, *Apis mellifera*. *J Neurosci* **2021,** *41* (14), 3192-3203.

19. Buatois, A.; Pichot, C.; Schultheiss, P.; Sandoz, J. C.; Lazzari, C. R.; Chittka, L.; Avargues-Weber, A.; Giurfa, M., Associative visual learning by tethered bees in a controlled visual environment. *Sci. Rep.* **2017,** *7* (1), 12903.

20. Buatois, A.; Laroche, L.; Lafon, G.; Avargues-Weber, A.; Giurfa, M., Higher-order discrimination learning by honeybees in a virtual environment. *Eur J Neurosci* **2020,** *51* (2), 681-694.

21. Lafon, G.; Howard, S. R.; Paffhausen, B. H.; Avarguès-Weber, A.; Giurfa, M., Motion cues from the background influence associative color learning of honey bees in a virtual-reality scenario. *Sci. Rep.* **2021,** *11* (1), 21127.

22. Geng, H.; Lafon, G.; Avarguès-Weber, A.; Buatois, A.; Massou, I.; Giurfa, M., Visual learning in a virtual reality environment upregulates immediate early gene expression in the mushroom bodies of honey bees. *Commun Biol* **2022,** *(in press)*.

23. Clayton, D. F., The genomic action potential. *Neurobiol Learn Mem* **2000,** *74* (3), 185-216.

24. Bahrami, S.; Drabløs, F., Gene regulation in the immediate-early response process. *Advances in Biological Regulation* **2016,** *62*, 37-49.

25. Minatohara, K.; Akiyoshi, M.; Okuno, H., Role of Immediate-Early Genes in Synaptic Plasticity and Neuronal Ensembles Underlying the Memory Trace. *Front. Mol. Neurosci.* **2015,** *8* (78), 78.

26. Kiya, T.; Kubo, T., Dance type and flight parameters are associated with different mushroom body neural activities in worker honeybee brains. *PLoS One* **2011,** *6* (4), e19301.

27. Singh, A. S.; Shah, A.; Brockmann, A., Honey bee foraging induces upregulation of early growth response protein 1, hormone receptor 38 and candidate downstream genes of the ecdysteroid signalling pathway. *Insect Mol Biol* **2018,** *27* (1), 90-98.

28. Iino, S.; Shiota, Y.; Nishimura, M.; Asada, S.; Ono, M.; Kubo, T., Neural activity mapping of bumble bee (*Bombus ignitus*) brains during foraging flight using immediate early genes. *Sci. Rep.* **2020,** *10* (1), 7887.

29. Ugajin, A.; Uchiyama, H.; Miyata, T.; Sasaki, T.; Yajima, S.; Ono, M., Identification and initial characterization of novel neural immediate early genes possibly differentially contributing to foraging-related learning and memory processes in the honeybee. *Insect Mol Biol* **2018,** *27* (2), 154-165.

30. Shah, A.; Jain, R.; Brockmann, A., Egr-1: A candidate transcription factor involved in molecular processes underlying time-memory. *Front. Psychol.* **2018,** *9* (865), 865.

31. Kiya, T.; Kunieda, T.; Kubo, T., Increased neural activity of a mushroom body neuron subtype in the brains of forager honeybees. *PLoS One* **2007,** *2* (4), e371.

32. Fujita, N.; Nagata, Y.; Nishiuchi, T.; Sato, M.; Iwami, M.; Kiya, T., Visualization of neural activity in insect brains using a conserved immediate early gene, Hr38. *Curr Biol* **2013,** *23* (20), 2063-70.

33. Duclot, F.; Kabbaj, M., The Role of Early Growth Response 1 (EGR1) in Brain Plasticity and Neuropsychiatric Disorders. *Front. Behav. Neurosci.* **2017,** *11* (35), 35.

34. de Brito Sanchez, M. G.; Serre, M.; Avarguès-Weber, A.; Dyer, A. G.; Giurfa, M., Learning context modulates aversive taste strength in honey bees. *J Exp Biol* **2015,** *218* (Pt 6), 949-59.

35. Aguiar, J.; Roselino, A. C.; Sazima, M.; Giurfa, M., Can honey bees discriminate between floral-fragrance isomers? *J Exp Biol* **2018,** *221* (Pt 14).

36. Ayestaran, A.; Giurfa, M.; de Brito Sanchez, M. G., Toxic but drank: gustatory aversive compounds induce post-ingestional malaise in harnessed honeybees. *PLoS One* **2010,** *5* (10), e15000.

37. Ugajin, A.; Kiya, T.; Kunieda, T.; Ono, M.; Yoshida, T.; Kubo, T., Detection of neural activity in the brains of Japanese honeybee workers during the formation of a "hot defensive bee ball". *PLoS One* **2012,** *7* (3), e32902.

38. Marchal, P.; Villar, M. E.; Geng, H.; Arrufat, P.; Combe, M.; Viola, H.; Massou, I.; Giurfa, M., Inhibitory learning of phototaxis by honeybees in a passive-avoidance task. *Learn Mem* **2019,** *26* (10), 412-423.

39. Okuno, H., Regulation and function of immediate-early genes in the brain: beyond neuronal activity markers. *Neurosci Res* **2011,** *69* (3), 175-186.

40. Schäfer, S.; Bicker, G., Distribution of GABA-like immunoreactivity in the brain of the honeybee. *J Comp Neurol* **1986,** *246* (3), 287-300.

41. Kiya, T.; Kubo, T., Analysis of GABAergic and non-GABAergic neuron activity in the optic lobes of the forager and re-orienting worker honeybee (*Apis mellifera* L.). *PLoS One* **2010,** *5* (1), e8833.

42. Chatterjee, A.; Bais, D.; Brockmann, A.; Ramesh, D., Search behavior of individual foragers involves neurotransmitter systems characteristic for social scouting. *Front Insect Sci* **2021,** *1* (4).

43. Keles, M. F.; Hardcastle, B. J.; Stadele, C.; Xiao, Q.; Frye, M. A., Inhibitory interactions and columnar inputs to an object motion detector in *Drosophila*. *Cell Rep* **2020,** *30* (7), 2115-2124 e5.

44. Keles, M. F.; Frye, M. A., Object-detecting neurons in *Drosophila*. *Curr Biol* **2017,** *27* (5), 680-687.

45. Rybak, J.; Menzel, R., Anatomy of the mushroom bodies in the honey bee brain: The neuronal connections of the alpha-lobe. *J Comp Neurobiol* **1993,** *334*, 444-465.

46. Lin, A. C.; Bygrave, A. M.; de Calignon, A.; Lee, T.; Miesenbock, G., Sparse, decorrelated odor coding in the mushroom body enhances learned odor discrimination. *Nat Neurosci* **2014,** *17* (4), 559-68.

47. Devaud, J. M.; Papouin, T.; Carcaud, J.; Sandoz, J. C.; Grunewald, B.; Giurfa, M., Neural substrate for higher-order learning in an insect: Mushroom bodies are necessary for configural discriminations. *Proc Natl Acad Sci U S A* **2015,** *112* (43), E5854-62.

48. Boitard, C.; Devaud, J.-M.; Isabel, G.; Giurfa, M., GABAergic feedback signaling into the calyces of the mushroom bodies enables olfactory reversal learning in honey bees. *Front. Behav. Neurosci.* **2015,** *9*.

49. Durrieu, M.; Wystrach, A.; Arrufat, P.; Giurfa, M.; Isabel, G., Fruit flies can learn non-elemental olfactory discriminations. *Proceedings of the Royal Society B: Biological Sciences* **2020,** *287* (1938), 20201234.

50. Honkanen, A.; Adden, A.; da Silva Freitas, J.; Heinze, S., The insect central complex and the neural basis of navigational strategies. *J Exp Biol* **2019,** *222* (Pt Suppl 1), jeb188854.

51. Mota, T.; Yamagata, N.; Giurfa, M.; Gronenberg, W.; Sandoz, J. C., Neural organization and visual processing in the anterior optic tubercle of the honeybee brain. *J Neurosci* **2011,** *31* (32), 11443-11456.

52. Mota, T.; Gronenberg, W.; Giurfa, M.; Sandoz, J. C., Chromatic processing in the anterior optic tubercle of the honeybee brain. *J Neurosci* **2013,** *33*, 4-16.

53. Massey, P. V.; Bashir, Z. I., Long-term depression: multiple forms and implications for brain function. *TINS* **2007,** *30* (4), 176-184.

54. Rose, D.; Blakemore, C., Effects of bicuculline on functions of inhibition in visual cortex. *Nature* **1974,** *249* (455), 375-7.

55. Sillito, A. M., Inhibitory mechanisms influencing complex cell orientation selectivity and their modification at high resting discharge levels. *J. Physiol.* **1979,** *289*, 33-53.

56. Tsumoto, T.; Eckart, W.; Creutzfeldt, O. D., Modification of orientation sensitivity of cat visual cortex neurons by removal of GABA-mediated inhibition. *Exp Brain Res* **1979,** *34* (2), 351-63.

57. von Holst, E.; Mittelstaedt, H., Das Reafferenzprinzip. *Naturwissenschaften* **1950,** *37* (20), 464-476.

58. Skinner, B. F., *The Behavior of Organisms. An Experimental Analysis*. Appleton-Century-Crofts: New York, **1938**; p 457.

59. Menzel, R., The insect mushroom body, an experience-dependent recoding device. *J Physiol Paris* **2014,** *108* (2-3), 84-95.

60. Devaud, J. M.; Papouin, T.; Carcaud, J.; Sandoz, J. C.; Grünewald, B.; Giurfa, M., Neural substrate for higher-order learning in an insect: Mushroom bodies are necessary for configural discriminations. *Proc Natl Acad Sci U S A* **2015,** *112* (43), E5854-62.

61. Guven-Ozkan, T.; Davis, R. L., Functional neuroanatomy of *Drosophila* olfactory memory formation. *Learn Mem* **2014,** *21* (10), 519-26.

62. Avargues-Weber, A.; Mota, T., Advances and limitations of visual conditioning protocols in harnessed bees. *J Physiol Paris* **2016,** *110* (3 Pt A), 107-118.

63. Avarguès-Weber, A.; Mota, T.; Giurfa, M., New vistas on honey bee vision. *Apidologie* **2012**, 1-25.

64. Kirschner, S.; Kleineidam, C. J.; Zube, C.; Rybak, J.; Grünewald, B.; Róssler, W., Dual olfactory pathway in the honeybee, *Apis mellifera*. *J Comp Neurol* **2006,** *499* (6), 933-952.

65. Ehmer, B.; Gronenberg, W., Segregation of visual input to the mushroom bodies in the honeybee (*Apis mellifera*). *J Comp Neurol* **2002,** *451* (4), 362-73.

66. Paulk, A. C.; Dacks, A. M.; Phillips-Portillo, J.; Fellous, J. M.; Gronenberg, W., Visual processing in the central bee brain. *J Neurosci* **2009,** *29* (32), 9987-99.

67. Kirkerud, N. H.; Schlegel, U.; Giovanni Galizia, C., Aversive learning of colored lights in walking honeybees. *Front. Behav. Neurosci.* **2017,** *11*, 94.

68. Plath, J. A.; Entler, B. V.; Kirkerud, N. H.; Schlegel, U.; Galizia, C. G.; Barron, A. B., Different roles for honey bee mushroom bodies and central complex in visual learning of colored lights in an aversive conditioning assay. *Front. Behav. Neurosci.* **2017,** *11*, 98.

69. Buehlmann, C.; Wozniak, B.; Goulard, R.; Webb, B.; Graham, P.; Niven, J. E., Mushroom Bodies Are Required for Learned Visual Navigation, but Not for Innate Visual Behavior, in Ants. *Curr Biol* **2020,** *30* (17), 3438-3443 e2.

70. Devaud, J. M.; Blunk, A.; Podufall, J.; Giurfa, M.; Grünewald, B., Using local anaesthetics to block neuronal activity and map specific learning tasks to the mushroom bodies of an insect brain. *Eur J Neurosci* **2007,** *26* (11), 3193-206.

71. Muller, D.; Staffelt, D.; Fiala, A.; Menzel, R., Procaine impairs learning and memory consolidation in the honeybee. *Brain Res* **2003,** *977* (1), 124-127.

72. Kamhi, J. F.; Barron, A. B.; Narendra, A., Vertical Lobes of the Mushroom Bodies Are Essential for View-Based Navigation in Australian Myrmecia Ants. *Curr Biol* **2020,** *30* (17), 3432-3437 e3.

73. Wolf, R.; Wittig, T.; Liu, L.; Wustmann, G.; Eyding, D.; Heisenberg, M., *Drosophila* mushroom bodies are dispensable for visual, tactile, and motor learning. *Learn Mem* **1998,** *5* (1-2), 166-78.

74. Heisenberg, M.; Borst, A.; Wagner, S.; Byers, D., *Drosophila* mushroom body mutants are deficient in olfactory learning. *J Neurogenet* **1985,** *2* (1), 1-30.

75. Ofstad, T. A.; Zuker, C. S.; Reiser, M. B., Visual place learning in *Drosophila melanogaster*. *Nature* **2011,** *474* (7350), 204-U240.

76. Vogt, K.; Schnaitmann, C.; Dylla, K. V.; Knapek, S.; Aso, Y.; Rubin, G. M.; Tanimoto, H., Shared mushroom body circuits underlie visual and olfactory memories in *Drosophila*. *Elife* **2014,** *3*, e02395.

77. Liu, L.; Wolf, R.; Ernst, R.; Heisenberg, M., Context generalization in Drosophila visual learning requires the mushroom bodies. *Nature* **1999,** *400*, 753-756.

78. Brembs, B.; Wiener, J., Context and occasion setting in Drosophila visual learning. *Learn. Mem.* **2006,** *13* (5), 618-628.

79. Tang, S.; Guo, A., Choice behavior of *Drosophila* facing contradictory visual cues. *Science* **2001,** *294*, 1543-1547.

80. Avarguès-Weber, A.; Giurfa, M., Cognitive components of color vision in honey bees: how conditioning variables modulate color learning and discrimination. *J. Comp. Physiol. A* **2014,** *200* (6), 449-461.

81. Bestea, L.; Rejaud, A.; Sandoz, J. C.; Carcaud, J.; Giurfa, M.; de Brito Sanchez, M. G., Peripheral taste

detection in honey bees: What do taste receptors respond to? *Eur J Neurosci* **2021,** *54* (2), 4417-4444.

82. R Development Core Team, *R: A Language and Environment for Statistical Computing*. The R Foundation for Statistical Computing: Vienna, Austria, **2016**.
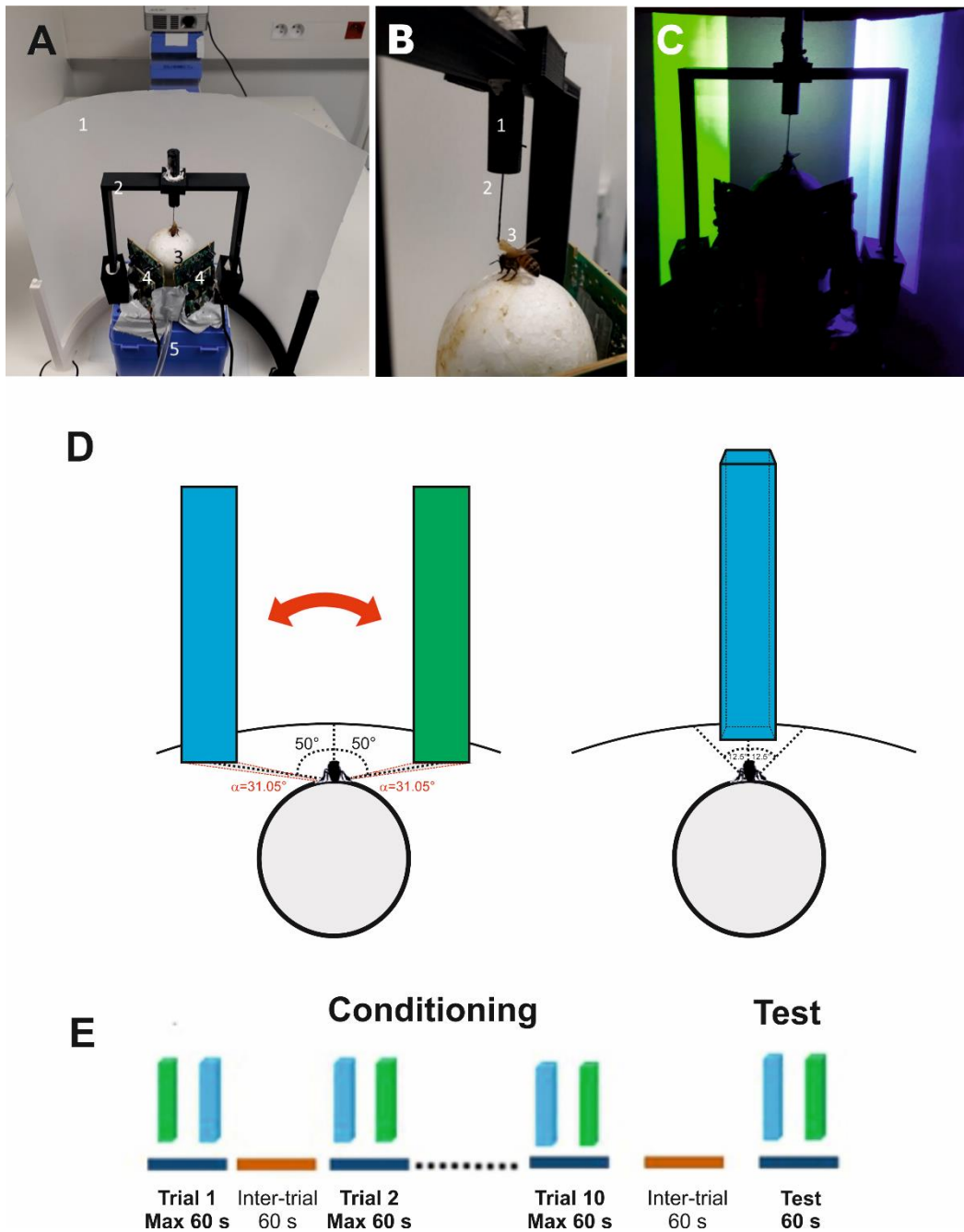
Figure 1. Experimental setup, choice criterion and conditioning procedure. A) Global view of the setup. 1: Semicircular projection screen made of tracing paper. 2: Holding frame to place the tethered bee on the treadmill. 3: The treadmill was a Styrofoam ball positioned within a cylindrical support (not visible) floating on an air cushion. 4: Infrared mouse optic sensors allowing to record the displacement of the ball and to reconstruct the bee's trajectory. 5: Air arrival. The video projector displaying images on the screen from behind can be seen on top of the image. **B) The tethering system.** 1: Plastic cylinder held by the holding frame; the cylinder contained a glass cannula into which a steel needle was inserted. 2: The needle was attached to the thorax of the bee. 3: Its curved end was fixed to the thorax by means of melted bee wax. **C) Color discrimination learning in the VR setup.** The bee had to learn to discriminate two vertical bars based on their different color and their association with reward and punishment. Bars were green and blue on a dark background. Color intensities were adjusted to avoid phototactic biases

independent of learning. Displacement of the bars was restricted to the 2D plane in front of the bee. **D) Left: view of the stimuli at the start of a trial or test.** The green and the blue virtual bars were a presented at -50° and +50° of the bee's longitudinal axis of the bee. Stimuli could be only displaced by the bee from left to right and vice versa (double red arrow). The red angles on the virtual surface indicate the visual angle subtended by each bar at the bee position ($\alpha = 31.05°$). **Right: Choice of a bar.** A choice was recorded when the bee kept the center of the object between -12.5° and +12.5° in front of it for 1 second. The bar image was then frozen during 8 s and the corresponding reinforcement (US) was delivered. **E) Conditioning protocol.** Bees were trained along 10 conditioning trials that lasted a maximum of 1 min and that were spaced by 1 min (intertrial interval). After the end of conditioning, and following an additional interval of 1 min, bees were tested in extinction conditions during 1 min.
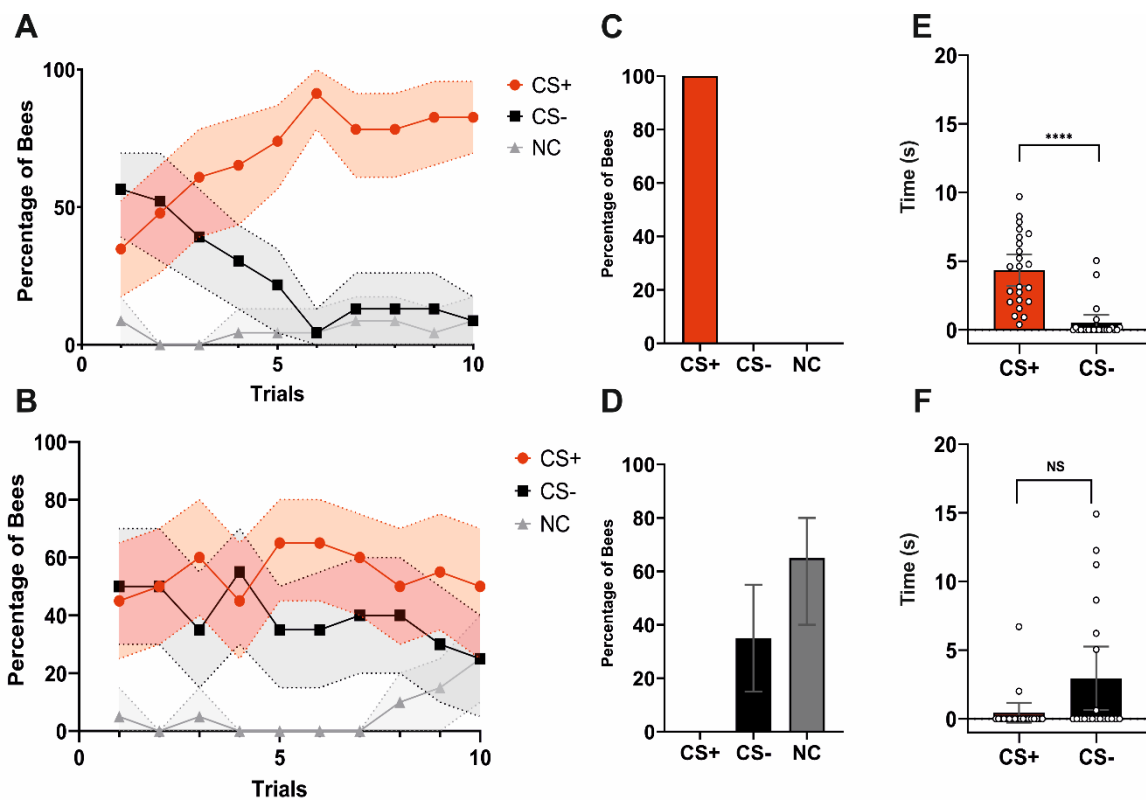
Figure 2. Acquisition and test performances of learners and non-learners. A) Acquisition performance of learners (i.e. bees that chose the CS+ in the non-reinforced test; n=23). The red, black and grey curves show the percentages of bees choosing the CS+, the CS- or not making a choice (NC), respectively. Bees learned the discrimination between CS+ and CS-. **B) Acquisition performance of non-learners** (i.e. bees that chose the CS- or did not make a choice in the non-reinforced test; n=17). These bees did not learn to discriminate the CS+ from the CS-. In **A)** and **B)** shaded areas around curves indicate the 95% confidence interval. **C) Test performance of learners** (% of bees choosing either the CS+, the CS- or not making a choice). Per definition these bees only chose the CS+ first. **D) Test performance of non-learners.** (% of bees choosing either the CS+, the CS- or not making a choice). Per definition these bees chose either the CS- or did not make a choice (NC). In **C)** and **D),** error bars represent the 95% confidence interval. **E) Time (s) spent by learners fixating the CS+ and the CS- during the test.** Learners spent more time fixating the CS+ consistently with their stimulus choice. Bars represent the time spent keeping the object within -12.5°/+12.5° in front of the bee. Scatter plots represent individual fixation times. ****: $p < 0.0001$. **F) Time (s) spent by non-learners fixating the CS+ and the CS- during the test.** Non-learners did not differ in their fixation time of the CS+ and the CS-. Bars represent the time spent keeping the object within -12.5°/+12.5° in front of the bee. Scatter plots represent individual fixation times. NS: non-significant. In **E)** and **F),** error bars represent the 95% confidence interval.
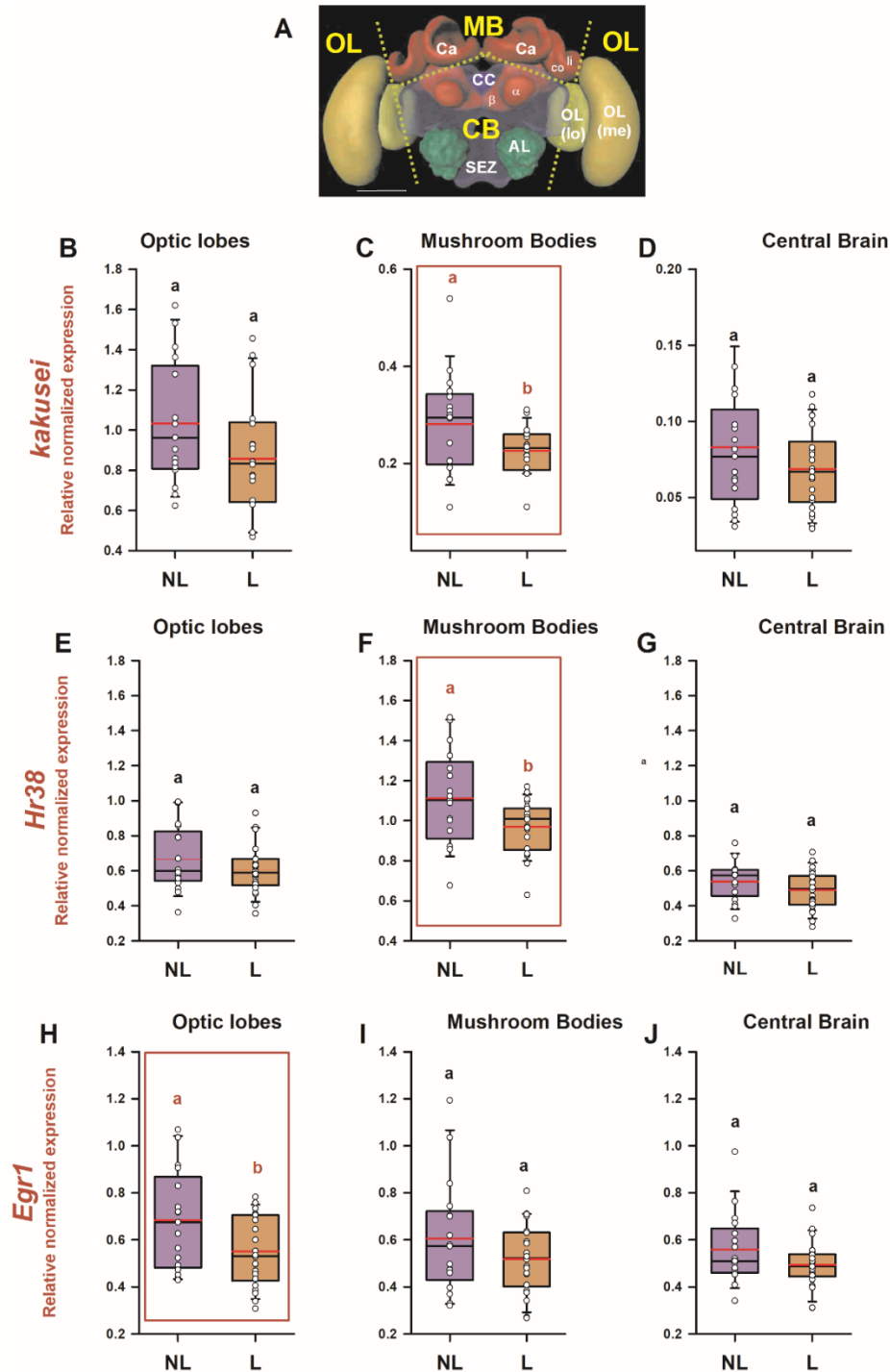
.

Figure 3. Differential IEG expression as a consequence of associative color learning in a 2D VR environment. (A) Honey bee brain with sections used for quantifying IEG expression. Yellow labels indicate the brain regions used for the analysis: MB: mushroom body; CB: central brain; OL: optic lobes. The dashed lines indicate the sections performed. Ca: calyx of the mushroom body; li: lip; co: collar; α and β: α and β lobes of the mushroom body; CC: central complex; AL: antennal lobe; SEZ: subesophagic zone; OL: optic lobe; Me: medulla; lo: lobula. **Relative normalized expression of (B-D) *kakusei*, (E-G) *Hr38* and (H-J) *Egr1* in three main regions of the bee brain, the optic lobes (B, E, H), the calyces of the mushroom bodies (C, F,**

I) and the central brain (D, G, J). The expression of each IEG was normalized to the geometric mean of *Actin and Ef1a* (reference genes). IEG expression was analyzed in individual brains of bees belonging to two categories: *learners* (L: conditioned bees that responded correctly and chose the CS+ in their first choice during the non-reinforced test) and *non-learners* (NL: conditioned bees that did not choose the CS+ in their first choice during the non-reinforced test). The range of ordinates was varied between panels to facilitate appreciation of data scatter. In all panels, n=22 for learners and n=17 for non-learners. Different letters on top of box plots indicate significate differences (two-sample t test; $p < 0.05$). Box plots show the mean value in red. Error bars define the 10th and 90th percentiles. Red boxes indicate cases in which significant variations were detected.
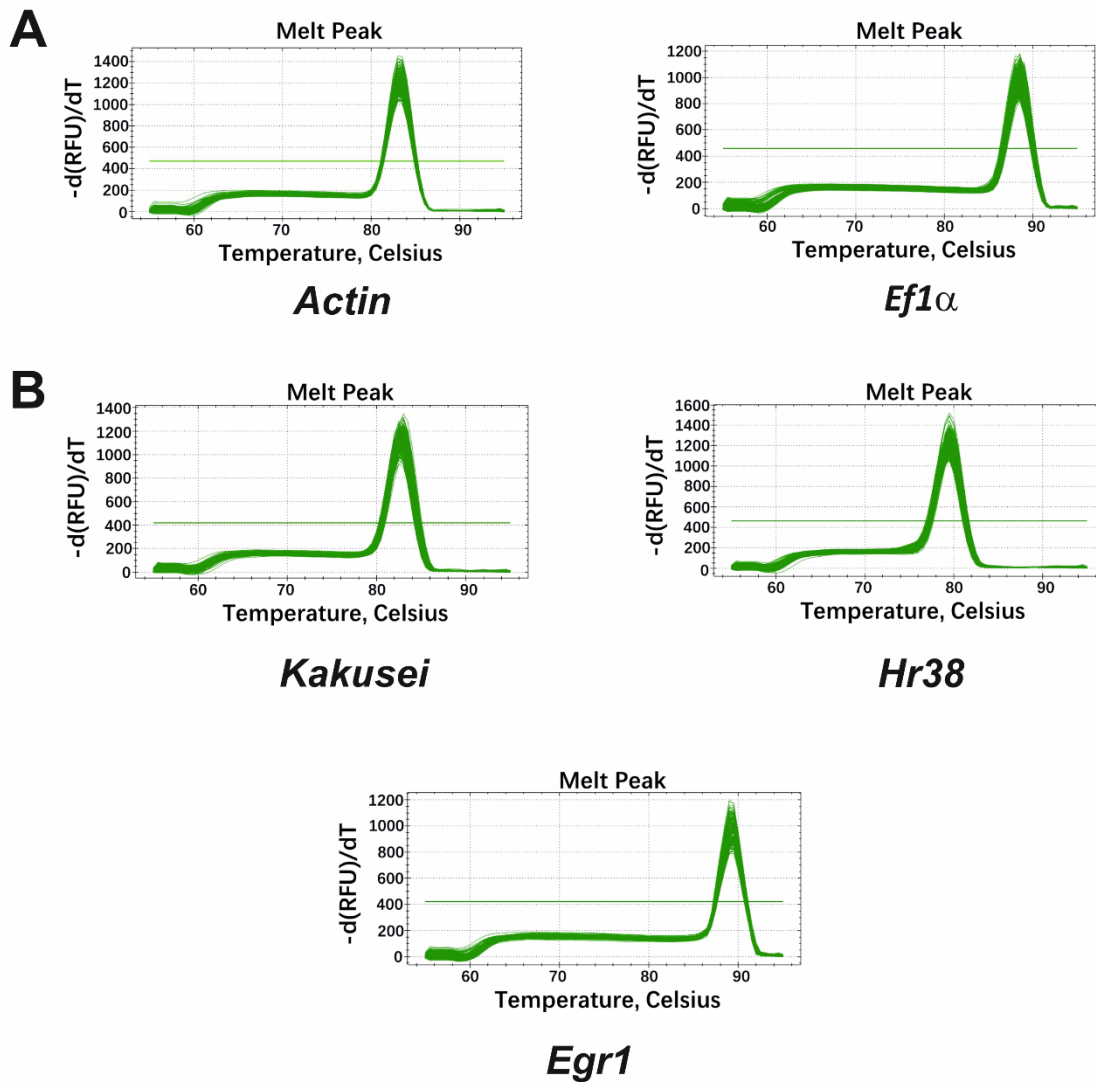
Table 1. Primer sequences used to quantify RNA expression of genes of interest and reference genes by RT-qPCR. Amplicon length (bp), efficiency (E, %) and the coefficient of correlation obtained for the standard curve (R^2) are also shown. *Hr38*: Hormone receptor 38 gene; *Egr1*: Early growth response gene-1; *Ef1α*: Elongation factor 1 α gene.

Type of gene	Target	Primer sequence 5' ➤3'	Amplicon length (bp)	E (%)	R^2
Target genes	*Kakusei*	CTACAACGTCCTCTTCGATT (forward) CCTACCTTGGTATTGCAGTT (reverse)	149	96.4	0.991
	Hr38	TGAGATCACCTGGTTGAAAG (forward) CGTAGCAGGATCAATTTCCA (reverse)	118	106	0.995
	Egr1	GAGAAACCGTTCTGCTGTGA (forward) GCTCTGAGGGTGATTTCTCG (reverse)	138	109	0.991
Reference genes	*Ef1α*	AAGAGCATCAAGAGCGGAGA (forward) CACTC TTAATGACGCCCACA (reverse)	148	106	0.993
	Actin	TGCCAACACTGTCCTTTCTG (forward) AGAATTGACCCACCAATCCA (reverse)	156	110	0.995

Supplementary Materials
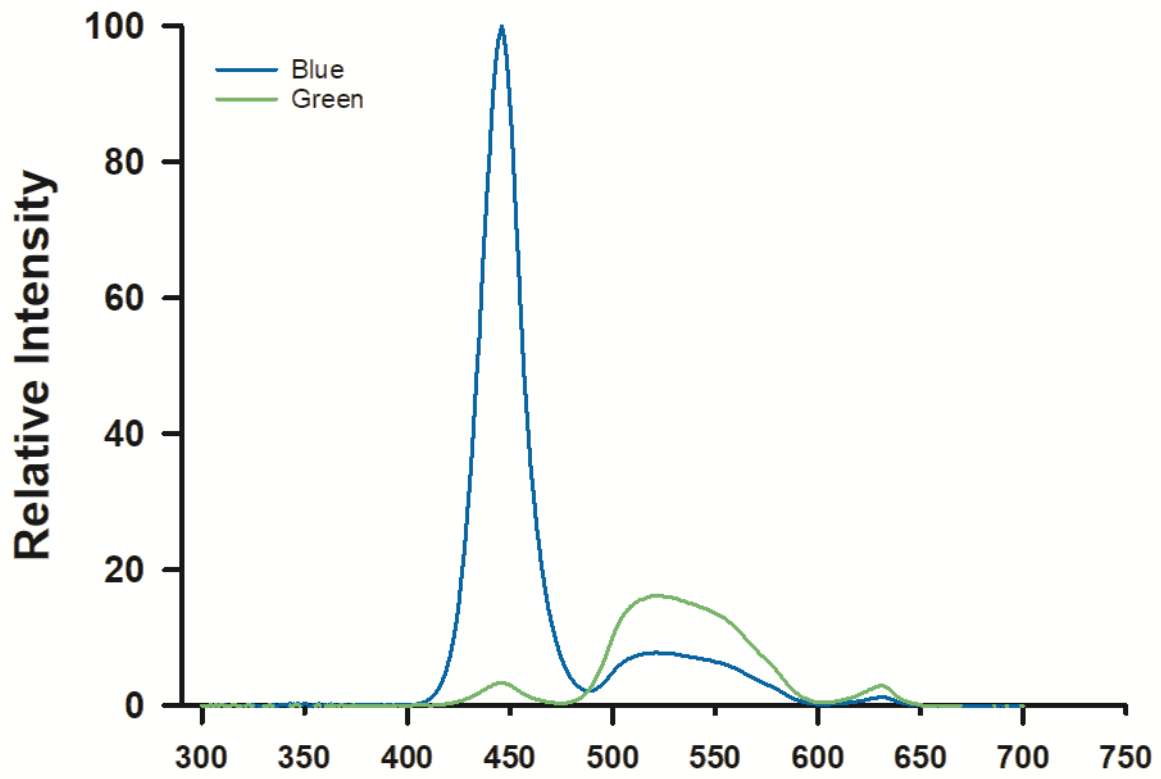
**Supplementary Figure 1.** Spectral distribution (relative intensity as a function of wavelength) of the blue light (dominant wavelength 446 nm) and the green light (dominant wavelength 528 nm) used to train the bees in the color discrimination task.

Supplementary Figure 2. Validation selectivity of gene-specific primers. Melting peaks of RT-qPCR. **A)** Reference genes. **B)** Target genes.
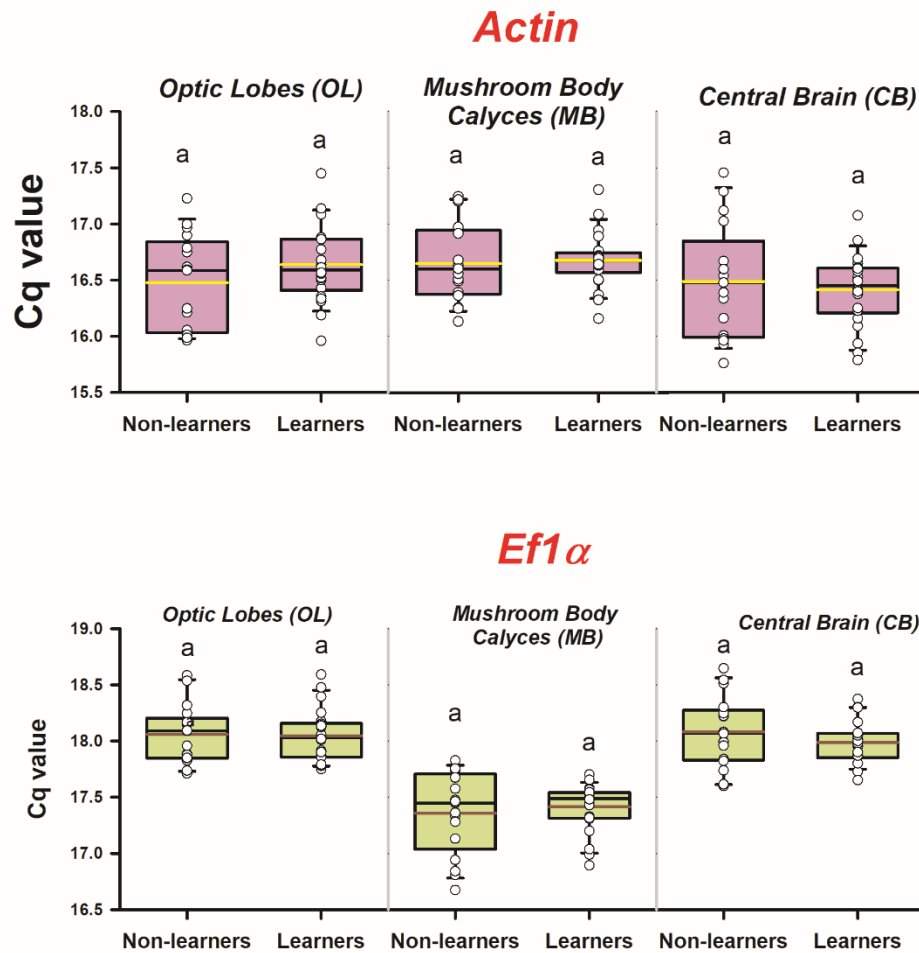
Supplementary Figure 3. Expression levels (Cq values) of the reference genes *Actin* (upper row) and *Ef1α* (lower row). Expression levels in the brain regions considered (optic lobes, mushroom body calyces and central brain) of learners and non-learners (n=22 and n=17, respectively, for both genes). Box plots show the mean value in yellow (*Actin*) or red (*Ef1α*). Sample sizes are indicated within parentheses below each group. Error bars define the 10th and 90th percentiles. Same letters on top of box plots indicate absence of significant differences (two-sample t test; $p < 0.05$).

Appendix

Research

Inhibitory learning of phototaxis by honeybees in a passive-avoidance task

Paul Marchal,[1,5] Maria Eugenia Villar,[1,4,5] Haiyang Geng,[1,2] Patrick Arrufat,[1] Maud Combe,[1] Haydée Viola,[3] Isabelle Massou,[1] and Martin Giurfa[1,2]

[1]Centre de Recherches sur la Cognition Animale (CRCA), Centre de Biologie Intégrative (CBI), Université de Toulouse, CNRS, UPS, F-31062 Toulouse cedex 09, France; [2]College of Bee Science, Fujian Agriculture and Forestry University, Fuzhou 350002, China; [3]Instituto de Biología Celular y Neurociencias (IBCN) "Dr Eduardo De Robertis," CONICET-Universidad de Buenos Aires, Buenos Aires (C1121ABG), Argentina

Honeybees are a standard model for the study of appetitive learning and memory. Yet, fewer attempts have been performed to characterize aversive learning and memory in this insect and uncover its molecular underpinnings. Here, we took advantage of the positive phototactic behavior of bees kept away from the hive in a dark environment and established a passive-avoidance task in which they had to suppress positive phototaxis. Bees placed in a two-compartment box learned to inhibit spontaneous attraction to a compartment illuminated with blue light by associating and entering into that chamber with shock delivery. Inhibitory learning resulted in an avoidance memory that could be retrieved 24 h after training and that was specific to the punished blue light. The memory was mainly operant but involved a Pavlovian component linking the blue light and the shock. Coupling conditioning with transcriptional analyses in key areas of the brain showed that inhibitory learning of phototaxis leads to an up-regulation of the dopaminergic receptor gene *Amdop1* in the calyces of the mushroom bodies, consistently with the role of dopamine signaling in different forms of aversive learning in insects. Our results thus introduce new perspectives for uncovering further cellular and molecular underpinnings of aversive learning and memory in bees. Overall, they represent an important step toward comparative learning studies between the appetitive and the aversive frameworks.

[Supplemental material is available for this article.]

Avoidance learning is a form of operant learning that allows animals to anticipate and elude noxious events in their environment (Krypotos 2015; LeDoux et al. 2017). Several protocols have been conceived to study the animals' capacity to learn that the emission or omission of a specific behavior results in the presence or the absence of an aversive stimulus (typically an electric shock). In rodents, for instance, active-avoidance and passive-avoidance learning protocols are commonly used to study avoidance learning. In active-avoidance learning, a specified response has to be produced by the animal to avoid the negative reinforcement (Wynne and Solomon 1955). For instance, a rat placed in a box with an electrified floor grid may learn that a discriminative stimulus (a light or a sound) anticipates shock delivery through the grid and that pressing a lever interrupts the punishment and the discriminative stimulus. The animal will thus exhibit shorter latencies and a higher frequency of lever pressing upon discriminative-stimulus onset. In passive-avoidance learning, on the contrary, a specified response needs to be suppressed to avoid the negative reinforcement (Venable and Kelly 1990; Kaminsky et al. 2001). For instance, rats, which spontaneously avoid bright illuminated areas to seek refuge in dark compartments learn that entering the dark compartment results in electric shock delivery. Learning results, therefore, in longer latencies to reenter the dark compartment as the animal inhibits its spontaneous response.

Despite their model status for research on invertebrate learning (Giurfa 2007; Menzel 2012), honeybees have been scarcely

studied using protocols of avoidance learning. Learning and memory in bees have been mostly studied using appetitive-learning protocols in which the animals learn to associate different types of sensory stimuli with sucrose reward, the equivalent of the nectar they search in flowers (Menzel 1985; Menzel and Müller 1996; Giurfa 2007). In a few studies, electric shock was used to establish either Pavlovian or operant aversive-learning protocols. For instance, in Pavlovian aversive learning, harnessed bees are trained to associate either olfactory, visual, or gustatory stimuli with an electric shock. In this case, the sting extension response is used as readout of learning and retention (Vergoz et al. 2007; Carcaud et al. 2009; Giurfa et al. 2009; Roussel et al. 2009, 2010, 2012; Mota et al. 2011; Guiraud et al. 2018). In addition, two operant variants of an active-avoidance learning protocol have been established in which freely walking bees confined into a tunnel learn to discriminate two sections displaying two different odors or colored lights, one paired with shock and the other not shocked (Agarwal et al. 2011; Kirkerud et al. 2013, 2017; Avalos et al. 2017). The bee has thus to avoid actively the color/odor paired with shock and move to the nonpunished stimulus. In this differential conditioning task, the amount of shock received by the bee depends, therefore, on the time spent in the reinforced compartment.

Passive-avoidance learning has been studied in harnessed bees, which learned to delay or withhold their proboscis when stimulated with an odorant paired with sucrose solution followed

by an electric shock (Smith et al. 1991). Yet, no protocol for the study of passive-avoidance learning has been established in the case of freely moving bees set under controlled laboratory conditions. Knowing that bees are positively phototactic when they leave a dark place and prepare to fly back to the hive (Menzel and Greggers 1985), we aimed at establishing a learning paradigm in which they would learn to inhibit this spontaneous behavior based on its pairing with an electric shock. We introduce here four main achievements: (1) the establishment of a novel passive-avoidance task in which bees learn to inhibit attraction to a blue light based on associating phototactic choice with electric shock; (2) the demonstration that this learning induces an avoidance memory that can be retrieved 24 h after training and that is specific to the learned light; (3) the characterization of the associations mediating this aversive learning; and (4) the finding that inhibitory phototaxis learning determines an up-regulation of the dopaminergic receptor gene *Amdop1* in the mushroom bodies, consistently with the role of dopamine signaling in different forms of aversive learning in insects.

Results

Honeybees learn to inhibit positive phototaxis in a passive-avoidance task

Bees were individually placed within the conditioning setup termed ICARUS (Fig. 1), which was made of two compartments interconnected via a small passage (see Fig. 1 and Materials and Methods). Both compartments were illuminated with red light ($\lambda = 640$ nm; Fig. 1E), which represents darkness for the bee confined in the setup (Fig. 1B). After a familiarization period, light in one of the compartments

Figure 1. ICARUS—a passive-avoidance setup for inhibitory conditioning of phototaxis in honeybees. (A) The ICARUS setup under red light. Red and black cables represent the electrodes connected to upper and lower metal grids by which the shock is delivered. (B–D) Top view images of the ICARUS setup taken with the camera used for video recording the experiments. (B) Background stimulation with red LEDs only. (C) Illumination of one compartment with blue LEDs. (D) Illumination of one compartment with green LEDs. (E) Spectral emittance (continuous lines; *left* ordinate) of the three types of LEDs used in the setup (blue, green, and red) and spectral sensitivity (dashed lines; *right* ordinate) of the three types of honeybee photoreceptors (S, M, and L, for short, mid, and long wavelengths, respectively) as a function of wavelength. Spectral analysis of quantum catches—the proportion of incident photons that are captured by the photo-pigments—showed that red LEDs induced negligible activation of photoreceptors ($Q_S = 0.6$, $Q_M = 0.64$, $Q_L = 1.84$) while green LEDs activated mainly the L photoreceptors ($Q_S = 0.84$, $Q_M = 3.25$, $Q_L = 44.22$) and blue LEDs activated both L and M photoreceptors ($Q_S = 0.36$, $Q_M = 21.42$, $Q_L = 23.19$). Quantum-catch values depend on the spectrum of the stimulating light and the spectral sensitivity of the photoreceptor considered; they are used to infer the signal generated at the photoreceptor level.

was switched to blue ($\lambda = 464$ nm; Fig. 1E), thus triggering phototactic attraction (Fig. 1A,C). Paired bees, unpaired bees, and no-shock bees were used in this experiment (Fig. 2A, left). Paired bees that entered the blue compartment received the electric shock and the blue light was switched off 2 sec afterward. Unpaired bees experienced noncontingent blue light and shock (the light was switched off 2 sec after the bee entered the blue-lit compartment and the shock was delivered 28 sec after shock offset, i.e., 30 sec after the bee entered the illuminated compartment). No-shock bees received the light stimulations but no electric shock (Fig. 2A, left).

Figure 2B shows that only the paired group progressively increased the latency to enter the blue-illuminated compartment during trials while no change in latency was found both for the unpaired and the no-shock group (ANOVA for repeated measurements; Groups: $F_{(2,46)} = 24.07$, $P < 0.001$; Trials: $F_{(3.145,144.7)} = 4.619$, $P < 0.01$). Moreover, we found a significant effect for the interaction of the two factors (Trials × Groups: $F_{(14,322)} = 4.24$, $P < 0.001$), confirming a difference in the dynamic of responses during trials between groups. A Dunnett's post-hoc test ratified the signifi-
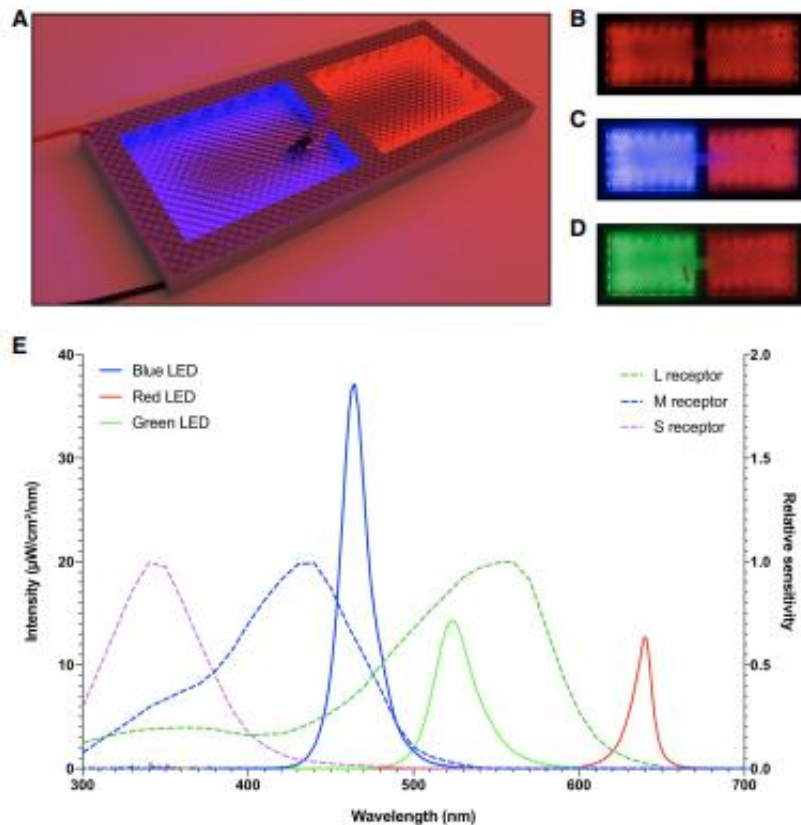
cant variation of latency between trials 1 and 8 for the paired group (mean diff = −91.77, $P < 0.05$) and the absence of difference for the unpaired and the no-shock groups (unpaired: mean diff = −1.273, $P = 0.99$; no-shock: mean diff = −4.17, $P = 0.07$). Thus, bees of the paired group learned to avoid the attractive blue light because they associated the action of entering into the blue-lit compartment with shock punishment (see Supplemental Fig. S1 and Supplemental Videos S1 and S2, which show the behavior of a paired bee towards blue light at the beginning and end of conditioning, respectively). Bees for which blue illumination and shock were not contingent (unpaired group) as well as bees that received no-shock (no-shock group) did not change their performance along with trials.

Inhibitory learning of phototaxis induces a 24-h specific memory

We then asked if this avoidance learning persists in time or if the fact of keeping them in darkness during 24 h away from the hive
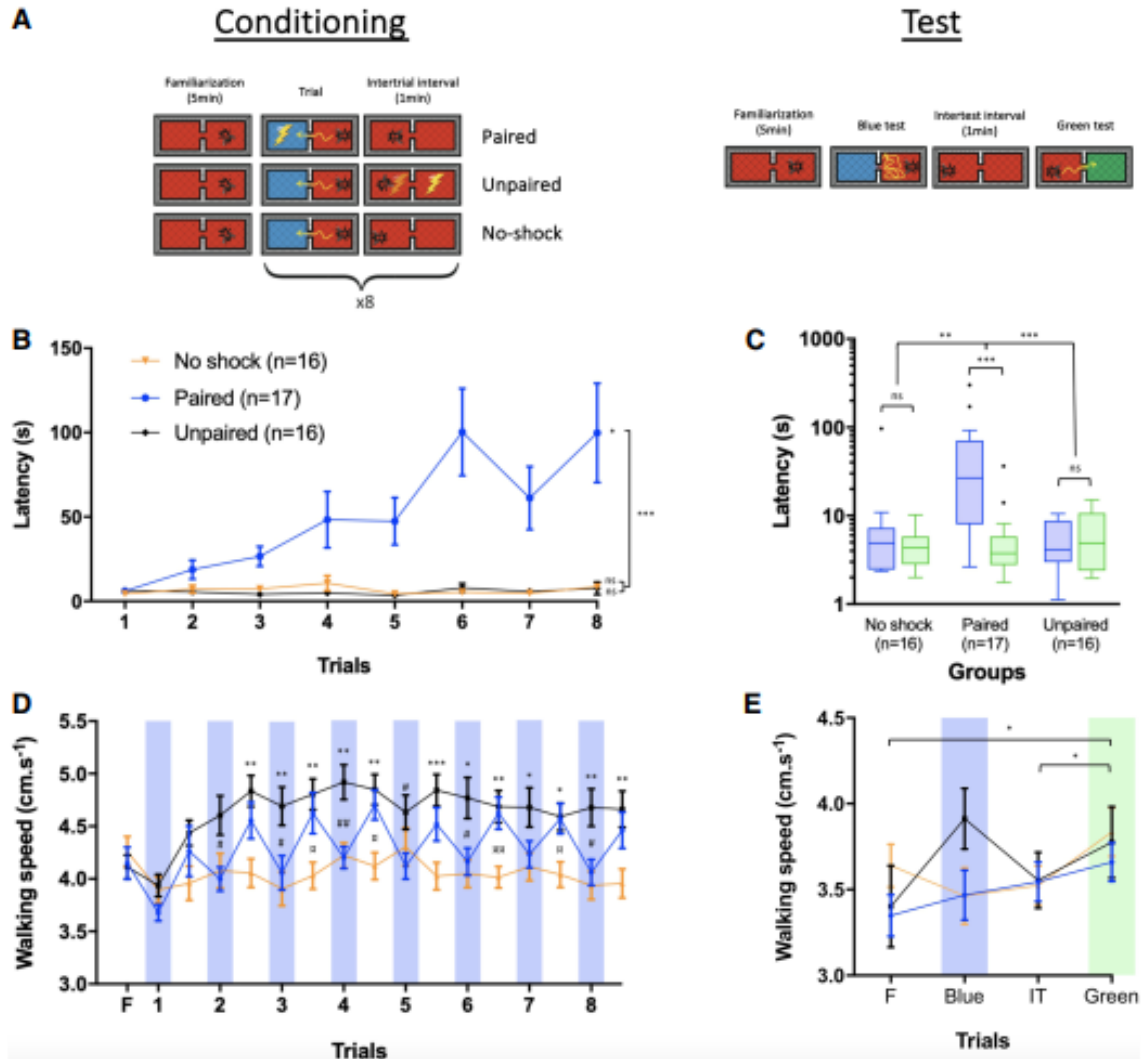
Figure 2. Multiple conditioning trials in a passive-avoidance task induce strong phototactic inhibitory learning and a memory retrievable 24 h after conditioning. (A) Schematic representation of the experimental protocol. After a familiarization period of 5 min in the setup under red light, three groups of bees (paired, unpaired, and no-chock) were subjected to three conditioning protocols in which the latency to enter a blue-lit compartment was measured as a proxy of learning and memory. The paired group received eight conditioning trials in which the action of entering the blue-lit compartment was paired with a mild electric shock. The unpaired group received eight trials consisting of stimulations with attractive blue light and mild electric shock separated by 30 sec. The no-shock group received eight trials consisting in which only the stimulation with the attractive blue light was present. In all groups, trials were separated by an intertrial interval of 1 min. Memory retention was tested 24 h after conditioning. The test session consisted of a familiarization period, and two tests separated by 1 min. In the first test, one of the compartments was illuminated with blue light; in the second test, one compartment was illuminated with green light. No-shock was delivered during tests. (B) Learning curves represented in terms of the latency (s) to enter the blue-lit compartment during conditioning trials for the three experimental groups. (C) Memory scores represented in terms of the latency (s) to enter the blue-lit and green-lit compartments. They are displayed in a logarithmic scale for better visualization. Each box extends from the 25th to 75th percentiles; the line in the middle of the box shows the median. Tukey's method was used for plotting whiskers and outliers. (D) Mean walking speed (cm/s) of bees of the three experimental groups during conditioning trials and intertrial intervals. Blue bars represent stimulations with blue light. #: significant difference between paired and unpaired. *: significant difference between unpaired and no-shock. ¤: significant difference between paired and no-shock. (E) Mean walking speed of bees (cm/sec) of each experimental group during the test session including familiarization, test trials, and intertest interval. Blue and green bars represent stimulation with blue and green lights, respectively. Error bars correspond to SEM. ns: nonsignificant, (*) $P < 0.05$, (**) $P < 0.01$, (***) $P < 0.001$.

results in either memory decay or in overriding of memory by enhanced phototaxis. To answer this question, we confined the bees from all three groups (paired, unpaired, and no-shock) individually in syringes and kept them in an incubator at 28°C, 70% humidity, in the dark during 24 h. We then tested them in a memory retention session (Fig. 2A, right) to determine if bees kept the memory of their prior learning. Furthermore, bees were subsequently tested for their response to a green-illuminated compartment ($\lambda = 523$

nm, Fig. 1D,E) to determine if phototactic behavior (to green light) was kept intact. Both tests were spaced by 1 min.

Figure 2C shows that the latency to enter the blue-illuminated compartment remained higher than the latency to enter the green-illuminated compartment only in the paired group (Wilcoxon signed-rank test; paired: $W = 147$, $P < 0.001$; unpaired: $W = -38$, $P = 0.30$; no-shock, $W = 26$, $P = 0.53$), thus confirming the presence of a 24-h memory in bees trained to suppress positive

phototaxis toward blue light (Fig. 2B). Additionally, for each individual, we computed the difference between the latencies to enter the blue-lit and the green-lit compartment ($\Delta_{latency}$ = latency$_{blue}$ − latency$_{green}$). The $\Delta_{latency}$ of the paired group was significantly higher than that of the control groups (Kruskal–Wallis test; K = 19.80, $P < 0.001$; Dunn's multiple comparisons; paired vs. unpaired: mean rank diff = 21.18, $P < 0.001$; paired vs. no-shock: mean rank diff = 15.93, $P < 0.01$). This result thus confirms that bees of the paired group formed and retained a memory of their aversive experience while bees of the two control groups, which did not learn, had obviously no such a memory.

Video tracking of bees during conditioning allowed to compare their mean walking speed during the familiarization period, the conditioning trials and the intertrial intervals (Fig. 2D). A two-way ANOVA for repeated measurements showed that the walking speed varied significantly along familiarization, trials, and intertrial intervals, and also between groups (Trials: $F_{(8.305, 382)} = 7.92$, $P < 0.001$; Groups: $F_{(2, 46)} = 6.82$, $P < 0.01$) and that the pattern of variation was different between groups (Trials × Groups: $F_{(32, 736)} = 3.32$, $P < 0.001$). A Tukey's post-hoc test showed that bees of the three groups varied in walking speed at several trials and intertrial intervals (see Supplemental Table S1 for statistics). In the two groups that received a shock (paired and unpaired groups), the walking speed increased overall from the first conditioning trial to the second intertrial interval, and then remained constant. The no-shock group maintained the same basal speed as in the familiarization period all along with the trials. Thus, the repeated experience of the shock tended to increase the speed of the bees within the setup. This was particularly visible for the unpaired group, which could not establish predictions about the shock and exhibited the higher speed. Finally, the paired group exhibited a decrease in walking speed when confronted to the attractive light, which may reflect their attempt to avoid receiving the shock. In the test session (Fig. 2E), the walking speed varied significantly during familiarization, tests, and intertest intervals for all groups (two-way ANOVA for repeated measurements; Groups: $F_{(2, 46)} = 0.44$, $P = 0.65$; Trials: $F_{(2.222, 102.2)} = 3.81$, $P < 0.05$; Trials × Groups: $F_{(6, 138)} = 1.96$, $P = 0.076$). More specifically, bees increased their walking speed between the familiarization period and the test with green light, and between the intertest interval and the test with green light (see Supplemental Table S1 for statistics).

Overall, these results validate a novel experimental procedure for the study of phototactic suppression using a passive-avoidance task. They show that bees learn to inhibit their strong innate tendency to go toward the light if kept in the darkness away from the hive and that this learning induces a memory that can be retrieved at least 24 h after conditioning. Bees behaved differently within the setup depending on having experienced or not an electric shock. Bees of the unpaired group, which could not predict the shock, moved faster while bees of the paired group, which learned the association between entering the blue-lit compartment and the shock, moved at intermediate speed. Bees of the no-shock group were slower.

Inhibitory learning of phototaxis is mainly operant but involves a Pavlovian component

In our protocol, the bee must inhibit phototactic responses to avoid receiving an electric shock. This scenario corresponds to a case of operant conditioning where the action of the animal is contingent to the reinforcement. Yet, learning could also rely on the contingency established between blue light and shock, which is of Pavlovian nature. Indeed, we previously demonstrated that the unpaired group (typical Pavlovian control) shows no sign of learning or memory. Yet, abolishing the temporal contingency between stimulus and reinforcement also abolishes the contingency

between the action of the animal and the reinforcement. Thus, to determine if the inhibitory learning of phototaxis has the characteristics of an operant-conditioning task, we conditioned a master and a yoked group in parallel (Fig. 3A). The master group was identical to the paired group of the previous experiment. The yoked group received the same amount of electric shock as the paired group but as shock was decided by the action of the master bee, it was not necessarily contingent with the action of entering the lit compartment (Fig. 3A, left). If learning were purely operant, an increase of latency should be observed in the master but not in the yoked group. After conditioning, both the master and the yoked groups were tested for 24-h memory retention by presenting sequentially the conditioned blue light and the unconditioned green light (Fig. 3A, right).

During conditioning, a significant difference in the latency to enter the blue-illuminated compartment was found between the master and the yoked group (Fig. 3B; two-way ANOVA for repeated measurements; Groups: $F_{(1, 32)} = 10.14$, $P < 0.01$). Responses varied during trials ($F_{(4.012, 128.4)} = 5.48$, $P < 0.001$) and a marginally non-significant interaction between factors was found (Trials × Groups: $F_{(7, 224)} = 1.88$, $P = 0.07$), thus showing that latencies increased mainly in the master group and that the pattern of variation tended to be similar in yoked and master bees. Indeed, both groups showed an increase in the latency to enter the blue-illuminated compartment during trials (latency below 10 sec both for master and yoked bees in the first trial, and around 100 and 25 sec in the eighth trial for master and yoked bees, respectively (master: mean diff = −81.91, $P < 0.05$; yoked: mean diff = −20.14, $P < 0.05$).

In the memory test (Fig. 3C), the yoked group showed a tendency to have a higher latency to enter the blue-lit compartment (Wilcoxon signed-rank test, $W = 73$, $P = 0.09$), which may confirm the results obtained at the end of the conditioning. Yet, this tendency has to be considered with caution in the light of the procedure used to quantify the latency of this group (see Materials and Methods). In any case, the master group presented a latency to enter the blue-lit compartment that was significantly higher than that for the green-lit one (Wilcoxon signed-rank test, $W = 153$, $P < 0.001$), consistently with the presence of a 24-h memory. Accordingly, a comparison between the $\Delta_{latencies}$ of both groups showed a significant difference in favor of the master group (Mann–Whitney test: $U = 82$, $P < 0.05$).

The walking speed of master and yoked bees varied significantly during familiarization, trials, and intertrial intervals but not between groups (Fig. 3D; two-way ANOVA for repeated measurements; Trials: $F_{(7.262, 232.4)} = 20.53$, $P < 0.001$; Groups: $F_{(1, 32)} = 0.99$, $P = 0.33$). Yet, the interaction between Trials and Groups was significant (Trials × Groups: $F_{(16, 512)} = 3.29$, $P < 0.001$), thus showing that the pattern of responses varied differently between master and yoked bees. In both groups, the walking speed increased after the first conditioning trial and then remained constant during the rest of the conditioning (see Supplemental Table S2 for statistics). It was high during intertrial intervals and low in the presence of blue light during trials. This similarity in performance is consistent with the occurrence of learning in both groups. This result confirms that bees increased their basal speed in response to the first shock acting as an arousing stimulus and that they decreased their walking speed when confronted to the attractive light acting as an inhibitory stimulus. Note that despite the absence of significant difference between groups, the master group tended to have a lower speed than that of the yoked group, in particular during certain intertrial intervals (Fig. 3D). In the test session (Fig. 3E), the walking speed varied significantly during familiarization, tests, and intertest interval for all groups (two-way ANOVA for repeated measurements; Trials: $F_{(2.74, 87.69)} = 5.29$, $P < 0.01$). Neither the group effect (Groups: $F_{(1, 32)} = 1.22$, $P = 0.28$) nor the interaction
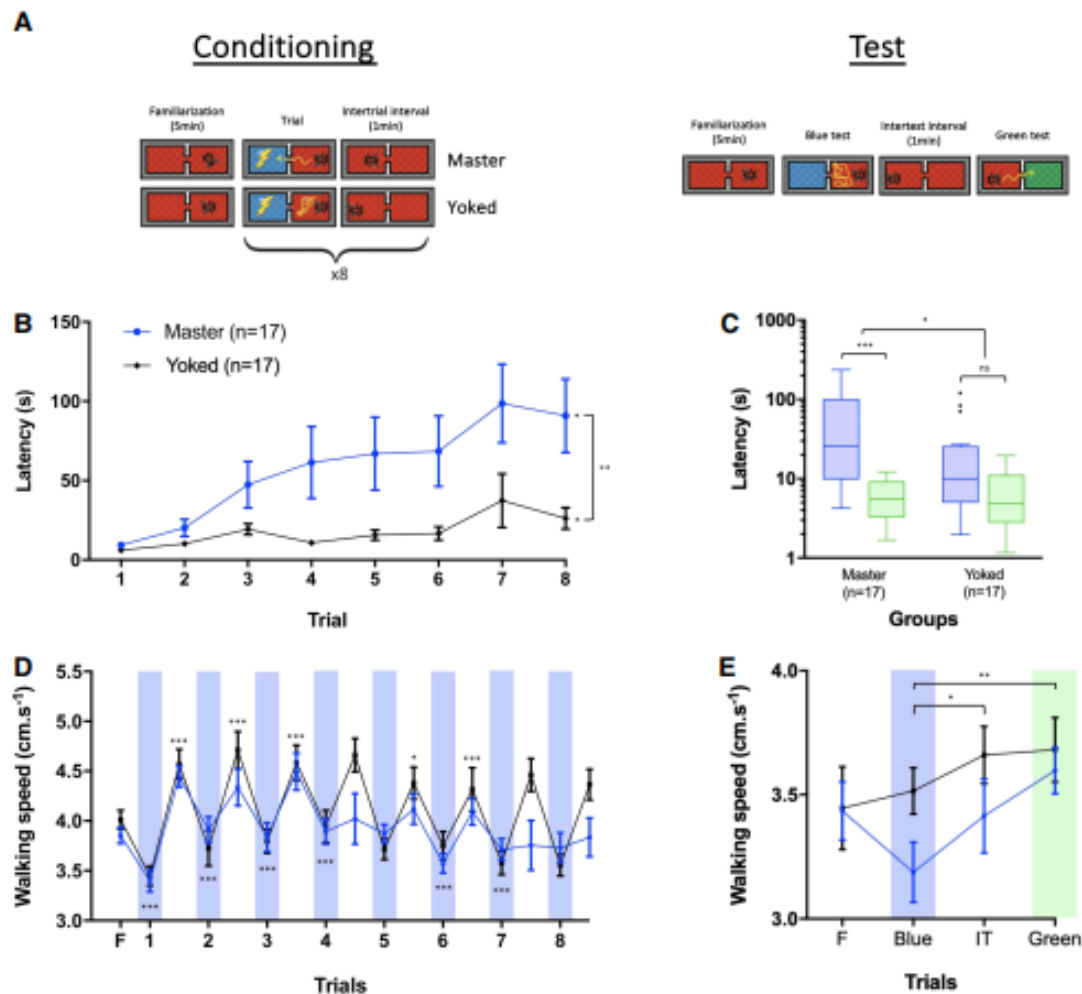
Figure 3. Inhibitory learning of phototaxis is mainly operant but involves a Pavlovian component. (A) Schematic representation of the experimental protocol. After a familiarization period of 5 min under red light in the setup, two groups of bees (master and yoked) were subjected to two conditioning protocols in which the latency to enter a blue-lit compartment was measured as a proxy of learning and memory. The master group received eight conditioning trials during which the action of entering the blue-lit compartment was paired with a mild electric shock. Each bee in the yoked group received eight trials consisting of stimulations with the attractive blue light and the mild electric shock following the exact same temporal sequence as that of its corresponding master bee. In both groups, trials were separated by intervals of 1 min. Memory retention was tested 24 h after conditioning. The test session consisted of a familiarization period, and two tests separated by 1 min. In the first test, one of the compartments was illuminated with blue light; in the second test, one compartment was illuminated with green light. No-shock was delivered during tests. (B) Learning curves are represented in terms of the latency (s) to enter the blue-lit compartment during conditioning trials for the two experimental groups. (C) Memory scores are represented in terms of the latency (s) to enter the blue-lit and green-lit compartments. They are displayed in a logarithmic scale for better visualization. Each box extends from the 25th to 75th percentiles; the line in the middle of the box shows the median. Tukey's method was used for plotting whiskers and outliers. (D) Mean walking speed (cm/s) of bees of each experimental group along with conditioning trials and intertrial intervals. Blue bars represent stimulations with blue light. (E) Mean walking speed of bees (cm/s) of each experimental group during the test session including familiarization, test trials, and intertest interval. Blue and green bars represent stimulation with blue and green lights, respectively. Error bars correspond to SEM. ns: nonsignificant, (*) $P < 0.05$, (**) $P < 0.01$, (***) $P < 0.001$.

(Trials × Groups: $F_{(3,96)} = 1.8$, $P = 0.15$) was significant. Both groups increased their walking speed after the test to the blue light (see Supplemental Table S2 for statistics).

Taken together, these results confirm the main operant nature of the inhibitory learning of phototaxis by honeybees and a contribution of a Pavlovian association between blue light and electric shock.

Inhibitory learning of phototaxis up-regulates *Amdop1* receptor in the calyces of the mushroom bodies

In a third experiment, we aimed at determining if inhibitory learning of phototaxis induces transcriptional changes immediately postlearning, which might participate either in memory consolidation or in amplifying the representation of reinforcement and/or the light used as discriminative stimulus. To this end, we performed RT-qPCR in individual brains of animals trained as in the previous experiments and focused on expression levels of the three dopamine-receptor genes *Amdop1*, *Amdop2*, and *Amdop3* (Beggs et al. 2011), the main octopamine receptor gene *AmoctaR1* (Farooqui et al. 2004; Sinakevitch et al. 2011) and the serotonin receptor gene *Am5-ht1a* (Thamm et al. 2010). These genes were selected based on the involvement of their associated signaling pathways in different forms of appetitive and aversive learning, as well as in visually mediated responses (see Materials and Methods).

Figure 4A shows the learning performance of bees of the paired and the unpaired groups. Bees of both groups differed in their latency to enter into the blue-lit compartment during trials. Indeed, we found a significant interaction between factors (two-way ANOVA for repeated measurements; Trials × Groups, $F_{(7,196)} = 6.74$, $P < 0.001$; Trials, $F_{(5.019, 140.5)} = 6.212$, $P < 0.001$; Groups, $F_{(1,28)} = 47.5$, $P < 0.001$), which shows that both groups responded differently along conditioning trials. Only the paired group increased the latency to enter the blue-illuminated compartment (from below 10 to ~150 sec from the first to the eighth trial; Dunnett's multiple comparisons tests; mean diff = −161.9, $P < 0.001$). On the contrary, no significant increase was found for the unpaired group (mean diff = −0.664, $P = 0.182$).

Bees were anesthetized on ice for 5 min immediately after conditioning; the head was then removed and frozen in liquid nitrogen to be stored at −80°C until dissection. Individual brains were dissected and separated in sections enriched in OL, MBc, AL, and CB (Fig. 4B). The RNA of each section was extracted, retrotranscripted and amplified (RT-qPCR). Levels of expression in each brain section in each individual were relativized and normalized to three reference genes (*Rps8*, *Rp49*, and *Ef1a*).

In the calyces of the mushroom bodies (Fig. 4C), we found a significant increase in the expression of the *Amdop1* receptor gene in the paired group with respect to the unpaired group (unpaired *t*-test; $t = 2.09$, df = 27, $P < 0.05$). No other difference was found with respect to the other receptor genes analyzed. In the
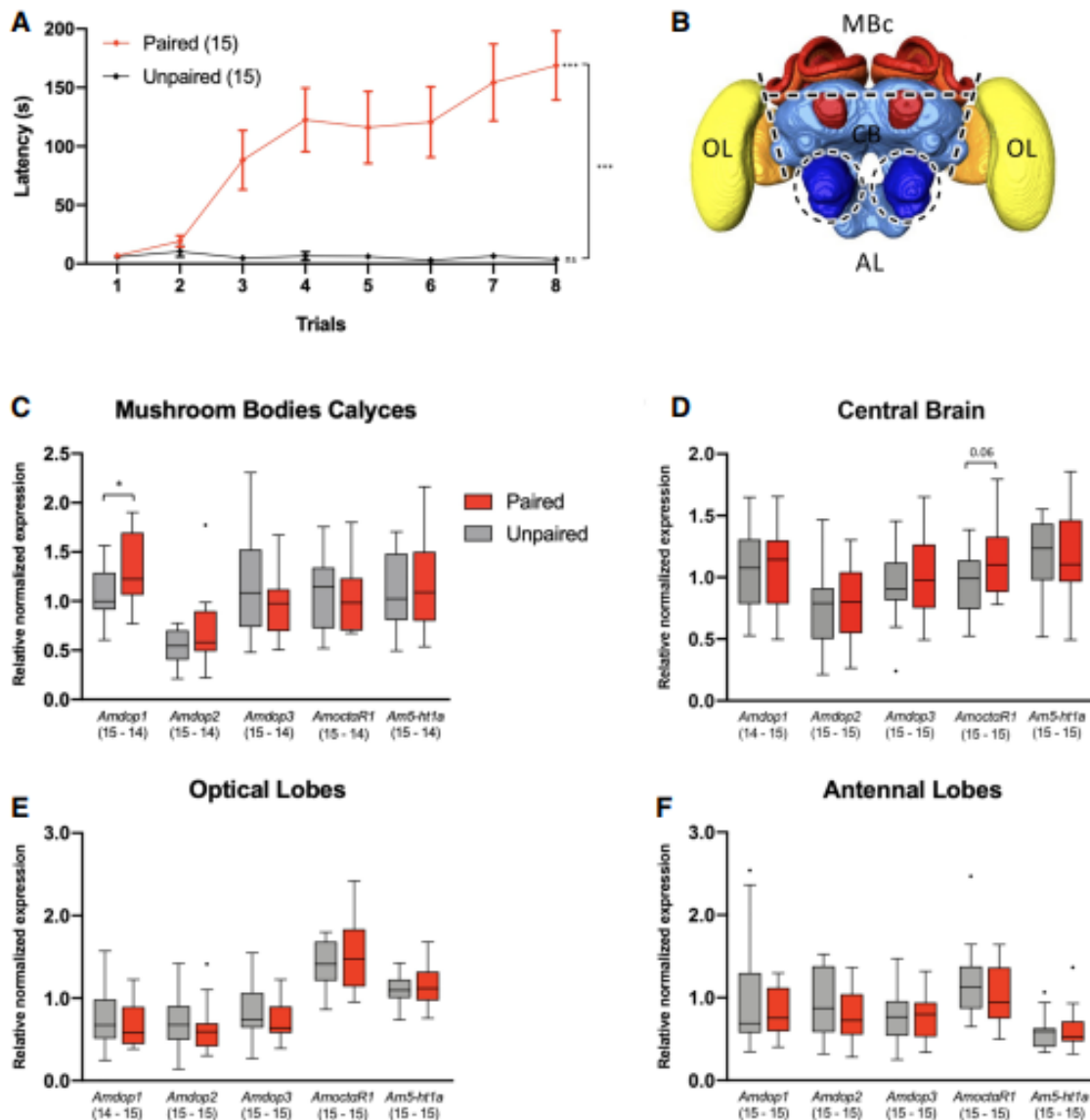

Figure 4. Inhibitory learning of phototaxis up-regulates *Amdop1* receptor genes in the calyces of the mushroom bodies. (*A*) Learning curves represented in terms of the latency (s) to enter the blue-lit compartment during conditioning trials for the two experimental groups, paired and unpaired. Error bars correspond to SEM. (*B*) Schematic representation of brain dissections. Brains were separated in four sections enriched in mushroom bodies calyces (MBc, red), optical lobes (OL, yellow), antennal lobes (AL, dark blue) and central brain (CB, light blue), respectively. (*C–F*) Relative normalized expression of five genes of interest (*Amdop1*, *Amdop2*, *Amdop3*, *AmoctaR1*, and *Am5-ht1a* receptors) in each of the four dissected brain regions of paired and unpaired conditioned bees. The expression of each gene of interest was normalized to the expression of three genes of reference (*Ef1a*, *Rps8*, *Rp49*) for each bee. Expression distribution is represented as boxplots. Each box extends from the 25th to 75th percentiles; the line in the middle of the box shows the median. Tukey method was used for plotting whiskers and outliers. ns: nonsignificant, (*) $P < 0.05$, (***) $P < 0.001$.

CB (Fig. 4D), no significant difference was found; yet a marginally nonsignificant tendency was found ($P=0.06$) in the case of the *AmoctaR1* gene, which was slightly increased in paired bees. In the cases of the OL (Fig. 4E) and the AL (Fig. 4F), no changes in receptor gene expression were detected between paired and unpaired bees.

Discussion

We used a novel passive-avoidance task to study the consequences of associating phototactic attraction toward a blue light with the negative reinforcement of an electric shock in honeybees. We found that bees learn to suppress this attraction and form a memory of this association that could be retrieved at least 24 h after the end of the training. Learning was mostly operant as the decision and behavior of the trained bees controlled shock delivery but included a nonnegligible Pavlovian component based on associating the blue light to the shock. Video recording and analysis of the bees' behavior during conditioning and retention tests revealed that the electric shock elicited higher walking speed, consistently with an arousing effect and with an intent to flee the aversive context. However, bees also reduced drastically their walking speed when facing the blue light. This fact may reflect a conflict situation between being attracted to the blue light-driven by phototaxis and the negative outcome experienced upon entering the blue-lit compartment. Finally, using RT-qPCR, we demonstrate that inhibitory learning of phototaxis correlates with a specific increase of the *Amdop1* receptor gene in the calyces of the mushroom bodies immediately after conditioning.

Phototaxis suppression was still observable 24 h after training, thus showing the strength of learning achieved in this passive-avoidance task. Indeed, given that phototaxis represents a strong innate behavior in bees (Menzel and Greggers 1985), which is accentuated by keeping the bees in darkness away from the hive during more than 24 h, one could have predicted that learning would be either overridden or outcompeted by phototaxis 1 d after conditioning. Yet, the fact that memory was still visible underlines the remarkable plasticity of bee behavior in which acquired information can overcome innate tendencies (Roussel et al. 2012). In the *Drosophila*'s heat box, a fly walking freely back and forth in a narrow alley in complete darkness is conditioned to avoid one half of the length of the alley by being heated instantaneously upon entering it (Wustmann et al. 1996; Wustmann and Heisenberg 1997). Conditioning is an operant process as flies learn to avoid the punished half of the chamber and spend more time on the "unpunished" half. In this setup, memory retention was measured right after training and it was shown to depend on a win-stay component (staying on the unpunished side after avoiding the last heat encounter) rather than on associative memory (Putz and Heisenberg 2002). This strategy is excluded in our case, as bees were tested 24 h after training and after being kept in a different context (an individual syringe placed in an incubator) until the memory test. This procedure also excludes the use of scent marks released during the shock given the time elapsed since training and the fact that tests were always done in the absence of shock. When a change of context was applied to flies trained in the heat box, retention tests revealed the presence of an aversive position memory that lasted only 2 h after the training (Putz and Heisenberg 2002). Although positional cues and heat may be less salient than the light and the electric shock used in our experiments, the 24-h memories present in bees underline again their remarkable behavioral plasticity.

The study of the associations established in our protocol confirmed the operant nature of the inhibitory learning of phototaxis by honeybees. Bees of the master group showed significant learn-

ing and retention performances, which were better than those of the yoked group (Fig. 3). Yet, the yoked group showed some evidence of learning, which could rely on the acquisition of a Pavlovian association between the blue light and the shock, independently of their motor actions. The residual learning of the yoked group could also be due to the fact that at the beginning of training the blue light was equally attractive to both master and yoked bees, thus resulting in coincident punishment delivery. This would induce learning in both groups, which would be further accentuated by successive trials in the master group. In the yoked group, the contingency between entering the blue-lit compartment and the shock would be progressively decreased.

The study of operant aversive learning has led to the establishment of two similar setups in the honeybee, which rely on active-avoidance (Kirkerud et al. 2013, 2017; Avalos et al. 2017; Dinges et al. 2017). In both cases, bees learn that one of two odors, or two colors, is paired with a shock so that they learn to choose the nonpunished stimulus and avoid the punished one. The response is expressed in terms of a preference index that takes into account the choice of the punished (CS+) versus the nonpunished stimuli (CS−). It is measured not only during the presentation of the CS+ but also during delivery of the shock that is associated to it, thus rendering response and acquisition evaluation difficult (Kirkerud et al. 2013, 2017; Avalos et al. 2017; Dinges et al. 2017). On the contrary, our behavioral readout, the latency to enter the blue-lit chamber, is an exclusive response to the blue light and does not involve the presence of shock during its quantification. So far, memory has not been assessed in the active-avoidance setups in which honeybee learning has been studied. It would be interesting to determine the memories arising in these protocols and compare them with those emerging in our passive-avoidance protocol.

Passive-avoidance tasks have been repeatedly used in rats to study learning and memory (Netto and Izquierdo 1985; Gold 1986; Izquierdo et al. 2000). In a step-through task, rats, which are innately photophobic, prefer to stay in a lit compartment when facing a choice between staying in a well-illuminated compartment and entering into a dark one. This avoidance is the result of having reinforced negatively the dark compartment with an electrical shock (McGaugh 1966; Roozendaal and McGaugh 2011). In a step-down task, a rat placed in an elevated platform steps down onto a metallic grid to explore it and receives thereby an electric shock. When the animal is placed back in the platform, it suppresses its stepping down (Jarvik and Kopp 1967; Viola et al. 2000; Tomaiuolo et al. 2015). Memories that last from 30 min to more than 30 d can be induced in both tasks by modifying the amount or the strength of electric shock experienced during the training (Izquierdo et al. 2006; Moncada and Viola 2007; Gonzalez et al. 2014; Tomaiuolo et al. 2015). Although we did not vary punishment intensity in our protocol, the possibility of inducing different memories through this variation is an interesting question for future experiments.

As biogenic-amine receptor genes mediate either appetitive or aversive reinforcement signaling (Giurfa 2006; Waddell 2010, 2013; Perry and Barron 2013; Das et al. 2016), we hypothesized that learning could be associated with rapid changes in the expression of these genes. Changes in gene expression related to memory formation, in particular in the case of long-term memories, may appear long after the period of 10–30 min postconditioning chosen in our work. Yet, here we did not put the accent on memory formation but on how learning may modify signaling pathways processing the sensory stimuli involved in our conditioning protocol (i.e., shock, light). We hypothesized that conditioning may enhance aminergic pathways underlying the processing of these stimuli as a way to enhance their salience. We thus chose to perform the quantification of RNA expression shortly after the end

of conditioning, in the same way as differences in immediate early genes expression are indicative of enhanced neural activity for a sensory stimulus. We found that inhibitory learning of phototaxis was associated with an up-regulation of the *Amdop1* receptor gene in the calyces of the mushroom bodies. This variation is coherent with previous findings that demonstrated the implication of dopamine in aversive learning in bees and other insects where it mediates the reinforcing properties of punishment-like stimuli (Unoki et al. 2005; Vergoz et al. 2007; Claridge-Chang et al. 2009; Mizunami et al. 2009; Aso et al. 2012; Dacks et al. 2012). It also underlines the implication of mushroom-body calyces in learning and memory (Heisenberg 2003; Giurfa and Sandoz 2012; Menzel 2014). The dopaminergic receptor genes *Amdop1*, *Amdop2*, and *Amdop3* code for three dopamine receptors termed AmDOP1, AmDOP2, and AmDOP3, respectively. While AmDOP1 and AmDOP2 are considered D1-like receptors because dopamine binding results in increased cAMP levels in cells expressing them, AmDOP3 is considered a D2-like receptor because dopamine binding results in a reduction of cAMP levels (Beggs et al. 2011). Differences exist between the two D-1 like dopaminergic receptors because AmDOP1 requires lower concentrations of dopamine for activation compared with AmDOP2 (Mustard et al. 2003). Differences are also found at the receptor-gene level. A study on age-related changes in the expression of dopaminergic receptor genes showed that *Amdop1* does not change its expression levels across the age groups tested. On the contrary, levels of expression of *Amdop2* were very variable, particularly during the first week of adult life (McQuillan et al. 2012). These characteristics render *Amdop1* particularly suitable to mediate the reinforcing properties of the electric shock in a stable, age-independent manner. Interestingly, we found a barely nonsignificant up-regulation of the octopaminergic receptor gene *AmoctaR1* in the CB section. Octopamine is involved in appetitive learning as it mediates sucrose-reward signaling (Hammer and Menzel 1998); yet, its role in vision should not be forgotten. Indeed, OA modulates motion-sensitive neurons in the lobula, one of the visual neuropils integrating the optic lobes of the bee brain (Erber and Kloppenburg 1995; Kloppenburg and Erber 1995). Moreover, high levels of OA are found in the optic lobes of pollen foragers, which exhibit reduced phototaxis (Scheiner et al. 2014). A similar relationship was not found for the mushroom bodies, and neither expression of *AmoctaR1* did vary between optic lobes and mushroom bodies in relation to phototaxis (Scheiner et al. 2014). However, our findings refer to an area of the brain (CB) that included neuropils not considered in the study of phototaxis in pollen foragers (Scheiner et al. 2014). It is thus possible that the tendency toward an up-regulation of *AmoctaR1* reflects learning-dependent phototaxis suppression and that it takes place in central areas of the brain such as the central complex (Pfeiffer and Homberg 2014).

Further studies should explore this possibility as well as determine the molecular underpinnings of the memories arising from our training. Exploration of this novel form of inhibitory learning opens the door for new comparative studies of operant learning in bees and flies and provides, therefore, new research avenues for the study of insect learning and memory.

Materials and Methods

Insects

Honeybees were obtained from outdoor hives of our apiary located in the campus of Paul Sabatier University. The bees used for the experiments were foragers collected at feeders filled with 40% (w/w) sucrose solution to which they were previously trained. Bees were collected each day and placed in a small plastic box where a 50% (w/w) sugar solution was made available. Each bee could obtain an average of 5 μL of that solution. The box was placed in an incubator at 28°C and 70% humidity during at least 30 min before the experiments began. If the time before experiments was longer, bees were fed every 3 h with 5 μL of 50% sugar solution to ensure high vitality.

Setup

The conditioning apparatus, termed ICARUS, consisted in a plastic rectangular box (14 cm × 7 cm × 0.8 cm, on the inside) made of two chambers connected by a small passage (1 cm width) (Fig. 1). The floor and ceiling were two metallic grids connected to a high-tension generator that allowed delivering an electric shock (1.3 kV, 65 μA, 200 msec) to the bee. The space between them was reduced so that the bee could only walk but not fly within the setup. Each chamber was surrounded by a set of 19 RGB LEDs (λ^{blue} = 464 nm, λ^{green} = 523 nm, and λ^{red} = 640 nm; Fig. 1) controlled by an Arduino Mega (Supplemental Fig. S2). In this way, both chambers could be lit in the same color, or in different colors. Red color was chosen to provide the equivalent of a dark surrounding to the bees given the absence of chromatic sensitivity in this range of the spectrum (Reisenman and Giurfa 2008). Experiments were recorded from the top by a HD video camera (Legria HF R806, Canon) (Fig. 1). Videos obtained can be used to observe and quantify behaviors (Supplemental Videos S1, S2). A video tracking software developed at the CRCA and under the CECILL free license of the CNRS allowed automated quantification of the bee position during the time (25 fps). As the only moving object in the scene was the bee, the software determines its position using the difference between successive images. Filters were applied to remove the noise related to the brightness changes. Thresholding of the three RGB channels of the image allowed detecting and identifying the chromatic stimuli. At the end of the analysis, postprocessing was performed to calculate the latencies to cross toward the light and the average walking speed of bees during familiarization, trials, and intertrial intervals. Post-processing also enables for retracing the trajectories of the bees during successive trials (Supplemental Fig. S1).

Conditioning protocol

All the experiments were conducted under red light (see above). The red LEDs of the setup were always on to facilitate tracking of the bee. In all experiments, the "paired" group experienced an electric shock upon entering the compartment that was lit in blue. Three different controls ("unpaired," "no-shock," and "yoked") were used in different experiments (see below, and Figs. 2A, 3A, left) and run in parallel with the paired group.

Training session, paired conditioning

During a phase of familiarization, the bee was allowed to explore freely the two chambers of the setup (under dark conditions, red-illuminated) for 5 min before the beginning of the first conditioning trial. A conditioning trial began when the compartment opposite to the one occupied by the bee was illuminated with a blue light. This only happened when the bee was located facing the wall opposite to the passage connecting the two compartments. This procedure allowed standardizing the position and distance to cross between bees. When the blue light was turned on, the bee driven by its innate positive phototaxis entered into the blue-illuminated compartment and received the electric shock during 200 msec. Two seconds after shock offset, the light was switched to red (only red light illumination remains). If 5 min after blue-light onset the bee did not enter the blue-illuminated chamber, the light was turned off and the trial finished without electric shock. This means that every trial had a possible maximal latency of 5 min. From all the bees subjected to paired conditioning (Figs. 2–4), 34.69% were in this situation in at least one of the conditioning trials. The intertrial interval was 1 min during which only red illumination was present. Overall, training consisted of familiarization and eight trials spaced by seven intertrial intervals. In all cases, we quantified the latency to enter into the blue-lit compartment, which is a proxy of learning and memory. Other parameters such

as the walking speed of each trained bee could be extracted from the videos. At the end of the training session, each bee was placed inside a 5 mL pierced plastic syringe and immediately fed with 5 µL of 50% (w/w) sugar solution. The solution was renewed every 3 h until the last feeding of the day, which took place at around 6 p.m. and which consisted of 20 µL of 50% sugar solution to overcome the night. The syringes containing the bees were placed in an incubator at 28°C and 70% until the 24 h test session. In the morning of the test-session day, bees were fed with 10 µL of 50% sugar solution, and if the test session occurred more than 3 h later, 5 µL of 50% sugar solution was further supplied.

Test session

Two memory-retention tests were performed 24 h after the end of conditioning (Figs. 2A, 3A, right). The test session included a familiarization period of 5 min inside the setup under red-light conditions, which was followed by the first test. This test was identical to a conditioning trial with the difference that no-shock was delivered upon entering the blue-lit compartment. Once the test 1 finished, and after an intertest interval of 1 min under red-light conditions, the second test was performed in which green light was used. The main goal of the test with the green light was to demonstrate that the innate phototactic tendency was still present and that the potential increase in the latency to enter the blue-lit compartment in the first test was only due to the previous aversive experience, instead of being due to motor fatigue or loss of light sensitivity, among others. Therefore, the test with green light was performed always after the test with blue light.

Experimental controls

The following control groups were used in different experiments: *no-shock group*: bees were trained in a way similar to the paired group but in the absence of electric shock. This group was used to determine if the increase in latency along trials of the paired group was due to sensory or motor fatigue or to a progressive loss of phototactic motivation; *unpaired group*: bees were trained with noncontingent blue light and electric shock; for these bees, a trial started when the opposite chamber was illuminated; the bee attracted by the light entered the lit compartment and 2 sec after this, the light was turned off. The electric shock was delivered 28 sec after the light was turned off, that is, under red-light conditions and 30 sec after the bee entered the lit compartment. In this way, we controlled for a possible Pavlovian association between light and shock; *yoked group*: bees of the yoked group received the electric shock independently of their behavior but dependently on the behavior exhibited by bees in a master group (paired group; see above). The yoked group is commonly used as a control in operant protocols as it allows determining if changes in latency in the master group are due to operant learning, that is, to the association between the action of entering the blue-lit compartment and the consequences of this action, receiving an electric shock. In shuttle boxes, in which subjects have to commute between a punished and a nonpunished compartment, yoked subjects should experience the blue light and the shock when the master group experienced them, taking into account the appropriate compartment for this experience. As for the master bees the light was switched on in the compartment opposite to their actual location to trigger phototaxis, a potential problem arises for yoked bees. Indeed, reproducing a master bee's situation may imply delivering the blue light either in the opposite chamber to the one where the yoked bee was located or to be forced to deliver it in the chamber where it was located. In the latter case, no latency to go to the light can be measured. Hence, no acquisition curve can be obtained. To avoid this problem, yoked bees in this situation were offered the blue light in the compartment opposite to their actual location. The onset of the electric shock was determined by the master bee's behavior. If the yoked bee exhibited a higher latency than its corresponding master bee, it received the shock without entering the lit compartment. In these cases, the latency assigned to the yoked bee was that of its corresponding master bee. Although this strategy may underestimate learning in the yoked group, it offers a conservative way to quantify latencies in both masters and yoked bees and overcomes the problem of yoked subjects commuting between two compartments in a shuttle box.

Molecular analyses

We quantified variations in receptor-gene expression resulting from inhibitory learning of phototaxis. We focused on biogenic-amine receptor genes given the fundamental role of biogenic amines for different forms of insect learning, where they mediate either appetitive or aversive reinforcement signaling (Giurfa 2006; Waddell 2010, 2013; Perry and Barron 2013; Das et al. 2016). We focused on the three dopamine-receptor genes identified for the honeybee *Amdop1*, *Amdop2*, and *Amdop3* (Beggs et al. 2011), given the essential role of dopamine for aversive reinforcement signaling in this insect (Vergoz et al. 2007; Tedjakumala and Giurfa 2013; Tedjakumala et al. 2014). We also quantified expression of the main octopamine receptor gene *AmoctaR1* (Farooqui et al. 2003, 2004; Beggs et al. 2011; Sinakevitch et al. 2011) due to the inverse relationship found between octopamine levels in the optic lobes of bee foragers and their phototactic responses (Scheiner et al. 2014). Finally, we also measured levels of the serotonin receptor gene *Am5-ht1a*, which has been shown to be highly expressed in brain regions involved in visual information processing and which has a strong impact on phototactic behavior (Thamm et al. 2010). As reference genes, we used the *Rps8* (ribosomal protein S8), the *Rp49* (ribosomal protein 49), and the *Ef1α* (translation elongation factor 1) genes, which are suitable genes for normalization in RT-qPCR analyses in the honeybee (Lourenço et al. 2008). Moreover, preliminary experiments allowed verifying that the two experimental groups did not differ with respect to these genes.

Paired and unpaired bees were put on ice for 5 min immediately after conditioning. They were then decapitated and the head was pasted to a slide with O.C.T compound (Mounting medium for cryotomy, VWR chemicals) and frozen in liquid nitrogen. All the brains were stored at −80°C until dissection.

Dissection

The frozen bee head was dissected on dry ice under a binocular magnifier. First, the antennae were removed and a window was cut in the upper part of the head capsule, removing the cuticle between the compound eyes and the ocelli. Second, the glands and tracheae around the brain were removed. Third, the retinas of the compound eyes were also removed. Finally, the brain was cut in four sections separating the AL, the OL, the upper part of the mushroom bodies (the mushroom-body calyces, MBc), and the remaining CB, which included mainly the central body, the subesophageal zone and the peduncula of the mushroom bodies (Fig. 4B). Samples were stored at −80°C before RNA extraction.

RNA extraction

The RNA from the four sections mentioned above (AL, OL, MBc, and CB) was extracted and purified using a Quick-RNA Miniprep Kit (Zimo Research). The final RNA concentration obtained was measured by spectrophotometry (NanoDrop, Thermo Scientific). A volume of 10 µL containing 30 ng of the RNA obtained was used for retro transcription following the procedure recommended in the Maxima H Minus First Strand cDNA Synthesis kit (Thermoscientific, 0.25 µL of random hexamer primer, 1 µL of 10 mM dNTP mix, 3.75 µL of nuclease-free H_2O, 4 µL 5× RT Buffer and 1 µL Maxima H Minus Enzyme Mix). Controls were performed in the absence of the retro transcriptase enzyme (RT-, reverse transcriptase negative control).

Quantitative polymerase chain reaction (qPCR)

All the primers used generated amplification products of ~200-bp (Table 1). The efficiencies of all the primers used were around 100% (*Amdop1*, 101.9%; *Amdop2*, 104%; *Amdop3*, 111.5%; *Amoa1*, 95.7%; *Am5-ht1a*, 107.5%; *Rps8*, 111%; *Rp49*, 101.5%;

Table 1. Primer sequences used to quantify RNA expression of genes of interest and reference genes by RT-qPCR

Type of gene	Primer target	Primer sequence	Amplicon length (bp)
Genes of interest	Amdop1	5'-GAGTTATCCGAAGAATGTT (forward) 5'-CGTTGAAGTTGATTATGAC (reverse)	148
	Amdop2	5'-GGATCAACAGCGGAATGAAT (forward) 5'-GCGAATCTTTGACTCGGTTT (reverse)	151
	Amdop3	5'-CGTTGCAAACTGTCACCAAT (forward) 5'-GACGTCCATTGCGATGTAAA (reverse)	155
	AmoctαR1	5'-GAACGCCATCCAAGTGTTCT (forward) 5'-GTGCTTCCAACCCTGTTGAT (reverse)	124
	Am5-HT1a	5'-GCCTCGATATTGCATCTGGT (forward) 5'-AGGATCCTTCCATCCGAGTT (forward)	168
Reference genes	Rps8	5'-ACGAGGTGCGAAACTGACTGA (forward) 5'-GCACTGTCCAGGTCTACTCGA (reverse)	176
	Rp49	5'-AAAGAGAAACTGGCGTAAACC (forward) 5'-CAGTTGGCAACATATGACGAG (reverse)	126
	Ef1a	5'-AAGAGCATCAAGAGCGGAGA (forward) 5'-CGTACCTTAATGACGCCCACA (reverse)	149

The length of the amplicons resulting from PCR is given.

Ef1α, 103.6%). Expression was quantified using a SYBR Green real-time PCR method. Real-time PCR was carried out in Hard-Shell 96-Well PCR Plates (Bio-Rad) cover with Microseal "B" PCR plate sealing Film (Bio-Rad). The PCR reactions were performed using the SsAdvanced Universal SYBR Green Supermix (Bio-Rad) in a final volume of 20 μL containing 10 μL of 2× SsAdvanced Universal SYBR Green Supermix, 2 μL of cDNA template (1:3 dilution from the reverse transcription reaction), 2.5 μL of 10 μmol of each primer (Table 1) and 5.5 μL of ultrapure water. The reaction conditions were as follows: 95°C for 30 sec followed by 40 cycles of 94°C for 5 sec, 55°C for 30 sec and plate read. and a final step at 95°C for 10 sec followed by a melt curve from 55°C to 95°C with 0.5°C per sec. The reaction was performed in a CFX Connect Real-Time PCR Detection System and analyzed with the software Bio-Rad CFX Manager.

Each sample was run in triplicates. If the triplicates showed too much variability (SD > 0.3), the furthest triplicate was discarded. If the two remaining triplicates still showed too much variability (SD > 0.3) the sample was discarded.

The samples were subjected to a relative quantification and normalization. First for each sample and for each reference gene per brain region, the relative quantity (Q_r) was computed using the difference between the mean Ct value of each sample and the highest mean Ct value (ΔCt), using the following formula: $Q_r = (1 + E)^{\Delta Ct}$ (with E = efficiency of the reaction). Then a normalization factor for each sample was obtained computing the geometric mean of the relative quantities obtained for the reference genes in the corresponding samples ($\Delta\Delta$Ct).

Data analysis

Latencies, velocities, and crossing events of behavioral experiments were extracted automatically by video analysis of the conditionings and memory tests. Learning curves were analyzed by performing two-way repeated measure analyses of variance (ANOVA) followed when necessary by post-hoc analysis using Dunnett's multiple comparisons test. If the sphericity criterion was not met for the repeated-measurement ANOVA, the Geisser–Greenhouse's correction was applied, thus resulting in corrected degrees of freedom for some Fischer statistics. Memory tests were analyzed by performing Kruskal–Wallis tests (or Mann–Whitney tests) on the difference between the latencies to cross toward blue and green-illuminated compartments ($\Delta_{latency}$ = latency$_{blue}$ − latency$_{green}$) followed when necessary by post-hoc analysis using Dunn's multiple comparisons test. Additionally, we assessed the presence of memory for each group by comparing the $\Delta_{latency}$ to a theoretical value of zero (indicating equal latencies to cross toward conditioned and unconditioned stimuli, hence the absence of memory) using Wilcoxon signed-rank test. Statistical differences between the gene expression of the paired and the unpaired groups

were assessed for a given gene and brain region using a Student *t*-test after transformation of the data to improve normality and homoscedasticity (or Welch *t*-test in case of heteroscedasticity). No cross-comparisons between brain regions or genes were performed. Statistical analyses were performed using GraphPad Prism 8 software.

References

Agarwal M, Giannoni Guzmán M, Morales-Matos C, Del Valle Díaz RA, Abramson CI, Giray T. 2011. Dopamine and octopamine influence avoidance learning of honey bees in a place preference assay. *PLoS One* **6**: e25371. doi:10.1371/journal.pone.0025371

Aso Y, Herb A, Ogueta M, Siwanowicz I, Templier T, Friedrich AB, Ito K, Scholz H, Tanimoto H. 2012. Three Dopamine pathways induce aversive odor memories with different stability. *PLoS Genet* **8**: e1002768. doi:10.1371/journal.pgen.1002768

Avalos A, Pérez E, Vallejo L, Pérez ME, Abramson CI, Giray T. 2017. Social signals and aversive learning in honey bee drones and workers. *Biol Open* **6**: 41–49. doi:10.1242/bio.021543

Beggs KT, Tyndall JDA, Mercer AR. 2011. Honey bee dopamine and octopamine receptors linked to intracellular calcium signaling have a close phylogenetic and pharmacological relationship. *PLoS One* **6**: e26809. doi:10.1371/journal.pone.0026809

Carcaud J, Roussel E, Giurfa M, Sandoz J-C. 2009. Odour aversion after olfactory conditioning of the sting extension reflex in honeybees. *J Exp Biol* **212**: 620–626. doi:10.1242/jeb.026641

Claridge-Chang A, Roorda RD, Vrontou E, Sjulson L, Li H, Hirsh J, Miesenböck G. 2009. Writing memories with light-addressable reinforcement circuitry. *Cell* **139**: 405–415. doi:10.1016/j.cell.2009.08.034

Dacks AM, Riffell JA, Martin JP, Gage SL, Nighorn AJ. 2012. Olfactory modulation by dopamine in the context of aversive learning. *J Neurophysiol* **108**: 539–550. doi:10.1152/jn.00159.2012

Das G, Lin S, Waddell S. 2016. Remembering components of food in *Drosophila. Front Integr Neurosci* **10**: 4. doi:10.3389/fnint.2016.00004

Dinges CW, Varnon CA, Cota LD, Slykerman S, Abramson CI. 2017. Studies of learned helplessness in honey bees (*Apis mellifera ligustica*). *J Exp Psychol Anim Learn Cogn* **43**: 147–158. doi:10.1037/xan0000133

Erber J, Kloppenburg P. 1995. The modulatory effects of serotonin and octopamine in the visual system of the honey bee (*Apis mellifera* L.) I. Behavioral analysis of the motion-sensitive antennal reflex. *J Comp Physiol A* **176**: 119–129. doi:10.1007/BF00197757

Farooqui T, Robinson K, Vaessin H, Smith BH. 2003. Modulation of early olfactory processing by an octopaminergic reinforcement pathway in the honeybee. *J Neurosci* **23**: 5370–5380. doi:10.1523/JNEUROSCI .23-12-05370.2003

Farooqui T, Vaessin H, Smith BH. 2004. Octopamine receptors in the honeybee (*Apis mellifera*) brain and their disruption by RNA-mediated interference. *J Insect Physiol* **50**: 701–713. doi:10.1016/j.jinsphys.2004 .04.014

Giurfa M. 2006. Associative learning: the instructive function of biogenic amines. *Curr Biol* **16**: R892–R895. doi:10.1016/j.cub.2006.09.021

Giurfa M. 2007. Behavioral and neural analysis of associative learning in the honeybee: a taste from the magic well. *J Comp Physiol A* **193**: 801–824. doi:10.1007/s00359-007-0235-9

Giurfa M, Sandoz J-C. 2012. Invertebrate learning and memory: fifty years of olfactory conditioning of the proboscis extension response in honeybees. *Learn Mem* **19**: 54–66. doi:10.1101/lm.024711.111

Giurfa M, Fabre E, Flaven-Pouchon J, Groll H, Oberwallner B, Vergoz V, Roussel E, Sandoz JC. 2009. Olfactory conditioning of the sting extension reflex in honeybees: memory dependence on trial number, interstimulus interval, intertrial interval, and protein synthesis. *Learn Mem* **16**: 761–765. doi:10.1101/lm.1603009

Gold PE. 1986. The use of avoidance training in studies of modulation of memory storage. *Behav Neural Biol* **46**: 87–98. doi:10.1016/S0163-1047 (86)90927-1

Gonzalez MC, Kramar CP, Tomaiuolo M, Katche C, Weisstaub N, Cammarota M, Medina JH. 2014. Medial prefrontal cortex dopamine controls the persistent storage of aversive memories. *Front Behav Neurosci* **8**: 408. doi:10.3389/fnbeh.2014.00408

Guiraud M, Hotier L, Giurfa M, de Brito Sanchez MG. 2018. Aversive gustatory learning and perception in honey bees. *Sci Rep* **8**: 1343. doi:10 .1038/s41598-018-19715-1

Hammer M, Menzel R. 1998. Multiple sites of associative odor learning as revealed by local brain microinjections of octopamine in honeybees. *Learn Mem* **5**: 146–156.

Heisenberg M. 2003. Mushroom body memoir: from maps to models. *Nat Rev Neurosci* **4**: 266–275. doi:10.1038/nrn1074

Izquierdo LA, Barros DM, Ardenghi PG, Pereira P, Rodrigues C, Choi H, Medina JH, Izquierdo I. 2000. Different hippocampal molecular requirements for short- and long-term retrieval of one-trial avoidance learning. *Behav Brain Res* **111**: 93–98. doi:10.1016/S0166-4328(00) 00137-6

Izquierdo I, Bevilaqua LRM, Rossato JI, Bonini JS, Medina JH, Cammarota M. 2006. Different molecular cascades in different sites of the brain control memory consolidation. *Trends Neurosci* **29**: 496–505. doi:10.1016/j.tins .2006.07.005

Jarvik ME, Kopp R. 1967. An improved one-trial passive avoidance learning situation. *Psychol Rep* **21**: 221–224. doi:10.2466/pr0.1967.21.1.221

Kaminsky O, Klenerova V, Stöhr J, Sida P, Hynie S. 2001. Differences in the behaviour of Sprague–Dawley and Lewis rats during repeated passive avoidance procedure: effect of amphetamine. *Pharmacol Res* **44**: 117–122. doi:10.1006/phrs.2001.0848

Kirkerud NH, Wehmann H-N, Galizia CG, Gustav D. 2013. APIS—a novel approach for conditioning honey bees. *Front Behav Neurosci* **7**: 29. doi:10 .3389/fnbeh.2013.00029

Kirkerud NH, Schlegel U, Giovanni Galizia C. 2017. Aversive learning of colored lights in walking honeybees. *Front Behav Neurosci* **11**: 94. doi:10 .3389/fnbeh.2017.00094

Kloppenburg P, Erber J. 1995. The modulatory effects of serotonin and octopamine in the visual system of the honey bee (*Apis mellifera* L.) II. Electrophysiological analysis of motion-sensitive neurons in the lobula. *J Comp Physiol A* **176**: 111–118. doi:10.1007/BF00197758

Krypotos A-M. 2015. Avoidance learning: a review of theoretical models and recent developments. *Front Behav Neurosci* **9**: 189. doi:10.3389/fnbeh .2015.00189

LeDoux JE, Moscarello J, Sears R, Campese V. 2017. The birth, death and resurrection of avoidance: a reconceptualization of a troubled paradigm. *Mol Psychiatry* **22**: 24–36. doi:10.1038/mp.2016.166

Lourenço AP, Mackert A, dos Santos Cristino A, Simões ZLP. 2008. Validation of reference genes for gene expression studies in the honey bee, *Apis mellifera*, by quantitative real-time RT-PCR. *Apidologie (Celle)* **39**: 372–385. doi:10.1051/apido:2008015

McGaugh LJ. 1966. Time-dependent processes in memory storage. *Science* **153**: 1351–1358. doi:10.1126/science.153.3742.1351

McQuillan HJ, Barron AB, Mercer AR. 2012. Age- and behaviour-related changes in the expression of biogenic amine receptor genes in the antennae of honey bees (*Apis mellifera*). *J Comp Physiol A* **198**: 753–761. doi:10.1007/s00359-012-0745-y

Menzel R. 1985. Learning in honey bees in an ecological and behavioral context. In *Experimental behavioral ecology and sociobiology* (ed. Hölldobler B, Lindauer M), pp. 55–74. Sinauer Associates, Stuttgart, Germany.

Menzel R. 2012. The honeybee as a model for understanding the basis of cognition. *Nat Rev Neurosci* **13**: 758–768. doi:10.1038/nrn3357

Menzel R. 2014. The insect mushroom body, an experience-dependent recoding device. *J Physiol Paris* **108**: 84–95. doi:10.1016/j.jphysparis .2014.07.004

Menzel R, Greggers U. 1985. Natural phototaxis and its relationship to colour vision in honeybees. *J Comp Physiol A* **157**: 311–321. doi:10 .1007/BF00618121

Menzel R, Müller U. 1996. Learning and memory in honeybees: from behavior to neural substrates. *Annu Rev Neurosci* **19**: 379–404. doi:10 .1146/annurev.ne.19.030196.002115

Mizunami M, Unoki S, Mori Y, Hirashima D, Hatano A, Matsumoto Y. 2009. Roles of octopaminergic and dopaminergic neurons in appetitive and aversive memory recall in an insect. *BMC Biol* **7**: 46. doi:10.1186/ 1741-7007-7-46

Moncada D, Viola H. 2007. Induction of long-term memory by exposure to novelty requires protein synthesis: evidence for a behavioral tagging. *J Neurosci* **27**: 7476–7481. doi:10.1523/JNEUROSCI.1083-07.2007

Mota T, Roussel E, Sandoz J-C, Giurfa M. 2011. Visual conditioning of the sting extension reflex in harnessed honeybees. *J Exp Biol* **214**: 3577–3587. doi:10.1242/jeb.062026

Mustard JA, Blenau W, Hamilton IS, Ward VK, Ebert PR, Mercer AR. 2003. Analysis of two D1-like dopamine receptors from the honey bee *Apis mellifera* reveals agonist-independent activity. *Brain Res Mol Brain Res* **113**: 67–77. doi:10.1016/S0169-328X(03)00091-3

Netto CA, Izquierdo I. 1985. On how passive is inhibitory avoidance. *Behav Neural Biol* **43**: 327–330. doi:10.1016/S0163-1047(85)91697-8

Perry CJ, Barron AB. 2013. Neural mechanisms of reward in insects. *Annu Rev Entomol* **58**: 543–562. doi:10.1146/annurev-ento-120811-153631

Pfeiffer K, Homberg U. 2014. Organization and functional roles of the central complex in the insect brain. *Annu Rev Entomol* **59**: 165–184. doi:10.1146/annurev-ento-011613-162031

Putz G, Heisenberg M. 2002. Memories in *Drosophila* heat-box learning. *Learn Mem* **9**: 349–359. doi:10.1101/lm.50402

Reisenman CE, Giurfa M. 2008. Chromatic and achromatic stimulus discrimination of long wavelength (red) visual stimuli by the honeybee *Apis mellifera*. *Arthropod Plant Interact* **2**: 137–146. doi:10.1007/ s11829-008-9041-4

Roozendaal B, McGaugh JL. 2011. Memory modulation. *Behav Neurosci* **125**: 797–824. doi:10.1037/a0026187

Roussel E, Carcaud J, Sandoz J-C, Giurfa M. 2009. Reappraising social insect behavior through aversive responsiveness and learning. *PLoS One* **4**: e4197. doi:10.1371/journal.pone.0004197

Roussel E, Sandoz J-C, Giurfa M. 2010. Searching for learning-dependent changes in the antennal lobe: simultaneous recording of neural activity and aversive olfactory learning in honeybees. *Front Behav Neurosci* **4**: 155. doi:10.3389/fnbeh.2010.00155

Roussel E, Padie S, Giurfa M. 2012. Aversive learning overcomes appetitive innate responding in honeybees. *Anim Cogn* **15**: 135–141. doi:10.1007/ s10071-011-0426-1

Scheiner R, Toteva A, Reim T, Søvik E, Barron AB. 2014. Differences in the phototaxis of pollen and nectar foraging honey bees are related to their octopamine brain titers. *Front Physiol* **5**: 116. doi:10.3389/fphys.2014 .00116

Sinakevitch I, Mustard JA, Smith BH. 2011. Distribution of the octopamine receptor AmOA1 in the honey bee brain. *PLoS One* **6**: e14536. doi:10 .1371/journal.pone.0014536

Smith BH, Abramson CI, Tobin TR. 1991. Conditional withholding of proboscis extension in honeybees (*Apis mellifera*) during discriminative punishment. *J Comp Psychol* **105**: 345–356. doi:10.1037/0735-7036.105 .4.345

Tedjakumala SR, Giurfa M. 2013. Rules and mechanisms of punishment learning in honey bees: the aversive conditioning of the sting extension response. *J Exp Biol* **216**: 2985–2997. doi:10.1242/jeb.086629

Tedjakumala SR, Aimable M, Giurfa M. 2014. Pharmacological modulation of aversive responsiveness in honey bees. *Front Behav Neurosci* **7**: 221. doi:10.3389/fnbeh.2013.00221

Thamm M, Balfanz S, Scheiner R, Baumann A, Blenau W. 2010. Characterization of the 5-HT1A receptor of the honeybee (*Apis mellifera*) and involvement of serotonin in phototactic behavior. *Cell Mol Life Sci* **67**: 2467–2479. doi:10.1007/s00018-010-0350-6

Tomaiuolo M, Katche C, Viola H, Medina JH. 2015. Evidence of maintenance tagging in the hippocampus for the persistence of long-lasting memory storage. *Neural Plast* **2015**: 603672. doi:10.1155/ 2015/603672

Unoki S, Matsumoto Y, Mizunami M. 2005. Participation of octopaminergic reward system and dopaminergic punishment system in insect olfactory learning revealed by pharmacological study. *Eur J Neurosci* **22**: 1409–1416. doi:10.1111/j.1460-9568.2005.04318.x

Venable N, Kelly PH. 1990. Effects of NMDA receptor antagonists on passive avoidance learning and retrieval in rats and mice. *Psychopharmacology (Berl)* **100**: 215–221. doi:10.1007/BF02244409

Vergoz V, Roussel E, Sandoz J-C, Giurfa M. 2007. Aversive learning in honeybees revealed by the olfactory conditioning of the sting extension reflex. *PLoS One* **2**: e288. doi:10.1371/journal.pone.0000288

Viola H, Furman M, Izquierdo LAI, Alonso M, Barros DM, de Souza MM, Izquierdo I, Medina JH. 2000. Phosphorylated cAMP response element-binding protein as a molecular marker of memory processing in rat hippocampus: effect of novelty. *J Neurosci* **20**: RC112. doi:10.1523/JNEUROSCI.20-23-j0002.2000.

Waddell S. 2010. Dopamine reveals neural circuit mechanisms of fly memory. *Trends Neurosci* **33**: 457–464. doi:10.1016/j.tins.2010.07.001

Waddell S. 2013. Reinforcement signalling in *Drosophila*; dopamine does it all after all. *Curr Opin Neurobiol* **23**: 324–329. doi:10.1016/j.conb.2013.01.005

Wustmann G, Heisenberg M. 1997. Behavioral manipulation of retrieval in a spatial memory task for *Drosophila melanogaster*. *Learn Mem* **4**: 328–336. doi:10.1101/lm.4.4.328

Wustmann G, Rein K, Wolf R, Heisenberg M. 1996. A new paradigm for operant conditioning of *Drosophila melanogaster*. *J Comp Physiol A* **179**: 429–436. doi:10.1007/BF00194996

Wynne LC, Solomon RL. 1955. Traumatic avoidance learning: acquisition and extinction in dogs deprived of normal peripheral autonomic function. *Genet Psychol Monogr* **52**: 241–284.

Inhibitory learning of phototaxis by honeybees in a passive-avoidance task

Paul Marchal, Maria Eugenia Villar, Haiyang Geng, et al.

General Discussion

In my thesis, I aimed at exploring molecular aspects of honey bee visual perception and learning, using a combination of molecular analyses and behavioral approaches. This led me to implement a novel CRISPR/Cas9 approach to target opsin receptor genes and to analyze the gene expression of IEGs in the brain of honey bees subjected to different kinds of tasks in a virtual reality landscape. In chapter I, I showed that my CRISPR/cas9 approach was successful and allowed me to study the differential contribution of *Amlop1* and *Amlop2* opsin receptor genes to an aversive form of color learning. I generated mosaic mutants and tested them in a visual learning protocol in which bees learned to inhibit attraction to light, based on an association between light and an electric shock (the Icarus setup; Marchal et al., 2019). In the following chapters (II and III), I used an IEG approach to determine neural activity in the brain of honey bees, subjected to two different forms of visual learning in a controlled virtual-reality (VR) scenario. I used ex vivo analyses of IEG expression in the case of three IEGs characterized for honey bees, *kakusei, Hr38, and Erg1* (Geng et al., 2022; Lafon et al., 2022), in order to determine which areas of the bee brain mediate color associative learning, and if observed changes in activity patterns resemble according to the way in which bees learn to solve same color discrimination. The goal was to determine which areas of the bee brain are active during visual learning, and if activity patterns differ between two learning protocols with different constraints. We showed that while 3D VR scenarios allowing for navigation and exploratory learning led to IEG upregulation, 2D VR scenarios in which movements are constrained may have induced higher levels of inhibitory activity in the bee brain, thus leading to IEG downregulation. Overall, we provide a series of new explorations of the visual system, including new functional analyses and the development of novel methods to study opsin function, which advances our understanding of honey bee vision and visual learning. In the following sections I discuss some of these findings, beyond the specific discussions provided in each chapter, and outline a general perspective for future research and work.

1. Addressing the role of honey bee opsin genes via a CRISPR/Cas9 approach

1.1 A change of perspective concerning visual learning in the Icarus setup

In Chapter 1, I aimed at establishing a CRISPR/Cas9 approach to knock out opsin genes characterized by the honey bee visual system. I first focused, as a proof of concept, on the *white* gene, which controls the external coloration of the compound eyes, because mutants can be easily detected due to the whitish coloration of the external surface of compound eyes. This strategy allowed me to verify that the CRISPR/Cas9 method I established worked efficiently, as I obtained mosaic bees with white spots in their compound eyes (see Fig. 1). I then targeted opsin genes, and I focused in particular on the two forms of green opsin that have been reported for the honey bee, *Amlop1* and *Amlop2*. These opsins are localized in different parts of the visual system, with *Amlop2* being in the ocelli and *Amlop1* in the ommatidia of the compound eyes (Velarde et al., 2005).
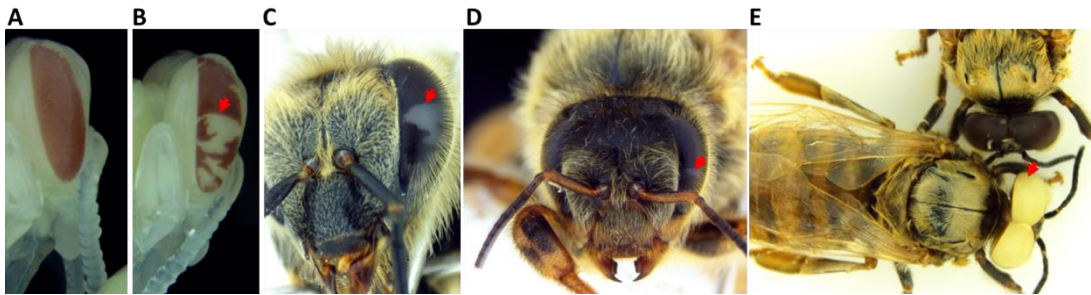

Figure 1. The honey bees show a white-eye phenotype after the white gene is knocked out by CRISPR/Cas9. Unpublished data. (Geng et al.) **(A)** Normal wild-type pupa **(B)** Mosaic pupa **(C)** Mosaic adult worker bee **(D)** Mosaic adult queen bee **(E)** Drone bees. Red arrow indicates white spots on compound eyes.

I verified via *in situ* hybridization that these two opsins are spatially segregated, as reported (Velarde et al., 2005), and then studied their functional implication in a protocol of visual learning that was established in our group. In this protocol, originally described as a case of phototactic inhibition via aversive associative learning (Marchal et al., 2019), bees are placed in a two-chamber compartment (the Icarus setup) where they learn to inhibit their attraction to a compartment lit with blue light, based on the association of this light with an electric shock. As a consequence, the latency to enter into the blue-lit compartment increases with trials. After generating our CRISPR/Cas9 *White, Amlop1* and *Amlop2* mutants, we placed them in this setup and studied their visual learning and memory. *White* and *Amlop2* mutants learned to inhibit spontaneous attraction to blue light, while *Amlop1* mutants failed to do so. These results indicate

that response to blue light, which is also partially sensed by green receptors, is mediated mainly by compound-eye photoreceptors containing *Amlop1* but not by the ocellar system, in which photoreceptors contain *Amlop2*. Accordingly, 24 hours later, *white* and *Amlop2* mutants exhibited an aversive memory for the punished color that was comparable to control bees, but *Amlop1* mutants exhibited no memory. Furthermore, the memory test showed that the bee response was specific to the blue light and was not generalizable to green light with the same intensity. Taken together, these findings highlight the fact that when learning the aversive light-shock association in the Icarus setup, bees are not necessarily inhibiting phototaxis, which may be mediated by the ocelli (but also by compound eyes) and which is essentially color blind (Menzel and Greggers, 1985). The performance of the bees is not color blind and reveals that learning in the Icarus setup is not a case of learning-based phototactic inhibition. It should be described as a case of aversive, associative color learning, given the different response to stimuli differing in chromatic contents but not in intensity.

1.2 The two green-sensitive opsins *Amlop1* and *Amlop2*

Previous phylogenetic analyses performed in hymenopterans other than honey bees (five bee species, *Bombus impatiens*, *B. terrestris*, *Diadasia afflicta*, *D. rinconis*, and *Osmia rufa*) (Spaethe and Briscoe, 2004), were the first to report the presence of a second green opsin, besides the one known and characterized at the level of the ommatidia of compound eyes. These analyses were unable to localize the second green-sensitive opsin, but proposed that it was more ancient than the known one, localized in the compound eyes. Later, Velarde et al (Velarde et al., 2005) expanded this finding to the honey bee, taking advantage of the existing drafts of the bee genome that would be published one year later. They were able to perform *in situ* hybridization analyses, which localized the second green opsin, termed then *Amlop2*, in reference to the known one *Amlop1*, at the level of the ocelli.

In terms of photoreceptor type composition, ocelli and compound eyes ommatidia, differ by the presence of an additional photoreceptor type in the latter. Indeed, ocelli always have the same photoreceptor composition, which includes a UV-sensitive and a green-sensitive photoreceptor expressing *Amuvop* and *Amlop2* opsins, respectively. Compound-eye ommatidia also express two

types of photoreceptors, according to their type, if the ninth photoreceptor is not considered, given its unclear nature and sensitivity. They all have 6 green photoreceptors expressing *Amlop1* and either two UV-sensitive, two blue-sensitive or one blue and one UV-sensitive photoreceptor (Wakakuwa et al., 2005). This means that color vision via the compound eyes, incorporated an additional photoreceptor type absent in the more primitive ocelli, the blue-sensitive photoreceptor expressing *Amblop*.

Recently, the spectral sensitivity of UV-sensitive and green-sensitive photoreceptors in the ocelli was characterized by means of electrophysiological analyses and stimulation, with a series of monochromatic flashes (340–600 nm) spaced by 20 nm (Ogawa et al., 2017). Interestingly, while the UV-sensitive photoreceptors showed a peak at around 360 nm, which is close to that exhibited by ommatidial UV photoreceptors (344 nm, $\Delta_\lambda = 16$ nm) (Peitsch et al., 1992), the green-sensitive photoreceptors had a peak at 500 nm, considerably altered towards shorter wavelengths when compared to the sensitivity of ommatidial green photoreceptors (544 nm, $\Delta_\lambda = 44$ nm) (see Fig. 2).
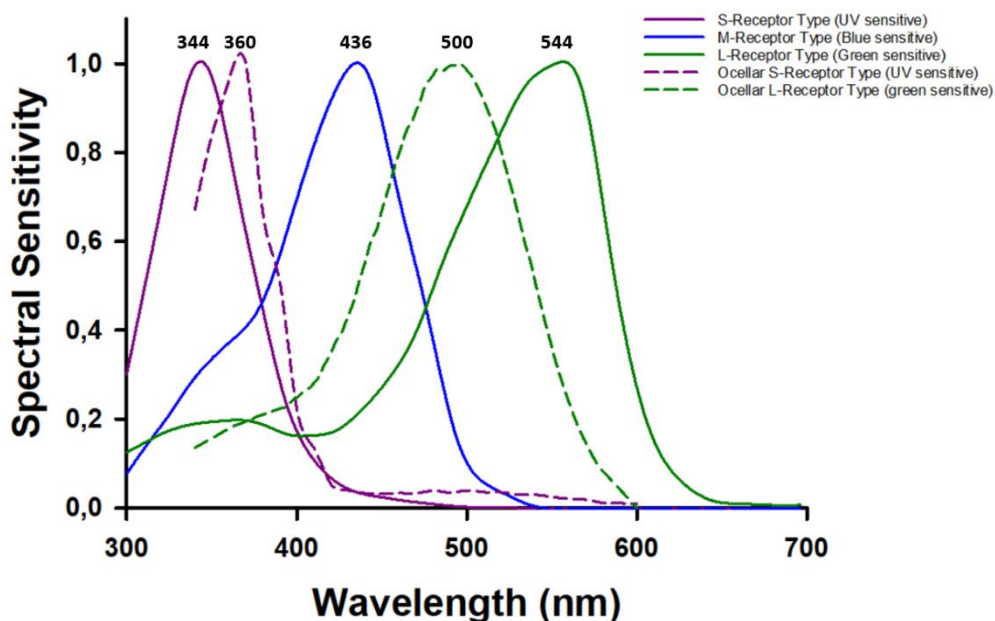
Figure 2. Spectral sensitivity of photoreceptors in honeybee compound eyes and ocelli. **Solid line:** Three types of photoreceptors with peak spectral sensitivities (λ_{max}) at 344 nm (UV, purple line), at 436 nm (Blue, blue line), and at 544 nm [green (G), green line] are present in the compound eyes. **Dashed line:** Two types of photoreceptors with peak spectral sensitivities (λ_{max}) at 360 nm (UV, purple line) and at 500 nm [green (G), green line] were present in the ocelli. Reconstructed after (Peitsch et al., 1992; Ogawa et al., 2017)

One explanation for this difference in λ may be related precisely to the incorporation of the additional blue photoreceptor whose sensitivity peaks between those of UV and green photoreceptors (436 nm). Displacing the sensitivity of the green ommatidial photoreceptor towards longer wavelengths may have given the opportunity to incorporate a "newer" photoreceptor without an excessive overlap between spectral sensitivity curves. This displacement is particularly important for color vision mediated by compound eyes, because it provides the basis for trichromatic color vision, and thus for a richer color experience of the environment, but also because it allows a higher wavelength discrimination. Indeed, the determination of the $\Delta\lambda$ function in honeybees shows that wavelengths at which bees achieve the best wavelength differentiation (i.e., discriminate wavelengths differing in few nm) are located at the intersection between adjacent spectral sensitivity curves (Von Helversen, 1972). It has even been shown that floral spectra have steeper curves precisely at these intersections, thus facilitating flower color discrimination (Chittka et al., 1992). Thus, shifting green receptor sensitivity allows not only adding another receptor type, but it also expands the range of chromatic differentiation, through a better separation of spectral sensitivity curves and consequently their intersection regions.

This interpretation needs to be taken cautiously, because the electrophysiological report on the spectral sensitivity of ocellar photoreceptors (Ogawa et al., 2017) requires further refined analyses. Indeed, the measurements provided present some deficits that were absent in the last and more precise characterization of ommatidial photoreceptors (Peitsch et al., 1992). In the latter case, and following the method established by Menzel and Blakers (Menzel and Blakers, 1976), measurements were performed from 300 to 700 nm using in 4 nm steps so that the precision of the curves reported for ommatidial photoreceptors was very high. For ommatidial photoreceptors, the range of measurements was limited from 340 to 600 nm and in 20 nm steps. In other words, important regions of the bee visual spectrum were absent, and the precision of recordings was 5 times lower. It would there be interesting to repeat the characterization of spectral sensitivity in the case of ocellar photoreceptors using a more precise methodology.

1.3 Technical challenges of the CRISPR/Cas9 approach in honey bees and how to overcome them

Looking back at the production process of gene-edited bees, we identified several challenges preventing researchers from gaining access to gene-edited bees, and we offer here some solutions. The first challenge is the collection of honeybee eggs within a 1.5 h period, following oviposition. The second challenge is the microinjection of age-appropriate bee eggs. The third challenge is the *in vitro* rearing of honey bee larvae after microinjection. Finally, the fourth challenge is the management and maintenance of mutant adult bees and mutant colonies.

1.3.1 Egg collection

Collecting eggs has been investigated by many researchers (Collins, 2002; Evans et al., 2010; Lee and Lee, 2019; Milne Jr et al., 1988; Omholt et al., 1995; Taber, 1961). The more common method is to establish multiple small nuclear colonies, where the queen bee is caged within a special queen-limited plastic box, allowing worker bees to enter freely into it and interact with the queen. The back of this plastic frame is a removable wax cup. After keeping the queen bee enclosed therein to lay eggs for 2 hours, the wax cup can be removed to collect the eggs. This method was used in several studies (Chen et al., 2021; Değirmenci et al., 2020; Hu et al., 2019; Roth et al., 2019; Schulte et al., 2014), but it has the double limitation that queen bees do not like to lay eggs in the plastic frame (Değirmenci et al., 2020), and that it requires considerable manpower and material resources. Moreover, due to seasonal conditions, this method can only be used during the breeding season (i.e., about 3 months in the Toulouse region). In order to solve such problems, we used new bee frames and caged the queen bee on the new frames to force her to lay eggs. Usually, the queen bee can lay thousands of eggs in 24 hours. We then removed the eggs from the restricted area of the frame and left some eggs as bait to lure the queen to further lay eggs. This method ensures that the queen bee lays eggs when the outdoor temperature is above 20°. In this manner, we could collect honeybee eggs every day for up to 7 months, (when experiments were not prevented by Covid-19 lockdowns). Furthermore, an average of hundreds of bee eggs could be harvested every day from one or two normal bee colonies.

1.3.2 Microinjection of bee eggs

Based on previous research (Chen et al., 2021; Değirmenci et al., 2020; Roth et al., 2019; Schulte et al., 2014), we further optimized the method for injecting eggs, which is crucial to achieve high hatching rates. In previous studies, a MK1 micromanipulator was used, which allows one to do microinjections using natural hand movements. Since the color of the bee eggs is similar to the color of the injection needle, it is difficult to control injection depth, which can affect egg survival. This point is critical and constitutes a major difficulty for a novice researcher injecting bee eggs. Without thousands of egg injections, it would be difficult to achieve a good performance (Değirmenci et al., 2020). To overcome these problems, we replaced the MK1 micromanipulator (Fig. 3A) by a M3301 micromanipulator (Fig. 3B), in which we fixed the injecting angle around 20 degrees (Fig. 3C). In other words, we standardized the injection process to make it more regular and controlled, and thus more efficient. The consequence of these procedural changes was a 95% hatching rate after injecting water, which is higher than all hatching rates reported in other studies (i.e., 56% hatching rate in (Roth et al., 2019); 61.4% hatching rate in (Değirmenci et al., 2020)).
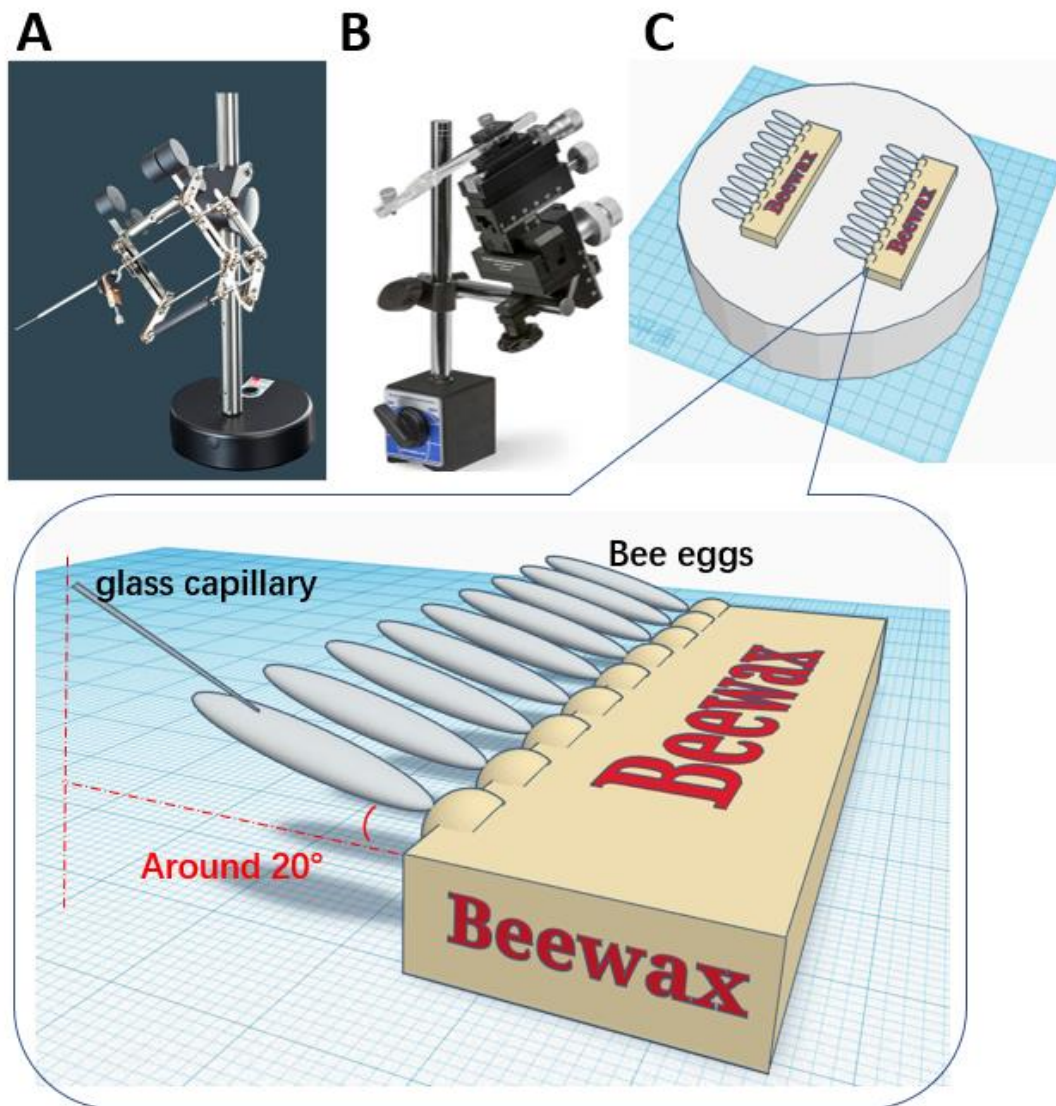
Figure 3. (A) the MK1 micromanipulator allows one to perform microinjections using natural hand movements, as opposed to using knobs. **(B)** The M3301 micromanipulator allows one to fix the injection angle, thus reducing injection variability. **(C)** Schematic diagram of bee egg microinjection. The bee eggs are aligned on a wax strip. The glass capillary is placed almost parallel to the eggs about 20 degrees with respect to the horizontal.

1.3.3 *In vitro* rearing of honey bee larvae after microinjection

There are currently many protocols for *in vitro* rearing of injected honey bee larvae (Büchler et al., 2013; Kaftanoglu et al., 2011; Schmehl et al., 2016). But so far, only a few laboratorys have managed to rear adult bees from injected bee eggs (Roth et al., 2019; Değirmenci et al., 2020; Wang et al., 2021). And the specific experimental steps were ignored in the published papers (Roth et al., 2019; Değirmenci et al., 2020; Wang et al., 2021). The difficulty resides mainly in the transition from bee eggs to small larvae. Normally, after injecting a mixture of sgRNA and Cas9

protein, bee eggs have a certain level of delayed hatching (Değirmenci et al., 2020; Hu et al., 2019). The transfer of eggs after hatching may induce a great deal of death and injury. Currently, researchers inject thousands of bee eggs to get only a small number of adult bees (Değirmenci et al., 2020). We reasoned that an important factor explaining this mortality was the lack of immediate access to food upon hatching. In order to correct this point, we added a layer of food underneath bee eggs which would hatch that day, so that the hatched small larvae would fall on the food. This important detail solved the problem of high mortality from bee eggs to larvae.

1.3.4 Management and maintenance of mutant adult bees and mutant colonies

A large number of chimeras are created in various species after gene editing (Allen et al., 2021; Mazo-Vargas et al., 2017; Mehravar et al., 2019; Zhang and Reed, 2016). The most effective way to overcome chimeras is to crossbreed, cultivate the next generation, and screen out homozygotes. But this is difficult to operate in social insects. In honeybees, homozygous mutants can only be obtained by means of artificial insemination.

The difficulty of artificial insemination of queen bees resides in the collection of drone semen. Normally, drones appear only during the spring breeding season. Only sexually mature drones have usable semen (Collins, 2004; Gillard and Oldroyd, 2020). The cultivation of gene-edited queen bees and drones requires experienced beekeepers to strictly control the time of artificial insemination and also requires sophisticated artificial insemination technology. So far, no reports show that gene-edited homozygous worker bees and fertile queen bees have been obtained by means of artificial insemination.

In our study, we succeeded in this goal and firstly obtained a queen bee with white eyes (*white* gene) and a mutant queen bee in which we targeted the *Amuvop* opsin gene. However, 3 days after artificial insemination, none of these queens was accepted by worker bees in the colony, and they did not survive. Another important factor to consider is the necessity of a large, secure flight cage from which mutants cannot escape, given the laws and restrictions imposed by European countries concerning the dispersal of genetically modified organisms. These secure green houses are very expensive, thus rendering research on gene-edited bees more difficult. Although in our previous experiments, we succeed in getting the mutant queens and mutant drone bees (G1) after knocking out the white gene (see Fig. 1), the process of obtaining gene-edited homozygous queens and

worker bees requires highly sophisticated and laborious treatments (i.e., multiple artificial inseminations, see Fig. 4) to produce, control, and maintain the respective genetic lines.

We therefore decided to use the first-generation mosaic worker bees (G0) to perform behavior experiments.
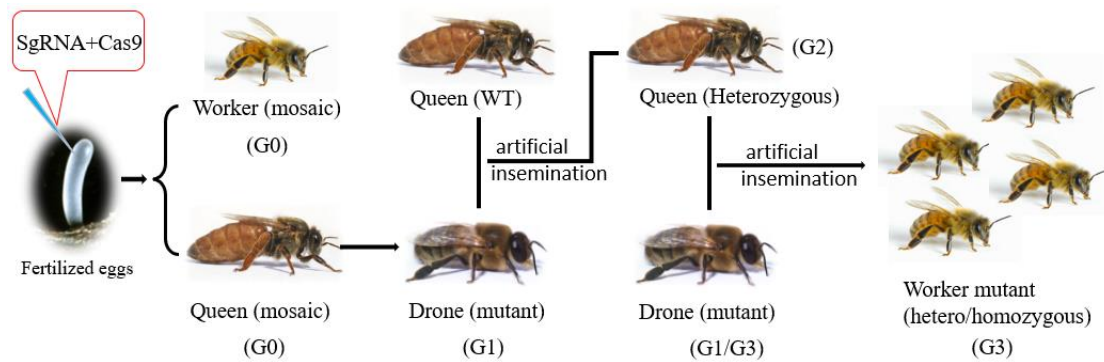

Figure 4. Processes to create genome-edited honeybee workers. Modified from (Kohno et al., 2016)**.** Overview of experimental procedures to create genome-edited honeybee workers by CRISPR/Cas9 is indicated. Queens whose germline cells are genome-edited [Queen (mosaic)] are produced by injecting sgRNA and Cas9 protein into fertilized embryos and rearing these embryos into queens. The queens are then induced to lay unfertilized eggs, which grow into drones, by transiently anesthetizing them with CO2. Genome-edited drones [Drone (mutant)] are selected from among drones produced by these mosaic queens, and sperm is collected from the genome-edited drones. A heterozygous queen is produced from a wild-type queen [Queen (WT)] artificially inseminated with sperm from the genome-edited drones. Heterozygous and homozygous mutant workers [Worker (heterozygous/homozygous mutant)] are produced from the heterozygous queen [Queen (heterozygous mutant)], which is again artificially inseminated with sperm from the genome-edited drones.

1.4 Difficulties faced while implementing the CRISPR/Cas9 approach

In our project, we had to work with mosaic bees (G0 in Fig. 4), and we could not establish the methodology to move from this level of mutation to that of homozygous mutants. Several reasons explain this limitation. The main one is the lack of time, due to the severe impact of successive lockdowns imposed by COVID-19 during my thesis. We had to review our original goals and aim at obtaining mosaic workers as a realistic strategy. Originally, we aimed at knocking out all opsin genes, i.e., *Amuvop, Amblop*, *Amlop1* and *Amlop2*. However, we were severely impacted by the successive lockdowns imposed by COVID-19 and we had to reduce our ambitions. We therefore decided to restrict our focus to the opsin genes *Amlop1* and *Amlop2*.

In order to obtain a higher gene mutation rate, we increased the microinjection volume (pl) of bee eggs from 800 pl to about 1500 pl. This may be the main reason for the decrease in hatching rate after microinjection. Yet, the mutation rate in the experimental group was around 90%, in line with our expectations.

Additional difficulties arose, which are specific to apiculture in the south of France (and to Europe in general) and which are related to the massive presence of Asian hornets, *Vespa velutina*, a fierce predator of honey bee colonies. As summer approaches and hornets become more abundant, the colonies get weak because bees respond to the hornet threat by not quitting the hive, and queens decrease their egg laying, thereby impairing the microinjection process. At the same time, the injected bee eggs had higher mortality at different stages of development, so that it was difficult to obtain 7-day-old adult mutant bees, even after having restricted our experiments to *Amlop1* and *Amlop2* mutants. It is worth mentioning that despite these multiple difficulties, we managed to obtain a few *Uvop* and *Blop* adult mutants. Many *Blop* and *Uvop* mutants had a very high death rate at the larval stage. In consequence, the number of mutants was not enough to complete behavioral experiments. In future experiments, trying more sgRNA sites for *Blop* and *Uvop* genes might allow one to obtain more mutants.

Further difficulties to in getting homozygous mutants refer both to the fact that artificial insemination can only be carried out during the spring when drones are available, and to the cost of maintaining mutant colonies. In addition, legal restrictions have to be considered when producing homozygous mutant bees (Kohno et al., 2016). However, once a homozygous mutant queen bee is produced, a considerable number of homozygous worker bees will be available for various months, because the life span of a queen bee can be as long as 3 years, and the annual number of eggs laid is considerable. This is an advantage compared with many other species with a shorter life span. In the future, new technologies for other nucleases (such as Cpf1, C2c1, C2c2, etc.), as well as gene knock-in will provide powerful and diverse gene-editing tools for scientific research in honey bees.

1.5 CRISPR/Cas9 approach in social insects

Based on our successful experience of gene knockout in honeybees and other studies on ants, in which the CRISPR/Cas9 genome editing was used (Trible et al., 2017; Yan et al., 2017; Chiu et al., 2020; Sieber et al., 2021), we summarize here some core challenges in the field of gene editing in social insects, which may be helpful for developing functional genetic studies in the future.

Gene editing in social insects, such as bees, ants, wasps, and bumblebees is very challenging, because of the social nature of these animals. First, the eggs of social insects are protected by many individuals, typically a specialized caste, and are not laid unprotected under leaves or in ponds such as in solitary insects, which have strong adaptability to harsh environments. Eggs of social insects cannot be isolated from the colony for longer periods and without attempting to reproduce colony environments, as they may easily die or result in abnormal development. The eggshell of social insect eggs is thin and flexible and thus can be easily damaged. Even if the eggs can be transferred out of the nest through an egg retrieval tool to reduce damage, it is difficult to guarantee a high hatching rate. Observing these unhatched eggs under a stereo microscope reveals some mechanical wounds on the surface of the eggs, which are invisible to the naked eye. Nurses in the colony tend to destroy injected embryos and reject and kill the larvae that develop from them. Also collecting eggs from the colony will make the defending adults aggressive, particularly in the case of honey bees.

Second, the larvae of social insect eggs need to be fed with fresh food provided by nurse workers every day. These larvae are not like those of non-social insects, which can eat food independently, without the need of nestmate care. In the honey bees, only a few laboratory protocols have managed to rear adult bees from micro-injected bee eggs (Roth et al., 2019; Değirmenci et al., 2020; Wang et al., 2021). And the specific experimental steps were ignored in the published papers (Roth et al., 2019; Değirmenci et al., 2020; Wang et al., 2021). In ants, younger nurses are used to feed the genetically engineered larvae in a small colony, to solve the feeding problem in the lab (Trible et al., 2017; Yan et al., 2017).

Third, gRNA and Cas9 injections into embryos create mosaic mutants (Allen et al., 2021; Mazo-Vargas et al., 2017; Mehravar et al., 2019; Zhang and Reed, 2016). Thus, obtaining stable mutant lines requires controlled genetic crosses, but most embryos develop into non-reproductive workers which cannot be mated. In ants, the problem has been overcome in *Harpegnathos saltator*

by using "gamergates", mated worker ants that can reproduce sexually and can be experimentally induced to become reproducing queen substitutes (Yan et al., 2017). Furthermore, clonal raider ants *Ooceraea biroi* can also be used as the colonies of these ants consist of only females, all of which reproduce parthenogenetically (Trible et al., 2017).

Fourth, generation of mutants in sexual species takes a long time (although in parthenogenetic species, such as *O. biroi*, homozygous mutants are obtained in the first generation). Homozygous mutants for the Odorant receptor co-receptor gene (*Orco*) in H. saltator could only be obtained in the fourth generation, which took a year and a half of work (Yan et al., 2017). Thus, considering life span is essential for implementing a better CRISPR/Cas9 strategy.

Fifth, some social insects need to fly out to mate in the sky. This is the case not only for honey bees but also for multiple ant species. Thus, CRISPR/Cas9 experiments require a stringent pre-release risk assessment of non-target effects to prevent unintended ecological consequences. Large-size fight cages can be used to this end, but the cost of highly secure (double wall) structures with UV transparent panels (required for enabling normal flight) is prohibitive.

Overall, in social insects, a dozen genes including *mrjp1*, *mKast*, *pax6*, *doublesex*, *fruitless*, *feminizer*, *loc552773*, *csd*, *Rdl*, *mGlutR1*, *Amyellow*, *Amgr3* and *Orco* have been knocked out in honey bees and in ants using CRISPR/Cas9 technology, thereby showing the suitability of this approach for the study of gene functions (Kohno et al., 2016; Trible et al., 2017; Yan et al., 2017; Kohno and Kubo, 2018; Hu et al., 2019; Roth et al., 2019; Değirmenci et al., 2020; Sinakevitch et al., 2020; Chiu et al., 2020; Sieber et al., 2021; Chen et al., 2021; Wang et al., 2021; Nie et al., 2021). So far, there is no report that CRISPR/Cas9 technology has been used in bumble bees. Of all these studies, only one has followed an approach similar to the one developed in my work in the sense that a sensory receptor was targeted (in this case, a gustatory receptor termed *AmGr3*) and mosaic worker mutants were obtained and tested behaviorally at the adult stage (Değirmenci et al., 2020). It was shown that AmGr3 is highly specific for fructose, and besides gustatory detection could also participate in internal fructose sensing for metabolic needs. So far, no study has focused on vision-related genes. Our goal was to induce opsin mutations and determine the effect of these mutations in controlled behavioral protocols for the study of visual perception and learning. Compared to previous studies, we standardized the injection process and had a 95% hatching rate after injecting water, which is above all hatching rates reported in other studies (i.e.,

56% hatching rate in (Roth et al., 2019), 61.4% hatching rate in (Değirmenci et al., 2020)).

2. Studying IEG expression in the bee brain following color discrimination learning in VR conditions

2.1 Visual learning in a virtual reality environment upregulates or downregulates immediate early gene expression in the mushroom bodies of honey bees according to the learning task

In chapters 2 and 3, I aimed at characterizing neural activity in the bee brain, following associative color learning in a VR environment and using an *ex vivo* IEG-quantification approach. As studies on neural activity during associative color learning are scarce, I used analyses of IEG expression in the case of three IEGs characterized for honey bees, *kakusei, Hr38,* and *Erg1*, in order to determine which areas of the bee brain mediate color associative learning, and if observed changes in activity patterns occur according to the way in which bees learn to solve same color discrimination. To answer this last question, I compared IEG expression under 3D (Experimental Chapter 2) and 2D VR conditions (Experimental Chapter 3), as these two scenarios impose different constraints on the control that the experimental bee can have on the virtual stimuli to be discriminated. In the 3D VR, successful learners exhibited *Egr1* upregulation only in the calyces of the mushroom bodies, thus uncovering a privileged involvement of these brain regions in associative color learning. Yet, in the 2D VR, *Egr1* was downregulated in the OLs of learners, while *Hr38* and *kakusei* were coincidently downregulated in the calyces of the MBs in the learner group. Although both VR scenarios point towards specific activation of the calyces of the mushroom bodies (and of the visual circuits in the 2D VR), the difference in the type of expression detected suggests that the different constraints of the two VRs may lead to different kinds of neural phenomena. While 3D VR scenarios allowing for navigation and exploratory learning may lead to IEG upregulation, 2D VR scenarios in which movements are constrained may require higher levels of inhibitory activity in the bee brain.

2.2 IEG analyses in the bee brain

Several studies have focused on Immediate Early Genes (IEGs) expression in the bee brain, as these genes are considered markers of neural activity (Kiya et al., 2007, 2008; Kiya and Kubo, 2011; Fujita et al., 2013; Singh et al., 2018; Iino et al., 2020). For instance, IEG expression was analyzed in response to isopentyl acetate (IPA), a releaser pheromone that communicates alarm in honey bees. Exposure to IPA affected behavioral responsiveness to subsequent exposures to IPA and induced the expression of the immediate early gene and transcription factor *c-Jun* in the antennal lobes (Alaux and Robinson, 2007), the primary olfactory center in the bee brain.

Most studies on IEG expression in brain areas of the honey bee have been performed in the broader contexts of foraging and navigation activities, thus trying to correlate changes in IEG expression with changes in foraging behavior, orientation close to the hive, circadian rhythms or even dance behavior (Lutz and Robinson, 2013; Shah et al., 2018; Singh et al., 2018; Ugajin et al., 2018; Iino et al., 2020).

The case of dance behavior (Kiya and Kubo, 2011) illustrates the difficulty inherent in by these studies performed in a natural context: even if changes in IEG expression could be found in the case of dancers vs. no dancers, this pattern of gene expression could be correlated to multiple uncontrolled variables such as motivational states, travel to the food source, flying speed, etc., which are difficult to disentangle in a natural context. This means that for an appropriate analysis of IEG expression and the assignment of expression variations to a specific behavior/task, controlled laboratory designs are necessary in which only the behavior under scrutiny can be the cause for expression variations. In most of the studies performed on natural behavior learning may have been involved; yet as this was neither explicitly demonstrated nor controlled, it is impossible to relate the variations observed to learning and/or memory.

Our use of the VR solved this problem and allowed us to analyze if and how visual learning induced changes in IEG expression. Our VR setup allowed full control of the animal experience and the separation of learners and non-learners, which differed only in learning success but not in their sensory experience, which was exactly the same as it was fully controlled by the experimenter, contrary to experiments with freely flying bees. Furthermore, analyses of locomotor performance in the setup showed that these motor variables were not related to changes in IEG expression observed between learners and non-learners. The variations were only due to differences in learning.

2.3 IEG Up- and downregulation in the bee brain

Immediate-early genes (IEGs) can be activated and transcribed within minutes after stimulation, without the need for de novo protein synthesis, and they are stimulated in response to both cell-extrinsic and cell-intrinsic signals (Bahrami and Drablos, 2016). They are commonly used as markers of neural activity in mammals where, for instance, *c-fos* or *zif268* are used as indicators of neural excitation in multiple brain areas.

Only in our 3D VR experiment was this expectation met, as we found an upregulation of *Egr1* in the calyces of the MBs of learners. In studies in which the behavior of bees was studied in uncontrolled conditions, foraging and reorientation activity following hive displacement (Kiya et al., 2007; Kiya and Kubo, 2010; Ugajin et al., 2018) increased *kakusei* expression not only in the mushroom bodies (Kiya et al., 2007) but also in the optic lobes (Kiya et al., 2008, 2007; Kiya and Kubo, 2010). In our 3D VR protocol, we did not find a significant difference in the bee brain between learner bees and non-learner bees in our study, neither for *kakusei* nor *Hr38*. However other temporal analyses of *kakusei* expression reported decay in expression beyond 30 min (Kiya et al., 2007), the possibility that our sampling period was too long to capture changes in *kakusei* expression cannot be excluded. The hormone-receptor gene (*Hr38*) has been indirectly related to learning and memory in honey bees and other insects (Singh et al., 2018; Iino et al., 2020) and is also upregulated by foraging experiences in honey bees (Singh et al., 2018) and bumblebees (Iino et al., 2020) and by orientation activities upon hive displacement (Ugajin et al., 2018). Despite its involvement in these activities, it did not reveal learning-dependent changes in neural activity in the experimental context defined by our setup and training protocol.

The most intriguing aspect of our IEG analyses refers to the findings obtained under the 2D VR protocol, where a consistent downregulation of IEG expression was found in visual neuropils and in the calyces of the mushroom bodies of learners but not in non-learners. This is intriguing, as IEGs are typically upregulated by neural activity (Franceschini et al., 2020). Our hypothesis on neural inhibition being the cause for this downregulation requires, therefore, to be considered with caution. Further experiments are necessary to validate it, using – for instance – cellular

preparations in which neural excitation and neural inhibition can be accessed and related to gene expression. A good candidate for this approach would be the use of hippocampus and/or cerebellum slices, where neural excitation and neural inhibition have been characterized as being responsible for the so called LTP (long-term potentiation) and LTD (long-term depression) phenomena, respectively (Bear and Malenka, 1994; Stanton, 1996). LTP is a synaptic enhancement that follows brief, high-frequency electrical stimulation in the hippocampus and other brain areas, while LTD is a long-lasting depression of synaptic transmission following a low-frequency stimulation (1 per second) of the Schaffer collateral axons. These phenomena are forms of synaptic plasticity that are considered to underlie different forms of learning and memory (Stuchlik, 2014). The induction of LTP in the dentate gyrus of the hippocampus is associated with a rapid and robust transcription of the immediate early gene *Zif268* (Jones et al., 2001), thus showing that this IEG is essential for the transition from short- to long-term synaptic plasticity. In fact, several IEGs have been related to LTP induction and to the encoding of plasticity-related proteins (PRPs) required for LTP maintenance and memory formation (Okuno, 2011; Minatohara et al., 2016). Analyses relating LTD and IEG expression are scarce. Thus, an appropriate test for our hypothesis that downregulated levels of IEG in the 2D VR protocol reflect higher levels of neural inhibition would be the quantification of IEG expression in an LTD preparation.

2.4 Technical challenges for IEG analyses in the bee nervous system

For our qPCR experiments, we optimized the protocol of RNA extraction from the different regions of single bee brains. When a single bee brain is cut into different parts, the first problem is the coarseness of the dissection. Using frozen brains at -80°C implies being limited to cutting coarse sections of the miniature brain of bees, as sectioning may easily destroy the frozen-brain block. This explains why the sections chosen could not resolve more precisely way brain structures such as the central complex or the antennal lobes, or even separate the entire mushroom bodies (and not just the calyces) from the rest of the brain. In future analyses, this problem can be overcome by, using laser-capture microdissection, which has been recently acquired by our team. In this case, one can use a laser to delineate and cut out specific brain regions (see Fig. 5) or even a single cell somata, thus allowing to refine the analyses performed so far.
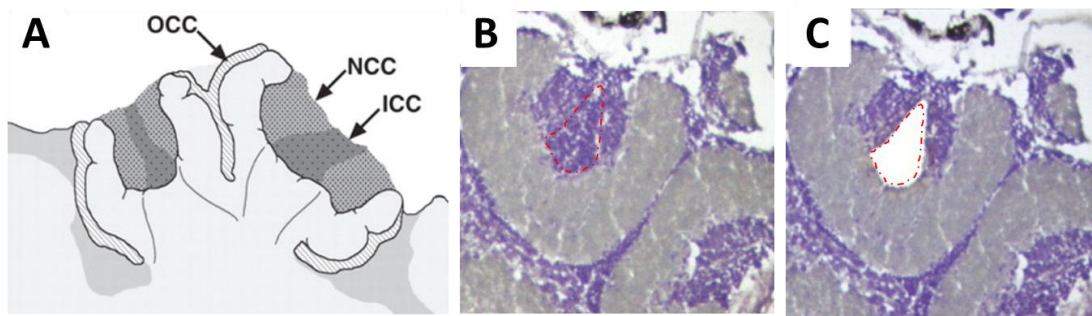
Figure 5. Adapted from (McQuillan et al., 2012) **(A)** a schematic diagram shows the structure of the MB and the location of inner-compact cells (ICC), noncompact cells (NCC), and outer compact cells (OCC). **(B)** histological section stained with hematoxylin and eosin. **(C)** The red dotted line indicates where inner-compact cell (ICC) was dissected by laser-capture microdissection.

Furthermore, another challenge of using single brains for analyses refers to the quality and quantity of extracted RNA, which in some cases cannot meet the requirements for the qPCR experiment. One solution adopted in some studies is to pool brain regions from two individual bees randomly chosen from each behavioral group to obtain sufficient genetic material for analysis (Avalos et al., 2021). But this solution sacrifices the possibility of relating single-brain changes to individual behavioral. Most studies used ice-cold bee saline to do the dissection (Reim and Scheiner, 2014; Scheiner et al., 2014b; Thamm et al., 2017). Then, each dissected tissue is transferred to a reaction tube, immediately frozen in liquid nitrogen, and stored at −80 °C until further use (Reim and Scheiner, 2014; Scheiner et al., 2014b). This solution cannot ensure the quality of RNA either, because in our previous experiment, we found that RNA degradation occurs primarily during the dissection of the bee brain, even if bee brains are placed into ice-cold bee saline. Therefore, we performed the dissection of bee brains under freezing conditions and used a closed RNA extraction method, thus ensuring the quality and quantity of RNA (Geng et al., 2022; Lafon et al., 2022).

In the future, the function of the *kakusei, Hr38,* and *Erg1* genes, among others can be further verified using tools such as RNAi or CRISPR/Cas9 knockout, which will allow one to confirm causal relationships between genes and phenotypes. In the case of complex behaviors, such as visual learning and memory, there must be more than one gene involved due to complex gene regulation. In that sense, the approach we chose, which is just to focus on 3 or 4 genes, is also limited but is commonly used in many studies on IEG expression (Lutz and Robinson, 2013; Shah

et al., 2018; Singh et al., 2018; Ugajin et al., 2018; Iino et al., 2020). Therefore, a first step would be to screen which genes are involved in the visual learning process of honeybees by means of transcriptome sequencing, and then select the target genes from the transcriptome database, and use RNAi or gene knockout to verify the specific functions of these genes.

In order to have a good understanding regarding the relationship between bee behavior and gene expression, the following steps are essential. First, transcriptome analysis is required to screen out differentially expressed genes from tens of thousands of bee genes (Li et al., 2019), and then RNAi may be used for behavioral validation analysis (Kohno and Kubo, 2019). If the relationship between the target gene and behavior can be determined, the gene-editing homozygote can be obtained by gene editing such as the CRISPR/Cas9 system (providing that CRISPR/Cas9 induced mutations are not lethal), and then the neural pathway research can be carried out. Thus, the gene-behavior-neural pathway can be established.

3. Studying aminergic gene expression during aversive color learning in the Icarus setup

Finally, I contributed to an analysis of aminergic gene expression in the context of aversive color learning in the Icarus setup. I aimed at determining if this aversive color learning induces transcriptional changes immediately post learning in the case of target aminergic receptor genes, which might participate either in memory consolidation, or in amplifying the representation of shock reinforcement and/or the light used as discriminative stimulus.

Aminergic receptor genes were chosen for this study because of the proved and recurrent role played by biogenic amines such as dopamine (DA), octopamine (OA), serotonin (5-HT) and tyramine (TH) to mediate reinforcement signals in the insect brain.

Dopamine (DA) has been linked to motivated behavior (Huang et al., 2022) and rewarding reinforcement in fruit flies (Krashes et al., 2009; Liu et al., 2012). In Drosophila, appetitive memory formation requires signaling through dopamine neurons providing reward information to the mushroom bodies, although the first relay neurons are octopaminergic (Burke et al., 2012). Dopamine also mediates, yet through a different set of dopaminergic neurons, aversive-reinforcement information in the Drosophila brain. A cluster of dopaminergic neurons convey the

information about electric shock and other forms of punishment (Riemensperger et al., 2005). In honeybees, dopamine signaling is also necessary for aversive olfactory learning (learning of odor-shock associations during the conditioning of the sting extension reflex (V. Vergoz et al., 2007) and other studies we did), where it plays a similar role as in Drosophila aversive olfactory conditioning.

Octopamine (OA) was originally considered to be the signal for reward in insect learnings (Hammer, 1993; Hammer and Menzel, 1998; Schwaerzel et al., 2003), but it seems that it only ensures this function in insects other than Drosophila. In honey bees and crickets (Hammer, 1993; Hammer and Menzel, 1998; Farooqui et al., 2003), OA has been shown to mediate the appetitive reward signal, as indicated by the case of the octopaminergic neuron VUMmx1 (Hammer, 1993) whose artificial activation replaces sucrose solution during olfactory conditioning, and therefore supports odor learning.

Serotonin (5-HT) may involve coordinated defensive action by honey bees (Nouvian et al., 2018). 5-HT is also a major neurotransmitter of the bee's visual system and participates in different forms of visual processing (Schürmann and Klemm, 1984; Erber and Kloppenburg, 1995; Erber et al., 1991). Tyramine (TH) is synthesized from tyrosine by the enzyme tyrosine decarboxylase, and then octopamine is synthesized from tyramine in one step by the action of the enzyme tyramine beta-hydroxylase (David and Coulon, 1985). Several studies showed that tyramine has sources and functions independent of octopamine, i.e., effecting olfactory behavior in Drosophila (Kutsukake et al., 2000), ruling behavior in locust (Roeder, 2005), inhibiting egg-laying in C. elegans (Alkema et al., 2005), division of foraging labor in honey bee (Scheiner et al., 2014a), defensive behavior in termite soldier (Ishikawa et al., 2016).

In the context of aversive color learning, we focused on the three dopamine receptor genes *Amdop1, Amdop2 and Amdop3* (Kyle T Beggs et al., 2011), given the essential role of dopamine for aversive-reinforcement signaling in honey bees (Tedjakumala et al., 2014; Tedjakumala and Giurfa, 2013; Vanina Vergoz et al., 2007) (See above). Furthermore, I quantified expression levels of the main octopamine receptor gene *AmoctαR1* (Kyle T. Beggs et al., 2011; Farooqui et al., 2004, 2003; Sinakevitch et al., 2011) due to the inverse relationship found between octopamine levels in the optic lobes of bee foragers and their phototactic responses (Scheiner et al., 2014b) (i.e., higher

phototactic responses correlate with lower OA levels). Finally, I also measured levels of the 5-HT receptor gene *Am5-ht1a*, which has been shown to be highly expressed in brain regions involved in visual information processing and which has a strong impact on phototactic behavior (Thamm et al., 2010).

I found that inhibitory color learning determines an up-regulation of the dopaminergic receptor gene *Amdop1* in the mushroom bodies, consistent with the role of dopamine signaling in different forms of aversive learning in insects.

As mentioned above, using frozen brains implies being limited to coarse sections of the miniature brain of bees. So, in future analyses, this problem can be overcome by using laser-capture microdissection. In this case, one can use a laser to delineate and cut specific brain regions (see Fig. 4) or even single-cell somata, thus refining to refine the analyses performed so far.

Outlook

Although honey bees do not offer the wide variety of genetic tools that are accessible in the fruit fly D*rosophila melanogaster*, they exhibit sophisticated forms of learning and memory, and social behaviors that are neither present in flies and other insects, nor even in many vertebrates. Thus, a fundamental goal for future research would be the molecular dissection of these complex behaviors that are unique to honey bees.

With the update of the honeybee genome and the development of bioinformatics, more and more genes in honeybees are annotated. This technical evolution increases the probability of explaining the relationship between genes and complex behaviors in bees, and eventually in other social insects. Transcriptome analyses allow one to quickly find the genes differentially expressed between two or more groups, such as learners vs. non-learners. Fluorescence *in situ* hybridization technology (FISH) allows one to visualiz the spatial expression of these differential genes in specific areas of the central nervous system. This approach could be used to obtain a refined study of IEG expression and move away from the coarse dissection methods used in the present work. After determining the spatial expression of target genes, functional hypotheses can be made related to their role and involvement in specific behavioral contexts. RNAi technology can then be used to verify whether these hypotheses are sound. Finally, transgenic bees could be produced by gene

knockout or gene knock-in (especially interesting would be the insertion of a fluorescent protein gene) to further verify how candidate genes affect behavior. For example, injecting related metabolites to see if behavioral phenotypes abolished in mutant bees can be rescued vis this knock in. Since the behavioral research of honeybees is very developed (i.e., PER, SER), the genes specific to various honeybee behaviors can be screened out by combining the above technologies. Then the door of the relationships and causations between candidate genes and honeybee, individual and social behaviors will be opened.

References

Alaux, C., Robinson, G.E., 2007. Alarm Pheromone Induces Immediate–Early Gene Expression and Slow Behavioral Response in Honey Bees. J Chem Ecol 33, 1346–1350. https://doi.org/10.1007/s10886-007-9301-6

Alkema, M.J., Hunter-Ensor, M., Ringstad, N., Horvitz, H.R., 2005. Tyramine functions independently of octopamine in the Caenorhabditis elegans nervous system. Neuron 46, 247–260. https://doi.org/10.1016/j.neuron.2005.02.024

Allen, S.E., Koreman, G.T., Sarkar, A., Wang, B., Wolfner, M.F., Han, C., 2021. Versatile CRISPR/Cas9-mediated mosaic analysis by gRNA-induced crossing-over for unmodified genomes. PLOS Biology 19, e3001061. https://doi.org/10.1371/journal.pbio.3001061

Avalos, A., Traniello, I.M., Pérez Claudio, E., Giray, T., 2021. Parallel mechanisms of visual memory formation across distinct regions of the honey bee brain. J Exp Biol 224. https://doi.org/10.1242/jeb.242292

Bahrami, S., Drablos, F., 2016. Gene regulation in the immediate-early response process. Adv Biol Regul 62, 37–49. https://doi.org/10.1016/j.jbior.2016.05.001

Bear, M.F., Malenka, R.C., 1994. Synaptic plasticity: LTP and LTD. Current opinion in neurobiology 4, 389–399. https://doi.org/10.1016/0959-4388(94)90101-5

Beggs, Kyle T, Tyndall, J.D., Mercer, A.R., 2011. Honey bee dopamine and octopamine receptors linked to intracellular calcium signaling have a close phylogenetic and pharmacological relationship. PLoS One 6, e26809. https://doi.org/10.1371/journal.pone.0026809

Büchler, R., Andonov, S., Bienefeld, K., Costa, C., Hatjina, F., Kezic, N., Kryger, P., Spivak, M., Uzunov, A., Wilde, J., 2013. Standard methods for rearing and selection of Apis mellifera queens. Journal of Apicultural Research 52, 1–30. https://doi.org/10.3896/IBRA.1.52.1.07

Burke, C.J., Huetteroth, W., Owald, D., Perisse, E., Krashes, M.J., Das, G., Gohl, D., Silies, M., Certel, S., Waddell, S., 2012. Layered reward signaling through octopamine and dopamine in Drosophila. Nature 492, 433–437. https://doi.org/10.1038/nature11614

Chen, Z., Traniello, I.M., Rana, S., Cash-Ahmed, A.C., Sankey, A.L., Yang, C., Robinson, G.E., 2021. Neurodevelopmental and transcriptomic effects of CRISPR/Cas9-induced somatic *orco* mutation in honey bees. Journal of Neurogenetics 35, 320–332.

https://doi.org/10.1080/01677063.2021.1887173

Chittka, L., Beier, W., Hertel, H., Steinmann, E., Menzel, R., 1992. Opponent colour coding is a universal strategy to evaluate the photoreceptor inputs in Hymenoptera. J Comp Physiol A 170, 545–563. https://doi.org/10.1007/BF00199332

Chiu, Y.-K., Hsu, J.-C., Chang, T., Huang, Y.-C., Wang, J., 2020. Mutagenesis mediated by CRISPR/Cas9 in the red imported fire ant, Solenopsis invicta. Insect. Soc. 67, 317–326. https://doi.org/10.1007/s00040-020-00755-8

Collins, A.M., 2004. Sources of variation in the viability of honey bee, Apis mellifera L., semen collected for artificial insemination. Invertebrate Reproduction & Development 45, 231–237. https://doi.org/10.1080/07924259.2004.9652594

Collins, A.M., 2002. Collection of honey bee eggs for cryopreservation. Journal of apicultural research 41, 89–95. https://doi.org/10.1080/00218839.2002.11101074

David, J.-C., Coulon, J.-F., 1985. Octopamine in invertebrates and vertebrates. A review. Progress in Neurobiology 24, 141–185. https://doi.org/10.1016/0301-0082(85)90009-7

Değirmenci, L., Geiger, D., Rogé Ferreira, F.L., Keller, A., Krischke, B., Beye, M., Steffan-Dewenter, I., Scheiner, R., 2020. CRISPR/Cas9-mediated mutations as a new tool for studying taste in honeybees. Chemical Senses 45, 655–666. https://doi.org/10.1093/chemse/bjaa063

Erber, J., Kloppenburg, P., 1995. The modulatory effects of serotonin and octopamine in the visual system of the honey bee (Apis mellifera L.). Journal of Comparative Physiology A 176, 111–118. https://doi.org/10.1007/BF00197757

Erber, J., Kloppenburg, P., Scheidler, A., 1991. Neuromodulation in the honeybee: autoradiography, behaviour and electrophysiology. The behaviour and physiology of bees 273–287. https://doi.org/10.1007/BF01929916

Evans, J.D., Boncristiani, H., Chen, Y., 2010. Scientific note on mass collection and hatching of honey bee embryos. Apidologie 41, 654–656. https://doi.org/10.1051/apido/2010009

Farooqui, T., Robinson, K., Vaessin, H., Smith, B.H., 2003. Modulation of early olfactory processing by an octopaminergic reinforcement pathway in the honeybee. The Journal of Neuroscience 23, 5370–80. https://doi.org/10.1523/JNEUROSCI.23-12-05370.2003

Farooqui, T., Vaessin, H., Smith, B.H., 2004. Octopamine receptors in the honeybee (Apis mellifera) brain and their disruption by RNA-mediated interference. Journal of Insect Physiology 50, 701–713. https://doi.org/10.1016/j.jinsphys.2004.04.014

Franceschini, A., Costantini, I., Pavone, F.S., Silvestri, L., 2020. Dissecting Neuronal Activation on a Brain-Wide Scale With Immediate Early Genes. Frontiers in Neuroscience 14. https://doi.org/10.3389/fnins.2020.569517

Fujita, N., Nagata, Y., Nishiuchi, T., Sato, M., Iwami, M., Kiya, T., 2013. Visualization of neural activity in insect brains using a conserved immediate early gene, Hr38. Curr Biol 23, 2063–70. https://doi.org/10.1016/j.cub.2013.08.051

Geng, H., Lafon, G., Avarguès-Weber, A., Buatois, A., Massou, I., Giurfa, M., 2022. Visual learning in a virtual reality environment upregulates immediate early gene expression in the mushroom bodies of honey bees. Commun Biol 5, 1–11. https://doi.org/10.1038/s42003-022-03075-8

Gillard, T.L., Oldroyd, B.P., 2020. Chapter One - Controlled reproduction in the honey bee (Apis mellifera) via artificial insemination, in: Jurenka, R. (Ed.), Advances in Insect Physiology.

Academic Press, pp. 1–42. https://doi.org/10.1016/bs.aiip.2020.08.001

Hammer, M., 1993. An identified neuron mediates the unconditioned stimulus in associative olfactory learning in honeybees. Nature 366, 59–63. https://doi.org/10.1038/366059a0

Hammer, M., Menzel, R., 1998. Multiple sites of associative odor learning as revealed by local brain microinjections of octopamine in honeybees. Learn Mem 5, 146–156. https://doi.org/

Hu, X.F., Zhang, B., Liao, C.H., Zeng, Z.J., 2019. High-Efficiency CRISPR/Cas9-Mediated Gene Editing in Honeybee (*Apis mellifera*) Embryos. G3 Genes|Genomes|Genetics 9, 1759–1766. https://doi.org/10.1534/g3.119.400130

Huang, J., Zhang, Z., Feng, W., Zhao, Y., Aldanondo, A., de Brito Sanchez, M.G., Paoli, M., Rolland, A., Li, Z., Nie, H., Lin, Y., Zhang, S., Giurfa, M., Su, S., 2022. Food wanting is mediated by transient activation of dopaminergic signaling in the honey bee brain. Science 376, 508–512. https://doi.org/10.1126/science.abn9920

Iino, S., Shiota, Y., Nishimura, M., Asada, S., Ono, M., Kubo, T., 2020. Neural activity mapping of bumble bee (*Bombus ignitus*) brains during foraging flight using immediate early genes. Scientific reports 10, 7887. https://doi.org/10.1038/s41598-020-64701-1

Ishikawa, Y., Aonuma, H., Sasaki, K., Miura, T., 2016. Tyraminergic and octopaminergic modulation of defensive behavior in termite soldier. PLoS One 11, e0154230. https://doi.org/10.1371/journal.pone.0154230

Jones, M., Errington, M.L., French, P.J., Fine, A., Bliss, T.V., Garel, S., Charnay, P., Bozon, B., Laroche, S., Davis, S., 2001. A requirement for the immediate early gene Zif268 in the expression of late LTP and long-term memories. Nature neuroscience 4, 289–296. https://doi.org/10.1038/85138

Kaftanoglu, O., Linksvayer, T.A., Page, R.E., 2011. Rearing Honey Bees, Apis mellifera, *in vitro*: Effects of Sugar Concentrations on Survival and Development. Journal of Insect Science 11, 1–10. https://doi.org/10.1673/031.011.9601

Kiya, T., Kubo, T., 2011. Dance type and flight parameters are associated with different mushroom body neural activities in worker honeybee brains. PloS one 6, e19301. https://doi.org/10.1371/journal.pone.0019301

Kiya, T., Kubo, T., 2010. Analysis of GABAergic and non-GABAergic neuron activity in the optic lobes of the forager and re-orienting worker honeybee (*Apis mellifera* L.). PloS one 5, e8833. https://doi.org/10.1371/journal.pone.0008833

Kiya, T., Kunieda, T., Kubo, T., 2008. Inducible- and constitutive-type transcript variants of kakusei , a novel non-coding immediate early gene, in the honeybee brain. Insect molecular biology 17, 531–6. https://doi.org/10.1111/j.1365-2583.2008.00821.x

Kiya, T., Kunieda, T., Kubo, T., 2007. Increased neural activity of a mushroom body neuron subtype in the brains of forager honeybees. PloS one 2, e371. https://doi.org/10.1371/journal.pone.0000371

Kohno, H., Kubo, T., 2019. Genetics in the Honey Bee: Achievements and Prospects toward the Functional Analysis of Molecular and Neural Mechanisms Underlying Social Behaviors. Insects 10, 348. https://doi.org/10.3390/insects10100348

Kohno, H., Kubo, T., 2018. mKast is dispensable for normal development and sexual maturation of the male European honeybee. Sci Rep 8, 11877. https://doi.org/10.1038/s41598-018-30380-2

Kohno, H., Suenami, S., Takeuchi, H., Sasaki, T., Kubo, T., 2016. Production of Knockout Mutants

by CRISPR/Cas9 in the European Honeybee, Apis mellifera L. Zoological science 33, 505–512. https://doi.org/10.2108/zs160043

Krashes, M.J., DasGupta, S., Vreede, A., White, B., Armstrong, J.D., Waddell, S., 2009. A neural circuit mechanism integrating motivational state with memory expression in Drosophila. Cell 139, 416–427. https://doi.org/10.1016/j.cell.2009.08.035

Kutsukake, M., Komatsu, A., Yamamoto, D., Ishiwa-Chigusa, S., 2000. A tyramine receptor gene mutation causes a defective olfactory behavior in Drosophila melanogaster. Gene 245, 31–42. https://doi.org/10.1016/s0378-1119(99)00569-7

Lafon, G., Geng, H., Avarguès-Weber, A., Buatois, A., Massou, I., Giurfa, M., 2022. The Neural Signature of Visual Learning Under Restrictive Virtual-Reality Conditions. Frontiers in Behavioral Neuroscience 16. https://doi.org/10.3389/fnbeh.2022.846076

Lee, J., Lee, S.H., 2019. Development of a film-assisted honeybee egg collection system (FECS). Apidologie 50, 804–810. https://doi.org/10.1007/s13592-019-00687-8

Li, Z., Yu, T., Chen, Y., Heerman, M., He, J., Huang, J., Nie, H., Su, S., 2019. Brain transcriptome of honey bees (Apis mellifera) exhibiting impaired olfactory learning induced by a sublethal dose of imidacloprid. Pesticide Biochemistry and Physiology 156, 36–43. https://doi.org/10.1016/j.pestbp.2019.02.001

Liu, C., Plaçais, P.-Y., Yamagata, N., Pfeiffer, B.D., Aso, Y., Friedrich, A.B., Siwanowicz, I., Rubin, G.M., Preat, T., Tanimoto, H., 2012. A subset of dopamine neurons signals reward for odour memory in Drosophila. Nature 488, 512–516. https://doi.org/10.1038/nature11304

Lutz, C.C., Robinson, G.E., 2013. Activity-dependent gene expression in honey bee mushroom bodies in response to orientation flight. The Journal of experimental biology 216, 2031–8. https://doi.org/10.1242/jeb.084905

Marchal, P., Villar, M.E., Geng, H., Arrufat, P., Combe, M., Viola, H., Massou, I., Giurfa, M., 2019. Inhibitory learning of phototaxis by honeybees in a passive-avoidance task. Learn Mem 26, 412–423. https://doi.org/10.1101/lm.050120.119

Mazo-Vargas, A., Concha, C., Livraghi, L., Massardo, D., Wallbank, R.W.R., Zhang, L., Papador, J.D., Martinez-Najera, D., Jiggins, C.D., Kronforst, M.R., Breuker, C.J., Reed, R.D., Patel, N.H., McMillan, W.O., Martin, A., 2017. Macroevolutionary shifts of WntA function potentiate butterfly wing-pattern diversity. Proc Natl Acad Sci USA 114, 10701–10706. https://doi.org/10.1073/pnas.1708149114

McQuillan, H.J., Nakagawa, S., Mercer, A.R., 2012. Mushroom bodies of the honeybee brain show cell population-specific plasticity in expression of amine-receptor genes. Learn. Mem. 19, 151–158. https://doi.org/10.1101/lm.025353.111

Mehravar, M., Shirazi, A., Nazari, M., Banan, M., 2019. Mosaicism in CRISPR/Cas9-mediated genome editing. Developmental Biology 445, 156–162. https://doi.org/10.1016/j.ydbio.2018.10.008

Menzel, R., Blakers, M., 1976. Colour receptors in the bee eye— Morphology and spectral sensitivity. Journal of Comparative Physiology A 108, 11–13.

Menzel, R., Greggers, U., 1985. Natural phototaxis and its relationship to colour vision in honeybees. Journal of Comparative Physiology A 157, 311–321.

Milne Jr, C.P., Phillips, J.P., Krell, P.J., 1988. Microinjection of early honeybee embryos. Journal of apicultural research 27, 84–89.

Minatohara, K., Akiyoshi, M., Okuno, H., 2016. Role of Immediate-Early Genes in Synaptic

Plasticity and Neuronal Ensembles Underlying the Memory Trace. Frontiers in Molecular Neuroscience 8. https://doi.org/10.3389/fnmol.2015.00078

Nie, H.-Y., Liang, L.-Q., Li, Q.-F., Zhu, Y.-N., Guo, Y.-K., Zheng, Q.-L., Lin, Y., Yang, D.-L., Li, Z.-G., Su, S.-K., 2021. CRISPR/Cas9 mediated knockout of Amyellow-y gene results in melanization defect of the cuticle in adult Apis mellifera. Journal of insect physiology 132, 104264. https://doi.org/10.1016/j.jinsphys.2021.104264

Nouvian, M., Mandal, S., Jamme, C., Claudianos, C., d'Ettorre, P., Reinhard, J., Barron, A.B., Giurfa, M., 2018. Cooperative defence operates by social modulation of biogenic amine levels in the honey bee brain. Proc Biol Sci 285, 20172653. https://doi.org/10.1098/rspb.2017.2653

Ogawa, Y., Ribi, W., Zeil, J., Hemmi, J.M., 2017. Regional differences in the preferred e-vector orientation of honeybee ocellar photoreceptors. Journal of Experimental Biology 220, 1701–1708. https://doi.org/10.1242/jeb.156109

Okuno, H., 2011. Regulation and function of immediate-early genes in the brain: beyond neuronal activity markers. Neuroscience research 69, 175–186. https://doi.org/10.1016/j.neures.2010.12.007

Omholt, S., Hagen, A., Elmholdt, O., Rishovd, S., 1995. A laboratory hive for frequent collection of honeybee eggs. Apidologie 26, 297–304.

Peitsch, D., Fietz, A., Hertel, H., de Souza, J., Ventura, D.F., Menzel, R., 1992. The spectral input systems of hymenopteran insects and their receptor-based colour vision. J Comp Physiol A 170, 23–40. https://doi.org/10.1007/BF00190398

Reim, T., Scheiner, R., 2014. Division of labour in honey bees: age- and task-related changes in the expression of octopamine receptor genes. Insect Molecular Biology 23, 833–841. https://doi.org/10.1111/imb.12130

Riemensperger, T., Völler, T., Stock, P., Buchner, E., Fiala, A., 2005. Punishment prediction by dopaminergic neurons in Drosophila. Curr Biol 15, 1953–1960. https://doi.org/10.1016/j.cub.2005.09.042

Roeder, T., 2005. Tyramine and octopamine: ruling behavior and metabolism. Annu. Rev. Entomol 50, 447–77. https://doi.org/10.1146/annurev.ento.50.071803.130404

Roth, A., Vleurinck, C., Netschitailo, O., Bauer, V., Otte, M., Kaftanoglu, O., Page, R.E., Beye, M., 2019. A genetic switch for worker nutrition-mediated traits in honeybees. PLoS Biol 17, e3000171. https://doi.org/10.1371/journal.pbio.3000171

Scheiner, R., Kulikovskaja, L., Thamm, M., 2014a. The honey bee tyramine receptor AmTYR1 and division of foraging labour. Journal of Experimental Biology 217, 1215–1217. https://doi.org/10.1242/jeb.098475

Scheiner, R., Toteva, A., Reim, T., Søvik, E., Barron, A.B., 2014b. Differences in the phototaxis of pollen and nectar foraging honey bees are related to their octopamine brain titers. Frontiers in Physiology 5, 1–8. https://doi.org/10.3389/fphys.2014.00116

Schmehl, D.R., Tomé, H.V., Mortensen, A.N., Martins, G.F., Ellis, J.D., 2016. Protocol for the *in vitro* rearing of honey bee (Apis mellifera L.) workers. Journal of Apicultural Research 55, 113–129. https://doi.org/10.1080/00218839.2016.1203530

Schulte, C., Theilenberg, E., Müller-Borg, M., Gempe, T., Beye, M., 2014. Highly efficient integration and expression of piggyBac-derived cassettes in the honeybee (Apis mellifera). PNAS 111, 9003–9008. https://doi.org/10.1073/pnas.1402341111

Schürmann, F., Klemm, N., 1984. Serotonin-immunoreactive neurons in the brain of the honeybee. Journal of Comparative Neurology 225, 570–580.

Schwaerzel, M., Monastirioti, M., Scholz, H., Friggi-Grelin, F., Birman, S., Heisenberg, M., 2003. Dopamine and octopamine differentiate between aversive and appetitive olfactory memories in Drosophila. J Neurosci 23, 10495–10502. https://doi.org/10.1523/JNEUROSCI.23-33-10495.2003

Shah, A., Jain, R., Brockmann, A., 2018. Egr-1: A candidate transcription factor involved in molecular processes underlying time-memory. Frontiers in Psychology 9. https://doi.org/10.3389/fpsyg.2018.00865

Sieber, K., Saar, M., Opachaloemphan, C., Gallitto, M., Yang, H., Yan, H., 2021. Embryo Injections for CRISPR-Mediated Mutagenesis in the Ant Harpegnathos saltator. JoVE (Journal of Visualized Experiments) e61930. https://doi.org/10.3791/61930

Sinakevitch, I., Kurtzman, Z., Choi, H.G., Pardo, D.A.R., Dahan, R.A., Klein, N., Bugarija, B., Wendlandt, E., Smith, B.H., 2020. Anti-RDL and Anti-mGlutR1 Receptors Antibody Testing in Honeybee Brain Sections using CRISPR-Cas9. JoVE (Journal of Visualized Experiments) e59993. https://doi.org/10.3791/59993

Sinakevitch, I., Mustard, J.A., Smith, B.H., 2011. Distribution of the octopamine receptor AmOA1 in the honey bee brain. PLoS ONE 6, e14536. https://doi.org/10.1371/journal.pone.0014536

Singh, A.S., Shah, A., Brockmann, A., 2018. Honey bee foraging induces upregulation of early growth response protein 1, hormone receptor 38 and candidate downstream genes of the ecdysteroid signalling pathway. Insect molecular biology 27, 90–98. https://doi.org/10.1111/imb.12350

Spaethe, J., Briscoe, A.D., 2004. Early Duplication and Functional Diversification of the Opsin Gene Family in Insects. Molecular Biology and Evolution 21, 1583–1594. https://doi.org/10.1093/molbev/msh162

Stanton, P.K., 1996. LTD, LTP, and the sliding threshold for long-term synaptic plasticity. Hippocampus 6, 35–42. https://doi.org/10.1002/(SICI)1098-1063(1996)6:1<35::AID-HIPO7>3.0.CO;2-6

Stuchlik, A., 2014. Dynamic learning and memory, synaptic plasticity and neurogenesis: an update. Frontiers in behavioral neuroscience 8, 106. https://doi.org/10.3389/fnbeh.2014.00106

Taber, S., III, 1961. Forceps Design for Transferring Honey Bee Eggs. Journal of Economic Entomology 54, 247–250. https://doi.org/10.1093/jee/54.2.247

Tedjakumala, S.R., Aimable, M., Giurfa, M., 2014. Pharmacological modulation of aversive responsiveness in honey bees. Frontiers in Behavioral Neuroscience 7. https://doi.org/10.3389/fnbeh.2013.00221

Tedjakumala, S.R., Giurfa, M., 2013. Rules and mechanisms of punishment learning in honey bees: the aversive conditioning of the sting extension response. The Journal of Experimental Biology 216, 2985–97. https://doi.org/10.1242/jeb.086629

Thamm, M., Balfanz, S., Scheiner, R., Baumann, A., Blenau, W., 2010. Characterization of the 5-HT1A receptor of the honeybee (Apis mellifera) and involvement of serotonin in phototactic behavior. Cellular and Molecular Life Sciences 67, 2467–2479. https://doi.org/10.1007/s00018-010-0350-6

Thamm, M., Scholl, C., Reim, T., Grübel, K., Möller, K., Rössler, W., Scheiner, R., 2017. Neuronal

distribution of tyramine and the tyramine receptor AmTAR1 in the honeybee brain. Journal of Comparative Neurology 525, 2615–2631. https://doi.org/10.1002/cne.24228

Trible, W., Olivos-Cisneros, L., McKenzie, S.K., Saragosti, J., Chang, N.-C., Matthews, B.J., Oxley, P.R., Kronauer, D.J.C., 2017. orco Mutagenesis Causes Loss of Antennal Lobe Glomeruli and Impaired Social Behavior in Ants. Cell 170, 727-735.e10. https://doi.org/10.1016/j.cell.2017.07.001

Ugajin, A., Uchiyama, H., Miyata, T., Sasaki, T., Yajima, S., Ono, M., 2018. Identification and initial characterization of novel neural immediate early genes possibly differentially contributing to foraging-related learning and memory processes in the honeybee. Insect molecular biology 27, 154–165. https://doi.org/10.1111/imb.12355

Velarde, R.A., Sauer, C.D., O. Walden, K.K., Fahrbach, S.E., Robertson, H.M., 2005. Pteropsin: A vertebrate-like non-visual opsin expressed in the honey bee brain. Insect Biochemistry and Molecular Biology 35, 1367–1377. https://doi.org/10.1016/j.ibmb.2005.09.001

Vergoz, V., Roussel, E., Sandoz, J.C., Giurfa, M., 2007. Aversive learning in honeybees revealed by the olfactory conditioning of the sting extension reflex. PloS one 2, e288. https://doi.org/10.1371/journal.pone.0000288

Vergoz, Vanina, Roussel, E., Sandoz, J.-C., Giurfa, M., 2007. Aversive learning in honeybees revealed by the olfactory conditioning of the sting extension reflex. PLoS ONE 2, e288. https://doi.org/10.1371/journal.pone.0000288

Von Helversen, O., 1972. Zur spektralen Unterschiedsempfindlichkeit der honigbiene. Journal of comparative physiology 80, 439–472.

Wakakuwa, M., Kurasawa, M., Giurfa, M., Arikawa, K., 2005. Spectral heterogeneity of honeybee ommatidia. Naturwissenschaften 92, 464–467. https://doi.org/10.1007/s00114-005-0018-5

Wang, X., Lin, Y., Liang, L., Geng, H., Zhang, M., Nie, H., Su, S., 2021. Transcriptional Profiles of Diploid Mutant Apis mellifera Embryos after Knockout of csd by CRISPR/Cas9. Insects 12, 704. https://doi.org/10.3390/insects12080704

Yan, H., Opachaloemphan, C., Mancini, G., Yang, H., Gallitto, M., Mlejnek, J., Leibholz, A., Haight, K., Ghaninia, M., Huo, L., Perry, M., Slone, J., Zhou, X., Traficante, M., Penick, C.A., Dolezal, K., Gokhale, K., Stevens, K., Fetter-Pruneda, I., Bonasio, R., Zwiebel, L.J., Berger, S.L., Liebig, J., Reinberg, D., Desplan, C., 2017. An Engineered orco Mutation Produces Aberrant Social Behavior and Defective Neural Development in Ants. Cell 170, 736-747.e9. https://doi.org/10.1016/j.cell.2017.06.051

Zhang, L., Reed, R.D., 2016. Genome editing in butterflies reveals that spalt promotes and Distal-less represses eyespot colour patterns. Nat Commun 7, 11769. https://doi.org/10.1038/ncomms11769